Molecular Imaging of STAT3 Signaling *In Vivo*

By

SHALINI DIMRI

[LIFE09201304001]

TATA MEMORIAL CENTRE

MUMBAI

A thesis submitted to the Board of Studies in Life Sciences

In partial fulfilment of requirements for the Degree of

DOCTOR OF PHILOSOPHY

of

HOMI BHABHA NATIONAL INSTITUTE

March, 2020

Homi Bhabha National Institute

Recommendations of the Viva Voce Committee

As members of the Viva Voce Committee, we certify that we have read the dissertation prepared by **Ms. Shalini Dimri** entitled "**Molecular Imaging of STAT3 Signaling *in vivo***" and recommend that it may be accepted as fulfilling the thesis requirement for the award of Degree of Doctor of Philosophy.

S. Chiplunkar — 10.08.2020

Chairperson – Dr. S.V Chiplunkar — Date:

Abhijit De — 10-08-2020

Guide – Dr. Abhijit De — Date:

10 August 2020

External Examiner – Dr. Veena K. Parnaik — Date:

Prasanna. — 10/8/2020.

Member – Dr. Prasanna Venkataraman — Date:

Sanjay — 10.08.2020

Member -Dr. Sanjay Gupta — Date:

Gupta — 10/8/2020

Invitee- Dr. Sudeep Gupta — Date

Final approval and acceptance of this thesis is contingent upon the candidate's submission of the final copies of the thesis to HBNI.

I hereby certify that I have read this thesis prepared under my direction and recommend that it may be accepted as fulfilling the thesis requirement.

Abhijit De 10-08-2020

Date: 10.08.2020
Place: Navi Mumbai

Dr. Abhijit De
Guide

STATEMENT BY AUTHOR

This dissertation has been submitted in partial fulfillment of requirements for an advanced degree at Homi Bhabha National Institute (HBNI) and is deposited in the Library to be made available to borrowers under rules of the HBNI.

Brief quotations from this dissertation are allowable without special permission, provided that accurate acknowledgement of source is made. Requests for permission for extended quotation from or reproduction of this manuscript in whole or in part may be granted by the Competent Authority of HBNI when in his or her judgment the proposed use of the material is in the interests of scholarship. In all other instances, however, permission must be obtained from the author.

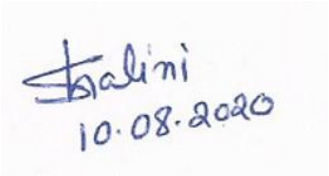

Ms. Shalini Dimri

DECLARATION

I, hereby declare that the investigation presented in the thesis has been carried out by me. The work is original and has not been submitted earlier as a whole or in part for a degree / diploma at this or any other Institution / University.

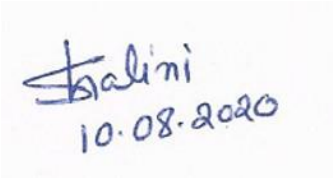

Ms. Shalini Dimri

List of Publications arising from the thesis

Journals

1. **“**Dynamic monitoring of STAT3 activation in live cells using a novel STAT3 Phospho-BRET sensor.” **Shalini Dimri**, Rohit Arora, Akshi Jasani and Abhijit De, American Journal of Nuclear Medicine and Molecular Imaging, 2019;9(6):321-334.

2. “Noncanonical pS727 post translational modification dictates major STAT3 activation and downstream functions in breast cancer.” **Shalini Dimri**, Renu Malhotra, Tanuja Shet, Smruti Mokal, Sudeep Gupta and Abhijit De. [Manuscript under Revision- Experimental Cell Research]

Patents

Provisional Indian Patent application filed with BCIL: “A Method for Detection of Protein Activation Using Phospho-BRET Imaging Sensor and Methods Thereof” (Ref. # 201921010208; filed on March 15, 2019).

Book chapters and Review articles

1. **Shalini Dimri**, Soumya Basu and Abhijit De. Use of BRET to Study Protein–Protein Interactions *in vitro*. The nuclear receptor superfamily, edited by Iain J. McEwan. Methods in Molecular Biology, Springer, New York 2016; 1443:57-78. **[Book Chapter]**

2. **Shalini Dimri**, Sukanya and Abhijit De. Approaching non-canonical STAT3 signaling to redefine cancer therapeutic strategy. Integrative Molecular Medicine,2017 4(1): 1-10 **[Review Article]**

Conference Abstracts (Published)

1. A novel molecular imaging sensor to elucidate functional role of non-canonical STAT3 activation in breast cancer. **Shalini Dimri**, Rohit Arora and Abhijit De. European Journal of Cancer, 2016 (54).

2. Non-canonical S727 STAT3 PTM activation governs its dimerization and downstream function in triple negative breast cancer. **Shalini Dimri**, Rohit Arora, Renu Malhotra, Tanuja Shet, Sudeep Gupta and Abhijit De. ESMO Open 2018; **3:** doi: 10.1136/esmoopen-2018-EACR25.706

Conferences and workshops

1. Attended and actively participated in workshop on - "Basic Course in Flow Cytometry-II-Hands on workshop" organized by Mumbai immunology group at ACTREC, 10-11th July 2014.

2. "Monitoring Stat3 Dimerization Dynamics in Live Cells Using Novel BRET Platform." Shalini Dimri, Rohit Arora and Abhijit De. 39th All India cell biology conference (AICBC)-cellular organization and dynamics held in Thiruvananthapuram, Kerala, 06-08th December 2015.

3. "Monitoring activation dynamics of STAT3 in Live Cells Using Novel BRET Platform". Shalini Dimri, Rohit Arora and Abhijit De. 11th National Research Scholars meet in Life Sciences held in ACTREC, Mumbai, 17-18th December 2015 and received **second best poster award**.

4. "A novel molecular imaging sensor to elucidate functional role of non-canonical STAT3 activation in breast cancer." Shalini Dimri, Rohit Arora and Abhijit De.75th TMC platinum jubilee "A Conference of New Ideas in Cancer: Challenging Dogmas" held in Mumbai, 26-28th February 2016.

5. "A novel molecular imaging sensor for monitoring *in vivo* STAT3 protein phosphorylation highlights important functional and biological role of non-canonical STAT3 PTMs." Shalini Dimri, Rohit Arora, Renu Malhotra, Tanuja Shet, Sudeep

Gupta and Abhijit De. International Congress of Cell Biology- "The Dynamic Cell-From molecules and Networks to form and function" held at Hyderabad, 27-31st January,2018.

6. "Non-canonical S727 STAT3 PTM activation governs its dimerization and downstream function in triple negative breast cancer." Shalini Dimri, Rohit Arora, Renu Malhotra, Tanuja Shet, Sudeep Gupta and Abhijit De. 25th Biennial Congress of the European Association for Cancer Research (EACR25) held at Amsterdam, Netherlands, 30th June – 03rd July 2018.

7. "Phospho-STAT3 BRET sensor for assessment of live cell STAT3 dimerization highlights functional and biological significance of non-canonical STAT3 activation in breast cancer." Shalini Dimri, Rohit Arora, Renu Malhotra, Tanuja Shet, Sudeep Gupta and Abhijit De. Society of Biological Chemists (SBC) Annual Meeting 2018-Mumbai Chapter held at Mumbai, 13th October 2018.

8. "A novel 'Phospho-STAT3 BRET' molecular sensor reveals non-canonical activation of STAT3 signaling in breast cancer." Shalini Dimri, Rohit Arora, Renu Malhotra, Tanuja Shet, Sudeep Gupta and Abhijit De. 7th Annual MPAI (Molecular Pathology Association of India) Meeting held at Mumbai, 12-13th January 2019 and received **best oral presentation award**.

Other Publications

Nishant Kumar Jain*, **Shalini Dimri***, Rajendra Prasad, Gayathri Ravichandran, V.G.M. Naidu, Abhijit De and Rohit Srivastava. Characteristics of molecularly engineered anticancer drug conjugated organic nanomicelles for site-selective cancer cell rupture and growth inhibition of tumor spheroids. (Manuscript Under Submission) (*Both the authors have contributed equally to the work)

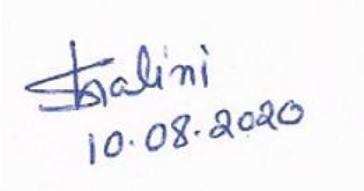

Ms. Shalini Dimri

Dedicated to my Mother and my elder Brother…

Acknowledgements

I would like to take this opportunity to acknowledge all those people who have supported and guided me through the entire duration of my Ph.D. journey.

First and foremost, I would like to sincerely acknowledge my supervisor Dr. Abhijit De for all his motivation and constant support throughout my Ph.D. work. I would like to sincerely express my heartfelt gratitude towards him for helping me to enhance my scientific skills to evolve as a good, honest and an independent researcher. He always knew how to encourage a student to bring the best of his/her research ideas from mind to benchwork and how to deal with excessive work pressure in a very flexible way. I would sincerely appreciate him for being a very humble, patient and down to earth person and for giving me the freedom to explore my scientific aptitude. I am extremely grateful that I got the opportunity to work in his lab and evolve both professionally and scientifically as a good researcher under his constant guidance.

I would like to extend my sincere gratitude towards ex- Directors Dr. Rajiv Sarin and Dr. S. V. Chipulnkar, present Director Dr. Sudeep Gupta and Deputy Director Dr. Prasanna Venkatraman for giving me the opportunity to pursue my Ph.D. study in ACTREC and for providing us with the wonderful infrastructure in the campus to work with.

I would express my heartfelt gratitude towards all the DC committee members; Dr. S.V. Chipulnkar (Chairperson), Dr. Prasanna Venkatraman, Dr. Sanjay Gupta, Dr. Sudeep Gupta; ex DC members Dr. Samit Chattopadhyay and Dr. Venugopal Bommireddy for their critical evaluation of the work, thorough scientific discussion and valuable suggestions in shaping my Ph.D. thesis work towards a right direction. I would like to specially acknowledge Dr. Pritha Ray, for all her valuable scientific inputs and constructive discussion during our scientific work presentations. I am extremely grateful to Dr. Tanuja Shet (TMH) and Ms. Smruti Mokal (TMH) for helping me with the clinical part of the study as a part of my thesis work.

I would like to acknowledge ACTREC for providing us with all the good infrastructure and staff members of common instrumentation facilities, Animal house unit, ACTREC molecular imaging facility, ACTREC digital imaging facility, Real Time PCR facility, genomics and flowcytometry facility for all their help and support during acquisition and analysis of the data. I am also thankful to library, administration, accounts department, purchase department and Student community of ACTREC for all their help and support. I

am thankful to ACTREC for providing me with the fellowship and Hostel facility during the entire duration of my Ph.D. work.

I am also grateful to HBNI, Sam Mistry and Patel Trust for providing me with the financial support for attending the international scientific conference – 25th EACR meeting at Amsterdam, Netherlands.

I would like to express my heartfelt gratitude towards all the past and present members of De lab. Having seniors like Dr. Sushmita, Dr. Madhura, Mr. Amir Ali and Mr. Rohit helped me a lot in learning new experiments and adapting to the lab environment very comfortably. I am extremely grateful to you, for all your support and help at scientific, professional and personal levels. I am also grateful to my juniors Sumit, Aaiyas, Arijit, Maitreyi, Pranay, Mansi and Chetna for developing and maintaining a very friendly and scientific environment in the lab. I am also thankful to Renu dee, Snehal, Gayathri and Jessica for helping me with various parts of my Ph.D. work. I would also like to thank past and current members of Ray lab; Dr. Ram, Dr. Snehal, Dr. Bhushan, Shubhoshree, Ajit, Aniketh, Abhilash, Shouvik, Pratham, Megha and Preeti for all their help and support.

I have been extremely lucky to have following people as my batchmates for Ph.D. journey; Dr. Ajay, Dr. Anuja, Dr. Vasudha, Asmita, Burhan, Dhanashree, Mahalakshmi, Mythreyi, Pravin, Ramchandra, Raghav, Raghupathi, Rahul, Rajashree, Raikamal and Shalaka. Every single day spent with you all is very special and has become a beautiful memory for lifetime. I am especially thankful to Ajay, Raghav, Pravin and Raikamal for being always there to support and encourage me during my tough days at work. Last but not the least, I am very grateful to my mother and my elder brother for the sacrifices they have made to help me achieve my dream. My journey would not have been complete without your unconditional love and support. Above all, I am and will always be grateful to God for looking after me every single day of my life.

Thank you all for your contributions.

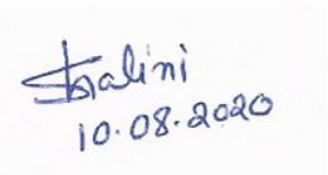

Ms. Shalini Dimri

TABLE OF CONTENTS

Synopsis

Homi Bhabha National Institute

SYNOPSIS OF Ph. D. THESIS

1. **Name of the Student:** Shalini Dimri
2. **Name of the Constituent Institution:** ACTREC, Tata Memorial Center
3. **Enrolment No.:** LIFE09201304001 (01.09.2013)
4. **Title of the Thesis:** Molecular Imaging of STAT3 Signaling *in vivo*
5. **Board of Studies:** Life Sciences

SYNOPSIS

Introduction

The Signal Transducers and activator of Transcription (STATs) is family of seven intracellular transcription factors, namely STAT1, STAT2, STAT3, STAT4, STAT 5a, STAT 5b and STAT6. The members of STAT family generally have a size ranging from 750-900 amino acids. Each member of STAT family has a conserved structure characterized by N-terminal domain, coiled-coiled domain (CC), central DNA binding domain (DBD), linker region, SH2 domain and a C-terminal transactivation domain (TAD)- comprising of Tyr705 and S727 residues (Turkson & Jove, 2000). STAT3, one of the important members of STAT family proteins, is a cytoplasmic factor that relays oncogenic signal from activated cytokine and growth factor receptor to nucleus where it regulates transcription of genes involved in various aspects of cancer progression like ; proliferation and cell survival- p53,Cyclin D1, Cyclin E1, migration/invasion- MMP9, MMP2, angiogenesis- VEGF,HIF-1-alpha, bFGF, immune evasion- IP-10,RANTES (Carpenter & Lo, 2014).

Activation of STAT3 pathway is detected by phosphorylation of its tyrosine residue (Y705) located on SH2 domain that leads to its dimerization, nuclear localization and transcriptional activation (canonical pathway)(Berishaj *et al*, 2007). For many years activation of STAT3 pathway has been ascribed based on phosphorylation status of tyrosine (Y705) residue of STAT3. Tumours expressing high levels of p-Y705 STAT3 were considered to be addicted to STAT3 oncogenic signaling while those expressing low levels or do not express pY705 do not rely majorly on STAT3 pathway (Zhang & Lai, 2014).

Recent studies have shown that activity of STAT3, either normal or oncogenic does not necessarily depend upon its Y705 phosphorylation status (Canonical pathway). Apart from phosphorylation of Y705 residue, STAT3 undergoes other post translational modifications like phosphorylation of S727 residue and acetylation of K685 residue on its C-terminus domain, that is equally important in gene activation (Noncanonical pathway)(Srivastava & DiGiovanni, 2016) function. Phosphorylation at S727 residue is known to activate transcription of target genes probably by interacting with different transcription co activators like CBP, cdk9 and SRC. There are number of emerging evidences that indicate that STAT3 via p-S727 can regulate cell survival and tumor growth independent of Y705 phosphorylation. For e.g. STAT3 phosphorylation on S727 has been reported in case of chronic lymphocytic leukaemia where it is required for cell survival functions even in the absence of Y705 phosphorylation (Hazan-Halevy *et al*, 2010), high levels of S727 phosphorylation has been detected in breast carcinoma which is independent of the Y705 phosphorylation status of the sample (Yeh *et al*, 2006), STAT3 phosphorylated on S727 and not on Y705 is required to induce transcription of DNA repair genes, upon treatment with irinotecan and oxaliplatin in colorectal cancer (Vigneron *et al*, 2008).

Upon cytokine stimulation STAT3 is known to undergo acetylation at K685 position via interaction with p300 and this acetylation is required for STAT3 to form stable dimers even in the absence of Y705 and S727 phosphorylation (Yuan *et al*, 2005). High levels of STAT3 K685 acetylation has been detected in colorectal cancer, melanoma and in ovarian cancer using immunohistochemistry(Li *et al*, 2013). Increased levels of K685 acetylation is associated with methylation of promoters of tumour suppressor genes e.g. p53 and increased tumour growth (Lee *et al*, 2012; Li *et al*, 2013). From these results it

seems that acetylation of K685 also plays a key role in STAT3 signaling apart from Y705 and S727 phosphorylation. Together, these studies indicate that different oncogenic PTM forms of STAT3 are present inside the cancer cells where they might be required for separate oncogenic programme. It is possible that these modifications might have different impacts on downstream cellular functions and therefore PTM specific therapy should be planned.

Considering the complexity of the STAT3 pathway (multiple receptors, variable ligands, differential PTM activation etc.), it is very much important to develop assay system that can delineate the molecular process and give true readout of the STAT3 signaling. Bioluminescence based BRET (Bioluminescence Resonance Energy Transfer) method is one such key approach. BRET is a highly sensitive assay for determining live cell protein-protein interactions. It is based on biophysical principle of resonance energy transfer, where non-radiative energy from excited donor-luciferase reaction is transferred to acceptor fluorophore located within a strict proximity of <10nm. When BRET is used for measuring protein dimerization, characteristic acceptor emission increases. BRET is essentially measured as a ratio of this acceptor signal over the bleed-through corrected donor signal, which increases as the proximity is achieved between the interacting proteins. With the potential applications of a BRET platform for precision measure of PTM specific dimerization and its competency for screening drug compounds using high-throughput live cell formats, we foresee the scope of developing and using a biosensor for measuring STAT3 PTM-specific *in vivo* modulations.

Rational & Objectives:

Based on evidences gathered from literature, it is evident that the classical canonical (pY705) PTM does not exclusively govern STAT3 signaling. The less known noncanonical (pS727 and K685ac) pathway can equally execute the activation and downstream biological functions of the STAT3 pathway. Despite numbers of compelling evidences, no reports are available to-date showing the interplay or cross-talk between the two signaling arms are simultaneous or segregated events. Whether pY705 activation precedes or depends upon pS727 and K685ac or vice versa, is still not clear. Further, with a few studies identifying transcriptional targets governed exclusively by the noncanonical activation, the possibility of PTM dependent transcriptional reprogramming of STAT3 is

also unknown. Thus, it is important to know if the classical targets of STAT3 (Cyclin D1, c-Myc, Socs3 etc.) are mutually regulated or there are separate set of PTM dependent oncogenic transcriptional program.

Based on the published data, independent expression of pS727 in the patient cancer tissue specimens are apparent in melanoma, chronic lymphocytic leukemia, glioblastoma, lung adenocarcinoma as well as in ER negative BC cases. However, the status of both pY705 and pS727 PTMs has not been reported in case of TNBCs. As *in vitro* studies have suggested important role of STAT3 signaling for survival of TNBC cells, it would be interesting and therapeutically important to investigate and identify whether canonical or noncanonical pathways operate individually or in coordination and mediate STAT3 function in this subtype of breast cancer.

STAT3 mediates its downstream function only after it forms a homodimer triggered by an extracellular ligand stimulus. Though pY705 mediated STAT3 dimerization is well documented, the role of pS727 and K685 is unclear to-date. Though in 2006 Yuan et.al. reported K685ac as key player in forming stable homodimer of STAT3, the role of pS727 or pY705 in combination with K685 were not tested. Along the line, development of an assay system is important so that individual or coordinated mode of operations via STAT3 PTMs can be distinguished and STAT3 activation from inside the live cells is possible. As none of the current assay systems provide such capacity, during this study a focus on developing a sensitive screening platform for STAT3 homodimerization is kept.

Hence to address the above issues related to STAT3 signaling, following objectives were designed:

1. ***To develop a molecular imaging guided experimental model to identify dynamic role of PTMs in STAT3 dimerization and transcriptional control over downstream genes.***

2. ***To identify the association of differentially regulated genes with different PTM status of STAT3.***

3. ***To study the association of STAT3 PTMs (e.g. Y705 and S727 phosphorylation as well as K685 acetylation) with respect to breast cancer outcome.***

Results:

Objective 1: To develop a molecular imaging guided experimental model to identify dynamic role of PTMs in STAT3 dimerization and transcriptional control over downstream genes

1.1 Development and optimization of Nluc-TurboFP based STAT3 Phospho BRET sensor

During this study, we plan to develop a molecular biosensor for STAT3 activation. We choose to use the newly established BRET platform in our laboratory, using Nanoluc as donor and TurboFP as acceptor, proven for its high specificity and feasibility of PPI detection from live cell environment. Fusion constructs of STAT3 with Nanoluc and TurboFP were established in both the orientations i.e. N-terminus and C-terminus. To demonstrate the activity of the STAT3 BRET sensor and to select the orientation in which the sensor works best with maximum amount of energy being transferred to the donor molecule we preformed BRET assay in two different cancer cell line models- HT1080 and PC3. HT1080 is a fibrosarcoma cell line with high STAT3 protein levels, whereas PC3 is a prostate cancer cell line reported to be null for STAT3 expression. HT1080 cells' expressing the STAT3 constructs in all the possible orientations i.e. Nluc-STAT3, Nluc-STAT3+TurboFP-STAT3, Nluc-STAT3+STAT3-TurboFP635, STAT3-Nluc, STAT3-Nluc+ STAT3-TurboFP635 and STAT3-Nluc+ TurboFP-STAT3 were treated with EGF in concentration ranging from 10-100ng/ml. Following ligand (EGF) addition a significant gain in BRET signal was observed for upto 60mins in all the four orientations tested. The spectral kinetics of BRET ratio in untreated versus EGF treated (10-100ng/ml) condition showed dimerization and activation of STAT3 with EGF trigger. However, of all the orientations tested we found that the gain obtained in BRET signal with N-terminally oriented Nluc/Turbo-STAT3 fusion was the highest (2.33mBu ±0.026, $p<0.01$). Also, in comparison to rest three orientations, only Nluc/Turbo-STAT3 showed ligand dependent increase in BRET signal.

To address whether endogenous pool of STAT3 has any effect on the BRET ratio, we performed similar experiment in STAT3 null PC3 cells **.**The activation kinetics of both HT1080 and PC3 cells remained same however the basal BRET ratio was high in PC3 cells (0.77mBu±0.002) as compared to HT1080 cells (0.42mBu±0.010) indicating that in

HT1080 cells the endogenous pool is able to compete with or quench a part of BRET STAT3 molecules. However, the difference in basal BRET ratio did not affect the maximum BRET signal achieved. Similar to HT1080, in PC3 cells also the N-terminus combination of Nluc/Turbo with STAT3 worked out best with maximum BRET ratio achieved upon EGF treatment (2.10 mBu±0.011, $p<0.01$) than rest of the combinations.

For performing the above BRET assay, both donor and acceptor plasmids fused to STAT3 were transiently co-expressed in the model cell line. To achieve higher BRET ratio, we engineered acceptor stable (TurboFP-STAT3 or STAT3-TurboFP) HT1080 cells. Similar to parental HT1080, in acceptor stables also a significantly higher BRET ratios obtained with Nluc/Turbo-STAT3 combination further confirmed the selected orientation (1.61mBu±0.036, $p<0.05$) as the most optimum dipole orientation for donor and acceptor to interact and transfer energy of excitation for efficient BRET signal

1.2 Validation of STAT3 Phospho BRET sensor across different cell lines and with variable STAT3 pathway ligands

Following optimization of Nluc-STAT3+TurboFP-STAT3 as most suitable BRET orientation, we next sought to validate the applicability of developed sensor to read activation of STAT3 pathway across different cancer types with multiple different ligands. To test verify this we overexpressed the STAT3 BRET sensor in multiple different cancer cell lines: MCF7, HT1080, PC3, A549 and MDA MB 231 and treated with two different ligands; IL6 and EGF. Irrespective of the cancer cell type and biological environment, the STAT3 phospho BRET sensor sensitively captured the activation phenomenon across all the tested cell lines (HT1080 [$p<0.01$], PC3 [$p<0.05$], MCF7 [$p<0.05$] and A549 [$p<0.01$]). Surprisingly, with two different ligands used, IL6 proved to be more potent as compared to EGF as it could achieve maximum activation signal with even 10-fold lower concentration than EGF. These observations indicate that the developed sensor can be extrapolated to any cell type for precise judgment of STAT3 pathway modulations

1.3 Determining the sensitivity and specificity of the STAT3 BRET sensor using potential STAT3 inhibitors and pathway blockers

Based on thorough validation of the developed STAT3 BRET sensor to determine the STAT3 pathway activation, we next questioned whether it can equally read the blockade of the pathway too. To determine this, we treated MCF7 cells stably expressing the STAT3 BRET sensor constructs with two potential STAT3 inhibitors; niclosamide and Stattic, at differential doses either with or without EGF. Over here, upon treatment of cells with either Niclosamide or Stattic did not change the basal BRET ratio, however upon stimulation with EGF, Niclosamide ($p<0.01$) continued to retain the inhibitory effect more strongly than Stattic ($p<0.05$). The inhibitory effect for both the drugs was seen in a dose dependent manner. Further immunoblotting for the activation levels of STAT3 and phospho forms confirmed the dual mode of inhibition for niclosamide (pY705 and pS727) while Stattic was majorly a pY705 blocker.

With EGF treatment an immediate increase is BRET signal was evidently seen. To strongly confirm that EGF mediated STAT3 phosphorylation, leads to homodimerization dependent gain in BRET signal, we used EGFR blocker. Prior treatment of MCF7 cells with EGFR blocking antibody showed a drastic decrease in BRET signal ($p<0.05$) despite giving EGF treatment. This result confirms that the gain obtained in BRET signal is a true representation of EGF-EGFR mediated STAT3 phosphorylation and activation event.

1.4 STAT3 Phospho-BRET sensor is high throughput compatible for screening STAT3 compound library

Based on successful development of STAT3 Phospho BRET system as a sensing model for STAT3 pathway modulation, we next sought to adapt it in a high throughput format as drug screening tool. For this, we seeded MCF7 cells genetically encoding STAT3 Phospho BRET sensor at a relatively 6-fold lesser adherent cell number in a 384 well plate. Upon treating the cells with a library of 12 different compounds at variable concentrations either in presence or absence of EGF gave significant results. From the BRET screen of compound library, we identified 6 drugs; Niclosamide, Stattic, Curcumin, Neratinib, ERK inhibitor and MS-275 with STAT3 inhibitory effect. Out of these 6 compounds, Neratinib, MS-275 and ERK inhibitors were newly identified candidates,

while curcumin, niclosamide and Stattic are previously known STAT3 inhibitors. Further, as compared to Stattic, niclosamide, curcumin, Neratinib and ERK inhibitor were found to be more potent ($p<0.01$) as they successfully attenuated the STAT3 activation upon EGF trigger. Of the remaining 6 drugs, three HDACi compounds (AR-42, Chidamide and CI-994) showed activation of STAT3 BRET sensor with EGF treatment ($p<0.01$). It is likely that these three HDACi compounds are increasing STAT3 activation by increasing overall acetylation of the genome, thereby increasing pool of STAT3 stimulators. The remaining three compounds Wortmannin (PI3K inhibitor), Fingolimod and Losartan (GPCRs inhibitors) are indirect inhibitors of STAT3 pathway that failed to retain the suppression of STAT3 activation upon EGF stimulation. Further, the corrected BRET signal captured from two different plate formats (96 vs. 384 well plate) were very similar indicating that the sensitivity of the developed biosensor is HTS compatible, requiring low number of cells, substrate or compound utility. To validate the findings from BRET inhibitor screen, we randomly selected 3 drugs; Stattic, Curcumin and Niclosamide, and treated MCF7 cells with differential doses for 24hrs. Upon immunoblotting, we found that both niclosamide and curcumin were able to inhibit the two phospho forms of STAT3 i.e. pY705 and pS727, while Stattic was only effective against pY705. These results from BRET screen justify that both niclosamide and curcumin are more effective as STAT3 inhibitor than Stattic. Collectively these results also implicate the high-throughput compatibility of the developed biosensor with potential for PTM target-specific drug screening.

Objective 2: To identify the association of differentially regulated genes with different PTM status of STAT3

2.1 Noncanonical pS727 PTM can independently drive STAT3 activation and cell survival functions

In order to understand how the three different PTM marks (pY705, pS727 and K685ac), regulate STAT3 activation and signaling independently, we engineered 3’UTR STAT3 knockdown MCF7 cells with stable overexpression of individual STAT3 PTM mutants i.e. Wt, Y705F, S727A and K685R, fused to nanoluc reporter gene. Upon stable overexpression and treatment with IL6 or EGF as ligand, we observed that both pS727

and pY705 activation can take place independently while K685ac requires prior pS727 activation.

STAT3 is a key signaling molecule that controls cell growth and proliferation under both normal and oncogenic conditions. To investigate how the loss of different PTM marks on STAT3 can affect cell proliferation, EdU incorporation assay was performed with STAT3 PTM mutant expressing cells. Loss of noncanonical activation marks (S727A and K685R) led to a significant decrease in proliferation ability of MCF7 ($p<0.01$) cells as compared to Wt or Y705F expression clones. The decrease in proliferation ability was also visible in clonogenic potential of the cells where both K685R and S727A mutants exhibited reduced number of colonies ($p<0.01$ and 0.05 respectively) of very small size (less than 25 cells). These results clearly indicate that non-canonical (pS727 and K685ac) pathway of STAT3 activation majorly controls proliferation and cell survival functions in breast cancer cells.

2.2 Noncanonical and canonical STAT3 activation exerts differential transcriptional effect on downstream STAT3 targets

To judge how the differential PTM status of STAT3 can control its transcriptional preference, the expression level of three known direct targets of STAT3- Cyclin D1, TWIST1 and SOCS3 was analyzed using quantitative real time PCR in all the STAT3 point mutants. Both TWIST1 and SOCS3 showed significantly enhanced expression ($p<0.05$) in Nluc-STAT3 (Wt) overexpression clone while their mRNA level decreased significantly in all three mutants (Y705F, S727A and K685R). Cyclin D1 levels majorly remain unchanged in both Wt and mutant background. This indicates that TWIST1 and SOCS3 expression requires the presence of all the three activation marks on STAT3 while Cyclin D1 levels can be maintained even if one of the STAT3 activation site is present. As a novel targets Her2 and ERα showed differential expression pattern in different STAT3 mutant clones. A significant decrease in the expression level of ERα was observed at protein level in K685R mutants expressing cells. Her2 expression was unaltered in either Wt or Y705F mutant while it increased significantly in S727A and K685R clones as observed with membrane staining in FACS and Immunofluorescence

assay. These results indicate that the non-canonical arm of STAT3 can regulate expression of Her2 and ERα (either directly or indirectly) in breast cancer cells.

2.3 pS727 activation is essential for stable homodimer formation in STAT3

Dimerization is a rate limiting step controlling STAT3 signaling. To elucidate how the different PTM marks of STAT3 can regulate its dimerization ability we made use of the STAT3 phospho BRET sensor developed in objective 1. A library of STAT3 PTM mutants for individual residue i.e. Y705, S727 and K685 was developed either in alone or in combination using site directed mutagenesis. A total of 8 such mutant combinations were developed. Upon testing these mutants in BRET platform using IL6 and EGF as ligands, we found that with the loss of S727 activation (S727A) a significant decrease is observed in the BRET activation signal ($P<0.001$). The decrease became more prominent in background of Y705 or K685 loss either alone or in combination. While individual point mutants of Y705F and K685R showed activation signal gain similar to wild type. The observations from BRET assay were further validated through pull down study where S727A mutants showed 2-fold lower stable homodimer formation ability as compared Wt, Y705F or K685R clones. In conclusion, these observations strongly confirm that noncanonical pS727 activation is essential for stable STAT3 homodimerization and signaling.

Objective 3: To study the association of STAT3 PTMs (e.g. Y705 and S727 phosphorylation as well as K685 acetylation) with respect to breast cancer outcome

3.1 Non canonical pS727 STAT3 activation predominates over canonical pY705 arm in TNBC cohort

Previous reports have highlighted significant role of STAT3 in controlling growth of triple negative breast cancer tumours (Qin *et al*, 2019). To investigate which pathway of STAT3 activation predominates in TNBCs, IHC analysis for total STAT3, pS727 and pY705 forms was performed in 76 TNBCs core biopsy and paired post NACT tumour tissues. Pathologist based Allred scoring method (Allred score 0-4= negative, 5-8= positive) showed that total STAT3 was present in more than 86% (66/76) of cases which

was constitutively phosphorylated at pS727 residue in more than 90% (70/76) cases. In comparison pY705 was present only in 15% (12/76) of STAT3 positive cases ($p<0.001$). Furthermore, IHC staining for both total and pS727 STAT3 showed intense to moderate nuclear staining while pY705 was either negative or low positive with cytoplasmic localization. The observations made using Allred scoring method was paralleled with digital scoring of the DAB stain using IHC profiler plug-in of imageJ software. Digital scoring method clearly indicated that majority of the TNBC cases had strong nuclear STAT3 expression (2+ to 3+ score) with predominate pS727 positivity (2+ to 3+ score) while pY705 was majorly absent or had weak positive score (0, 1+). In paired post NACT specimens the expression of total STAT3, pS727 and pY705 STAT3 decreased significantly from 86.2% to 63.2% ($p<0.001$), 92.1% to 64.4% ($p<0.001$) and 15.8% to 3.4% respectively, after chemotherapy as analyzed with both Allred and IHC profiler scoring. Furthermore, by performing correlation analysis of total STAT3 with pS727 or pY705 independently in both core biopsy and post NACT specimens, a significantly strong to moderate positive association ($r=0.4987$, $p<0.0005$) between pS727 and total STAT3 expression was obtained. While, pY705 showed insignificantly low positive correlation ($r=0.2086$, $p<0.$ 0.0808) with total STAT3 expression. These observations clearly suggest that pS727 mediated activation of STAT3 is the major pathway that is present in TNBCs as compared to classical pY705 activation.

When the expression pattern of total STAT3, pS727, pY705 was correlated with clinicopathological parameters, a positive association of pS727 STAT3 expression was observed with apoptosis ($p<0.001$) and necrosis ($p<0.017$) in core biopsy specimens. Both total STAT3 and pS727 also showed positive correlation with mitotic score in core biopsy ($p<0.001$) as well as paired NACT samples ($p<0.017$, $p<0.008$). Lymphocytic infiltration was found to be high in post NACT cases with high STAT3, pS727 and pY705 expression ($p=0.010$, 0.004 and 0.044 respectively). A chi-square test of independence was also performed to examine the relationship between STAT3, pS727 and pY705 score and response status after NACT. No significant difference in total and phospho forms of STAT3 expression was observed with respect to the pathological response post adjuvant chemotherapy. However, based on medical case records, cases with high STAT3 score or positive cases (89.58%) tend to have an incomplete response when compared with STAT3 negative cases (61.11%). No such observations of response

status post NCAT was found for pS727 and pY705 expression. Also, no significant difference in the expression of STAT3, pS727 and pY705 was observed with respect to age, menopausal status or stromal fibrosis in both before and after chemotherapy specimens.

3.2 STAT3 signaling is essential for growth, survival as well as maintenance of stem cell population in TNBC cell lines

To investigate the role of STAT3 signaling in triple negative breast cancer as observed in above IHC results, stable STAT3 knockdown (KD) MDA MB 231 cells were engineered using 3'UTR shRNA approach. STAT3 knockdown population was enriched with consecutive GFP sorting and the depletion of STAT3 along with activated forms (pY705, pS727 and K685ac) was confirmed using immunoblotting. Over here with loss of STAT3 expression in MDA MB 231 cells a significantly reduced cell proliferation was observed in KD population as compared to parent counterpart ($p<0.01$). Knockdown of STAT3 not only reduced the number of colonies formed during colony formation assay but the size of the colonies formed was also appreciably smaller ($p<0.01$). Furthermore, the anchorage independent growth assessed with soft agar colony formation assay also showed more than 50% reduction ($p<0.01$) in overall colony formation ability of the STAT3 knockdown cells. The effect of STAT3 loss was also observed in $CD44^{+}/CD24^{-or\ low}$ population of MDA MB231 cells. A significant shift from $CD44^{+}/CD24^{-or\ low}$ (79% in parent cells) to $CD44^{-/low}/CD24^{+/high}$ (73.9% in STAT3 knockdown cells) population was observed upon STAT3 depletion. Along with decrease in $CD44^{+}/CD24^{-or\ low}$ pool, STAT3 loss also led to a significant reduction in the mRNA expression of stem cell markers like Oct4 ($p<0.05$) and Sox2 ($p<0.01$). These results indicate that STAT3 expression is very crucial for survival and tumorigenesis potential of TNBC cells along with the maintenance of stem cells pool.

3.3 Niclosamide exhibits excellent anticancer activity against TNBC both *in vitro* and *in vivo*

Based on results from patient data and in vitro experiments, it is evident that noncanonical STAT3 activation is essential for TNBCs. Hence chemotherapeutic approaches targeting the noncanonical pathway are essential for treating this subtype of breast cancer. From our study, we have shown that as compared to Stattic, well know

STAT3 inhibitor, Niclosamide is more potent as it sufficiently blocks both pS727 and pY705 activation marks with complete STAT3 blockade and enhanced cell killing in vitro. To further validate the anticancer efficacy of niclosamide *in vivo*, we developed an orthotopic tumour xenograft model using luciferase labelled MDA MB231-Luc-D3H2LN cells. When the tumours attained approximate size of $100mm^{3,}$ mice were randomly segregated into two groups; vehicle control (n=3) and treatment (50mg/kg, n=3). Growth of primary tumour from luciferase labelled MDA MB 231-Luc cells was monitored using non-invasive BLI (bioluminescence) imaging at every 7^{th} day of the treatment. Over here mice receiving 50mg/kg niclosamide consecutively for 21 days via intraperitoneal route showed significant inhibition in tumour growth as compared to the vehicle control group ($p<0.001$)**.** Reported to be highly metastatic and aggressive in nature we also monitored metastatic spread to other organs. Ex vivo BLI imaging of nearest thigh bone (femur) from the same side as that of primary tumour showed no bone metastasis with niclosamide treatment. While, as compared to control group, lung metastasis in response to niclosamide administration though not completely blocked but was significantly reduced. The body weight of both control and treatment group however did not change much throughout the treatment phase. Collectively these results confirm the efficacy of niclosamide as potent drug inhibitor against TNBCs both *in vitro* and *in vivo*.

Conclusion

STAT3 signaling is reported to be upregulated in majority of primary tumours and cancer cell lines. Classical approach for presence or absence of canonical pY705 activation mark is still used as stratification criteria for STAT3 based therapeutic approaches. However, with the identification of an alternate noncanonical (pS727 and K685ac) activation mechanism, the clinical paradigm of terming pY705 as sole activation mark for STAT3 pathway is changing. The present study here carefully demonstrates the role and functions of the two STAT3 activation arms and how they can be targeted effectively in a subset of breast cancer.

To better inhibit the STAT3 pathway, it is important to decipher the biology of STAT3 activation from natural biological environment. However, so far there are no sensor-based approaches available that can determine the STAT3 pathway modulation in real time manner from live cells. Hence this study for the first time reports the development of

phosphorylation driven STAT3 homodimerization BRET sensor. STAT3 fused to Nanoluc as donor and TurboFP as acceptor at the C-terminus very precisely demonstrated the EGF mediated STAT3 activation in a time dependent manner. Additionally, the biosensor very sensitively detected the modulation of STAT3 pathway even across different cancer cell type (HT1080, PC3, A549, MCF7) and with variable pathway ligands. Adapting to a high throughput screening platform, the BRET biosensor clearly identified the potential activators (AR42, CI-994 and Chidamide) and inhibitors (Curcumin, Niclosamide, ERK inhibitor and MS-275) of the STAT3 pathway. Of which, Niclosamide being dual blocker (pY705 and pS727) was found to be more potent STAT3 inhibitor than previously known Stattic compound, which can only block pY705 phospho- activation mark.

To determine how the two signaling arms (canonical and noncanonical) govern STAT3 activation and molecular functions in breast cancer, we engineered 3'UTR STAT3 knocked down MCF7 cells, in which stable over expression of either wild type or point mutants of STAT3 PTMs (Y705F, S727A and K685R) were introduced. Over here we found that both canonical (pY705) and noncanonical (pS727 and K685R) activations can operate independently while pS727 PTM mark necessarily cooperate with K685ac. With differential downstream transcriptional execution, both pS727 and K685ac were identified to play a dominant and essential role in controlling proliferation and cell survival functions in BC cells over canonical pY705 PTM. Further taking advantage of the Phospho BRET sensor developed, we constructed a library of STAT3 clones harboring mutation in individual PTM residue either alone or in combinations and subjected them to BRET platform in presence or absence of ligands (IL6 and EGF). Collective observation form all the mutants screened, identified pS727 and not Y705, as key residue required for stable STAT3 homodimer formation in breast cancer cells.

Intrigued by the dominant role played by noncanonical pS727 activation in governing STAT3 homodimerization and downstream biological functions *in vitro* in breast cancer cells, we next decided to explore whether the same situation prevails even in clinical scenario. To determine this, we performed retrospective analysis for pY705, pS727 and total STAT3 expression in 76 core biopsy and paired post NACT TNBC cases. Quantitative assessment for the IHC DAB staining with two different scoring methods

identified pS727 (more than 90% positive cases) as predominant STAT3 PTM form present over pY705 (less than 15% positive cases). Also, the cases positive for total STAT3 showed moderate to strong positive Pearson correlation value with pS727 PTM mark while it was low positive for pY705 STAT3. These observations made from patient samples were in accordance with the *in vitro* data and identified noncanonical pS727 pathway as key mode of operation for STAT3 functions in TNBCs. With the aberrant activation of STAT3 signaling seen in TNBCs, as expected, knocking down its expression in MDA MB 231 cells (TNBC cell line) led to a significant decrease in cell proliferation, survival, and tumorigenic potential along with depletion in $CD44^{high}/CD24^{low}$ like stem cell pool. Based on clinical and *in vitro* data it is evident that STAT3 pathway is essential for survival of TNBCs. Hence to therapeutically target TNBC, we developed *in vivo* tumour xenograft model using reporter labelled MDA MB 231cells and treated the mice with, dual STAT3 blocker Niclosamide (as identified from the BRET inhibitor screen) inhibitor. With potent STAT3 inhibitory functions Niclosamide treatment not only retarded the primary tumour growth but it significantly reduced the metastasis to distant organs like lungs and bones.

In summary, based on experimental and clinical data gathered during the study, here for the first time we report that noncanonical pS727, but not the canonical pY705, is the key PTM driving major STAT3 activation and functions in TNBC subtype of breast cancer. We have further demonstrated that pS727 STAT3 PTM operates independently and is crucial requirement for STAT3 homodimerization, activation and downstream oncogenic functions in breast cancer cells. As a therapeutic target, Niclosamide, a repurposed anti-helminthic drug, is demonstrated as dual blocker of phospho-STAT3 (pY705 and pS727) and thus act with enhanced anti-cancer activity than Stattic (which specifically block pY705 only) both *in vitro* and *in vivo* condition. Finally, with the robust drug screening platform developed using Phospho-STAT3 BRET sensor, the way for comprehensive analysis of STAT3 signaling is paved and in future it is expected to provide with an opportunity to screen large combinatorial anti-STAT3 drug libraries using live cell across multiple cancer types.

References:

Berishaj, M., S. P. Gao, S. Ahmed, K. Leslie, H. Al-Ahmadie, W. L. Gerald, W. Bornmann & J. F. Bromberg (2007) Stat3 is tyrosine-phosphorylated through the interleukin-6/glycoprotein 130/Janus kinase pathway in breast cancer. *Breast Cancer Res,* 9**,** R32.

Carpenter, R. L. & H. W. Lo (2014) STAT3 Target Genes Relevant to Human Cancers. *Cancers (Basel),* 6**,** 897-925.

Hazan-Halevy, I., D. Harris, Z. Liu, J. Liu, P. Li, X. Chen, S. Shanker, A. Ferrajoli, M. J. Keating & Z. Estrov (2010) STAT3 is constitutively phosphorylated on serine 727 residues, binds DNA, and activates transcription in CLL cells. *Blood,* 115**,** 2852-63.

Lee, H., P. Zhang, A. Herrmann, C. Yang, H. Xin, Z. Wang, D. S. Hoon, S. J. Forman, R. Jove, A. D. Riggs & H. Yu (2012) Acetylated STAT3 is crucial for methylation of tumor-suppressor gene promoters and inhibition by resveratrol results in demethylation. *Proc Natl Acad Sci U S A,* 109**,** 7765-9.

Li, J., G. Cui, L. Sun, S. J. Wang, Y. L. Li, Y. G. Meng, Z. Guan, W. S. Fan, L. A. Li, Y. Z. Yang, Y. Q. You, X. Y. Fu, Z. F. Yan & K. Huang (2013) STAT3 acetylation-induced promoter methylation is associated with downregulation of the ARHI tumor-suppressor gene in ovarian cancer. *Oncol Rep,* 30**,** 165-70.

Qin, J. J., L. Yan, J. Zhang & W. D. Zhang (2019) STAT3 as a potential therapeutic target in triple negative breast cancer: a systematic review. *J Exp Clin Cancer Res,* 38**,** 195.

Srivastava, J. & J. DiGiovanni (2016) Non-canonical Stat3 signaling in cancer. *Mol Carcinog,* 55**,** 1889-1898.

Turkson, J. & R. Jove (2000) STAT proteins: novel molecular targets for cancer drug discovery. *Oncogene,* 19**,** 6613-26.

Vigneron, A., E. Gamelin & O. Coqueret (2008) The EGFR-STAT3 oncogenic pathway up-regulates the Eme1 endonuclease to reduce DNA damage after topoisomerase I inhibition. *Cancer Res,* 68**,** 815-25.

Yeh, Y. T., F. Ou-Yang, I. F. Chen, S. F. Yang, Y. Y. Wang, H. Y. Chuang, J. H. Su, M. F. Hou & S. S. Yuan (2006) STAT3 ser727 phosphorylation and its association with negative estrogen receptor status in breast infiltrating ductal carcinoma. *Int J Cancer,* 118**,** 2943-7.

Yuan, Z. L., Y. J. Guan, D. Chatterjee & Y. E. Chin (2005) Stat3 dimerization regulated by reversible acetylation of a single lysine residue. *Science,* 307**,** 269-73.

Zhang, H. F. & R. Lai (2014) STAT3 in Cancer-Friend or Foe? *Cancers (Basel),* 6**,** 1408-40.

Publications in Refereed Journal:

a. Published: **Shalini Dimri**, Rohit Arora, Akshi Jasani and Abhijit De. Dynamic monitoring of STAT3 activation in live cells using a novel STAT3 Phospho-BRET sensor. American Journal of Nuclear Medicine and Molecular Imaging, 2019;9(6):321-334.

b. Accepted: NA

c. Under Preparation: **Shalini Dimri**, Renu Malhotra, Tanuja Shet, Smruti Mokal, Sudeep Gupta and Abhijit De. Noncanonical pS727 post translational modification dictates major STAT3 activation and downstream functions in breast cancer. [Manuscript under Revision- Experimental Cell Research]

Patents:

Provisional Indian Patent application filed with BCIL: "A Method for Detection of Protein Activation Using Phospho-BRET Imaging Sensor and Methods Thereof" (Ref. # **201921010208**; filed on March 15, 2019).

Other Publications:

a. Book Chapter/Review Article

1. Shalini Dimri, Soumya Basu and Abhijit De, Use of BRET to Study Protein–Protein Interactions in vitro. *In*. The nuclear receptor superfamily, edited by Iain J. McEwan. Methods in Molecular Biology, Springer, New York 2016; 1443:57-78. **[Book Chapter]**

2. Shalini Dimri, Sukanya and Abhijit De, approaching non-canonical STAT3 signaling to redefine cancer therapeutic strategy. Integrative Molecular Medicine, 2017 4(1): 1-10. **[Review Article]**

b. Conference/Symposium

1. Attended and actively participated in workshop on- "Basic Course in Flow Cytometry-II-Hands on workshop" organized by Mumbai immunology group at ACTREC (10-11 July 2014).

2. 39th All India cell biology conference (AICBC)-cellular organization and dynamics held in Thiruvananthapuram, Kerala, 06-08th December 2015.

3. 11th National Research Scholars meet in Life Sciences held in ACTREC, Mumbai, 17-18th December 2015 and received **second best poster award**.

4. 75th TMC platinum jubilee "A Conference of New Ideas in Cancer: Challenging Dogmas" held in Mumbai, 26-28th February 2016.

5. International Congress of Cell Biology- "The Dynamic Cell- From molecules and Networks to form and function held at Hyderabad, 27th-31st January,2018.

6. 25th Biennial Congress of the European Association for Cancer Research (EACR25) held at Amsterdam, Netherlands, 30th June – 03rd July 2018.

7. Society of Biological Chemists (SBC) Annual Meeting 2018- Mumbai Chapter held at Mumbai, 13th October 2018.

8. 7th Annual MPAI (Molecular Pathology Association of India) Meeting held at Mumbai, 12th-13th January 2019 and received **best oral presentation award**.

Signature of Student: Shalini

Date: 10.01.2020

Doctoral Committee:

S. No.	Name	Designation	Signature	Date
1.	Dr. Shubhada V. Chiplunkar	Chairman	S.Chiplunkar	10/01/2020
2.	Dr. Abhijit De	Guide	Abhijit De	10-01-2020
3.	Dr. Prasanna Venkataraman	Member	V. Prasanna	10-01-2020
4.	Dr. Sanjay Gupta	Member	Sanjay	10-01-2020
5.	Dr. Sudeep Gupta	Invitee	Sudeep	14-JAN-2020

Forwarded Through:

S.Chiplunkar 23/1/2020

Prof. S.V. Chiplunkar,
Chairperson, Academic &
Training Programme, ACTREC

(Prof. Dr. S. V. Chiplunkar)
Chairperson, Academic &
Training Programme , ACTREC

27/1/2020

Prof. S. D. Banavali,
Dean (Academics)
T.M.C.

PROF. S. D. BANAVALI, MD
DEAN (ACADEMICS)
TATA MEMORIAL CENTRE
MUMBAI – 400 012.

Chapter 1

Introduction and Review of Literatures

Introduction

1.1 STAT Family Protein

Signal Transducers and activator of transcription (STAT) proteins were initially identified as cytoplasmic transcription factors that mediate their cellular response in treatment to cytokines or growth factors (Darnell, 1997; Darnell *et al*, 1994). Till date, the STAT family comprises of seven different members, namely STAT1, STAT2, STAT3, STAT4, STAT5a/5b and STAT6 (Leonard & O'Shea, 1998). In general the members of STAT family are 750-800 amino acid long and comprises of six conserved domains in the structure; N-terminal domain comprising of 3 alpha helices is required for STAT3 to interact with DNA and translocate to nucleus; CCD (coiled coil domain) interacts with regulatory proteins; DNA binding domain interacts with specific enhancer regions of STAT3 target gene promoters; Linker domain for stabilising DNA binding; SH2 domain contains Tyrosine-residue that is phosphorylated by activated receptor (pY) and it is also involved in reciprocal interaction of pY and SH2 domain on opposite STAT3 dimers and a C-terminal transactivation domain (TAD) comprises of conserved Tyrosine and Serine residue that gets phosphorylated upon STAT3 activation, it is also involved in intramolecular CCD and SH2 domain interaction to enhance binding to receptor (Kiu & Nicholson, 2012; Schindler *et al*, 2007). While activation of STAT 1, 2, 4 and 6 is induced in response to specific cytokines or interferons, both STAT3 and 5 can be activated by multiple other ligands (Murray, 2007) **(Figure 1.1)**.

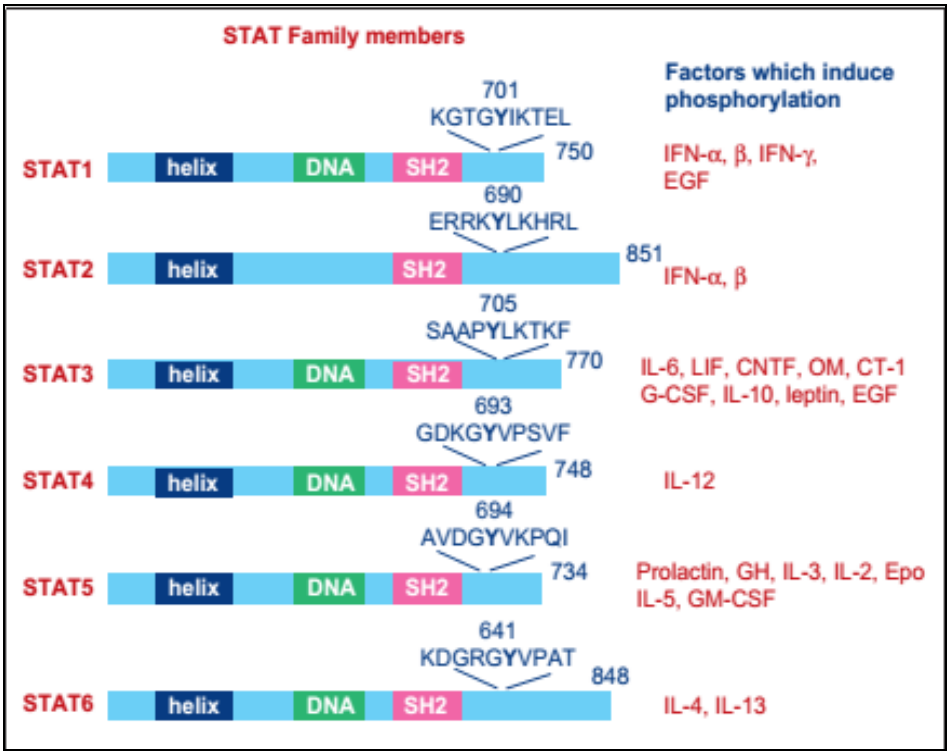

Figure 1.1. Domain organization and stimulating ligands of STAT family proteins (Akira, 1999).

Members of STAT family are known to be activated by receptors either with or without intrinsic tyrosine kinases activity (RTK). RTKs with intrinsic tyrosine activity involves EGFR, PDGF-R, colony stimulating factor-1 receptor (CSF-1R) and GPCRs such as angiotensin II receptor and serotonin 5-HT2A receptor (O'Shea *et al*, 2002; Schindler *et al*, 2007). Investigations on transcriptional response of STAT protein to interferons led to identification of Janus Kinase – STAT signaling pathway. JAKs are group of receptors associated cytoplasmic tyrosine kinases that plays a critical role in phosphorylation of STAT at tyr residue. There are currently four members in this nonreceptor protein kinase family; JAK1, JAK2, JAK3 and TYK2 that possess intrinsic kinase activity (Imada & Leonard, 2000; Leonard & O'Shea, 1998).

The basic mechanism by which the members of STAT family are activated is as follows, in the inactive state, STAT proteins lie majorly in the cytoplasm while JAK kinases remain bound to the cytoplasmic region of the receptor. Upon ligand stimulation, JAK kinases

become catalytically active and phosphorylate the receptor, this leads to recruitment of cytoplasmic STAT protein to the activated receptor. Once bound to receptor, the activated JAK kinases then phosphorylate STAT at tyrosine residue. Thereafter, the phosphorylated STAT dissociates from the receptor and either in the form of a heterodimer or homodimer it translocates to nucleus and regulate expression of its target genes by binding to STAT consensus sequence in the promoter region (Kiu & Nicholson, 2012; Vinkemeier *et al*, 1996). STAT1, STAT3, STAT4, STAT5 and STAT6 majorly form homodimer complexes, while STAT1 and 3 can for heterodimers as well. STAT2 primarily forms heterotrimer complex with STAT1 and interferon regulatory factor 9 (IRF9) but it can also act independent of STAT1 **(Figure 1.2)** (Copeland *et al*, 1995).

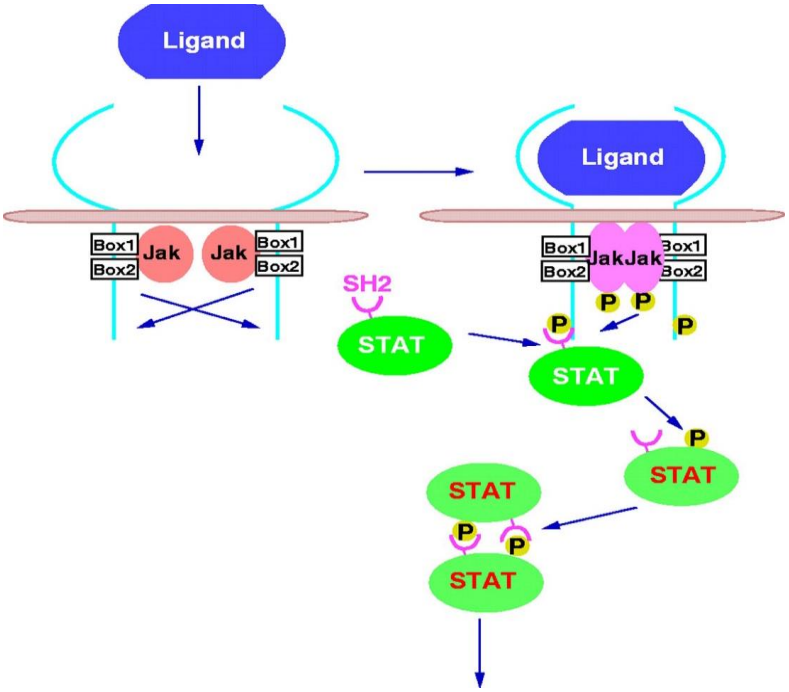

Figure 1.2. Basic mechanism for ligand mediated activation of STAT family proteins. *Upon ligand binding, the receptor homodimerizes followed by autophosphorylation of receptor by JAK kinases and cross phosphorylation of STAT protein. Following phosphorylation, two STAT monomers dissociate from receptor , dimerize and translocates to nucleus to works as a transcription factor (Akira, 1999).*

Members of STAT family play an important role in many biological processes including immunity, haematopoiesis and embryonic development. While a deregulated STAT signaling leads to chronic inflammation and various malignant progression like blood malignancies (lymphomas or leukaemia) or solid tumours (breast cancer, prostate cancer etc.). The primary role of individual STAT family member was identified based on specific knockout (KO) mouse model system **(Table 1.1) (Akira, 1999)**.

Targeted gene	Phenotype
STAT1	Compromised innate response to microbial pathogens and viruses.
STAT2	Increased susceptibility to viral infection and a loss of biological response to type I IFN.
STAT3	Early embryonic lethality.
STAT4	Impaired natural killer cell cytotoxicity and Th1 cell response.
STAT5a and 5b	No mammary gland development or lactogenesis.
STAT6	No Th2 cells development.

Table 1.1. Table summarising the phenotypic effect of individual STAT protein loss in mouse model (Kamran et al, 2013).

STAT1 plays critical role in controlling Type I and Type II interferons mediated biological responses (Durbin *et al*, 1996; Shuai *et al*, 1992).

STAT4 is essential for IL-12 dependent functions like cell proliferation, enhancement of natural killer cell cytotoxicity, production of IFN-γ and Th1 cell differentiation (Kaplan *et al*, 1996; Thierfelder *et al*, 1996).

STAT6 controls IL-4 mediated responses like class switching to IgE, T- and B-Cell proliferation, induction of MHC class II, CD23 and Th2 cell development (Shimoda *et al*, 1996; Takeda *et al*, 1996).

STAT 5 consists of two isoforms STAT5a and 5b, which resulted from gene duplication event and share more than 96% amino acid sequence similarity (Teglund *et al*, 1998). STAT 5a KO led to impairment of mammary lobuloalveolar outgrowth (Liu *et al*, 1997) while loss of STAT 5b led to sexually dimorphic pattern of pituitary growth hormone secretion (Udy *et al*, 1997).

STAT3 KO mice died embryonically at day E6.5–7.5, indicating role of STAT3 in early embryonic development (Takeda *et al*, 1997). The role of STAT3 was further investigated using dominant negative STAT3 mutant (DN). Overexpression of STAT3 DN in myeloid leukemic M1 cells led to abolished response to IL6 or LIF (Boeuf *et al*, 1997). STAT3 is also important for IL6 or IF mediated cortical neuroepithelial cells differentiation (Bonni *et al*, 1997). STAT3 deficiency in adult mice led to impaired IL6 mediated T-cell proliferation. STAT3 loss in macrophages and neutrophils led to endotoxin shock and enhanced production of inflammatory cytokines such as IL-1, TNF-α and INF-γ. Further STAT3 expression loss in skin cells led to impaired skin wound healing and reduced motility of epidermal cells in culture condition (Takeda *et al*, 1998). Taken together, STAT3 was identified as important member in STAT family that controls variety of biological functions including cell growth, proliferation depending upon cell type and stimulus.

1.2 Signal Transducer and Activator of Transcription 3 (STAT3)

STAT3, the third member of STAT family (in chronology) was initially identified as acute phase response factor (APRF) that gets rapidly activated in response to IL6 (Wegenka *et al*,

1993). Zhong et.al in 1994, identified STAT3 from a cDNA library screen for proteins that bind to DNA in response to IL6 treatment (Zhong *et al*, 1994). Subsequently Akira et.al in 1994 purified and cloned APRF gene and showed binding of APRF to IL6 responsive elements of acute phase genes promoters (Akira *et al*, 1994). Role of STAT3 in oncogenesis came forward with initial transformation studies using v-src oncoprotein. In 1996, Cao et.al. reported that STAT3 is constitutively active in v-src transformed cell lines (Cao *et al*, 1996; Yu *et al*, 1995). In 1998, Bromberg et.al. reported that STAT3 activation is essential for oncogenic transformation mediated by v-src (Bromberg *et al*, 1998; Bromberg *et al*, 1999; Turkson *et al*, 1999).

STAT3 gene located on chromosome 17q21.31 has four different isoforms STAT3 α, β, γ and δ (Choi *et al*, 1996). STAT3 α is the most predominantly expressed isoform with an average length of about 770 amino acids and molecular weight of 88KDa (Maritano *et al*, 2004). All major functions ascribed to STAT3 are performed by the STAT3α isoform. Structural organization of STAT3 is similar to other members of STAT family. It also consists of an N-terminal domain, DNA binding domain, Coiled-coil domain, Src-homology domain (SH2) and a C-terminal transactivation domain **(Figure 1.3)** (Ren *et al*, 2008). The N-terminal domain forms an interface for dimer-dimer interaction during gene transcription. The SH2 domain contain three sites that are solvent accessible sub pockets which plays an important role in stabilizing the STAT3-STAT3 dimer and STAT3-receptor interaction. DNA binding domain offers interface for DNA-protein interaction so that STAT3 can interact with DNA to proceed with gene transcription functions (Vinkemeier *et al*, 1996; Xu *et al*, 1996).

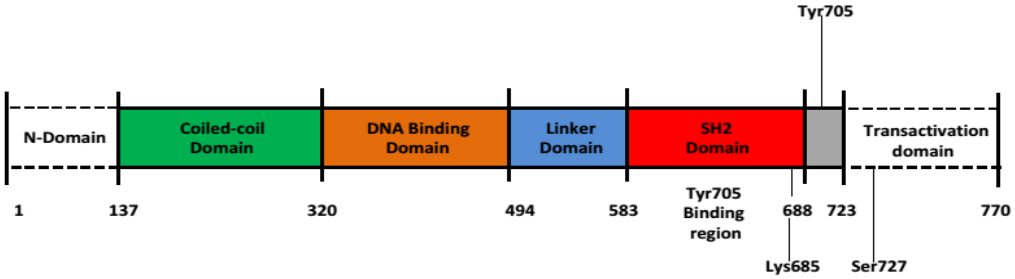

Figure 1.3. Domain organization of STAT3 protein (Wake & Watson, 2015).

STAT3 activation can be driven either by cytokine mediated activation of gp130-JAK complex or growth factors mediated receptor tyrosine kinases activation. In either case upon ligand binding to the receptor, the receptor undergoes a conformational change and dimerizes (Berclaz *et al*, 2001). During this process, the pTyr residue in the SH2 domain of receptor gets phosphorylated either by intrinsic tyrosine kinase activity or due to associated JAK kinases. Upon receptor activation, the monomeric STAT3 from the cytoplasm gets recruited to the receptor via STAT3 SH2-domain and pTyr residue -receptor interaction, this leads to phosphorylation of Y705 residue in the c-terminal domain of STAT3. Following phosphorylation, STAT3 dissociates from the receptor and dimerizes with another pY705-STAT3 residue in a pTyr-SH2 domain interaction fashion on the opposite monomer. The dimeric STAT3 than translocates to nucleus and initiate transcription of genes involved in various biological process and oncogenic growth of the cells (Hemmann *et al*, 1996) **(Figure 1.4)**. STAT3 is known to either form homodimer or heterodimerize with STAT1 due to high sequence similarity. This eventually enhances the number of genes under its transcription (Ho & Ivashkiv, 2006).

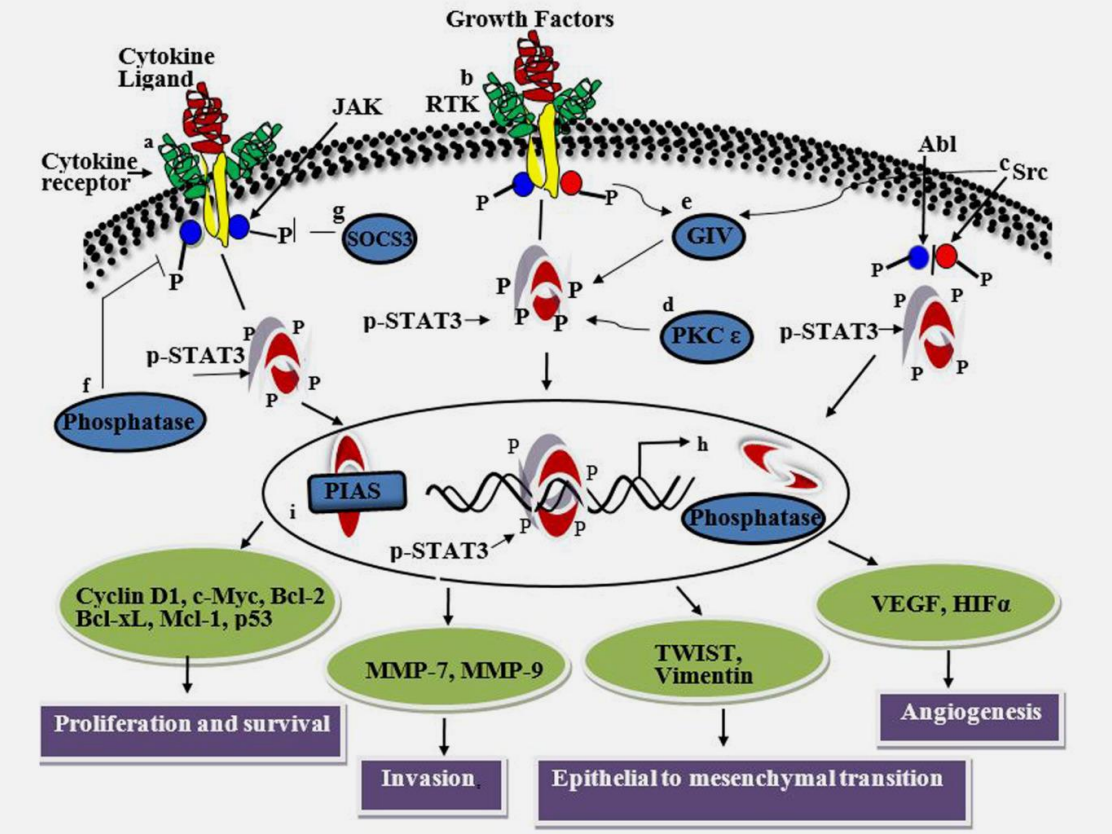

Figure 1.4. Mechanism of STAT3 activation and functioning. *Upon growth factors or cytokine stimulation, STAT3 gets phosphorylated by the activated receptors, phosphoSTAT3 then dimerizes with another phosphoSTAT3 molecule and this dimeric complex then translocates to nucleus where it controls transcription of genes involved in proliferation, invasion, EMT and angiogenesis. The hyper activation of STAT3 pathway is kept under control by various inhibitory molecules such as SOCS3, PIAS and PTPs inside the cell (Banerjee & Resat, 2016).*

1.3 Activators and Inhibitors of STAT3 pathway

Activation and inhibition of STAT3 signaling under both and oncogenic condition is a highly regulated process. There are various activation and inhibition mechanisms developed by the cell to keep a proper check on STAT3 function. Some of the potential regulators of STAT3 pathway are discussed below.

1.3.1 Activators of STAT3 pathway

Though elevated levels of pY705 STAT3 has been reported in case of primary tumours and tumor-derived cell lines, so far there are no mutations reported in STAT3 that can lead to its constitutive activation. However, there are multiple potential upstream modulators that can induce STAT3 signaling like, receptor tyrosine kinase family members -EGFR, FGFR, Her2, PDGFR, VEGFR; non-receptor tyrosine kinases such as Src and JAK; IL6-gp130 receptors and several other GPCRs. Along with receptors, there are multiple growth factors e.g. EGF, FGF, VEGF, PDGF, CSF1 as well as cytokine for e.g. IL6, IL10, IL11, LIF, CNTF and Oncostatin M, that have been reported to initiate STAT3 pathway activation (Kamran *et al*, 2013; Shalini Dimri, 2017) **(Figure 1.4)**. Either elevated levels or constitutive activation of components that can trigger STAT3 pathway have been reported in many different cancer types and are associated with poor prognosis. For e.g. mutation or overexpression of EGFR, mutations in JAK receptor and overexpression of Src are few of the molecular events in tumour cells that can induce persistent STAT3 pathway. Apart from receptors, even elevated levels of ligands such as IL6 and TGFα, either in serum or tumour microenvironment has been reported in variety of human malignancies. High level of these ligands in serum or tumor stroma can initiate and sustain constitutive STAT3 signaling either in paracrine, autocrine or endocrine manner (Laudisi *et al*, 2018; Leonard & O'Shea, 1998). Additionally, mutations that can lead to loss of epigenetic control for the regulators of STAT3 pathway has also been identified for many human malignancies (Wu *et al*, 2019).

1.3.2 Inhibitors of STAT3 pathway

Phosphorylation and dephosphorylation event play a key role in regulating levels of phosphorylated STAT3 pool in the cells. Several protein tyrosine phosphatases (PTP) such as PTP1B, PTPεC, SHP-1, SHP-2 and TC45 have been implicated in termination of STAT3

phosphorylation **(Figure 1.4)** (Chen *et al*, 2004). The family of PTPs can be divided into two major groups; receptor like PTPs for e.g. CD45 and nonmembrane PTPs containing SH2 domain i.e. SHP1, SHP2, PTP1B and TCPTP (T-cell protein tyrosine phosphatase). Similar to SHP-1, SHP-2 also contains two SH-2 domains in the N-terminal region and one PTP domain in the C-terminus. It is ubiquitously expressed throughout the body. By the virtue of two SH2 domains, SHP-1 interacts with pY residue on gp130 receptor, growth factor receptors, cytokine receptors, STAT3, JAKs and members of Src- tyrosine kinase family. All the pY containing proteins in STAT3 signaling are potential substrates for PTPs. In nucleus TC45 PTP is involved in dephosphorylation of nuclear phospho STAT3 and terminate transcriptional activation (Neel & Tonks, 1997). Considering their important function in supressing overtly activated STAT3, downregulation of these PTPs in various cancers thus promotes activation of STAT3 pathway. TCPTP and PTPN9 (non-receptor type 9 PTP; PTPMeg2) are reported to be downregulated in various breast cancer cell lines and primary triple negative breast cancer tumours, thereby facilitating cell proliferation *in vitro* and primary tumor growth *in vivo (Han et al, 2006; Irie-Sasaki et al, 2001)*.

PIAS (peptide inhibitor of activated STAT3) are endogenous proteins that controls the amount and duration of STAT3 activation **(Figure 1.4)**. PIAS protein comprises of 5 family members- PIAS1, PIAS3, PIASγ, PIASxα and PIASxβ. All the members of PIAS family have a conserved structure, it comprises of N-terminal domain (SAP domain) that recognizes and bind to AT rich DNA sequences along with various nuclear receptors and their coregulators (Shuai, 2000). The PINIT (Pro-Ile-Asn-Ile-The) motif is involved in nuclear accumulation of the PIAS protein. RLD or Ring finger like zinc binding domain and a C-terminal AD domain (highly acidic) that contain motif for interaction with sumoylated proteins i.e. SIM motif (Liu *et al*, 2001). PIAS is known to bind STAT3 and specifically blocks its DNA binding and transcriptional activity (Chung *et al*, 1997). Each member of

PIAS family is reported to regulate function of individual STAT family member for e.g. PIAS1 regulate STAT1 and p53, PIASxα interact with androgen receptor, PIASγ with LEF1, while PIAS3 interacts with STAT3, STAT5a and 5b (Arora *et al*, 2003). With the Sumo E3 ligase activity, PIAS is also suspected to be involved in sumoylation of STAT3 to further inhibits its function. The expression of PIAS in the cancer cells is post-transcriptionally suppressed thereby elevating STAT3 oncogenic functions (Clevenger, 2004).

Another potential inhibitor of STAT3, is a family of SOCS proteins (suppressor of cytokine signaling) that comprises of 8 members, SOCS 1-7 and CIS. All members of SOCS family contain an N-terminal domain of variable length, central SH2 domain and a C-terminal SOCS box domain. Due to presence of SOCS SH2 domain, members of SOCS family can interact with pY residue containing region in gp130, cytokine and JAK receptors and regulate STAT3 binding. The C-terminal SOCS box domain binds to E3 ubiquitin ligase thereby facilitating the ubiquitination and proteasomal degradation of SOCS binding proteins. SOCS3, one of the members of SOCS family is transcriptionally activated by STAT3 (Shuai, 2000; Wormald & Hilton, 2004). High levels of SOCS3, suppress hyperactivation of STAT3 either by competing with STAT3 for binding to activated receptor, by directly binding and inhibiting JAKs and by directly binding to STAT3 signaling proteins and directing them for proteasomal degradation **(Figure 1.4)**. In response to cytokine stimulation, elevated STAT3 expression in turn induce SOCS3 expression that in a negative feedback loop suppresses STAT3 activation (Kamran *et al*, 2013). Therefore, in oncogenic condition, the expression of SOCS3 is often silenced by promoter methylation thus favouring cancer cell growth (Weber *et al*, 2005).

1.4 STAT3 Pathway in Oncogenesis

The direct evidence for STAT3 as an oncogenic signaling came from the study where cells transformed using Epstein-Barr virus or Human T-lymphotropic virus-1 showed constitutive STAT3 signaling (Migone *et al*, 1995; Weber-Nordt *et al*, 1996). Further blocking STAT3 activity in cells prior to v-src transformation significantly compromised the transforming ability of the cells. More importantly, implanting normal mouse fibroblast expressing the mutant STAT3 construct (STATC), that rapidly form STAT3 dimers, led to tumor formation. Apart from mouse fibroblast, expression of STAT3C construct even in variety of other cells led to upregulation of essential oncogenic and angiogenic factors like VEGF, MMP and C-terminal tensin like protein (Bromberg *et al*, 1999). All these evidences strongly pinpoint the role played by STAT3 as a potential oncogenic molecule.

Aberrant expression and abnormal activation of STAT3 has been reported for several haematological malignancies and solid tumours. Unlike other oncogenes, mutation in STAT3 molecule that can lead to constitutive activation, are not very common. An exception to that is, inflammatory hepatocellular adenomas where 12% of tumours, lacking any mutation in IL6 receptor, have somatic mutations in region coding for SH2 domain of STAT3. These mutations lead to IL6 independent, STAT3 activation and homodimerization (Pilati *et al*, 2011). However, for majority of the cancer type, persistent STAT3 activation is a result of deregulated upstream signaling either in the form of overexpressed or constitutive receptor activation and abundance of growth factors or cytokine secretion.

Primary difference in the normal and oncogenic activation of STAT3 lies in the duration and level of pathway activation. Under normal condition, a substantial amount of ligand induction is required for acute STAT3 activation. While under oncogenic condition, even lower amount of ligand can lead to prolonged STAT3 induction. In many cases, the cancer cells even

become dependent upon or are addicted to STAT3 signaling and when such activity is blocked it leads to tumour regression and enhanced cell death (Regis *et al*, 2008). Apart from cellular level, STAT3 activity in the tumor microenvironment also controls tumour proliferation and metastasis. For e.g. hyperactivation of STAT3 leads to enhanced expression and secretion of inflammatory cytokines such as IL6 and angiogenesis prompting factors such as VEGF and HIF1-α (Xu *et al*, 2005). Abundance of these cytokines in the tumour stroma not only favours faster wound healing but also modulate the cancer cells for further activation of JAK/STAT pathway **(Figure 1.5)**. Additionally, secretion of these cytokines in the tumor microenvironment also suppress the immune cell functioning (Regis *et al*, 2008).

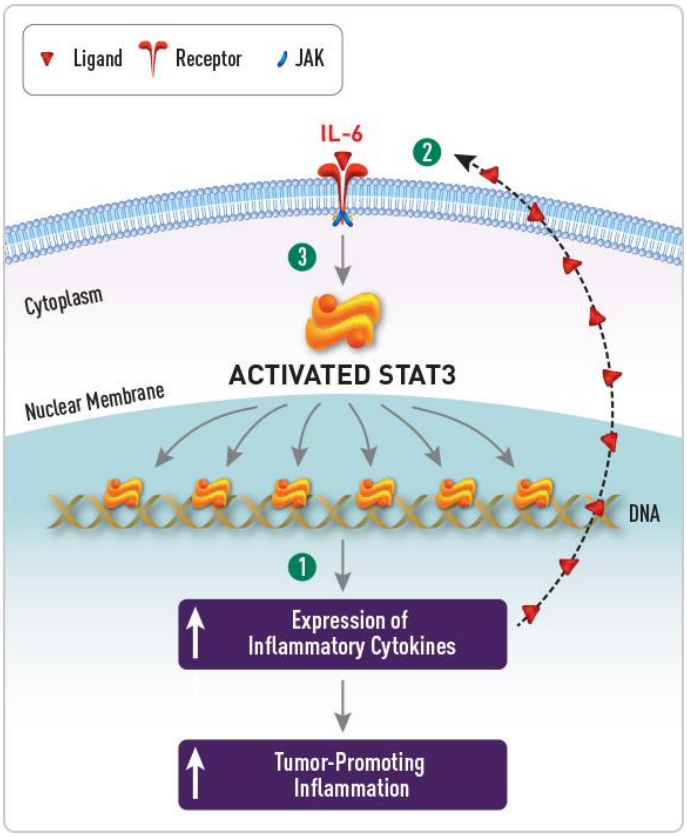

Figure 1.5. Oncogenic STAT3 induction. *Hyperactivated STAT3 in tumour cells lead to cytokine secretion, which in turn further elicits JAK/STAT pathway in an autocrine and paracrine manner. As a result, apart from modulating cancer cells, STAT3 also alters the tumour microenvironment (Chang et al, 2019).*

Mounting number of evidences strongly suggest STAT3 as a bondafide oncogenic molecule. Constitutive activation of STAT3 by tyr705 phosphorylation has been reported in breast carcinomas, head and neck carcinoma, lymphomas, leukemias, ovarian, brain, prostate and pancreatic cancers. Apart from being overtly expressed STAT3 is even identified as a poor prognostic biomarker for many cancers. A meta-analysis from previously published 63 studies in which expression of pTyrSTAT3 was assessed with overall survival in the patients with solid tumor (comprising of hepatic, pancreatic, lung, prostate and gastric cancer with advanced stage tumours) showed worse overall and disease-free survival for high pTyrSTAT3 expression (Wu *et al*, 2016). From meta-analysis of 17 studies (n=2346) exclusively comprising of colorectal cancer also identified pTyrSTAT3 expression association with poor prognosis and lymph node metastasis (Ji *et al*, 2016). In case of breast cancer, analysis of TCGA data sets with STAT3 activation identified strong correlation with basal like-TNBC gene signatures. Signatures corresponding to STAT3 activation were seen in TNBC samples that had reduced metastasis free survival (Tell & Horvath, 2014). Combined experimental and clinical observation strongly put forward STAT3 as a potential candidate that strongly controls tumour growth and cell survival functions thereby providing promising avenue for therapeutic intervention.

1.5 Mechanisms of STAT3 Activation

STAT3 is reported to be activated by following two mechanisms in cancer.

1.5.1 Canonical Pathway

In classical canonical pathway, STAT3 activation takes place primarily by phosphorylation at Y705 residue in response to cytokines or growth factors treatment. Once phosphorylated, STAT3 shuttles to nucleus and mediate its DNA binding and transcriptional activity. For many years activation of STAT3 has been attributed to pY705 mediated functions that in turn

controls expression of genes involved in various aspects of cancer progression such as proliferation (Cyclin D1, c-Myc), Cell survival (p53, survivin and Bcl-xL), migration (MMPs), invasion (Rho1, E-cadherin) , angiogenesis (VEGF,HIF1 alpha) and immune evasion (RANTES,IL6) (Carpenter & Lo, 2014) **(Figure 1.6)**. For both *in vitro* and *in vivo* studies pY705 has been used as marker to determine STAT3 activation status. In clinical scenario, activation of STAT3 pathway in tumor samples is determined based on pY705 positivity. pY705 is even used as biomarker to predict disease prognosis and overall survival in case of colon cancer, breast cancer, lung cancer and several other cancers (Cocchiola *et al*, 2017; Shalini Dimri, 2017). Based on this, the clinical paradigm of STAT3 was established. Tumours that express pY705 STAT3 are positive for STAT3 pathway activation and hence should be administered anti-STAT3 inhibitors. While tumours that don't express pY705 STAT3 are not considered to be STAT3 addicted and hence STAT3 inhibitors should not be given (Sellier *et al*, 2013). In this context, all therapeutic development and clinical studies consider pY705 STAT3 as prime parameter for judging the STAT3 pathway activation. Additionally, since STAT3 plays an important role in drug resistance, one could speculate that tumours with high pY705 expression would be more resistant to chemotherapeutic treatment. Hence prior detection of pY705 expression in tissue samples can help in stratifying patients that would show resistance or incomplete response to the conventional chemotherapy regime (Barre *et al*, 2007).

1.5.2 Noncanonical Pathway

Apart from classical canonical pTyr705 mediated activation, STAT3 is reported to go undergo post translational modifications at other sites that can equally activate the STAT3 molecule. Serine residue located at the C-terminal domain of STAT3 at position 727 is known to undergo phosphorylation upon IL6 or EGF stimulation. There are multiple kinases

reported to be involved in phosphorylating STAT3 at S727 site such as JNK, MAPK, PKC family members, CDK5 and Casein kinase (Decker & Kovarik, 2000; Tkach *et al*, 2013) **(Figure 1.6)**. When initially discovered, pS727 was identified as secondary modification event following pY705 occurrence to fully activate the STAT3 molecule (Wen *et al*, 1995). However, data from recent studies clearly highlight independent oncogenic role of pS727 site in STAT3 functions.

In case of infiltrating ductal breast carcinoma, pS727 STAT3 was found to be involved in pathogenesis of breast cancer in ER dependent manner, irrespective of pY705 STAT3 expression. Breast tumour tissues positive for pS727 expression showed negative correlation with ER status of the sample and a positive association with both tumour stage and grade (Yeh *et al*, 2006). In case of both chronic lymphocytic leukemia and melanoma, STAT3 was constitutively phosphorylated at S727 residue irrespective of pY705 status. Activation of STAT3 at pS727 was found to be essential for DNA binding, transcriptional activation and cell survival of the cells (Hazan-Halevy *et al*, 2010). In glioblastoma, pS727 expression was found to contribute toward tumorigenesis, resistance to chemotherapy and radiotherapy and samples with high pS727 positivity showed poor clinical outcome. Additionally, treating GBM cells with inhibitor that led to pS727 STAT3 inactivation radio sensitizes the cells toward radiation induced cell death. While no such effect was observed with pY705 STAT3 depletion (Lin *et al*, 2014; Ouedraogo *et al*, 2016). Even in case of prostate cancer, pS727 driven STAT3 activation was found to be sufficient and dominant to drive tumorigenesis independent of pY705 STAT3 activation (Qin *et al*, 2008). Similarly, for colorectal cancer, treatment with Topoisomerase I inhibitor led to activation of STAT3 specifically at pS727 site. pS727 dependent STAT3 activation transcriptionally enhanced expression of Eme1 gene (endonuclease) that favoured faster repair of damaged DNA and imparts chemoresistance

(Vigneron *et al*, 2008). Exclusive pS727 expression is even essential at the embryonic state for differentiation of mESC to neuronal lineage (Huang *et al*, 2014).

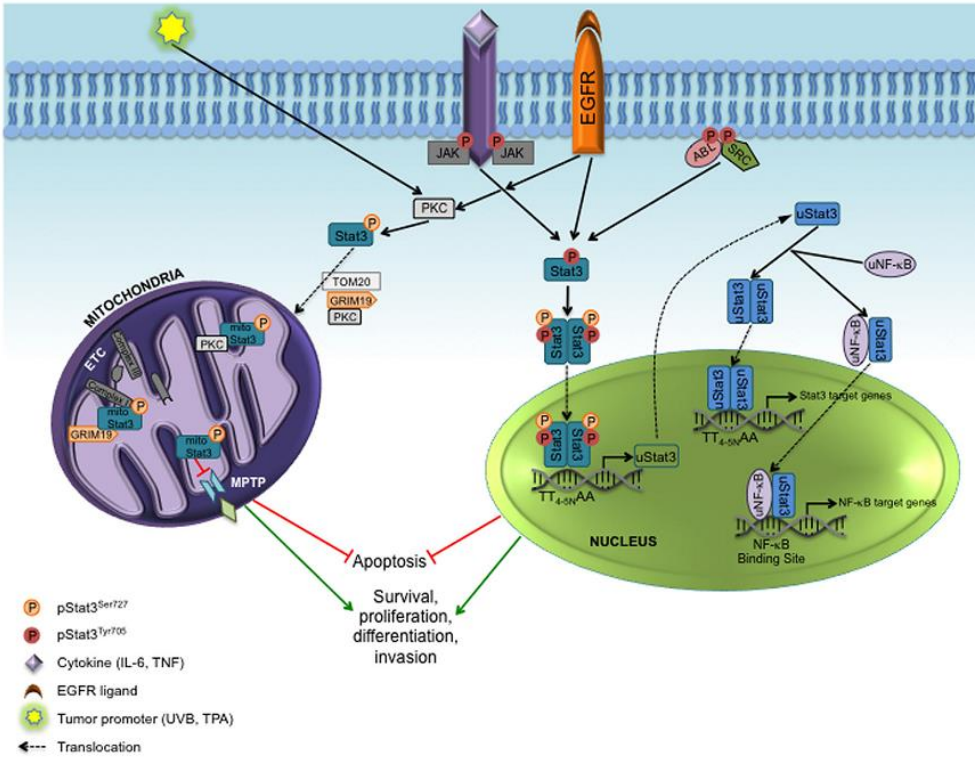

Figure 1.6. Canonical and noncanonical STAT3 activation. *Canonical activation of STAT3 is driven by pY705 phosphorylation that leads to dimerization, nuclear translocation and transcriptional activity of STAT3 molecule. In noncanonical activation (pS727 and K685ac- uSTAT3) the ligand or stimulation is not known. However, under the influence of PKC, STAT3 gets S727 phosphorylation and localizes either to mitochondria or nucleus and controls cell survival functions. While U-STAT3 or K685ac STAT3 can interact with NF-kB and regulate expression of genes with NF-kB response elements* (Srivastava & DiGiovanni, 2016).

Another important post translational modification that influences STAT3 activation is acetylation of lysine residue at 685 position (K685ac). STAT3 is known to interact with CBP/p300 protein that acetylates STAT3 at K685 residue and this acetylation is essential for

nuclear localization, DNA binding and transcriptional activity of STAT3 molecule (Wang *et al*, 2005). In 2005, Yuan et.al. reported that acetylation of STAT3 at K685 residue is essential for STAT3 to form stable homodimers irrespective of pY705 and pS727 presence. K685ac was essential for cell to proliferate and regulate expression of cell survival genes such as cyclin D1, Bcl-xL and c-Myc (Yuan *et al*, 2005). Enhanced expression of K685ac STAT3 was reported even in case of melanoma, ovarian cancer, colorectal cancer and lung cancer (Lee *et al*, 2012; Li *et al*, 2013; Yang *et al*, 2010). Acetylation of STAT3 at K685 was found to be essential for interaction of STAT3 with DNMT1. With this interaction STAT3-DNMT1 methylates the promoter of tumor suppressor genes such as TP53, STAT1, SOCS3, CDKN2A and DLEC1 and downregulate their expression (Lee *et al*, 2012). Acetylated STAT3 in gastric cancer, is also reported to interact with CD44 and regulate expression of Cyclin D1 gene (Lee *et al*, 2009). Inhibition of STAT3 acetylation by garcinol (acetyltransferase inhibitor) led to suppression of proliferation, induction of apoptosis and regression of xenograft tumours in hepatocellular carcinoma mouse model (Sethi *et al*, 2014). STAT3 acetylation is even reported to be involved in processing of NF-κβ protein. STAT3 once acetylated activates IKKα kinase that further phosphorylates p100 for proteolytic cleavage to give rise to p52 (Nadiminty *et al*, 2006). Additionally, acetylated STAT3 is also reported to form a complex with NF-κβ protein and regulate expression of different set of genes such as IL8, MET, MRAS, IL6 and RANTES (Dasgupta *et al*, 2014).

Apart from having differential post translational modification (PTM) mediated nuclear STAT3 functions, there are evidences PTM dependent altered localization of STAT3 (Avalle & Poli, 2018). Once phosphorylated at pS727 site, STAT3 interacts with GRIM-19 and get translocated to mitochondrial inner membrane. STAT3 is incorporated to the ETC chain 1 of mitochondria where it regulates generation of ROS (reactive oxygen species) and apoptosis induction. There are even reports on mitochondrial STAT3 interacting with ETC I, II and II

and contributing to dysfunctional mitochondria respiration and enhanced tumour growth (Wegrzyn *et al*, 2009). In case of breast cancer, mitoSTAT3 activated at pS727 site was found to be essential for tumorigenesis. Cells expressing mutant STAT3 (S727A) showed reduced ETC complex 1 activity and enhanced ROS accumulation under hypoxic condition (Zhang *et al*, 2013). Recently, STAT3 was even reported to localize to endoplasmic reticulum where it regulates ER-mitochondrial calcium release. STAT3 activated at pS727 residue localizes to ER and degrades calcium channel IP3R3 during stress thereby controlling calcium release to cytoplasm. While loss of STAT3 expression in these cells leads to calcium release form ER via IP3R3 channel and initiation of intrinsic apoptotic pathway (Avalle *et al*, 2019; Banerjee *et al*, 2017).

Additional to pS727 and K685ac there are other sites on STAT3 that are reported to undergo post translational modification. K679, K707 and K709 lysine residues in STAT3 are deacetylated by SirT1 to inhibit its activation and promote gluconeogenesis (Nie *et al*, 2009). STAT3 is also reported to undergo reversible dimethylation at K140 residue by Set9 enzyme and it is deactivated by LSD1 demethylase enzyme. K140 is a nuclear event that takes place specifically inside nucleus before DNA binding and it occurs only after pS727 STAT3 activation (Yang *et al*, 2010). However so far, the functional role of K140 dimethylation is not well identified.

1.6 STAT3 Inhibitors

STAT3 is considered to be one the most important molecule for therapeutic targeting in any cancer. Considering the prevalent role of STAT3 signaling in controlling various oncogenic process, therapeutic approaches for targeting STAT3 has been developed that majorly includes; direct inhibition and indirect inhibition methods **(Table1.2)**.

Indirect inhibitors of STAT3				
Classification	**Inhibitors**	**Year**	**Target site**	**Mode of targeting STAT3**
Small-molecule inhibitors	Ruxolitinib	2012	JAK1/2	Phosphorylation
	Tofacitinib	2013	JAK3	Phosphorylation
	AZD1480	2011	JAK1/2	Phosphorylation
	SB1578	2010	JAK2	Unknown
	WP1066	2010	JAK2	Phosphorylation
	AG490	1996	JAK2	Phosphorylation
	Naringenin	2013	SOCS3	Unknown
	Flavone	2013	SOCS3	Unknown
Natural inhibitors	Tricin	2014	JAK1/2	Phosphorylation
Direct inhibitors targeting the SH2 domain of STAT3				
Classification	**Inhibitors**	**Year**	**Target site**	**Mode of targeting STAT3**
Peptides and peptide-like inhibitors	PpYLKTK	2001	SH2	Dimerization
	pYLPQTV	2003	SH2	Dimerization
	Acetyl-pYLKTKF	2007	SH2	Dimerization
Small-molecule inhibitors	STA-21	2009	SH2	Dimerization
	LLL12	2012	SH2	Phosphorylation
	OPB-31121	2013	SH2	Phosphorylation
	OPB-51602	2015	SH2	Phosphorylation
	Stattic	2006	SH2	Phosphorylation
	S31-201 & analogs	2007	SH2	Dimerization
Natural inhibitors	Curcumin	2014	SH2	Phosphorylation
	Cucurbitacin E	2010	SH2	Phosphorylation
	Alantolactone	2015	SH2	Unknown
	Cryptotanshinone	2009	SH2	Unknown
	Piperlongumine	2015	SH2	Unknown
	Silibinin	2015	SH2	Unknown
Direct inhibitors targeting DBD and other domains of STAT3				
Classification	**Inhibitors**	**Year**	**Target site**	**Mode of targeting STAT3**
Small-molecule inhibitors	C48	2011	DBD	DNA binding
	InS3-54 & analogs	2014	DBD	DNA binding
	MMPP	2017	DBD	DNA binding
Platinum compounds	IS3-295	2005	DBD	DNA binding
	CPA-1	2004	DBD	DNA binding
	CPA-7	2004	DBD	DNA binding
	Platinum (IV) tetrachloride	2004	DBD	DNA binding
Natural inhibitors	Galiellalactone	2014	DBD	DNA binding
	Peptides	2007	ND	Transcriptional activity
	ST3-Hel2A-2	2013	ND	Transcriptional activity
	K116	2018	TAD	Dimerization

Table 1.2. Potential direct and indirect inhibitors of STAT3 pathway (Chen et al, 2019).

1.6.1 Direct Inhibition

STAT3 SH2 domain binders: For disrupting STAT3 homodimerization various SH2 binding peptides, peptidomimetics and nonpeptidic chemical inhibitors have been developed. PY*LKTK, ISS 610, Y*LPQTV peptide and several other modified versions including hydro cinnamoyl-Tyr (PO3H2)-Leu- *cis*-3,4-methanoPro-Gln-NHBn was identified that selectively binds to STAT3 and prevent STAT3 DNA binding activity in vitro (Ren *et al*, 2003; Ren *et al*, 2008; Turkson *et al*, 2004a). Based on structure driven computational screening of STAT3, SH2 domain binding STA-21 peptide (Song *et al*, 2005) and a small molecule

inhibitor -Stattic was identified (Schust *et al*, 2006) that showed potent STAT3 inhibitory activities.

Blockers for DNA Binding domain of STAT3: Disrupting DNA binding activity of STAT3 will stall the transcriptional function and tumor promoting activity of the cancer cells. In these lines various platinum (IV) compounds like IS3 295, CPA-1, CPA-7, and platinum (IV) tetrachloride are used. These platinum (IV) compounds showed significantly better in vitro inhibitory activity against STAT3 in comparison to peptides, peptidomimetic or nonpeptide molecules (Turkson *et al*, 2005; Turkson *et al*, 2004b).

Oligonucleotide based approach: Targeting STAT3 using small interfering RNA (siRNA), antisense RNA and decoy oligodeoxynucleotide (ODN) leads to transcriptional repression of target genes. Use of synthetic STAT3 decoy ODN (5-CATTTCCCGTAAATC-3) successfully blocked STAT3 dependent transcription functions and led to reduction in proliferation, induction of apoptosis in various cancer cell lines (Tomita *et al*, 2003). Recently new class of ODN has been developed, known as G-rich ODN that form inter and intramolecular G- quartet structures that disrupts STAT3 homodimers (Jing *et al*, 2003).

N-terminal domain targeting: The N-terminal domain is important for STAT3 dimers to interact with the target DNA, transcriptional regulators and activators. A short category of peptides, derived from helix 2 of STAT3 have been identified that specifically binds to STAT3 molecule represses its transcriptional activity without affecting the phosphorylation status. When these peptides were fused with Penetratin (RQIKIWFPNRR-Nle-KWKK-NH2 protein transduction motif) to increase cell permeability, they showed specific inhibition of cell growth and induction of apoptosis in MDA-MB-231, MDA-MB-435 and MCF-7 breast cancer cells (Becker *et al*, 1998; Timofeeva *et al*, 2007).

1.6.2 Indirect Targeting of STAT3

Indirect targeting of STAT3 majorly involves blocking the upstream tyrosine kinases that activate the STAT3 molecule. Apart from existing tyrosine kinase inhibitors such as EGFR and Src kinase, there are few new tyrosine kinase blockers identified that suppress STAT3 phosphorylation by indirect blocking of the upstream tyrosine kinase activity. For e.g. JSI-124 (Blaskovich *et al*, 2003) , JAK kinase inhibitor- AG490, WP1066 and TG101209, Src-Kinase inhibitors – resveratrol and indirubin, Receptor Tyrosine Kinase inhibitor – tyrphostins and JAK-STAT3 pathway blocker such as curcumin (Ferrajoli *et al*, 2007; Kotha *et al*, 2006; Levitzki, 1992; Pardanani *et al*, 2007; Yue & Turkson, 2009).

Despite so much of knowledge on STAT3 signaling pathways with different alternative approaches available to target, very few STAT3 inhibitors have actually cleared the clinical trials **(Table 1.3)**. This demands for an urgent need to re-examine the drug development and targeting approach against the STAT3 pathway. With extensive cross talk and alternative signaling STAT3 pathway present, limits the usage of single targeting agent against the STAT3 molecule as prime approach. Further, with the identification of canonical and noncanonical mode of STAT3 pathway activation, the use of only pY705 mediated STAT3 inhibition strategy is in question. In this scenario, a comprehensive analysis of STAT3 PTM presence and the mode of activation need to explored thoroughly for individual tumor. This will not only aid the development of STAT3 specific drug but will also provide patient specific section of the inhibitors to improve the treatment response. One of the potential ways to amplify and specify the drug development approach is to develop molecular imaging based live cell biosensors that can be used as a read-out tool for STAT3 pathway modulation directly from living system. The inhibitors identified from live cell screening offers high chances of showing therapeutic effect as compared to the candidates screened using conventional virtual structure-based approaches and then validated *in vitro*.

Inhibitor	Indication	Study Phase	Status	NCT Identifier
AZD9150 IONIS-STAT3Rx (STAT3 antisense oligonucleotide)	NSCLC, advanced solid tumors	I/II	Recruiting	*NCT03421353*
	Advanced pancreatic cancer, NSCLC, and CRC	II	Recruiting	*NCT02983578*
	Advanced/metastatic hepatocellular cancer	I	Completed	*NCT01839604*
	DLBCL	I	Recruiting	*NCT02549651*
	Advanced solid tumors, metastatic HNSCC	I/II	Recruiting	*NCT02499328*
	Advanced tumors, DLBCL, lymphoma	I/II	Completed	*NCT01563302*
OPB-31121 (STAT3 SH2 domain)	Advanced cancer, solid tumors	I	Completed	*NCT00955812*
	Advanced solid tumors	I	Unknown	*NCT00657176*
	Hepatocellular carcinoma	I/II	Completed	*NCT01406574*
OPB-51602 (STAT3 SH2 domain)	Advanced tumors	I	Completed	*NCT01423903*
	Multiple myeloma, NHL, AML, ALL, and CML	I	Completed	*NCT01344876*
	Advanced solid tumors	I	Completed	*NCT01184807*
OPB-111077 (STAT3 phosphorylation)	Advanced tumors	I	Completed	*NCT01711034*
Napabucasin DSP-0337 (STAT3 SH2 domain)	Metastatic pancreatic adenocarcinoma	III	Recruiting	*NCT02993731*
	Metastatic CRC	II	Not yet recruiting	*NCT03647839*
	Advanced solid tumors	I	Not yet recruiting	*NCT03416816*
STAT3 DECOY (STAT3 response element)	HNSCC	Early I	Completed	*NCT00696176*
TTI-101 (STAT3 SH2 domain)	Advanced tumors	I	Recruiting	*NCT03195699*

ALL, acute lymphoblastic leukemia; AML, acute myeloid leukemia; CML, chronic myeloid leukemia; CRC, colorectal cancer; DLBCL, diffuse large B-cell lymphoma; HNSCC, head and neck squamous cell carcinoma; NHL, non-Hodgkin lymphoma; NSCLC, non-small-cell lung cancer; SH2, Src homology domain 2; STAT3, signal transducer and activator of transcription 3.

Table 1.3. List of STAT3 inhibitors currently in clinical trials (Segatto et al, 2018).

1.7 Optical Imaging

Optical imaging (OI) refers to techniques employing light in the near infrared (NIR) region (700-1000nm) and visible region (400-700nm) to reveal or interrogate molecular, functional or morphological information from cells, tissues or living systems (plants and animals). With innovative combination of molecular biology and chemistry, optical imaging methods thus facilitates deeper understanding of disease biology, mechanistic details or cellular processes *in vivo* in a real time manner. Because of its advantages like easy to adopt utility, rapid results output with cost effectiveness, optical imaging methods are increasingly gaining popularity at both preclinical and clinical application set up (Luker & Luker, 2008; Shah & Weissleder, 2005). Fluorescence and Bioluminescence imaging are the two most widely used optical

imaging approaches in current scenario that holds great potential for future intervention **(Figure 1.7)**.

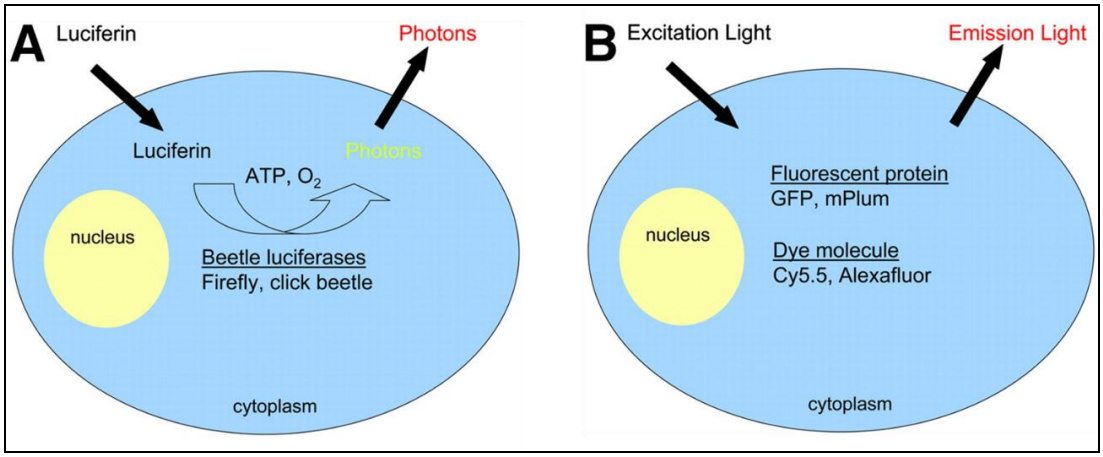

Figure 1.7: Diagrammatic representation of Bioluminescence and Fluorescence optical imaging methods. *(A) Bioluminescence imaging involves catalysis of specific substrate by luciferase enzymes (firefly, beetle luciferase etc.) in presence of ATP and O_2 to emit light of defined spectral property. (B) Fluorescence imaging requires excitation of the fluorophore with a specific wavelength to produce characteristic emission signal for the fluorophore (Luker & Luker, 2008).*

1.7.1 Fluorescence Imaging

Fluorescence imaging utilizes endogenous or exogeneous probe or material that emits light at defined wavelength upon excitation with external light source. In principal, when a fluorescent probe or molecule is excited using a light or electromagnetic radiation of specific wavelength, it results in excitation of electrons within the molecule causing them to transit from low energy ground state to high energy excited state. After, a lag period of few nanoseconds i.e. fluorescence lifetime, the excited electrons return back to their ground state by releasing the energy in the form of a photon. Due to high energy relaxation while transiting, the emitted light always has a low energy and high wavelength. The difference between the excitation wavelength and the emission wavelength is termed as “stokes shift” (Dunst & Tomancak, 2019) **(Figure 1.8)**.

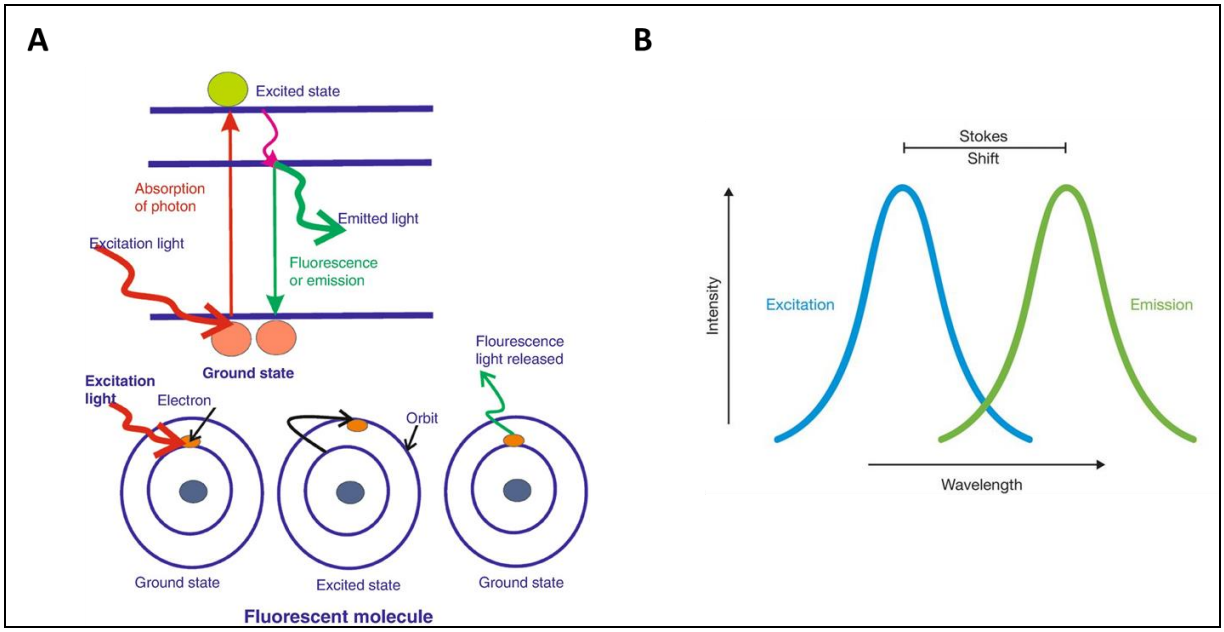

Figure 1.8. Principle of resonance energy transfer. *Upon illumination of fluorescent molecule with light source of specific wavelength leads to excitation of electron to high energy state. While coming back to ground state the, it emits light that can excite nearby fluorescent molecule with overlapping excitation wavelength (Dunst & Tomancak, 2019).*

Fluorescence imaging is constantly being utilised for determining protein localization or aberrant protein expression in normal versus pathological condition. Apart from this, fluorescence imaging is routinely utilised for studying intracellular trafficking, labelling cell organelles or superficial structures, monitoring tumour growth or response to specific drug treatment or developing biosensors for protein-protein interactions (BiFC, FRET etc) (Hassan & Klaunberg, 2004). The most commonly utilised fluorophore in fluorescence imaging are GFP and its derivatives YFP (yellow fluorescent protein – 527nm emission), blue (450nm emission) and cyan fluorescent proteins (500nm emission) (Tsien, 1998); Ds Red and its improved RFP variants such as mCherry, mOrnage, mRaspberry (Zhang *et al*, 2002); TurboFP635 (635nm emission) and TagRFP (580nm emission) derived from sea anemone, *Entacmaea quadricolor* (Gurskaya *et al*, 2001).

1.7.2 Bioluminescence Imaging

Bioluminescence refers to biophysical phenomenon where a light is produced upon chemical reaction between luciferase enzyme and its natural substrate. Bioluminescence imaging is mostly employed for cellular and molecular imaging in small animals (Widder, 2010). This phenomenon of independent light production is a natural process known to exist in many organisms and utilised for various purposes; as a defence mechanism, evading predators or demonstrating sexual behaviour. Some of the well-known luciferases utilising this phenomenon include; *Renilla* luciferase (RLuc), firefly luciferase (Fluc), *Gaussia Metridia* and *Vargula* luciferase. Since its discovery, scientists have successfully extrapolated this natural process to bench side for demonstrating and determining various cellular process from living systems. One of the potential applications of bioluminescence both in natural and experimental set up is bioluminescence resonance energy transfer (Hoshino, 2009; Seliger & Mc, 1960).

1.7.2.1 Bioluminescence Resonance Energy Transfer

Bioluminescence resonance energy transfer or BRET is a naturally occurring phenomenon in marine organisms such as sea pansy *Renilla reniformis* and jellyfish *Aequorea Victoria*. For. E.g. in *Aequora Victoria*, aequorin is a calcium dependent photoprotein that produces flashes of blue light. These blue lights are transferred to GFP protein that in turn emits green light upon excitation **(Figure 1.9)**. The basic principle of this natural phenomenon is that, upon binding to specific substrate, the luciferase enzyme catalysis it, as a result it gets excited and goes to high energy state. After a lag period it relaxes and transition to low energy state by dissipating some amount of energy as heat due to random collision and remaining electronic relaxation energy as non-radiative dipole-dipole coupling to adjacent acceptor fluorophore **(Figure 1.10)**. The acceptor fluorophore in turn is excited and transition from low to high

energy state and while relaxing it emits signal at respective acceptor wavelength (Drinovec *et al*, 2012; Xu *et al*, 1999).

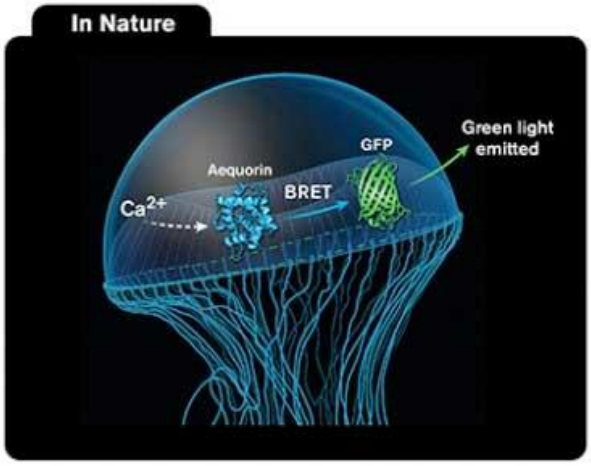

Figure 1.9. BRET in Aequorea Victoria under natural environment. *Calcium flux causes aequorin membrane protein to emit blue light that in turn excites GFP protein to give green emission signal (Bhuckory et al, 2019).*

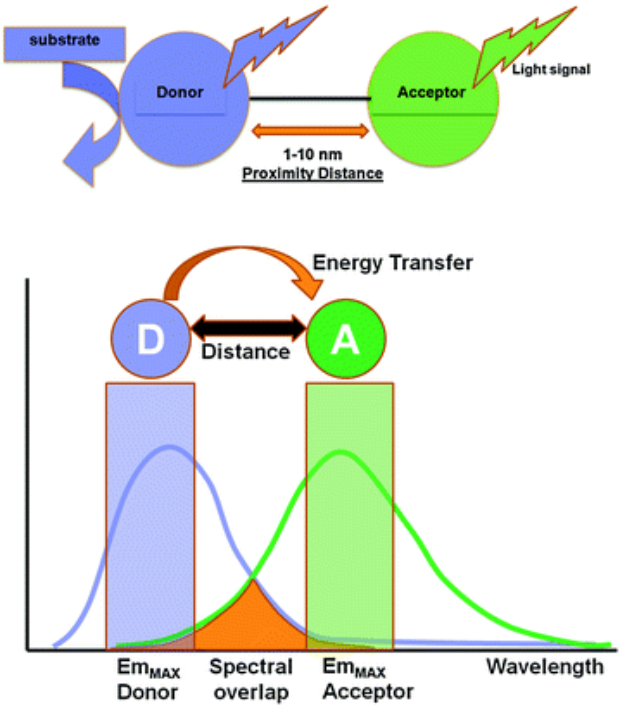

Figure 1.10. Working model of BRET assay system. *When donor and acceptor are in close proximity, the energy from donor upon catalysis of its substrate is transferred to acceptor molecule*

resulting in acceptor emission at respective wavelength. In BRET upon positive interaction, two resultant peaks are obtained, donor emission and acceptor emission (Abhijit De, 2014).

Exploiting this underlying principle of BRET from natural environment, scientists have developed BRET pair using either the native or modified luciferase enzyme and coupled the with various fluorophores for establishing BRET system. **Table 1.4** highlights some the exiting BRET pairs that have been developed using native or mutant RLuc as donor (Dimri *et al*, 2016). The development of these BRET system enabled scientist to monitor various biological process directly from live cells or live organism in their natural environment. With the potential advantages like high signal to background ratio and no requirement of excitation light that takes care of photobleaching and autofluorescence signal, makes BRET a better system than existing protein interaction approaches (El Khamlichi *et al*, 2019).

Assay	Donor	Acceptor	Substrate	Spectral resolution (nm)	Dynamic range	Efficiency
BRET[1]	RLUC 480 nm (Improved version using RLUC2/ RLUC8)	YFP/EYFP 535 nm	Clz /Enduren™	55	Small	Moderate
BRET[2]	RLUC 400 nm (Improved version using RLUC2/ RLUC8)	GFP[2] 515 nm	Clz400 /protected Clz400	115	Very large	Moderate
BRET3	RLUC8 480 nm	mOrange 564 nm	Clz /Enduren™	85	Large	Moderate
BRET4	RLUC8 480 nm	TagRFP 584 nm	Clz/ Enduren™	104	Large	High
BRET5	RLUC8 515 nm	TagRFP 584 nm	Clz -v	70	Moderate	Low
BRET6	RLUC8.6 535 nm	TagRFP 584 nm	Clz /Enduren™	50	Large	High
BRET7	RLUC8 480 nm	TurboFP 635 nm	Clz-v	155	Small	Low
BRET8	RLUC8.6 535 nm	TurboFP 635 nm	Clz /Enduren™	100	Moderate	Moderate

Table 1.4. List of different BRET systems developed using native and mutant version of Renilla luciferase with their substrate, spectral separation and efficiency (Dimri et al, 2016) .

1.7.2.2 Factors affecting BRET Signal

The efficiency of any BRET system developed depends upon following factors that need to keep in consideration before establishing the sensor (Ciruela *et al*, 2010; Stryer & Haugland, 1967; Wu & Brand, 1994).

Spectral overlap: the emission of donor should overlap the excitation wavelength of the acceptor molecule. Higher the spectral overlap better is the energy transfer.

Distance between donor and acceptor pair: the distance between donor and acceptor is inversely proportional to efficiency of energy transfer. The optimal distance for Foster resonance energy transfer for any natural biological interaction is 1-10nm. Increase in distance more that 10nm leads to decrease in energy transfer from donor to recipient acceptor and accounts for a negative or no interaction.

Dipole orientation: the relative alignment of donor and acceptor dipoles is extremely essential, as energy transfer will happen only when the two are in same dipole angle and aligned together.

Quantum yield of donor: the quantum efficiency of the donor should be high enough to excite the fluorophore before losing it out as non-radiative decay energy. Additionally, higher the efficiency of donor luciferase better are the chances of coupling it with fluorophores with red shifted emission.

1.7.2.3 Luciferase and Fluorophores utilised for BRET study

The most commonly utilised luciferase for BRET study is native RLuc or *Renilla* luciferase (Angers *et al*, 2000). However, since the emission of RLuc majorly lie in the blue green region it was further mutated to give RLuc8 (with eight single site mutations). RLuc8 had more than 50hrs of half-life, high quantum yield and shift of 5nm in emission wavelength as compared to native RLuc (Loening *et al*, 2006). Further to extend application of RLuc8 for deep tissue imaging, a mutant version RLuc8.6 was developed that had emission towards red shifted region (Loening *et al*, 2007). Along with modifying the luciferase enzyme, the substrate coelenterazine was also altered to have better luminescence efficiency (Clz-h, CLz-v, CLz400, EnduRen^{TM} and ViviRen^{TM}) (Levi *et al*, 2007; Otto-Duessel *et al*, 2006). Another commonly utilised luciferase is *Firefly* luciferase from *Photinus pyralis*. Fluc is an ATP dependent luciferase that utilises ATP for light production during bioluminescence reaction with emission maxima at 562nm (Green & McElroy, 1956). Fluc has been employed for several BRET applications by pairing with red and far-red shifted fluorophores such as DsRed and variants of mKate (Arai *et al*, 2002; Chiu & Christopoulos, 1999). One of the most widely used luciferase in current scenario is Nanoluciferase (NLuc). Nanoluc is a mutant derived from parent *Oplophorus* luciferase (OLuc) which is a tetramer. NLuc is a monomeric enzyme of 19KDA molecular weight with high stability and quantum efficiency as compared to native Rluc and Fluc enzymes (Mo & Fu, 2016).

As acceptor pair, many fluorophores have been utilised for pairing with the existing luciferase system. Some of the commonly utilised fluorophores include; GFP and its variants such as EGFP (Muller-Taubenberger & Anderson, 2007), TurboGFP, AcGFP, and EmeraldGFP; Yelow fluorescent protein (EYFP) derived from wtGFP and its successors such as mCitrine, Venus and YPet; Red fluorescent proteins such as DsRed , mOrange, mCherry, mTangerine, TagRFP,TurboFP635 etc (Baird *et al*, 2000; Shaner *et al*, 2004). More recently

near-infrared (NIR) probes are being explored as partner for luciferase donor that facilitates whole body or deep tissue imaging due to reduced light scattering. Bacterial phytochrome-based NIR red fluorescent proteins (iRFP) is one such example. iRFPs have a second soret peak at 380nm that makes them favourable acceptor for RLuc8 luciferase that gives acceptor emission at NIR region using conventional coelenterazine substrate (Nishihara *et al*, 2019; Rumyantsev *et al*, 2016).

Considering the high sensitivity and versatile nature of BRET assay system, in the present study we have attempted to develop a phosphorylation based STAT3 homodimerization sensor using this approach. Based on initial parameters of dipole orientation we first selected the optimal dipole alignment for STAT3 pair using Nluc as donor and TurboFP635 as acceptor. After that we showed the applicability of developed sensor against multiple parameters and established its high throughput compatibility as a drug screening tool.

Rational of the Study

Rational of the Study

Aberrant activation of STAT3 has been observed in different type of tumours and tumour derived cell lines. Based on its biological relevance as an essential functional molecule, STAT3 has long been known as a key oncogenic driver. Consequently, pertaining to its position in the signaling hierarchy and ability to control multiple oncogenic pathways, it is even considered as one of the most promising candidates in the field of cancer therapy. However, defining STAT3 PTM mediated activation and their role in downstream signaling in various cancer population is very important for development of successful treatment strategies against this molecular target.

Literature evidences suggest that the classical canonical (pY705) PTM does not exclusively govern STAT3 signaling in many cancer types or subtypes. The less known noncanonical (pS727 and K685ac) pathway can equally execute the activation and downstream biological functions of the STAT3 pathway. Despite numbers of compelling evidences, no reports are available to-date showing the interplay or cross-talk between the two signaling arms are simultaneous or segregated events. Whether pY705 activation precedes or depends upon pS727 and K685ac or vice versa, is still not clear. Further, a few studies have identified transcriptional targets governed exclusively by the noncanonical activation, but the possibility of PTM dependent transcriptional reprogramming of STAT3 is still not very clear. Thus, it is important to know if the classical targets of STAT3 (Cyclin D1, c-Myc, Socs3 etc.) are mutually regulated or there are separate set of PTM dependent oncogenic transcriptional control.

On the basis of published data, independent expression of pS727 in the cancer tissue specimens are apparent in melanoma, chronic lymphocytic leukemia, glioblastoma, lung adenocarcinoma as well as in ER negative BC cases. However, the status of pY705 or pS727

PTM mediated STAT3 activation is not known, at least in TNBC cases. As *in vitro* data from various studies have suggested important role of STAT3 signaling for survival of TNBC cells, it would be important and therapeutically relevant to investigate whether canonical or noncanonical pathways operate individually or in coordination and mediate the STAT3 function in this subtype of breast cancer.

STAT3 mediates its downstream function only after it forms a homodimer triggered by an extracellular ligand stimulus. Though pY705 mediated STAT3 dimerization is well documented, the role of pS727 and K685 is unclear to-date. Though in 2006 Yuan et.al. reported K685ac as key player in forming stable homodimer of STAT3, the role of pS727 or pY705 in combination with K685 was not tested. Along the line, development of an assay system is important so that individual or coordinated mode of operations via STAT3 PTMs can be distinguished and STAT3 activation from inside the live cells is possible. As very limited assay systems provide such capacity, during this study a focus on developing a sensitive screening platform for STAT3 homodimerization is kept.

Hence to address the above issues related to STAT3 signaling, following objectives were designed:

1. ***To develop a molecular imaging guided experimental model to identify dynamic role of PTMs in STAT3 dimerization and transcriptional control over downstream genes.***
2. ***To identify the association of differentially regulated genes with different PTM status of STAT3.***
3. ***To study the association of STAT3 PTMs (e.g. Y705 and S727 phosphorylation as well as K685 acetylation) with respect to breast cancer outcome.***

Objective 1 is covered in chapter 2, objective 2 and objective 3 are covered in Chapter 3 and 4 of the Thesis, respectively.

Chapter 2

Development of Novel Phospho-STAT3 BRET Sensor

Objective 1: To develop a molecular imaging guided experimental model to identify dynamic role of PTMs in STAT3 dimerization and transcriptional control over downstream genes

2.1 Introduction

The intricate and complex network of signaling from external stimuli to inside the cells is a highly regulated process. Post translational modifications (PTM), including phosphorylation, is the heart of this highly complexed process that controls diverse protein functions in eukaryotes (Prabakaran *et al*, 2012). Many of these protein PTMs also serve as a biomarker for detection and diagnosis of pathological or disease conditions like cancer (Krueger & Srivastava, 2006). In the era of high throughput genomics and proteomics a constant hunt for developing methods or techniques for fast, accurate and sensitive detection of protein PTMs either *in vitro* or *in vivo* is the burning goal (Fonseca *et al*, 2013) .

Among all the signaling cascades controlled by protein phosphorylation, Signal transducer and activator of transcription 3 (STAT3) pathway stands out. STAT3 is a key oncogenic signaling molecule whose activation and inhibition is tightly controlled by phosphorylation and dephosphorylation event (Zhang *et al*, 2007) . Upon ligand surge i.e. IL6, EGF etc. surface receptors (such as EGFR, gp130 respectively) for STAT3 undergoes auto- and cross-phosphorylation events to allow cytoplasmic pool of non-phospho monomeric STAT3 to bind to the receptor through SH2 domain followed by which STAT3 is also phosphorylated at Y705 residue. Thereafter pY705 STAT3 dissociates from the receptor and dimerize with another monomeric pY705 STAT3 via pY705-SH2 domain interaction. Activated STAT3 dimers then translocate to nucleus and function as a transcription factor to control expression of its target genes (Berishaj *et al*, 2007). Under normal biological conditions, activation of STAT3 via pY705 residue is tightly controlled by different phosphatases (PTPs) that rapidly

dephosphorylate STAT3 at Y705 residue leading to its dissociation and cytoplasmic localization (Huang, 2007; Yeh *et al*, 2006). Constitutive activation of STAT3 as detected by pY705 form is reported to be present in many cancers like breast cancer (Hughes & Watson, 2018), oral cancer (Gkouveris *et al*, 2017), melanoma (Kulesza *et al*, 2019), prostate cancer (Don-Doncow *et al*, 2017) as well as in hematological malignancies like CML (Nair *et al*, 2012) . Because of its extensive role in cancer, STAT3 has now become a very promising pharmacological target (Johnston & Grandis, 2011).

Considering the essential role of STAT3 pathway in many cancers, efforts have been made to therapeutically target the STAT3 molecule at multiple levels; either by inhibiting phosphorylation, disrupting homodimerization, preventing binding of STAT3 to DNA or STAT3 nuclear translocation (Johnston & Grandis, 2011). However, considering the significant failures of majority of the STAT3 inhibitors in clinical trials demands for a much more strategic approach. One such key approach is to develop a sensor-based methodology where the biology of STAT3 pathway can be explored more extensively. Efforts have been made in past towards this direction, FRET based STAT3 biosensor has been made using CFP and YFP as partners, to show cytoplasmic-nucleus shuttling kinetics of STAT3 molecules from live cells (Kretzschmar *et al*, 2004). Optical reporter for Y705 residue (Trp564 mutated to 7-hydroxycoumarin-4-yl) is also developed, that specifically shows Y705 phosphorylation upon incubation with Src-kinase only (Lacey *et al*, 2011). BRET (Rluc and EYFP) has also been utilized to demonstrate the existence of STAT3 as a high molecular weight protein complex in cytoplasm prior to EGF treatment, that forms stable homodimers after the ligand stimulation (Schroder *et al*, 2004). However, one of the major drawbacks with existing methods is their inability to be taken forward in a high throughput format. Neither the sensors developed have been validated for their sensitivity on multiple parameters for accurate read out ability of the signaling kinetics from *in vitro* and *in vivo* settings as a unified platform.

Despite so many methods available for detecting protein-protein interactions, BRET (Bioluminescence Resonance Energy Transfer) approach clearly stands out. With high sensitivity, enhanced signal to background ratio and detecting multiple protein interactions in single platform, BRET offers superior advantages than all the existing methodologies (De, 2011). As mentioned previously, BRET works on the principle of resonance energy transfer where upon catalysis of substrate by the donor molecule, the energy of excitation is transferred to the acceptor molecule non-radiatively within a close proximity of 10nm. Since the discovery of BRET many novel luciferase and luciferase variants were subsequently developed for pairing with fluorophores having emission maxima within the detection limit (Abhijit De, 2014; De *et al*, 2013). Nanoluciferase (Nluc), one of the brightest members of luciferase family is a 19KDa monomeric protein derived from parent *oplophorus luciferase.* It is an ATP independent luciferase with stable luminescence and a very high quantum output (England *et al*, 2016). Because of its superior property than existing luciferases, Nluc is currently being utilized extensively for both *in vitro/in vivo* and commercial applications (Boute *et al*, 2016; Machleidt *et al*, 2015).

TurboFP635 or Katushka is a far-red mutant developed from *Entacmaea quadricolor*. It is super bright far red fluorescent protein with high photo stability and fast maturation cycle. With emission maxima beyond 600nm, TurboFP gives less autofluorescence and is a suitable candidate for developing FRET or BRET based PPI interaction sensors (Shcherbo *et al*, 2007).

In the current study, taking advantage of the BRET principle we have designed a very versatile STAT3 protein phosphorylation and homodimerization sensor using Nluc and TurboFP as donor-acceptor pair. With extensive validation, the developed sensor demonstrates its innate ability to work as a reporter system for sensitive measurement of STAT3 activation across multiple different cancer cell types with variable activators or

inhibitors of STAT3 pathway in a live cell format. It also shows excellent compatibility with high throughput screening format and thus holds great potential to be taken forward as drug screening tool or to study STAT3 biology (PTM dependent activation) for therapeutic intervention.

2.2 Materials and Methods

2.2.1 Materials

EGF (#AF-100-15) and IL6 (#200-06) were purchased from Peprotech (USA). Anti-Nluc antibody and plasmid was provided as a generous gift from Promega corporation. Antibodies like anti–total STAT3 (#9139), anti-EGFR blocking antibody (#54359) and anti-pY705 STAT3 (#D3A7) were bought from Cell signaling (USA). Furimazine (#N1110) was procured from Promega and Lipofectamine 2000 (#11668019) transfection reagent was bought from Thermo Fischer. Coelenterazine (native, #C-7001) was purchased from Biosynth International (Switzerland). Inhibitors like Stattic (#S7024), Neratinib (#S2150), Losartan (#S1359) and Fingolimod (#S5002) were purchased from Selleckchem (USA). CI-994(#1742), AR-42 (#2716), Chidamide (#2261) and MS-275 (#1590) were from Biovision (USA). Wortmanin (#W1628), Niclosamide (#N3510), Curcumin (#08511) were from Sigma (USA) and ERK inhibitor U0126 (#9903) was from Cell signaling (USA). Gibco DMEM (#12100046) and RPMI1640 (#31800022) media as well as other growth supplements are from Thermo Fisher, USA. BRET measurements were done using IVIS Spectrum In Vivo Imaging System from Perkin Elmer (USA) equipped with filters ranging from 500-850nm with 20nm bandwidth.

2.2.2 BRET plasmid preparation

Nanoluciferase (Nluc) gene was provided as a generous gift from Promega. For developing pCMV-GGS-Nluc plasmid, full length Nluc gene (516 bp) with stop codon was PCR

amplified flanked with XhoI-BamHI restriction sites and inserted into pCMV-GGS empty vector. TurboFP635 plasmid was purchased from Evrogen. For developing TurboFP-Nluc fusion construct, full length TurboFP gene (711 bp) without stop codon was PCR amplified with restriction sites EcoRI and BglII and inserted at the N-terminus of above prepared pCMV-GGS-Nluc vector. A spatial distance of 12 amino acids is kept constant. pCMV-TurboFP-GGS plasmid was prepared by inserting PCR amplified EcoRI-TurboFP-BglII fragment into empty pCMV-GGS vector.

For STAT3 BRET construct preparation following strategy was adopted. Full length human STAT3 cDNA was PCR amplified from STAT3 (Y705F)-TAL-Luc (gift from Afshin Dowlati, Addgene plasmid # 46933) plasmid without stop codon, flanked with NheI- SalI restriction sites. The amplified NheI-STAT3-SalI (2.3 kb) fragment was then inserted at the N-terminus of pCMV-GGS-Nluc and pCMV-GGS-TurboFP vectors to give pSTAT3-Nluc and pSTAT3-TurboFP fusion constructs with a linker separation of 10 amino acids.pNluc-STAT3 and pTurboFP-STAT3 constructs were prepared by inserting PCR amplified XhoI-STAT3 (Y705F)-BamHI fragment with stop codon at the C-terminus of pCMV-Nluc-GGS and pCMV-TurboFP-GGS vectors. A spatial separation of 12 amino acids is achieved in this orientation. Mutant STAT3 (Y705F) was converted to wild type STAT3 by site directed mutagenesis using following SDM primers:

Forward primer: 5’AGCGCTGCCCCATACCTGAAGACC 3’,

Reverse primer: 5’GGTCTTCAGGTATGGGGCAGCGCT 3’

2.2.3 Cell culture & Transfection

HT1080 and PC3 cells were maintained in DMEM medium (Gibco, USA) with 10% fetal bovine serum (Gibco, USA) and 1% penicillin/streptomycin (Thermo Fischer, USA). MCF7 and A549 cells were cultured in RPMI medium (Gibco, USA) supplemented with 10% fetal

bovine serum (Gibco, USA) and penicillin/streptomycin (Thermo Fischer, USA). All cell lines were maintained in sterile humidified atmosphere at 37ºC with 5% CO_2 supply.

For transfection, cells were seeded at an appropriate number to achieve 70-80% confluency next day. Transfection was performed using Lipofectamine 2000 transfection reagent as per the manufacturer's instructions. For BRET study, donor and acceptor plasmids were transfected in 1:1 ratio with one set of donor alone transfected and untransfected cells. 5-6hrs post transfection, the medium was replaced and cells were maintained at 37ºC with 5% CO_2 supply till further use.

For acceptor stable model generation, HT1080 cells were transfected with STAT3-TurboFP or TurboFP-STAT3 constructs. The clones were selected and maintained using Zeocin (Invitrogen, USA) as mammalian antibiotic selection marker (500µg/ml).

2.2.4 Immunoblotting

Cell were trypsinized, harvested and washed with by 1XPBS. Cell pellet was resuspended in 1X cell lysis buffer containing - 10 mM Tris-HCl (pH 7.5), 140 mM NaCl, 5 mM EDTA, 2mM EGTA, 100mM NaF,100mM Na_3VO_4 ,100mM PMSF and protease inhibitor cocktail. Lysis was performed by sonication method at 10% amplitude with 10sec on/off cycle. The sample was centrifuged at 14000rpm/30min/4ºC and supernatant was collected in separate tube. Protein estimation was done using Bradford reagent and approx. 50-60µg protein was loaded on 7.5% SDS-PAGE gel. Protein transfer was done in semidry Trans blot assembly at 15V for 1hr at room temperature. Blocking was performed in 5% non-fat dry milk for 1hr at room temperature followed by primary antibody incubation [STAT3 1:1000, pY705 STAT3 1:500, pS727 STAT3 1:1000, α-Tubulin 1:1000] overnight/4ºC. Next day, secondary-HRP antibody treatment was given followed by developing the blot using ECL substrate in ChemiDoc system (Biorad, USA).

2.2.5 Real time PCR

Total RNA from the cells was extracted using RNA extraction minikit (QIAGEN). 2µg RNA was used for preparation of cDNA using SuperScript III (Invitrogen) kit as per the manufacturer's instructions. Real time PCR was done using Sybr green reagent and GAPDH was used as normalization control. Primer sequence for EGFR and GAPDH gene is as follows:

EGFR Fwd : 5' AGGCACAAGTAACAGGCTCAC ;

EGFR Rev: 5'AAGGTCGTAATTCCTTTGCAC

GAPDH Fwd : 5' TGCACCACCAACTGCTTAGC;

GAPDH Rev: 5'GGCATGGACTGTGGTCATGAG

2.2.6 Fluorescence microscopy

For fluorescence microscopy, HT1080 cells stably expressing TurboFP-STAT3 or STAT3-TurboFP construct were seeded onto a coverslip at a confluency of 70-80%. Next day, cells were fixed with 4% paraformaldehyde at 37ºC/ 10mins and stained with DAPI to mark the nucleus. Images were acquired in Zeiss LSM 780 Confocal Microscope (Germany) at 633nm filter for TurboFP and 460nm filter for DAPI.

2.2.7 Live cell luciferase Imaging

For live cell luciferase imaging, HT1080 cells expressing Nluc-STAT3 or STAT3-Nluc constructs were seeded at a density of 10,000 or 20,000 cells per well (in duplicates) in a black well plate with clear bottom using 100µl culture medium volume. After the cells were adhered, 50µl furimazine substrate (1:1000 diluted in culture medium) was added to each well and signal was acquired in 500nm (donor channel) filter with integration time of 1sec in

IVIS spectrum. Post-acquisition, ROI was drawn on individual well to determine the average radiance signal.

2.2.8 BRET imaging and calculation

24-30hrs post transfection, untransfected, donor alone, donor-acceptor transfected cells were trypsinized and seeded at required cell number in 96 black well plate with clear bottom (in duplicate) in 100µl medium volume. Next day, 50µl furimazine (1:1000 diluted in medium) was added to each well and spectral scan was performed in IVIS spectrum from 500-680nm±20 filter range with integration time of 1sec/filter.

For STAT3 Phospho-BRET study, 30hrs post transfection, donor alone (Nluc-STAT3/STAT3-Nluc), donor + acceptor (Nluc-STAT3/STAT3-Nluc +Turbo-STAT3/STAT3-Turbo) expressing cells were seeded at a cell number of 20,000 cell /well in 96-black well plate or 5000 cell/well for 384 black well plate, with clear bottom in serum negative medium. 24hrs post serum starvation, 50µl furimazine substrate (1:1000 diluted in serum negative medium) was added to each well and cells were stimulated with or without EGF/IL6 in variable concentration. For EGFR blocking assay, 24hrs post serum starvation, cells were incubated with EGFR blocking antibody (1:100 dilution) for 4hrs at 37ºC followed by EGF or substrate addition. While for inhibitor related studies, serum starved cells were incubated with respective drug concentrations for 24hrs prior before adding ligand and luciferase substrate.

Immediately after ligand stimulation signal was acquired in donor (500nm) and acceptor (640nm) filter sets with acquisition time of 30sec/filter using IVIS spectrum. ROI was drawn on each well and Average radiance was determined in both donor and acceptor filters. BRET ratio was calculated by using following equation (Dimri *et al*, 2016; Dragulescu-Andrasi *et al*, 2011):

$$\text{BRET Ratio} = \frac{BL_{emission}\,(\text{Acceptor } \lambda) - C_f \times BL_{emission}\,(\text{Donor } \lambda)}{BL_{emission}\,(\text{Donor } \lambda)}$$

$$\text{where, } Cf = \frac{BL_{emission}\,(\text{Acceptor } \lambda)_{\text{donor only}}}{BL_{emission}\,(\text{Donor } \lambda)_{\text{donor only}}}$$

2.2.9 *In vivo* BRET study

All animal experiments were approved and performed in compliance with the standard protocols for animal care and handling designed by the Institutional animal ethics committee (IAEC). Briefly, $3X10^6$ luciferase labelled HT1080 cells (Nluc only or TurboFP-Nluc) were implanted subcutaneously onto the dorsal right flank of 6-8 weeks old nude mice (N=3). Donor only cells (Nluc) were implanted near upper right shoulder while donor-acceptor fusion cells (TurboFP-Nluc) were injected onto the lower right side of the back. 30mins post implantation, 100µl furimazine substrate (1:20 diluted in saline) was injected intraperitoneally. The mice were anesthetized in 2.5% (vol/vol) gaseous isoflurane in oxygen. Bioluminescence signal was captured in both donor (500nm) and acceptor (640nm) filters with 60sec integration time/filter settings in IVIS spectrum. BRET ratio and double ratio (DR) were calculated by drawing ROI (region of interest) on the subject and determining the average radiance. BRET ratio was calculated as mentioned above (2.2.8), while following equation was employed for calculating the double ratio (Dragulescu-Andrasi *et al*, 2011) (Abhijit De, 2014):

$$DR = \frac{\left(\frac{BL_{\text{acceptor channel}} \times \mu_t(\text{acceptor channel})}{BL_{\text{donor channel}} \times \mu_t(\text{donor channel})}\right)_{\text{Donor + Acceptor}}}{\left(\frac{BL_{\text{acceptor channel}} \times \mu_t(\text{acceptor channel})}{BL_{\text{donor channel}} \times \mu_t(\text{donor channel})}\right)_{\text{Donor alone}}}$$

Where, μ_t is total attenuation coefficient. Here, DR is independent of μ_t.

2.2.10 Statistical analysis

For all statistical analysis student t-test was used (paired and two tailed), where p-value <0.05 was considered as statistically significant.

2.3 Results

2.3.1 Nanoluc (NLuc) and TurboFP635 as suitable pair for *in vitro* and *in vivo* BRET studies

Nluc being a very bright luciferase with very high quantum output, while TurboFP is a red shifted fluorophore with emission maxima beyond 600nm (as compared to mOrange or TagRFP) made them an obvious choice for development of BRET pair **(Figure 2.1A)**. Hence fusion construct of Nluc and TurboFP was established in previously optimized dipole orientation i.e. TurboFP-Nluc with a flexible GGS linker separation of 12 a.a. **(Figure 2.1B)**. In order to determine the compatibility of NLuc to serve as donor for TurboFP acceptor, we overexpressed TurboFP-NLuc (fusion protein), TurboFP+ NLuc (separate plasmids) and

NLuc only (donor alone) plasmids in HT1080 cells. Upon utilizing furimazine as substrate, NLuc was able to sufficiently excite TurboFP in fusion protein only, resulting in acceptor emission peak at 640nm **(Figure 2.1C)**. While no such emission peak was obtained when both NLuc and TurboFP were co-expressed individually. Further, because of minimal bleed through from Nluc to acceptor channel and high spectral resolution, the BRET ratios obtained for TurboFP-Nluc fusion was (189.98mBu±0.015) significantly high ($p<0.001$) as compared to donor alone or donor + acceptor co-transfected cells (9.64mBu±0.031 and 10.63mBu±0.040 respectively) **(Figure 2.1D)**. These results confirm the fact that both Nluc and TurboFP are not naturally interacting partners and energy transfer from Nluc to TurboFP will not happen until they are in vicinity of physiological interaction (less than 10nm) as achieved with GGS linker separation. Additionally, it also shows that BRET is strictly a proximity dependent assay that is unaffected by overcrowded protein mediated non-specific interaction.

Further to confirm that the strength of BRET signal does not change upon stable or transient expression of the BRET components, we developed HT1080 cells stably expressing TurboFP-Nluc or Nluc alone plasmids and compared them with transient expression system. As expected, the BRET ratios and spectral behavior of the donor-acceptor molecules obtained in transient expression (186.98mBu±0.012) did not change significantly upon stable expression of the BRET constructs (211.96mBu±0.040) **(Figure 2.1E-F)**. Hence, both Nluc and TurboFP are suitable as a pair for development of BRET system.

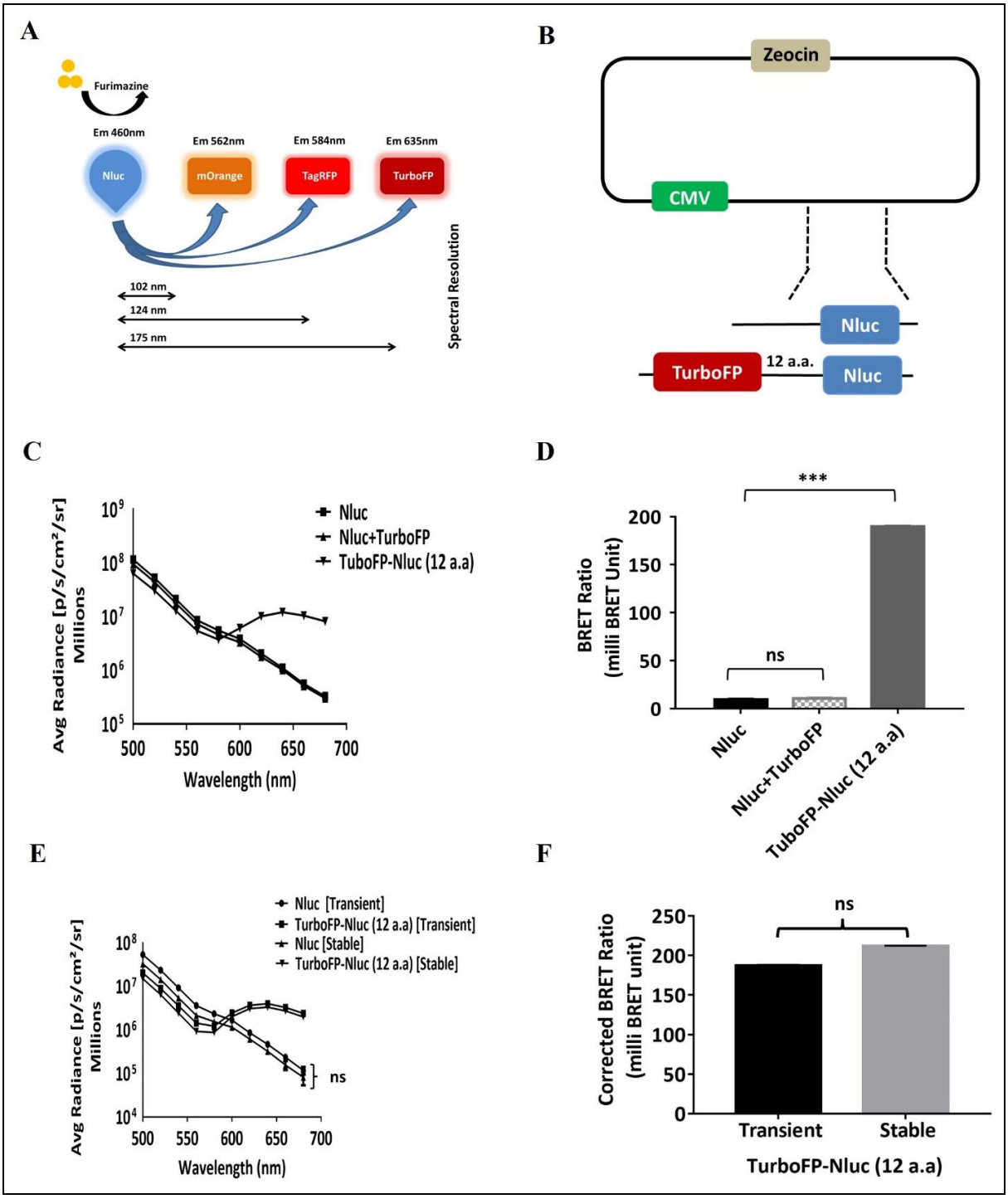

Figure 2.1. Establishment of Nluc and TurboFP as optimal BRET pair. *(A) Schematic representation of spectral separation between emission maxima of Nluc as donor and emission wavelength of different red shifted fluorophores (mOrange, TagRFP or TurboFP). (B) Diagrammatic representation of pCMV vector expressing Nluc alone or in fusion with TurboFP having a spatial separation of 12 a.a. GGS linker (Gly-Gly-Ser) repeat. (C) Spectral scan of HT1080 cells expressing*

*Nluc alone, Nluc+ TurboFP co-transfected or TurboFP-Nluc fusion constructs from 500-680nm ± 20nm filter range using furimazine substrate. (D) BRET ratios calculated for the constructs in (C). (E) Spectral scan of HT1080 cells expressing Nluc or TurboFP-Nluc either stably or with transient transfection. (F) Corrected BRET ratio graph for constructs in (E). For all BRET studies Nluc emission was measured at 500nm and TurboFP at 640nm using furimazine as substrate in IVIS spectrum with integration time of 1s/filter. Each graph represents mean value ± SEM. Significance levels are *p< 0.05, **p< 0.01, ***p< 0.001 and ns as non-significant.*

Finally, to determine the compatibility of TurboFP-Nluc pair for detecting PPI even from deep tissues, we implanted HT080 cells stably expressing Nluc only (upper flank) or TurboFP-Nluc (bottom flank) onto the dorsal right flanks of nude mice. Upon intraperitoneal injection of furimazine substrate, the BRET signal was captured in respective donor (500nm) and acceptor filters (640nm) **(Figure 2.2A-B)**. The corrected ratios (bleed through subtracted signal) obtained for *in vivo* BRET (0.6±0.002mBU) were 3-fold higher ($p<0.001$) as compared to *in vitro* BRET values (0.18±0.001mBU). The difference in BRET ratios obtained for same donor-acceptor pair (TurboFP-NLuc) is due to difference in attenuation of light for short wavelength emission under two different experimental set up (live cells versus *in vivo*). Hence, double ratio (DR) was calculated. DR analysis does not depend upon μt i.e. total attenuation coefficient, hence signal attenuation from acceptor emission is minimised. A similar DR values obtained for BRET from live cells (12.07±0.50mBu) and living subject (13.30±0.24mBu) indicates that both Nluc and TurboFP mediated interactions are ratiometric and they can function as superior BRET pair for detecting PPI events even from *in vivo* biological system **(Figure 2.2C)**. Based on above observations, we selected Nluc and TurboFP as suitable pair for development of STAT3 BRET sensor.

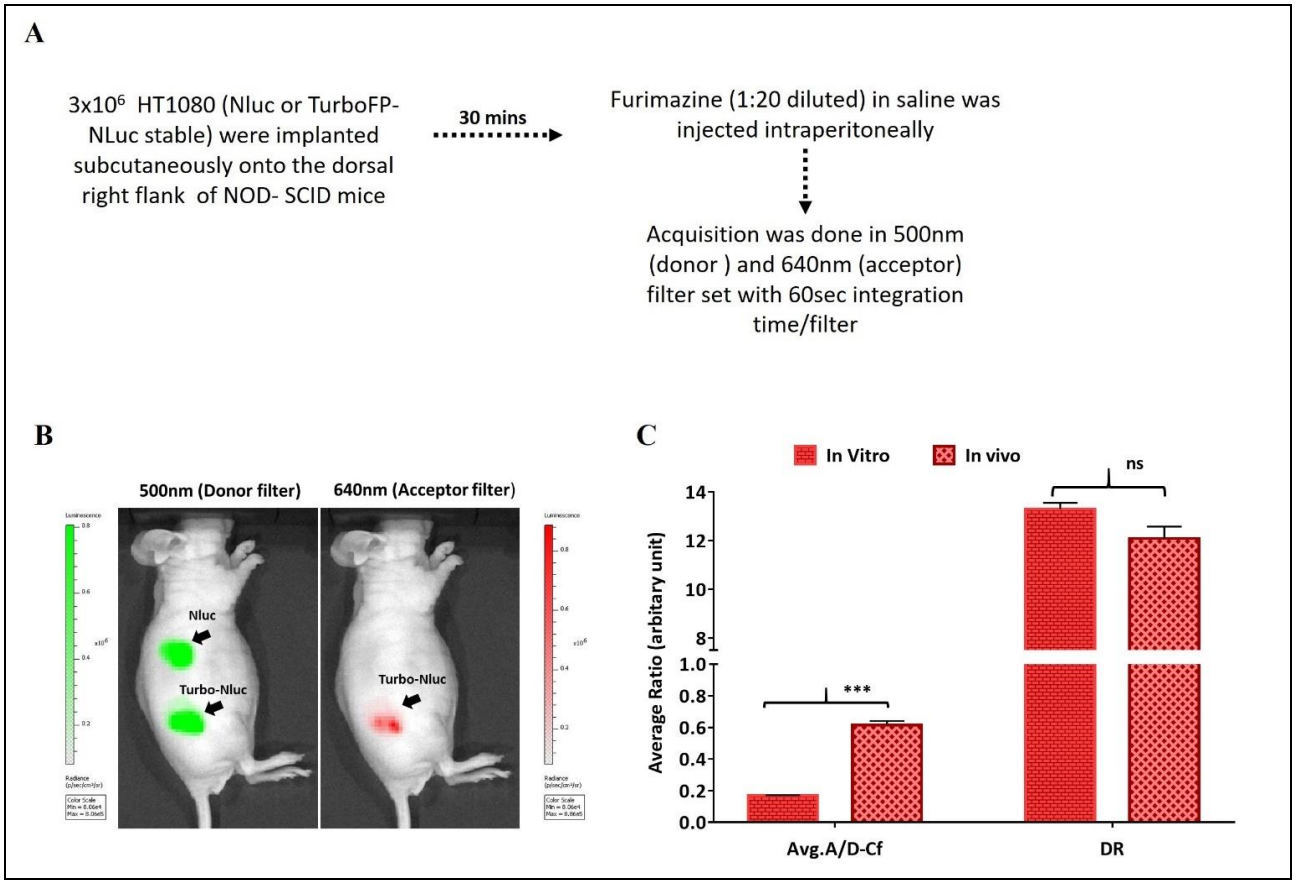

Figure 2.2. In vivo validation of TurboFP-Nluc as suitable BRET pair. *(A) Schematic work flow for performing in vivo BRET with TurboFP-Nluc BRET pair. (B) Representative image of nude mice expressing Nluc alone (top) or TurboFP-Nluc fusion protein (bottom) in respective donor and acceptor channel. Image acquisition was done in IVIS spectrum using furimazine substrate with integration time of 60sec/filter. (C) Graph comparing the BRET ratio and double ratio as determined from in vitro or in vivo BRET assay system. For all BRET studies Nluc emission was measured at 500nm and TurboFP at 640nm using furimazine as substrate in IVIS spectrum with integration time of 1s/filter. Each graph represents mean value ± SEM. Significance levels are *p< 0.05, **p< 0.01, ***p< 0.001 and ns as non-significant.*

2.3.2 Development of Phospho-STAT3 BRET sensor

With the selection of optimal donor-acceptor pair for BRET system, we next cloned STAT3 in fusion with respective reporter genes i.e. nanoluc (donor) and TurboFP635 (acceptor) in

two different orientations i.e. N-terminus and C-terminus. A total of four such different orientation combinations were established for selecting the best BRET partners for future studies **(Figure 2.3A)**. Briefly, the principle on which this sensor works is that, in the absence of any ligand for STAT3 pathway, STAT3 is inactive and hence remain majorly in monomeric state in cytoplasm. As a result of which Nluc and TurboFP will be located at a distance beyond physiological interaction and feasibility of resonance energy transfer. Adding luciferase substrate in this condition will only result in signal from donor channel due to catalysis of substrate by luciferase enzyme, with no resulting emission form acceptor filter. However, upon addition of specific ligand that triggers STAT3 phosphorylation, stable homodimers of STAT3 will be formed where both Nluc and TurboFP will achieve closest proximity (<10nm). Adding luciferase substrate in this condition will give signal from two different filters; donor (500nm) filter due to luciferase-substrate reaction and acceptor (640nm) filter due to excitation of acceptor via transfer of energy from donor molecule **(Figure 2.3B)**. The BRET ratios calculated will give precise judgement of STAT3 homodimerization event with substantial deduction of donor bleed through signal.

Following the development of STAT3 BRET constructs, primary validation for functionality of the fusion protein was performed. Live cell luciferase assay with donor-STAT3 constructs showed that fusing Nluc with STAT3 does not affects its ability to catalyse furimazine substrate and that both the STAT3 constructs give functional luciferase signal **(Figure 2.3C)**. Further to determine that the fusion proteins are stable and fully translated, we overexpressed the four-STAT3 BRET constructs in HT1080 cells. Immunoblotting for total and pY705 STAT3 marks confirmed proper fusion protein translation while pY705 levels indicated that the fusion- STAT3 is equally recognized and activated by the endogenous cellular machinery **(Figure 2.3D)**.

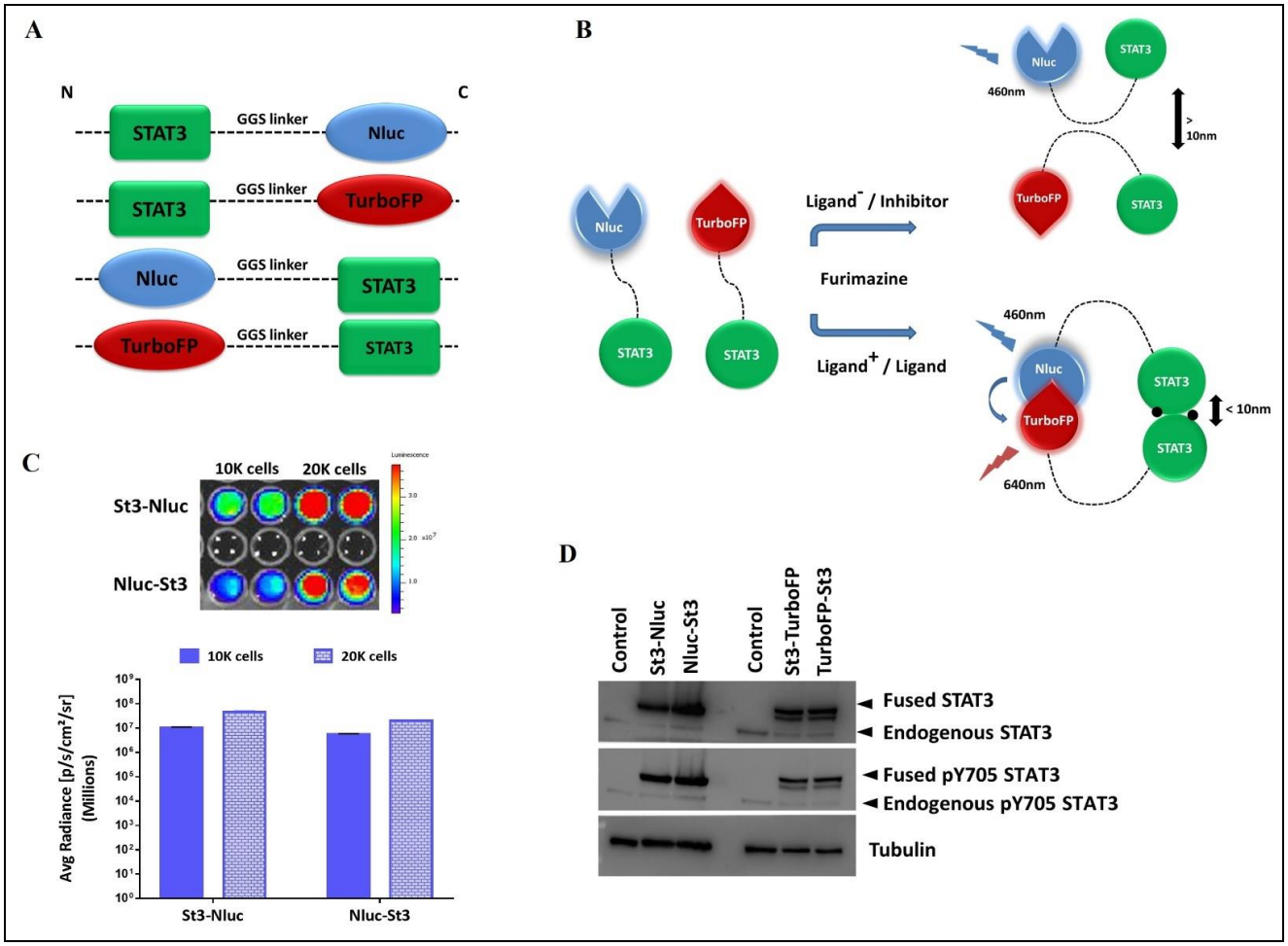

Figure 2.3. Development of Nluc and TurboFP based Phospho STAT3 BRET Sensor. *(A) Diagrammatic representation of STAT3 BRET constructs prepared by fusing with Nluc or TurboFP in different orientations. (B) Schematic depiction for working model of STAT3 BRET sensor. In the absence of ligand or presence of inhibitor the two STAT3 molecules will be in monomeric state, as a result of which upon luciferase substrate addition the energy of excitation from donor moiety will not be transferred to the acceptor fluorophore. Hence, signal will be seen only in donor channel. However, in the presence of stimulating ligand, the two STAT3 molecules will dimerize as a result of which both Nluc and TurboFP will achieve closest proximity of natural interacting distance. In this case, upon substrate addition, the energy of excitation will be successfully transferred to the acceptor molecule and we will get two resultant signals; one from donor filter and the other from acceptor filter. (C) Representative plate image of live cell luciferase assay for HT1080 cells expressing Nluc-STAT3 or STAT3-Nluc seeded at two different cell density (in duplicates), performed in open filter*

settings using furimazine substrate. Bottom graph represents average luciferase signal calculated from each well for individual constructs. (D) Immunoblot of HT1080 cells expressing all the four STAT3 BRET constructs, probed for total and pY705 STAT3 levels. Untransfected parental HT1080 cells were used as control. Each graph represents mean ± SEM value, error bars represent SEM.

For determining the optimal dipole orientation where Nluc and TurboFP will be in closest proximity upon STAT3 homodimerization event, we overexpressed the STAT3 BRET pairs in all the possible combinations i.e. Nluc-STAT3+TurboFP-STAT3, Nluc-STAT3+STAT3-TurboFP, STAT3-Nluc+STAT3-TurboFP and STAT3-Nluc+ TurboFP-STAT3, in HT1080 cells **(Figure 2.4A)**. The cells expressing the STAT3 BRET pairs were stimulated with variable EGF concentrations (0-100ng) and BRET ratio was determined as mentioned in **Materials and Methods section 2.2.8**. Within 5mins of EGF treatment, a significant gain in BRET ratio was achieved for the all the orientations tested (except St3-Nluc+TurboFP-St3) **(Figure 2.4B)**. The BRET signal measured for a duration of 60mins scan showed a stable STAT3 activation profile **(Figure 2.4C)**. However, of all the orientations screened, the C-terminally STAT3 oriented dipole pair i.e. Nluc-STAT3+TurboFP-STAT3 showed a maximum gain in BRET ratio (2.33mBu, $p<0.01$ for 100ng EGF) with dose dependent increment in BRET signal.

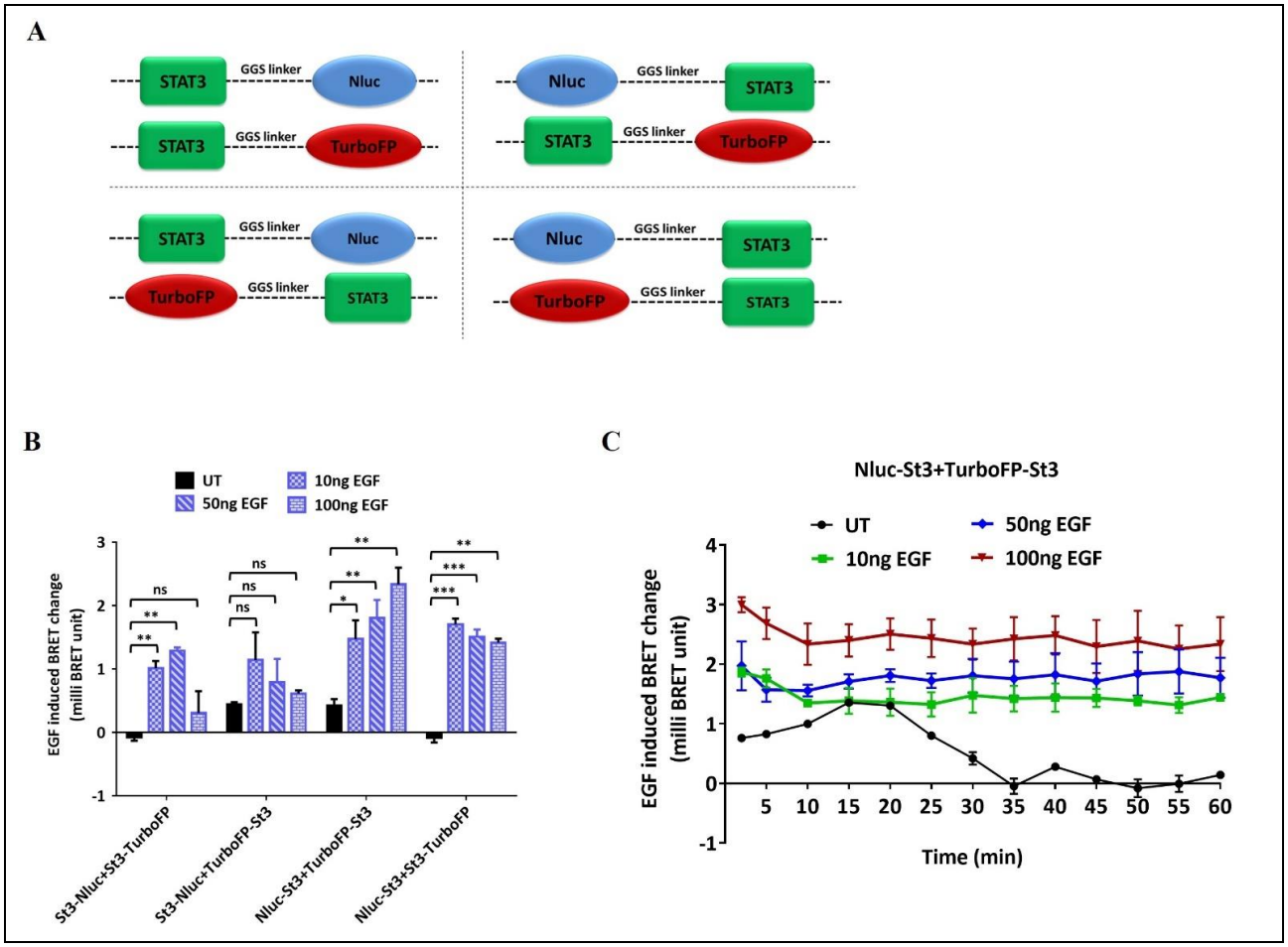

Figure 2.4. Defining optimal orientation of Phospho STAT3 BRET Sensor. *(A) Schematic representation of probable four combination of dipole orientations developed for STAT3 BRET sensor. (B) Corrected BRET ratio graph of HT1080 cells expressing the four different dipole orientations of STAT3 constructs 30mins post EGF treatment at variable concentrations. (C) Time kinetic graph of BRET ratio change for all the four combinations, post EGF trigger for a duration of 60mins. For all BRET studies Nluc emission was measured at 500nm and TurboFP at 640nm using furimazine as substrate in IVIS spectrum with integration time of 30s/filter. Each graph represents mean value ± SEM. Significance levels are *p< 0.05, **p< 0.01, ***p< 0.001 and ns as non-significant.*

Further, to ensure that the gain obtained in BRET signal is a true representation of EGF induced STAT3 phosphorylation - homodimerization event, we expressed STAT3 BRET

construct in HT1080 cells and determined the pY705 activation levels simultaneously along with BRET signal kinetics. Over here we observed that the EGF induced STAT3 BRET signal is maximum at 2hrs post EGF trigger and declined subsequently to basal level by 24hrs **(Figure 2.5A-B)**. Immunoblotting for the levels of activated and total STAT3 also followed the similar trend where pY705 STAT3 activation peaked to maximum at 2hrs and fell down gradually to basal level by 24hrs **(Figure 2.5C)**. This indicates that EGF induced STAT3 phosphorylation precedes homodimerization of STAT3 molecule and a subsequent gain in Phospho-BRET signal is thus obtained.

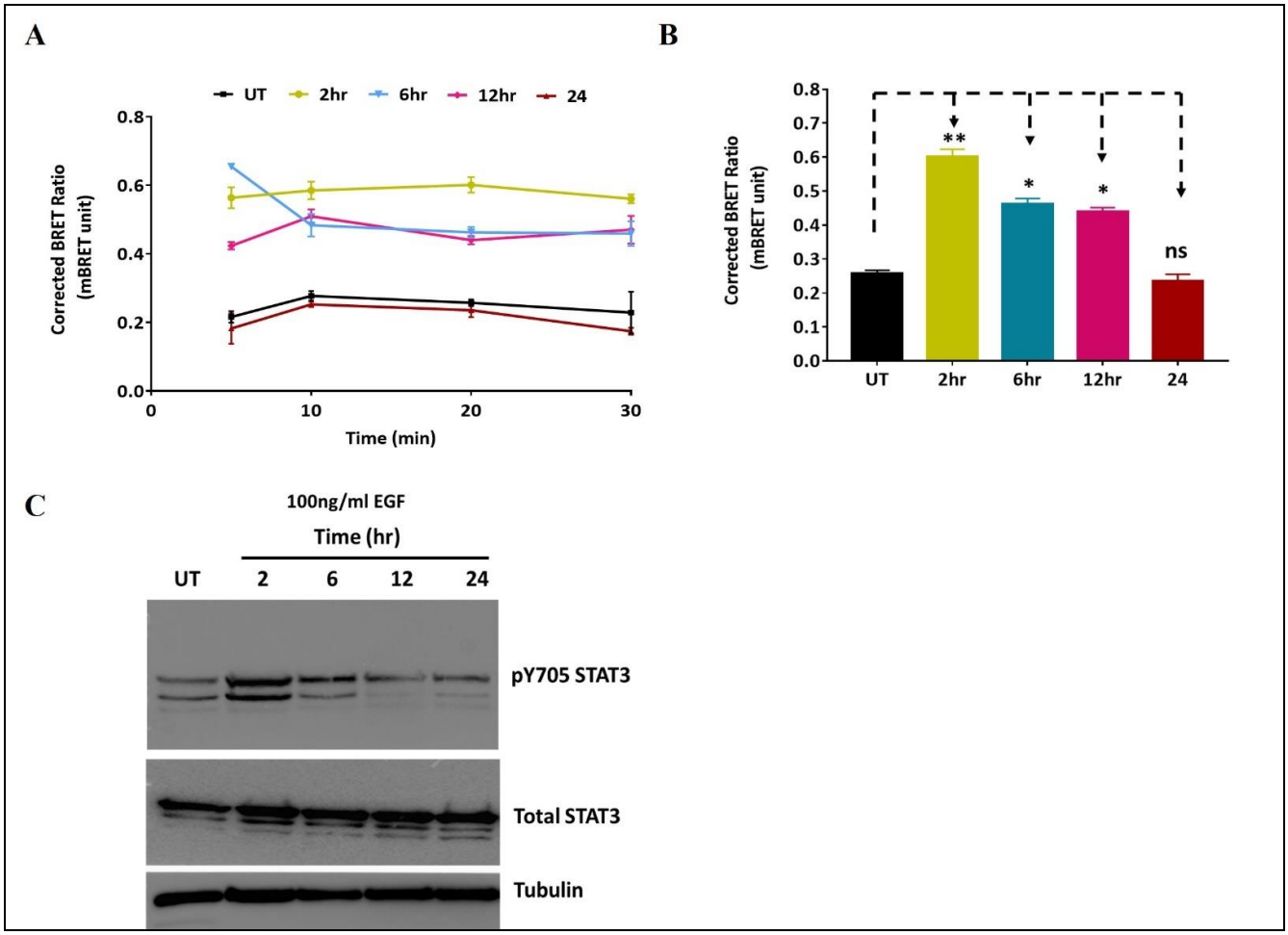

Figure 2.5. Determining STAT3 activation kinetics using Phospho STAT3 BRET Sensor. *(A) Dynamics of BRET ratio changes in HT1080 cells expressing STAT3 BRET sensor post 100ng EGF*

*treatment at different time points. (B) Corrected BRET ratio graph (for 20mins time point) for samples in (A) treated with EGF at variable time points. Untreated cells were taken as control for basal BRET ratio determination. (C) Immunoblot of HT1080 cells expressing Nluc-STAT3 construct and treated with EGF for respective time points before lysate preparation. Blots were probed for total and activated pY705 STAT3 levels. Tubulin was used as loading control. For all BRET studies Nluc emission was measured at 500nm and TurboFP at 640nm using furimazine as substrate in IVIS spectrum with integration time of 30s/filter. Each graph represents mean value ± SEM. Significance levels are *p< 0.05, **p< 0.01, ***p< 0.001 and ns as non-significant.*

2.3.3 Validation of Phospho-STAT3 BRET sensor across different STAT3 genetic background of cell

Following the initial screen of STAT3 BRET constructs in STAT3 positive HT1080 cells, we further validated the developed STAT3 sensor in different genetic backgrounds (i.e. STAT3 null or acceptor-STAT3 fusion stable cells) to address whether the endogenous pool of STAT3 has any effect on the BRET ratios.

PC3 is a prostate cancer cell line reported to be null for STAT3 expression and hence an appropriate model for our validation **(Figure 2.6A)**. When STAT3 fusion constructs in different orientations were overexpressed in PC3 cells, similar to HT1080, a positive gain in BRET signal was evident in all the tested orientations. The increase in BRET signal was obtained within 2mins of ligand addition and continued for upto 1hr of spectral scan performed. The activation kinetics of both STAT3 high-HT1080 and STAT3 null-PC3 cells remained same however the basal BRET ratio obtained in case of PC3 cells was high(0.77mBu±0.002 PC3; 0.42mBu±0.010 HT1080 UT condition), indicating that in HT1080 cells the endogenous pool is able to compete with or quench a part of BRET STAT3 molecules **(Figure 2.6B-D)**. However, the difference in basal BRET ratio did not affect the

maximum BRET signal achieved. Similar to HT1080, in PC3 cells also the N-terminus combination of Nluc/Turbo with STAT3 worked out best with maximum attainment of BRET signal in an EGF concentration dependent manner (2.10 mBu±0.011, $p<0.01$) than rest of the combinations **(Figure 2.6E)**.

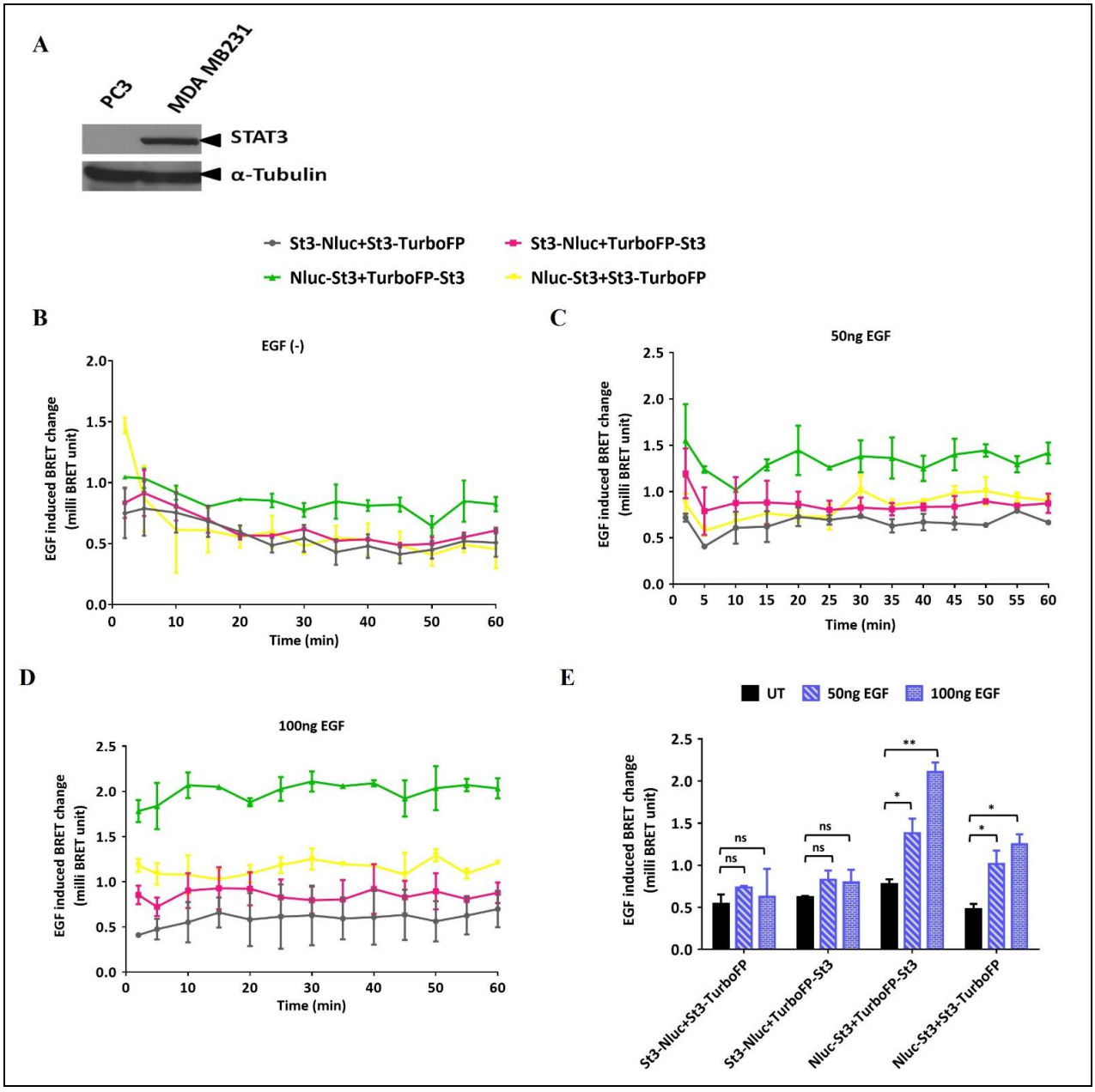

Figure 2.6. Validating Phospho STAT3 BRET in STAT3 null background. *(A) Immunoblot of PC3 cells probed for total STAT3 protein expression. MDA MB 231 cells were taken as positive control for*

*STAT3 protein and tubulin as loading control. (B-D) Dynamics of BRET ratio change for PC3 cells expressing STAT3 BRET constructs in different dipole orientations, upon EGF trigger (0-100ng). Acquisition was performed in every 5mins for a duration of 60mins post EGF stimulation. (E) Corrected BRET ratio graph for all the constructs in (B-D) at 30mins post EGF trigger. For all BRET studies Nluc emission was measured at 500nm and TurboFP at 640nm using furimazine as substrate in IVIS spectrum with integration time of 30s/filter. Each graph represents mean value ± SEM. Significance levels are *p< 0.05, **p< 0.01, ***p< 0.001 and ns as non-significant.*

For performing the above BRET assays, we had transiently transfected both donor and acceptor plasmids fused to STAT3 in the model cell line. To further affirm that the orientations that did not show significant induction upon EGF trigger is not due to experimental or technical flaw of transfection and to see whether we can achieve higher BRET ratio we engineered acceptor stable i.e. TurboFP-STAT3 and STAT3-TurboFP HT1080 cells **(Figure 2.7A)**. Upon transfecting the donor counterparts in acceptor stable cell background, we observed that again Nluc-STAT3+TurboFP-STAT3 orientation showed maximum BRET signal gain [1.61mBU ($p<0.05$)] upon EGF trigger then rest of the orientations. Though , the kinetics of STAT3 BRET signal gain in transient versus acceptor stable HT1080 cells remained same, the highest BRET ratio was achieved even at lowest EGF concentration (10ng) in stable background **(Figure 2.7B-C)**.Hence based on above observation, Nluc-STAT3+TurboFP-STAT3 orientation was selected as final orientation for Phospho-STAT3 BRET sensor establishment.

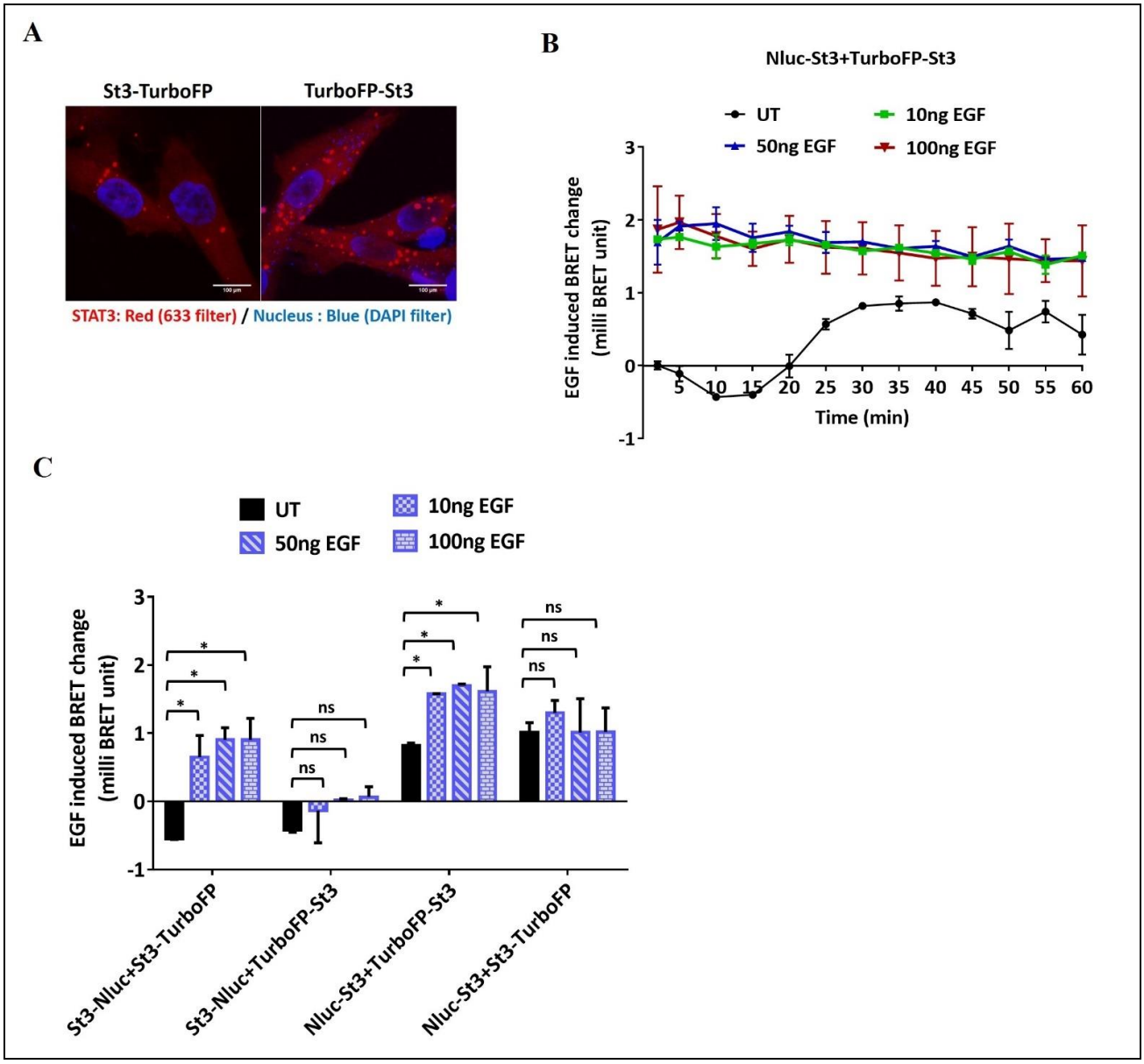

Figure 2.7. Validating Phospho STAT3 BRET in acceptor stable cells. *(A) Fluorescence microscopy images of HT1080 cells stable expressing STAT3-TurboFP or TurboFP-STAT3 constructs. Cells were stained with DAPI to mark nucleus. TurboFP signal was acquired in 633nm filter and DAPI at 460nm. (B) Kinetics of BRET ratio changes in acceptor stable HT1080 cells expressing donor-STAT3 constructs in different orientations, upon EGF treatment. (C) Corrected BRET ratio graph for constructs in (B) at 30mins time point post EGF treatment. For all BRET studies Nluc emission was measured at 500nm and TurboFP at 640nm using furimazine as substrate in IVIS spectrum with integration time of 30s/filter. Each graph represents mean value ± SEM. Significance levels are *p< 0.05, **p< 0.01, ***p< 0.001 and ns as non-significant.*

2.3.4 Validation of Phospho-STAT3-BRET sensor across multiple cancer cell types and with different ligands

Following thorough validation of developed Phospho-STAT3 BRET sensor on multiple parameters for selecting optimal orientation. We next sought to determine, whether the STAT3 phosphorylation sensor can detect activation of STAT3 pathway mediated by other receptors apart from EGFR and whether it can work as a sensing model for capturing STAT3 activation across different cancer cell types.

To test verify this we overexpressed the Phospho-STAT3 BRET constructs in panel of multiple cancer cell lines; HT1080 (Fibrosarcoma), PC3 (Prostate cancer), A549 (Adenocarcimomic human alveolar basal epithelial cells) and MCF7 (Breast cancer), and triggered STAT3 activation using IL6, another potential ligand of STAT3 pathway. Irrespective of differential endogenous STAT3 level and biological background of cancer cell line, the Phospho-STAT3 BRET sensor precisely captured the STAT3 activation phenomenon across all the tested model cell lines; HT1080 [2.14 mBU, $p<0.01$], PC3 [2.3mBU, $p<0.05$], MCF7 [1.57mBU< $p<0.05$] and A549 [4.43mBU, $p<0.01$] using 10ng IL6 **(Figure 2.8A-D)**. The activation of STAT3 as observed previously with EGF, was triggered within 2mins of IL6 addition and continued for upto 1hr in PC3 cells **(Figure 2.8B)**. For all the BRET experiments, 100ng EGF treated sample was taken as a positive control. Further the increment obtained in BRET signal showed a dose dependent pattern with IL6 concentration, except in case of MCF 7 cells. Surprisingly, pertaining to its potency, IL6 turned out to be a better ligand for STAT3 pathway than EGF, as it could achieve BRET ratio similar to EGF treatment with even 10-fold lower ligand concentration [HT1080- 10ng IL6 (2.14mBU) and 100ng EGF (2.20mBU)].

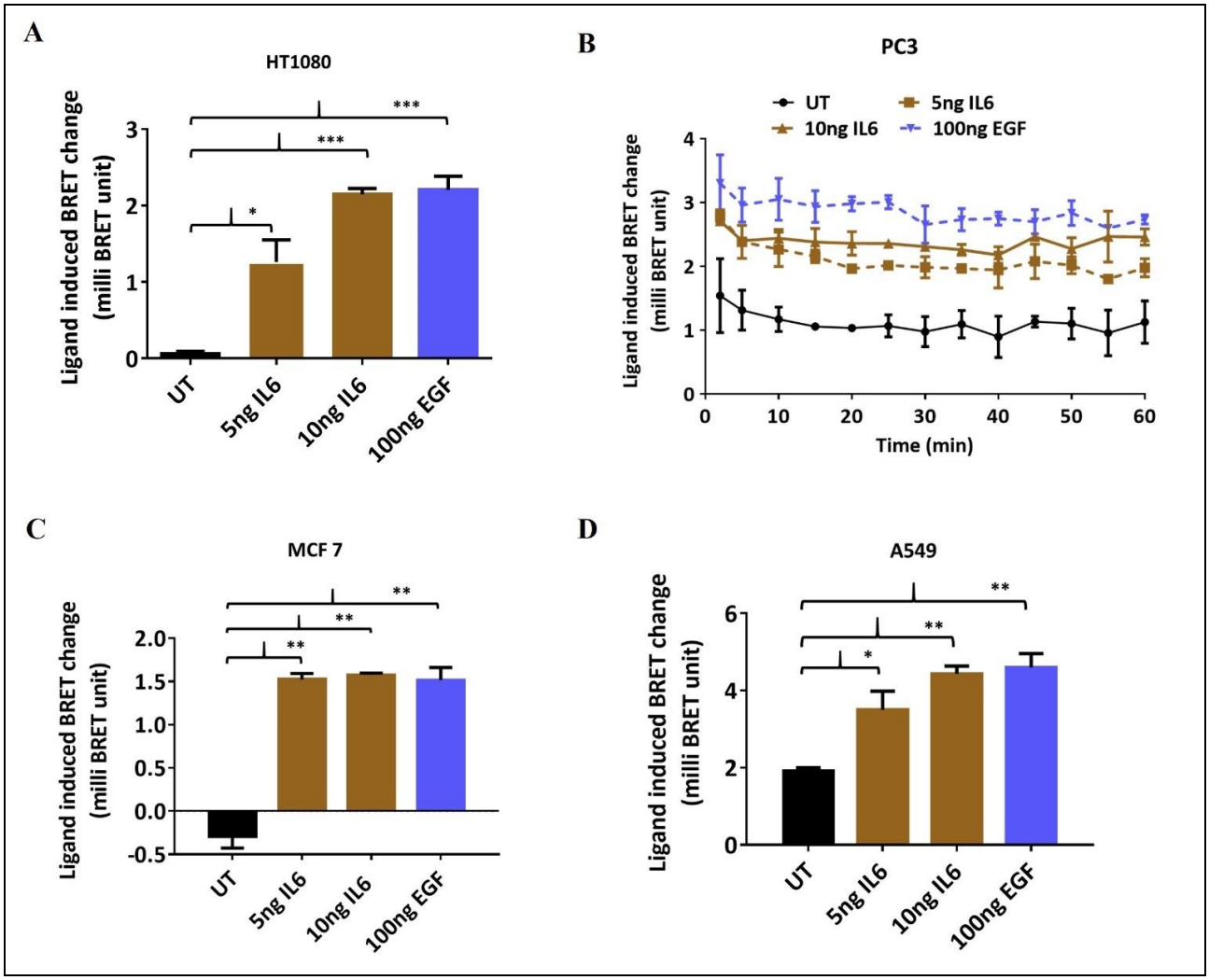

Figure 2.8. IL6 induced STAT3 activation across multiple different cancer cell lines. *(A) Corrected BRET graph for HT1080 cells expressing STAT3 BRET sensor in response to IL6 treatment at different concentrations. 100ng EGF treated set was used a positive control. (B) Dynamics of BRET ratio changes for a duration of 60mins post IL6 treatment at variable concentrations. (C-D) Corrected BRET ratio graph for MCF 7 and A549 cells respectively, upon treatment with IL6 at different concentrations. For all BRET studies Nluc emission was measured at 500nm and TurboFP at 640nm using furimazine as substrate in IVIS spectrum with integration time of 30s/filter. Each graph represents mean value ± SEM. Significance levels are *p< 0.05, **p< 0.01, ***p< 0.001 and ns as non-significant.*

Further, the difference in BRET ratios obtained across multiple cancer cell line-MCF7, PC3, A549 and HT1080 cells, despite using same EGF concentration indicated that the EGFR receptor expression might plays a key role in affecting the level of STAT3 activation achieved. Hence, quantitative assessment for EGFR mRNA transcript level and comparative analysis of BRET ratio gain in individual model cell line was performed **(Figure 2.9A)**. Over here we observed that the levels of EGFR transcript and BRET ratio gain in respective cell line showed a similar trend **(Figure 2.9B)**. The cells with high EGFR expression (A549) has significantly higher BRET ratio (4.17mBU) as compared to the low EGFR [MCF7 (1.48mBU) and HT1080 (2.20mBU) expressing cell line ($p<0.05$). PC3 though has EGFR levels similar to A549 but due to genetically STAT3 null condition it was unable to achieve BRET ratio similar to A549 ($p<0.05$). Collectively, the observations made from above experiments highlights the versatile nature, inherent strength and high sensitivity of the Phopsho-STAT3 BRET sensor as a live cell read out tool for STAT3 pathway activation.

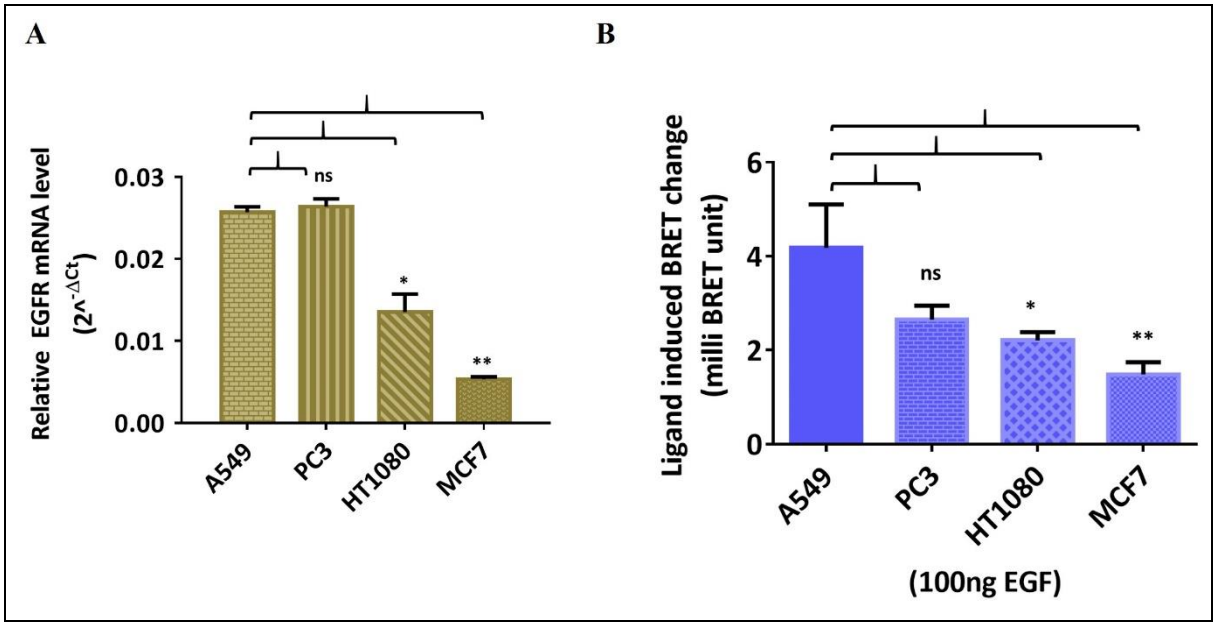

Figure 2.9. Effect of EGFR expression on STAT3 BRET signal. *(A) Quantitative real time PCR analysis of relative EGFR transcript levels across all the model cell lines used. GAPDH was used as normalization control. (B) Corrected BRET ratio graph for different cancer cell lines in response to*

*100ng EGF treatment. For all BRET studies Nluc emission was measured at 500nm and TurboFP at 640nm using furimazine as substrate in IVIS spectrum with integration time of 30s/filter. Each graph represents mean value ± SEM. Significance levels are *p< 0.05, **p< 0.01, ***p< 0.001 and ns as non-significant.*

2.3.5 Phospho-STAT3 BRET sensor sensitively detects augmentation in STAT3 activation signaling

Wide application of any biosensor depends upon its utility to sensitively report perturbation in the respective signaling pathway. Hence, with the thorough validation for ability of Phospho-STAT3 BRET sensor to detect activation of STAT3 signaling in a real time manner, we next questioned whether it can equally read the blockade of the STAT3 pathway too. To determine this, we subjected our developed sensor to treatment with different STAT3 inhibitors or specific pathway blockers.

For this we selected two different STAT3 inhibitors; Stattic and Niclosamide (NSA) and treated MCF7 cells expressing the Phopsho-STAT3 BRET constructs with differential drug doses for 24hrs. Upon triggering the drug treated cell either with or without EGF (100ng), activation signal was recoded to determine the BRET ratios. With Stattic treatment, the basal BRET ratios dropped from 0.643mBu for untreated (UT) cells to 0.379mBu for 20µM Stattic ($p<0.05$). However, when the Stattic pre- treated cells were challenged with EGF, the inhibitory effect of the drug was lost in a dose dependent manner [0.904mBu for 10µM to 0.745mBu for 20µM (Stattic + EGF)] ($p<0.05$) **(Figure 2.10A)**. For NSA treated samples, the drop in basal BRET ratio was much more significant [0.643mBu for UT to 0.190mBu for 8µM NSA] ($p<0.01$) from the basal BRET signal. Further when NSA treated cells were given EGF stimulation, NSA was able to strongly retain the STAT3 inhibitory effect even upto 8µM of drug concentration [0.222mBu for 4µM to 0.151mBu for 8µM (NSA + EGF)]

($p<0.001$) **(Figure 2.10B)**. Collectively, these observations indicate that Niclosamide is more potent and specific inhibitor of STAT3 pathway as it could strongly attenuate the STAT3 activation signal at drug concentration even 2.5-fold lower [0.224mBu for 4µM NSA versus 0.904mBu for 10µM Stattic, $p<0.001$ and 0.05 respectively] than Stattic irrespective of EGF presence or absence.

To validate the findings from BRET study, we further treated the MCF7 cells with NSA or Stattic in increasing drug concentrations and determined the levels of total and activated STAT3 protein from cell lysates using immunoblotting. Both NSA and Stattic treatment was able to deplete the levels of activated phopsphoY705 STAT3 in a dose dependent manner. However, surprisingly only NSA was also able to block phosphoS727 STAT3 activation mark, for which Stattic was ineffective **(Figure 2.10C).** These observations indicate that the significant decrease observed in STAT3 BRET signal with NSA is due to its ability to target the dual STAT3 activation marks i.e. pY705 and pS727. Stattic on the other hand though failed to inhibit pS727 STAT3 activation but it successfully blocked the activation of STAT3 at pY705 residue only.

Binding of EGF activates EGFR receptor which in turn induces phosphorylation of STAT3, thus activating STAT3 dependent downstream functions **(Figure 2.10D)**. Hence to show that the activation obtained in BRET signal upon EGF treatment is via EGF-EGFR-STAT3 pathway, we pre-blocked the MCF7 cells expressing the Phospho-STAT3 BRET sensor with EGFR neutralizing antibody. Over here, EGFR-Ab treatment did not alter the basal BRET ratio obtained, however with prior blocking of EGFR receptor, EGF was unable to bind and induce EGFR- STAT3 mediated gain in BRET signal **(Figure 2.10E)** ($p<0.05$). Hence, these observations indicate that the EGF mediate gain obtained in BRET signal is a true event of EGF-EGFR mediated STAT3 phosphorylation and homodimerization process. Collectively,

these results clearly demonstrate the high specificity of the Phopsho-STAT3 BRET sensor to capture STAT3 activation or inhibitory events directly from live cells.

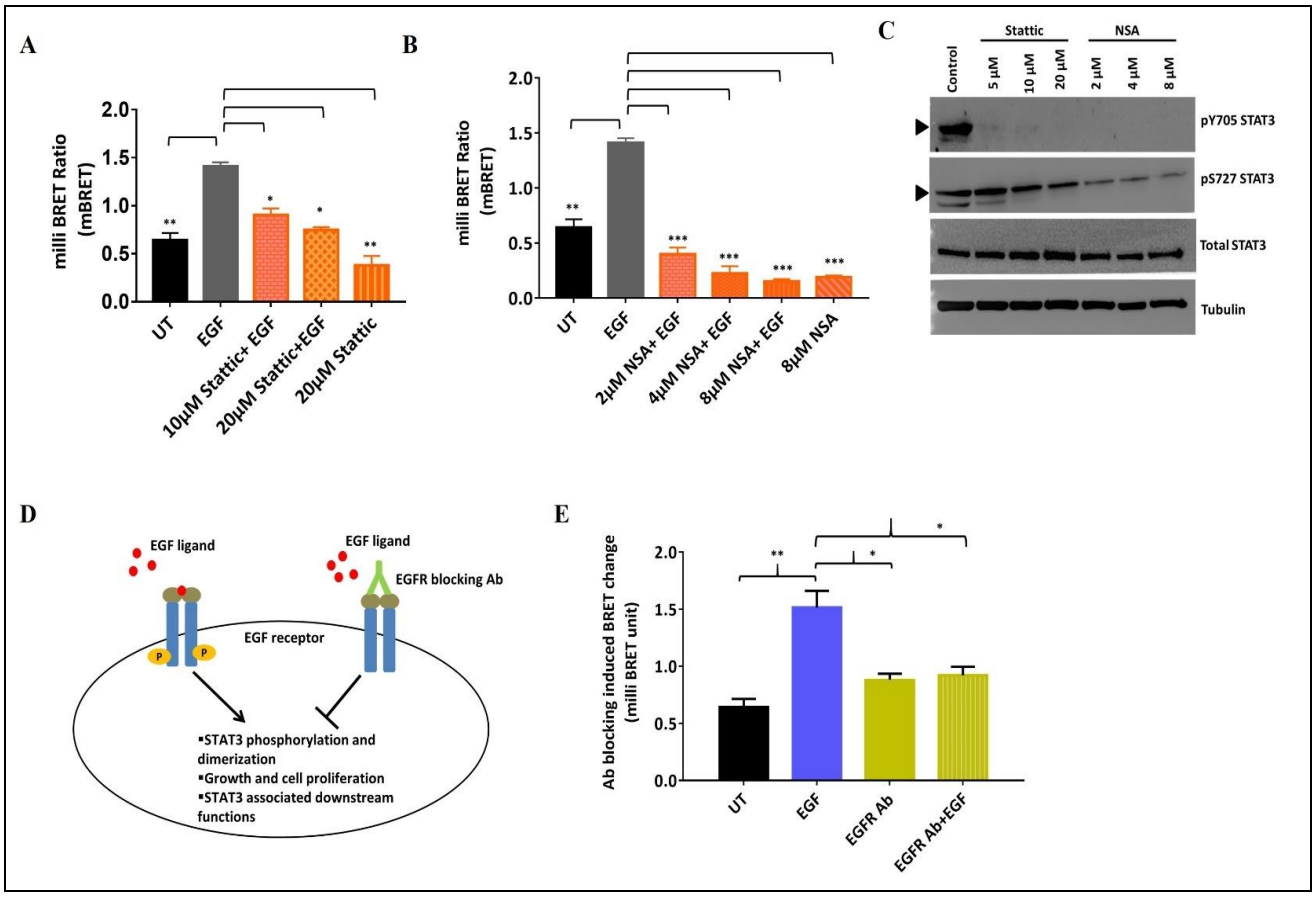

Figure 2.10. Detecting inhibition of STAT3 pathway with Phospho STAT3 BRET Sensor. *(A-B) Graphs representing the corrected BRET ratios of MCF 7 cells expressing Phospho STAT3 BRET sensor upon treatment with Stattic and Niclosamide, respectively, in presence or absence of EGF. (C) Immunoblot of MCF 7 cells treated with differential doses of Niclosamide or Stattic for 24hrs. Blot was probed for total and activated (pY705 or pS727) STAT3 levels with tubulin as loading control. (D) Schematic representation for EGF-EGFR mediated STAT3 activation process and effect of blocking with EGFR neutralising antibody. (E) Representative graph of corrected BRET ratio for MCF 7 cells expressing STAT3 BRET constructs, upon treatment with EGFR blocking antibody either in presence or absence of EGF. For all BRET studies Nluc emission was measured at 500nm and*

*TurboFP at 640nm using furimazine as substrate in IVIS spectrum with integration time of 30s/filter. Each graph represents mean value ± SEM. Significance levels are *p< 0.05, **p< 0.01, ***p< 0.001 and ns as non-significant.*

2.3.6 Phospho-STAT3 BRET: a semi-throughput platform for screening potential STAT3 inhibitors

For identifying potential inhibitors against STAT3 pathway, we need a system where different compound libraries can be screened on multiple parameters and in panel of cancer cell types with a highly sensitive readout, all in one platform. Pertaining to the excellent sensitivity and versatile nature of developed Phospho-STAT3 BRET sensor, we next sought to adapt it to a high throughput screening platform. To achieve this, we transfected MCF7 cells with STAT3 BRET constructs and seeded them at relatively 6-fold less adherent cell number in 384 well plate. Upon treating the cells with a library of 12 different compounds either in presence or absence of EGF gave different results **(Figure 2.11A-B)**. Out of twelve, six compounds (Niclosamide, Stattic, Curcumin, Neratinib, Wortmannin and ERK inhibitor U0126) showed STAT3 inhibitory functions. Of these 6 compounds, Neratinib (-0.109mBU), MS-275 (-0.157mBU) and ERK inhibitor (-0.149mBU) were newly identified candidates, while curcumin (-0.367mBU), niclosamide (-0.287mBU) and Stattic (0.325mBU) are previously known STAT3 inhibitors. Among these six inhibitory compounds identified, niclosamide, curcumin, ERK inhibitor and Neratinib were found to be more potent (more than 70% inhibition, $p<0.001$) with higher level of STAT3 inhibitory activity while both Wortmannin and Stattic though suppressed STAT3 BRET signal but failed to retain the inhibition post EGF stimulus **(Figure 2.12A)**.

Losartan (Angiotensin receptor blocker) and Fingolimod (Sphingosine 1-phosphate receptor blocker) are GPCR inhibitors with known inhibitory effect on STAT3 activation. However,

both the inhibitors failed to block STAT3 activation upon EGF trigger, as EGF activates STAT3 via EGF-EGFR pathway that is unaffected by both the GPCR blockers. As an activator, HDAC inhibitors like AR-42, CI-994 and chidamide showed induction of BRET signal post EGF stimulation with maximum activation effect observed with both AR-42 (71%) and Chidamide (69%) followed by CI-994 (41%). MS-275 on contrary failed to activate the STAT3 pathway **(Figure 2.12A)**.

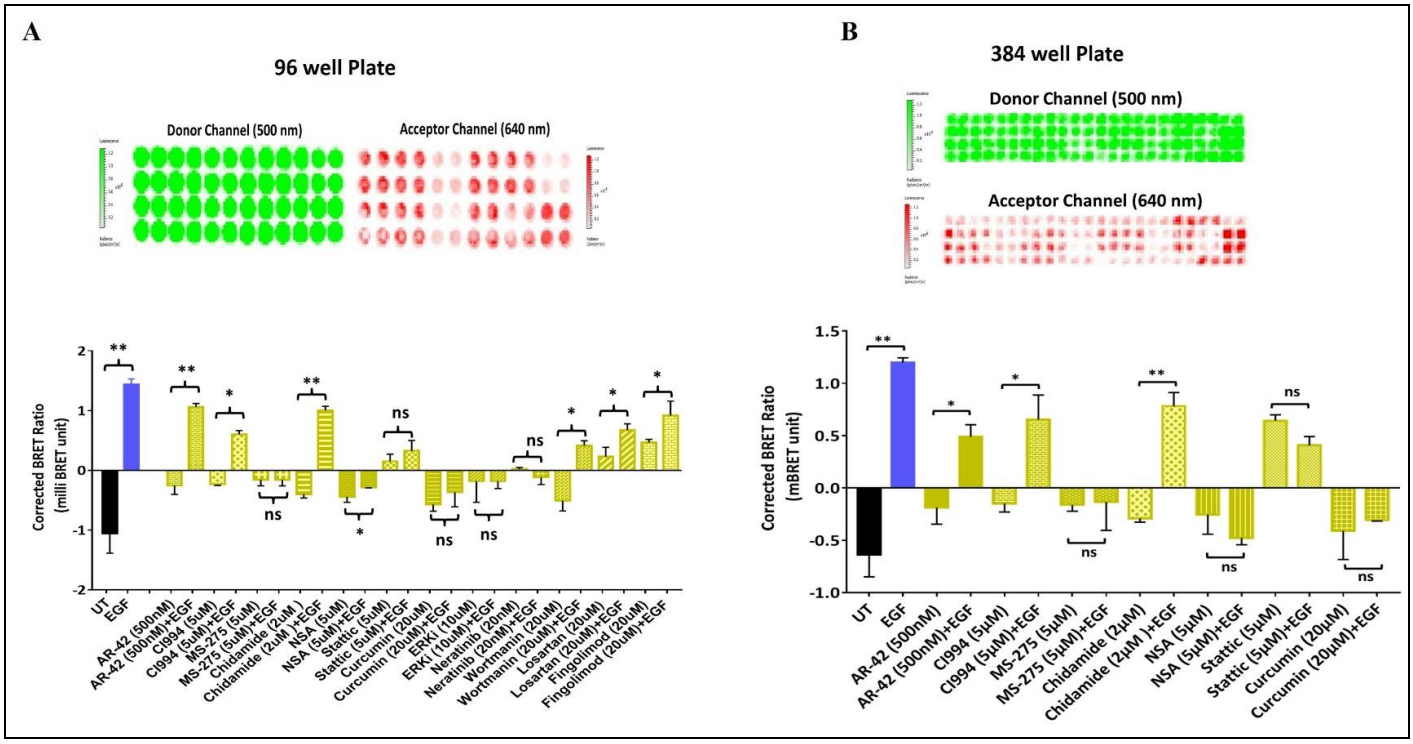

Figure 2.11. High throughput adaptability of Phospho STAT3 BRET Sensor. *(A-B) Representative image of 96 and 384- well plates, respectively, for MCF 7 cells expressing Phospho STAT3 BRET sensor in respective donor and acceptor filters upon treatment with compound library. Bottom graph in each case represents the calculated corrected BRET ratio for each drug treatment in presence or absence of EGF. For all BRET studies Nluc emission was measured at 500nm and TurboFP at 640nm using furimazine as substrate, in IVIS spectrum with integration time of 30s/filter. Each graph represents mean value ± SEM. Significance levels are *p< 0.05, **p< 0.01, ***p< 0.001 and ns as non-significant.*

Furthermore, comparing the sensitivity of Phosho-STAT3 BRET sensor from two different plate formats, a comparable bleed through subtracted BRET signal showed uncompromised sensitivity of the sensor despite adapting to miniature platform with limiting substrate utility and cell number **(Figure 2.12B)**. Finally, as a proof to validate the findings from STAT3 BRET screen, we randomly selected curcumin (80% inhibition) with inhibitory effect comparable to Niclosamide and treated MCF7 cells with variable doses. Immunoblotting for the levels of total and activated STAT3 showed that Curcumin also inhibited the dual activation marks on STAT3 (pY705 and pS727) in a dose dependent manner and thus justify its potency level equivalent to NSA **(Figure 2.12C)**. Collectively these results clearly demonstrate the sensitivity and strength of the Phosho-STAT3 BRET platform as a technology tool for high throughput screening of STAT3 activators or inhibitors either alone or in combination with differential effects and promising output.

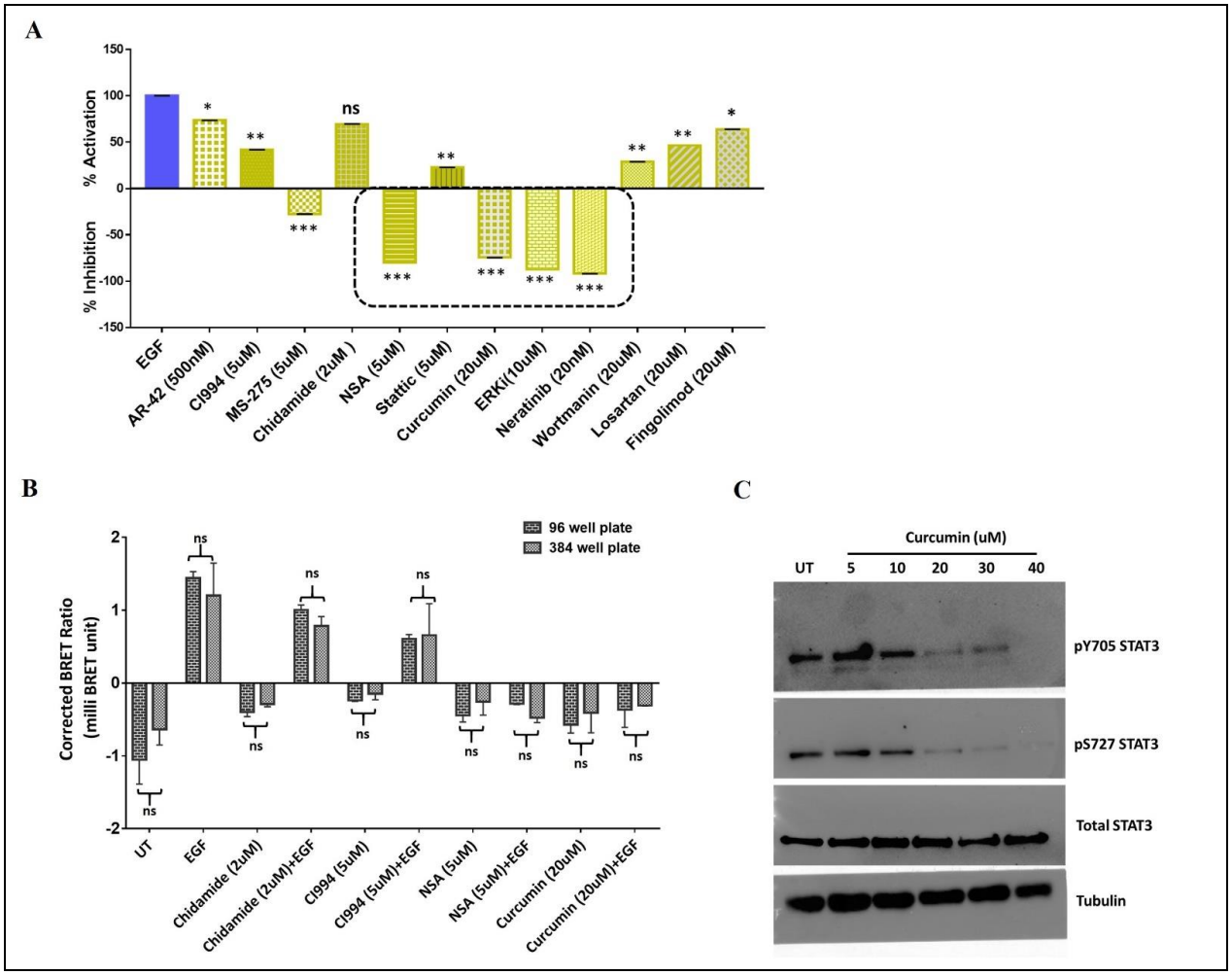

Figure 2.12. High throughput adaptability of Phospho STAT3 BRET Sensor. *(A) Representative graph for percent inhibition or activation in BRET signal with respect to EGF treated control, for individual drug treatment. Percent activation is calculated by dividing corrected ratio of drug treated sample with EGF treated control *100. For percent inhibition the above calculated value is subtracted from 100. (B) Comparison of corrected BRET ratios from two different plate formats - 96 versus 384 well plate. (C) Immunoblot of MCF 7 cell treated with differential concentration of curcumin and probed for total and activated (pY705 and pS727) STAT3 expression. Tubulin was used as loading control. Each graph represents mean value ± SEM. Significance levels are *p< 0.05, **p< 0.01, ***p< 0.001 and ns as non-significant.*

2.4 Discussion

STAT3 signaling is known to be activated in majority of the cancers including breast cancer where more than 60% breast cancer cases are found to be positive for both total and pY705 STAT3 (Chung S.S., 2014). Ligand induced Y705 phosphorylation followed by homodimerization holds the key step in regulating STAT3 activation. Because of its indispensable role in maintaining normal and oncogenic cellular function, STAT3 is a prime target for drug discovery and therapeutic intervention in current scenario. Extensive efforts are being made majorly by adopting high throughput screening strategies like virtual screening of inhibitors for binding and in silico docking of putative binders onto SH2-STAT3 domain followed by validation *in vitro* to identify STAT3 specific inhibitors (Liu *et al*, 2014; Yuriev, 2014). The lacuna of the structure-based drug identification strategy is its lack of absolute specificity and sensitivity for the pathway. Majority of the potential binders may not even show relevant biological effect in *in vitro* or *in vivo* conditions (Liu *et al*, 2014). To overcome these issues, in the present study here, we developed a very reliable and high throughput live cell reporter sensor for dynamic monitoring of phosphorylation dependent STAT3 activity.

For developing a STAT3 phosphorylation sensor, we first characterized the ability of Nluc to serve as a compatible donor for spectrally well separated TurboFP635 fluorophore. Despite an appreciable difference of more than 175nm in spectral overlap, Nluc could sufficiently excite TurboFP in fusion protein state with minimal bleed-through from the donor channel irrespective of the transient or stable expression condition. Due to lesser tissue attenuation for light emitted at 640 nm, a comparable double ratios (DRs) obtained for both cell culture and animal imaging experiment further highlight the superiority of selected pair for deep tissue imaging of biological PPI.

Because of bright and stable luminescence from Nluc and high spectral resolution along with feasibility to be adopted for in vivo imaging with TurboFP made them an appropriate candidate of choice to develop the STAT3 phosphorylation sensor. Thereafter, rational selection for optimal dipole orientation of STAT3 BRET sensor was performed in cell lines with differential endogenous STAT3 expression level using known ligand EGF at variable concentration. Despite using either STAT3 positive (HT1080), STAT3 null (PC3) or acceptor-stable HT1080 cell line, C-terminally oriented STAT3 configuration is identified as the most suitable orientation because of its drastic difference from the basal BRET signal and a concentration dependent readout in the assay. Additionally, the compounding factor of endogenous STAT3 did not compromise the ratiometric judgement of STAT3 sensor for EGF mediated STAT3 activation in all the backgrounds tested. However, with acceptor stable cells, as expected, maximum STAT3 activation was achieved even with low EGF concentration. As reported previously, STAT3 phosphorylation at Y705 is induced within 3min of ligand addition and continues high for more than 6hrs (Verma *et al*, 2015). Our model also very elegantly highlighted the similar activation kinetics of STAT3 pathway as observed for upto 1hr of signal scan post ligand induction.

STAT3 is reported to be constitutively active in majority of cancer cell lines and primary tumor (Zhang & Lai, 2014). Where apart from EGF, various other ligands like IL6, PMA etc can also activate the STAT3 molecule (Berishaj *et al*, 2007; Rebe *et al*, 2013). Hence, using IL6 as new ligand and EGF as positive control, we further validated the ability of above identified Nluc-ST3+TurboFP-ST3 BRET combination in panel of cancer cell lines - HT1080, MCF7, A549 and PC3 to determine STAT3 activation. In all the model cell lines tested IL6 proved to be a better ligand in comparison to EGF as it successfully and sensitively mimicked the biological condition of phosphorylation mediated dimerization and gain in BRET signal even at low ligand concentration (10 ng/ml vs. 100 ng/ml for EGF).

Additionally, we also observed a ligand-receptor stoichiometry dependent gain in STAT3 BRET signal, where quantitative analysis of the EGFR mRNA level in all the four cell lines correlated well with the BRET ratio obtained using EGF (100ng/ml) as ligand. Further selective blocking of cells with EGFR blocking antibody to prevent EGF-EGFR mediated STAT3 activation also showed loss of BRET signal in EGF induced pre-blocked cells. Indicating that the activation response obtained with STAT3 BRET sensor upon EGF treatment was a true event of EGF mediated STAT3 phosphorylation and homodimerization.

HTS compatibility for an assay system depends on high detection sensitivity without compromising the specificity. While a majority of HTS assays rely on 96 well plate format, here we have shown that STAT3 phospho BRET sensor works even in 384 well format while using the same imaging equipment for photonic quantification. Achieving this ability can certainly justify STAT3 phospho BRET sensor as an efficient as well as a cost-effective screening tool. As the results suggest, between 96 well to 384 well format, use of a 6-fold lower number of cells has no effect on donor and acceptor photon detection or ratiometric readouts of the samples. Of the 12 compounds screened in the BRET platform, 6 compounds (curcumin, niclosamide, Stattic, ERK-inhibitor, neratinib and MS-275) were identified as potential STAT3 inhibitors, among which Neratinib (Segovia-Mendoza *et al*, 2015), ERKi (Marampon *et al*, 2009) ,curcumin(Hahn *et al*, 2018) and niclosamide(Shi *et al*, 2017) showed STAT3 inhibitory activity (more than 70% inhibition), even better than the known Stattic inhibitor (Schust *et al*, 2006). Of the remaining 6 drugs, three HDACi compounds (AR-42, Chidamide and CI-994) showed activation of STAT3 BRET sensor with EGF treatment ($p<0.01$). It is likely that these three HDACi compounds are increasing STAT3 activation by increasing overall acetylation of the genome, thereby increasing pool of STAT3 stimulators (Suraweera *et al*, 2018). The remaining three compounds Wortmannin (PI3K inhibitor) (Bito *et al*, 2011), Fingolimod and Losartan (GPCRs inhibitors) (He *et al*, 2014;

Lankadasari *et al*, 2018) are indirect inhibitors of STAT3 pathway that failed to retain the suppression of STAT3 molecule upon EGF stimulation. Comparable corrected ratios obtained for individual drug compound in two different plate formats (96 and 384 well plate) further provides confidence in the detection system and highlights the sensitivity of the assay system.

In summary, the STAT3 phospho BRET assay system developed is able to measure STAT3 protein phosphorylation in vivo. The reporter sensor captures the kinetics of STAT3 homodimer formation as a result of protein activation from live cell environment. The sensor shows sufficient sensitivity and specificity against activator and inhibitor molecules tested and thus can be designated as HTS ready. In future this technology can be used for studying role of key PTMs of STAT3 in its dimerization as well as screening potential inhibitors either alone or in combination against this master transcriptional regulator of various oncogenic pathways.

2.5 Significance of the Study

This study for the first-time reports' development a very versatile and sensitive STAT3 phosphorylation dependent homodimerization sensor (STAT3 Phospho-BRET). With thorough screening and multiparametric optimization the sensor developed in this study shows potential applications like; detecting STAT3 activation in different genetic background, multiple cancer cell type with differential activating ligands, sensitive response to activation or blockade signals from upstream receptors as well as high throughput screening of compound library to identify stimulators or inhibitors of STAT3 Signaling.

Considering the current challenges for STAT3 inhibitors in clinical trials, we believe that rational approaches like developing sensors for real time live cell screening will significantly aid the drug discovery process. The inhibitors identified through live cell screening approach are much more reliable candidates, with high chances of showing desirable response at both preclinical and clinical testing. In future the STAT3 Phospho-BRET sensor can be utilised for high throughput screening of chemotherapeutic drugs either alone or in combination, against the STAT3 pathway irrespective of any cancer cell type. Additionally, with the identification of new PTM (post translational modification) sites on STAT3, the application of this sensor can further be extended to demonstrate their individual role in governing STAT3 dimerization or downstream signaling **(Figure 2.13)**.

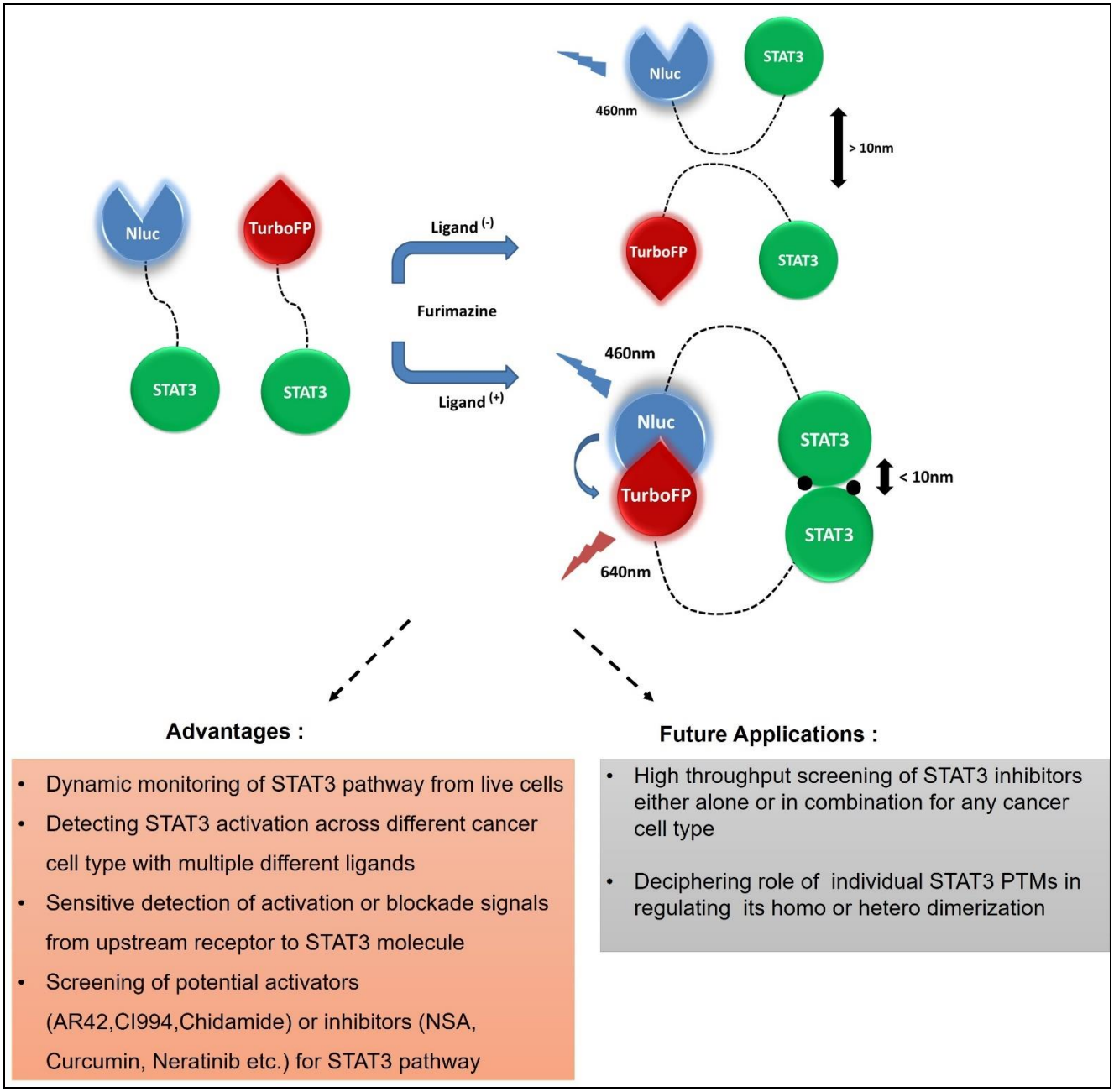

Figure 2.13: *Schematic representation of the current and future advantages of STAT3 Phospho BRET sensor.*

Chapter 3

Role of PTM Dependent STAT3 Signaling in Breast Cancer

Objective 2: To identify the association of differentially regulated genes with different PTM status of STAT3

3.1 Introduction

STAT3, one of the most important members of STAT family protein, is a cytoplasmic factor that is activated upon phosphorylation of tyrosine 705 residue in the C-terminal domain of the protein. Upon activation of STAT3 via its classical canonical (pY705) route, it serves to regulate expression of genes involved in various aspects of cancer progression for e.g. proliferation, survival, angiogenesis, immune evasion, metastasis etc. (Rebe *et al*, 2013) . For many years' activation of STAT3, in primary tumours or cancer cell line is determined based on pY705 expression levels. pY705 is even used as a biomarker to predict overall survival or response to chemotherapy for many cancers including breast cancer, colorectal cancer, lung adenocarcinoma, osteosarcoma etc (Sellier *et al*, 2013). Hence, anti-STAT3 therapeutic approaches have always considered blocking the pY705 activation as key step to block the STAT3 pathway. Eventually the clinical notion of giving STAT3 inhibitors only to patients with pY705 positive expression was conceived (Johnston & Grandis, 2011). However, this clinical notion is now put to test due to the identification of alternate STAT3 activation pathways.

Apart from classical canonical(pY705) activation, recently STAT3 is reported to be upregulated by an alternate arm known as noncanonical pathway. The major residues known to be involved in noncanonical STAT3 activation are pS727 and K685ac (Srivastava & DiGiovanni, 2016; Wen *et al*, 1995). With the initial discover, phosphorylation at S727 site was thought to be required for full transactivation of STAT3, following pY705 induction (Wen *et al*, 1995) . However, recent studies indicate that both pS727 and pY705 might be playing an independent role in controlling STAT3 functions. Activation of STAT3 at pS727

residue is known to initiated by multiple cytoplasmic kinases like - JNK, MAPK/ERK, PKC, CK5 and CDK5 (Wen & Darnell, 1997). In case of infiltrating ductal carcinoma breast cancer tissue samples STAT3 was found to be constitutively phosphorylated at pS727 residue independent of canonical pY705 activation. All the cases with highpS727 expression showed negative association with the ER status and positive association with tumor stage and grade of the sample (Yeh *et al*, 2006). In case of both CML and AML, majority of the samples were found to be positive for pS727 STAT3 with very little or no pY705 expression, where it controls both nuclear localization and cell survival functions for the cancer cell (Hazan-Halevy *et al*, 2010). Similar reports are available even in case of glioblastoma where, pS727 expression is associated with enhanced intrinsic radio resistance and leads to poor overall survival. Apart from S727 phosphorylation, acetylation at K685 residue is equally implicated to play an important role in STAT3 activation (Lin *et al*, 2014; Ouedraogo *et al*, 2016). C-terminal domain of STAT3 is known to interact with CBP/P300 protein that acetylates the STAT3 molecule at K685 residue (Wang *et al*, 2005). Enhanced expression of acetylated K685 STAT3 has been reported in melanoma, lung adenocarcinoma and ovarian cancer tissue samples. High levels of acetylated STAT3 interacts with DNMT1 and methylates the promoter of tumor suppressor genes like P53, SOCS3, CDKN2A etc., thereby promoting tumour growth (Lee *et al*, 2012; Li *et al*, 2013) . In case of colorectal cancer acetylated STAT3 interacts with CD44 protein and regulate expression of Cyclin D1 gene (Lee *et al*, 2009). Acetylation of STAT3 is also essential for processing of p100 protein and activation of NF-κβ pathway (Nadiminty *et al*, 2006). More importantly, K685ac was reported to be extremely essential for stable homodimerization of STAT3 molecule that in turns regulate expression of its downstream target genes like Cyclin D1, c-Myc etc (Yuan *et al*, 2005).

Controlling the STAT3 activity at transcriptional level, there are number of reports available that hints towards noncanonical activation mediated transcriptional reprogramming of

STAT3 molecule. In case of mESC, pS727 and pY705 STAT3 levels are differentially regulated to control the stem cell fate of mESC. While high level of pY705 is required for self-renewal of mESC population, hyper activation of STAT3 at pS727 residue shifts the equilibrium from pluripotency to neuronal commitment (Huang *et al*, 2014). Upon treating the colorectal cancer cell lines with topoisomerase inhibitor, I, activation of STAT3 is specifically induced at pS727 and not at pY705 site. STAT3 activated at pS727 residue in turn downstream enhances the expression of DNA repair enzyme Eme1 to facilitate faster DNA repair and increase cell survival (Vigneron *et al*, 2008). Recently, it was found that K685ac plays a very limiting role in regulating expression of pY705 dependent STAT3 target genes. Rather acetylation of STAT3 at K685 is required for controlling expression of genes involved in response to angiotensin II treatment that controls development of cardiac hypertrophy and dysfunction (Dasgupta *et al*, 2014).

Collective observations from the literature clearly identifies prevalent role of noncanonical pathway (pS727 and K685ac) in controlling STAT3 dependent biological function and growth of cancer cells. However, since the two activation pathways of STAT3 are never studied together, some of the basic and essential information about the STAT3 signaling is still unanswered. First, it is not known how the two arms of STAT3 activation regulate or cross talk with each other in case of breast cancer. Second, apart from K685ac, whether pS727 activation plays any role in controlling STAT3 homodimerization. And lastly, whether with the different PTM status of STAT3, the transcriptional preference of STAT3 in altered or not.

In the present study, we engineered a 3'UTR STAT3 knockdown model system with stable overexpression of Nluc-STAT3 variants i.e. Wt, Y705F, S727A and K685R. With the model system established and taking advantage of the Phospho STAT3 BRET sensor, we systematically demonstrate the role of individual PTM site in cross regulating each other and

controlling STAT3 homodimerization. We further performed various functional and biological assays to decipher the role of canonical and noncanonical STAT3 pathway activation in breast cancer cells. Finally, we demonstrate that dual blocking of STAT3 PTMs as achieved with Niclosamide inhibitor is a better approach than conventional pY705 blockers, to achieve complete blockade of the STAT3 pathway.

3.2 Materials and Methods

3.2.1 Materials

Stattic (#S7024) was purchased from Selleckchem (USA) and Niclosamide (#N3510) from Sigma-Aldrich, USA. IL6 (#200-06) and EGF (#AF-100-15) were bought from Peprotech (USA). Mouse-anti-STAT3 (#9139), rabbit-anti-pY705 STAT3 (#9145) and rabbit-anti acetyl-K685 (#2523) antibodies were from Cell Signalling (USA). Mouse-anti-Her2 antibody (ab8054), rabbit-anti-ERα (ab3575) antibody, rabbit-anti-pS727-STAT3 (#E121-31), mouse-anti-RFP (#ab125244) and rabbit-anti-Cyclin D1 (#ab134175) antibodies were from Abcam. Secondary antibodies like anti-mouse HRP (#ab6728) from Abcam, anti-mouse dylight633 (#33512) and anti-rabbit dylight633(#35562) from Thermo Fischer scientific and anti-rabbit-HRP (#31460) from Invitrogen. iClick EdU AndyFluor647 cell proliferation kit was procured from Genecopia (USA, #A006). Nanoluc antibody and gene sequence was provided as a generous gift and Furimazine substrate (#N1110) was purchased from Promega Corporation (USA). For live cell imaging IVIS Spectrum pre-clinical *in vivo* imaging system was used that is equipped with 20nm bandpass filters covering the range of 500-850nm.

3.2.2 Recombinant Plasmid DNA Construction

Nluc-STAT3 (Wt) and TurboFP-STAT3 (Wt) fusion constructs were established as mentioned in **Chapter 2 (Section 2.2.2 Materials and Methods).** For developing site

specific point mutants, sequential site directed mutagenesis was performed and the primer list is given below. For knockdown studies, shRNA oligos against 3'UTR region of STAT3 were annealed and cloned in pLL3.7-GFP vector under U6 promoter using HpaI and XhoI restriction sites as per the standard protocol (De *et al*, 2008).

Fwd STAT3 K685R: 5' GCATTCGGAAGGTATTGTCGGCCA

Rev STAT3 K685R: 5'TGGCCGACAATACCTTCCGAATGC

Fwd STAT3 S727A: 5' ACCTGCCGATGGCCCCCCGCA

Rev STAT3 S727A: 5'TGCGGGGGGcCATCGGCAGGT

Fwd STAT3 Y705F: 5'AGCGCTGCCCCATTCCTGAAGACC

Rev STAT3 Y705F: 5'GGTCTTCAGGAATGGGGCAGCGCT

Fwd 3'UTRshRNA STAT3 – 5'GCTACATACTCCTGGCATTGC3'

Rev 3'UTRshRNA STAT3 – 5'GCAATGCCAGGAGTATGTAGC 3'

3.2.3 Cell Culture

MCF7 cells were grown in RPMI-1640 medium supplemented with 10% FBS (Gibco, USA) and 1% Pen-Strep (Invitrogen, USA) and maintained at 37ºC with 5% CO_2. MDA MB231 cells were cultured in L-15 medium (Sigma, USA) without $NaHCO_3$ supplemented with 10% FBS (Gibco, USA) and 1% Pen-step (Invitrogen, USA) in a CO_2 free incubator at 37ºC. MCF 7 / MDA MB 231 cells overexpressing Nluc-STAT3 fusion constructs (Wt,Y705F,S727A and K685R) were generated by transfecting individual mutant plasmid and selecting clones using 500µg/ml Zeocin antibiotic selection. Final screening of the clones was done with live cell luciferase assay using furimazine substrate.

For knocking down endogenous STAT3 expression in the PTM mutant stable clones, we prepared lentiviral particles in HEK293FT cells by transfecting with pLL3.7-GFP lentiviral vector containing 3'UTR STAT3 shRNA cassette along with virus envelope plasmids. Both MCF 7 and MDA MB 231 cells were stably transduced with the virus containing shRNA against STAT3 and with high GFP assisted FACS sorting, knocked down clones were enriched with subsequent passages.

3.2.4 Real Time PCR

Total RNA from the cells was extracted using RNA extraction minikit (QIAGEN). 2µg RNA was used for preparation of cDNA using SuperScript III (Invitrogen) kit as per the manufacturer's instructions. Real time PCR was done using Sybr green reagent and GAPDH was used as normalization control. Primer sequence for STAT3, CYCLIN D1, TWIST1, SOCS3 and GAPDH gene is as follows:

Fwd STAT3: 5' GGAGGAGTTGCAGCAAAAAG

Rev STAT3: 5' TGTGTTTGTGCCCAGAATGT

Fwd CYCLIN D1: 5'TATTGCGCTGCTACCGTTGA

Rev CYCLIN D1: 5'CCAATAGCAGCAAACAATGTGAAA

Fwd TWIST 1: 5' GGCCGGAGACCTAGATG

Rev TWIST 1: 5' ACGGGCCTGTCTCGCTTTCT

Fwd SOCS3: 5'ACCCTCCGCGCTCAGCCTTT

Rev SOCS3: 5'AGCGGAGCAGGGAGTCCAAGT

Fwd GAPDH: 5' TGCACCACCAACTGCTTAGC

Rev GAPDH: 5'GGCATGGACTGTGGTCATGAG

3.2.5 Immunoblotting

For immunoblotting cells were seeded in a 6-well plate and serum starved for 24hours before giving IL6 (10ng/ml) or EGF (100ng/ml) stimulation for next 2hours. Control cells kept in serum negative medium. Post 2hrs of incubation cell were trypsinized, harvested and washed with by 1XPBS. Cell pellet was resuspended in 1X cell lysis buffer containing - 10 mM Tris-HCl (pH 7.5), 140 mM NaCl, 5 mM EDTA, 2mM EGTA, 100mM NaF,100mM Na_3VO_4 ,100mM PMSF and protease inhibitor cocktail. Lysis was performed by sonication method at 10% amplitude with 10sec on/off cycle. The sample was centrifuged at 14000rpm/30min/4ºC and supernatant was collected in separate tube. Protein estimation was done using Bradford reagent and approx. 50-60µg protein was loaded on 7.5% SDS-PAGE gel. Protein transfer was done in semidry Trans blot assembly at 15V for 1hr at room temperature. Blocking was performed in 5% non-fat dry milk for 1hr at room temperature followed by primary antibody incubation [STAT3 1:1000, pY705 STAT3 1:500, pS727 STAT3 1:1000, K685ac STAT3 1:500, α-Tubulin 1:1000, Her2 1:500] overnight/4ºC. Next day, secondary-HRP antibody treatment was given followed by developing the blot using ECL substrate in ChemiDoc system (Biorad, USA).

3.2.6 Immunoprecipitation

For Co-immunoprecipitation assay, Nluc-STAT3 PTM mutant clones were seeded in duplicates at an appropriate density. Next day, Turbo-STAT3 PTM mutant constructs were transfected in respective donor counterpart wells.48hrs post transfection, cells were serum starved for 24hours and then IL6 induction (10ng/ml) was given for 2hrs. Cells were harvested and lysed in ECS lysis buffer containing ;50mM Tris-Cl pH 8.0, 0.5% NP40, 2mM EGTA, 125mM NaCl, 5mM EDTA, 100mM Na_3VO_4, 100mM NaF, 10ul/ml protease inhibitor (Sigma, USA) and 2ul/ 1ml PMSF. Lysate was centrifuged at 14000rpm for 30mins

at 4ºC and supernatant was collected. Protein estimation was done using Bradford reagent (Sigma, USA). Protein G-Sepharose beads were equilibrated by sequential washing with NETN buffer (100mM NaCl, 1mM EDTA, 20mM Tris-Cl pH 8.0 and 0.1% NP40) at 1000rpm/5mins/4°C. Beads were blocked in 5% BSA (in NETN buffer) for 3hrs/13rpm/4°C. For binding, 1µg protein was incubated with 1µg of anti-RFP antibody and 20µl Protein G beads in a total volume of 1ml NETN buffer and incubated overnight at 13rpm/4°C. Next day, bound fraction and unbound fraction was separated by centrifuging the complex at 1000rpm/5mins/4°C. Final beads in the pellet was resuspended in 1X denaturing buffer and loaded onto 7.5% SDS PAGE gel. Immunoblotting was performed sequentially with anti-Nluc and anti- RFP antibody.

3.2.7 Immunofluorescence

Cells were fixed with 4% paraformaldehyde for 10 minutes at 37ºC, followed by permeabilization using 0.5% triton X100 for 10 minutes at room temperature. Blocking was done with 5% BSA in 1XPBS for 1hr at room temperature. Primary antibody (Her2 and E-Cadherin -1:50 diluted) incubation was done at 4ºC overnight in humidified chamber. Secondary antibody incubation was given for 1hr at room temperature in dark, followed by DAPI staining and mounting. Images were acquired using Zeiss LSM780 microscope with 633nm and 460nm filter sets and final images were processed in ImageJ software.

3.2.8 Cell Survival and Proliferation Assay

For EdU cell proliferation assay, EdU AndyFluor647 proliferation kit (Origene, USA) was used. Briefly, cells seeded at an appropriate density on a coverslip. Next day, EdU was added to each sample and incubated for 16hrs.Processing of the coverslips was done as per the manufacturer’s instructions. Images were acquired in LSM780 (Leica) microscope with 633nm filter for EdU and 460nm filter for DAPI.

For clonogenic assay, 1000 cells were counted and seeded in a 6-well plate in duplicates. Clones were allowed to form for 14days, after which the colonies were fixed with chilled methanol and stained with 0.5% crystal violet stain.

3.2.9 Live Cell luciferase assay

For live cell luciferase assay, Nluc-STAT3 PTM mutant expressing MCF 7 cells were seeded at two different cell numbers; 5000 and 10,000 cells/well in triplicate in black well plate with clear bottom. For live cell imaging 50µl furimazine (1:1000) was added to each well and luminescence signal was acquired in IVIS spectrum using open filter settings.

3.2.10 BRET assay

For BRET assay, Nluc-STAT3 constructs (Cl1-Cl8) expressing engineered MCF 7 cells / MDA MB 231 cells (with endogenous STAT3 knock down) were seeded at a density of $1X10^5$ cells/ well in 12-well plate. Next day Turbo-STAT3 plasmids (Cl1-Cl8) were transfected in respective well and one set of donor alone set was kept separate. 36hrs post transfection, cells were counted and seeded at a density of 20,000 cell/well in 96 black well plate (duplicate) with clear bottom in serum negative medium. Post 24hrs of serum starvation, cells were stimulated with IL6 (10ng/ml) reconstituted in serum negative medium followed by furimazine substrate addition (1:1000 diluted). Signal acquisition was performed in IVIS spectrum with 500nm as donor and 640nm as acceptor channel with integration time of 30sec/filter. For analysing BRET signal, ROI was drawn on individual wells and following equation was applied to derive both BRET ratio and corrected ratios from the signal (Dimri *et al*, 2016; Dragulescu-Andrasi *et al*, 2011).

$$\text{BRET Ratio} = \left(\frac{BL_{\text{acceptor channel}} - Cf}{BL_{\text{donor channel}}} \right)_{\text{Donor +Acceptor cells}}$$

$$\text{Where, } Cf = \left(\frac{BL_{\text{acceptor channel}}}{BL_{\text{donor channel}}} \right)_{\text{Donor alone cells}}$$

3.2.11 Statistical analysis

For all statistical analysis, student t-test was employed and p value <0.05 was considered as statistically significant.

3.3 Results

3.3.1 Development of 3'UTR STAT3 knockdown PTM mutant expressing MCF7 breast cancer cell line

In order to determine whether the two activation arms of STAT3; canonical (pY705) and noncanonical (pS727 and K685ac) mediate their functions independently or in an interdependent manner in breast cancer, we developed the following model system. We first knocked down the endogenous STAT3 expression in MCF 7 cell line using 3'UTR STAT3 shRNA approach in lentiviral plasmid vector. The stable STAT3 knockdown population was selected and enriched with subsequent GFP mediated FACS sorting to give a final 97-98% pure GFP^+ clones **(Figure 3.1A)**. Depletion in STAT3 levels upon knockdown was confirmed at both protein and transcript levels. Immunoblot for total and pY705 activated forms confirmed more than 90% reduction in STAT3 protein expression **(Figure 3.1B)**.

While a depletion of more than 3-fold was evident at the mRNA transcript levels using quantitative real time PCR **(Figure 3.1C)**.

Taking advantage of the STAT3 BRET plasmids developed in Chapter 2, we took STAT3 fused with Nluc (i.e. Nluc-STAT3) as template and performed site directed mutagenesis. Each PTM site on the wild type STAT3 template was substituted with another un-reactive amino acid individually to finally give rise to following 4 constructs: Nluc-STAT3 - Wt/Y705F/S727A or K685R **(Figure 3.1D).** Finally, we merged the two-model systems, by stably overexpressing the individual STAT3 Wt or PTM mutants in endogenous STAT3 knocked MCF 7 cell background. Stable clones were established upon antibiotic selection while STAT3 null condition was maintained with GFP assisted cell sorting. The model system developed here thus offers following two main advantages; least interference form endogenous STAT3 pool; and true representation of PTM loss on functional and biological activity of STAT3 molecule **(Figure 3.1E)**. The model system established was thus used for further functional or phenotypic assays.

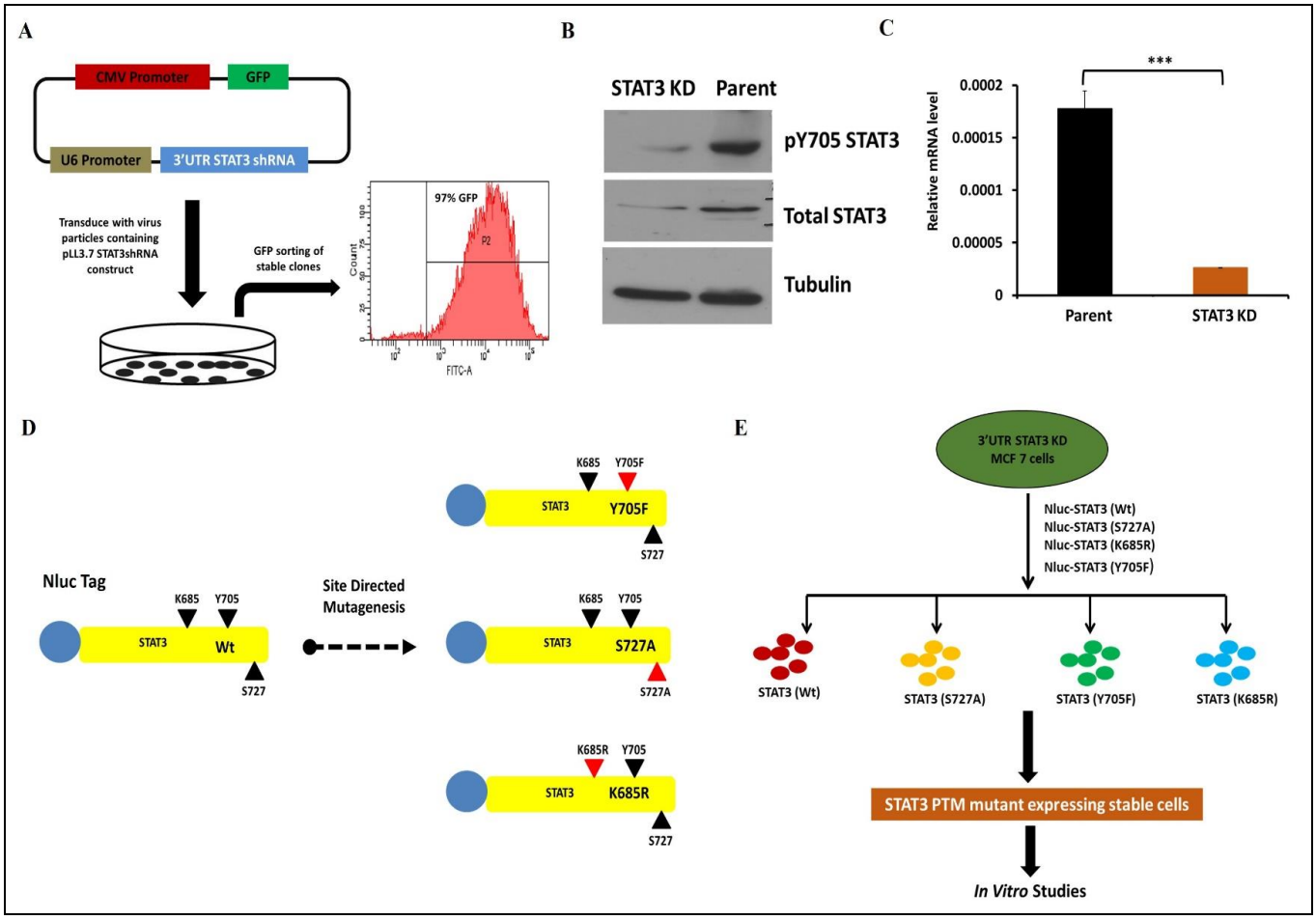

Figure 3.1. Development of 3'UTR STAT3 knock down and PTM mutant overexpressing MCF 7 cell line. *(A) Schematic representation for 3'UTR knock down of STAT3 in MCF 7 cells. shRNA against 3'UTR region of STAT3 was cloned in pLL3.7 lentiviral vector and virus particles were prepared in HEK293FT cells that were used to stably transduce MCF 7 cells. Positive clones were selected based on GFP sorting to finally give a 97% pure STAT3 KD positive clones. (B) Immunoblot of parent and STAT3 KD MCF 7 cells, probed for total and pY705 STAT3 levels. Tubulin was used as loading control. (C) Quantitative mRNA transcript levels of STAT3 in parent and STAT3 KD cells. (D) Schematic representation for preparation of STAT3 PTM mutant clones. Nluc-STAT3 (Wt) was used as template and site directed mutagenesis was performed for individual PTM (Y-F, S-A and K-R) site to establish the mutant constructs. (E) Diagrammatic work flow for generation of engineered MCF 7 STAT3 KD cell with stable over expression on STAT3 PTM mutants on which all the in vitro experiments were performed. Each graph represents mean value ± SEM. Significance levels are * $p<0.05$, ** $p<0.01$, and *** $p<0.001$ and ns as non-significant.*

3.3.2 Noncanonical pS727 activation is independent of canonical pY705 STAT3 activation

With the establishment of engineered MCF 7 cells with 3'UTR STAT3 knockdown and stable overexpression of individual STAT3 point mutants fused to Nanoluciferase (Nluc-STAT3 Wt, Y705F, S727A and K685R), we went ahead to address how the cross talk among these key PTM sites **(Figure 3.2A)** regulate STAT3 activation**.** Following the development of these stable clones, we first performed live cell luciferase assay to demonstrate that fusion of STAT3 with nanoluc does not affect the ability of NLuc to catalyse its substrate and that the fusion construct gives functional Nluc activity **(Figure 3.2B)**. Thereafter to ensure proper translation of the fusion constructs and to check the effect of single site loss on other PTM residues, we performed immunoblotting of these stable clones and probed for all the three STAT3 activation marks. Over here we observed that with loss of pY705 PTM (Y705F), pS727 and K685 ac was intact while with loss of K685ac (K685R), both pY705 and pS727 was unaffected. Surprisingly, in S727A mutant, though pY705 activation was unaltered but K685ac was completely lost. These observations were validated in two different model cell lines – MCF 7 and MDA MB231 with stable STAT3 KD **(Figure 3.2C-D)**. Additionally, the faint band of K685ac observed in K685R mutant is due to non-specific recognition of adjacent lysine residues i.e. K679, 707 and 709 (Nie *et al*, 2009).

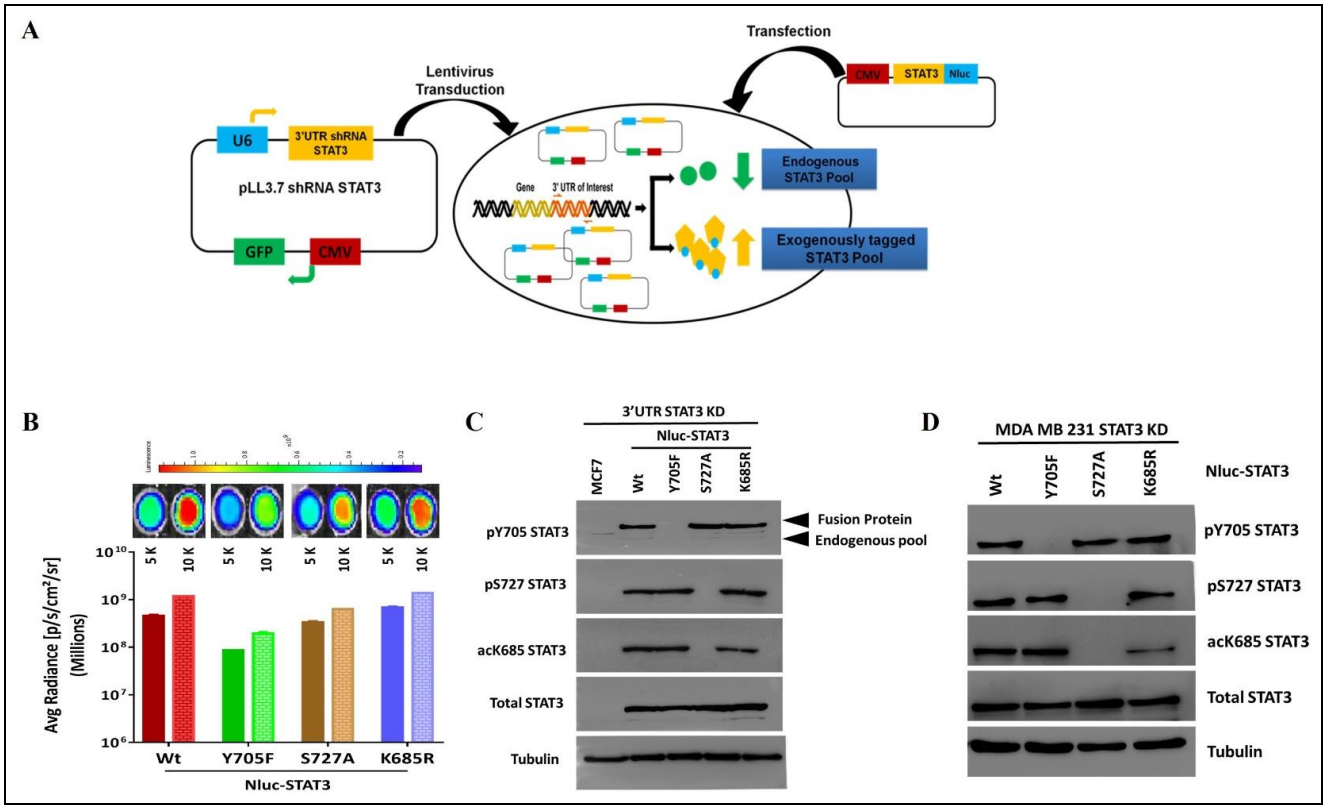

Figure 3.2. Canonical (pY705) and noncanonical (pS727 & K685ac) STAT3 activation are independent of each other. *(A) Schematic model for the MCF 7 or MDA MB 231 cells with endogenous STAT3 KD and overexpression of PTM mutant STAT3 clones. (B) Live cell luciferase assay of the 4 Nluc-STAT3 PTM mutant clones at two different cell density. Furimazine was used as substrate (1:1000) and luminescence signal was acquired in IVIS spectrum with open filter settings. (C-D) Immunoblot of MCF 7 and MDA MB 231 cells with endogenous STAT3 KD background probed for total and all the three STAT3 activation marks (pY705, pS727 and K685ac) in different PTM mutant lines.*

To further strengthen the above interesting observations, we treated the above four mutants with IL6 and EGF for 2hours before lysate preparation and probed for all the three activation marks again. In Y705F and S727A clones due to point mutations, phospho-activation site was completely lost. Further in Y705F mutant, not much change was observed in pS727 levels, while K685ac showed significant induction upon IL6 or EGF trigger. In K685R clones also,

pS727 and pY705 levels enhanced post ligand treatment. However, again in case of S727A, though pY705 levels increased in response to IL6 or EGF addition but K685ac was completely abrogated **(Figure 3.3A-C)**. These results clearly indicate that both canonical pY705 and noncanonical pS727 pathways operate independently and can be activated individually, while K685ac requires prior pS727 presence.

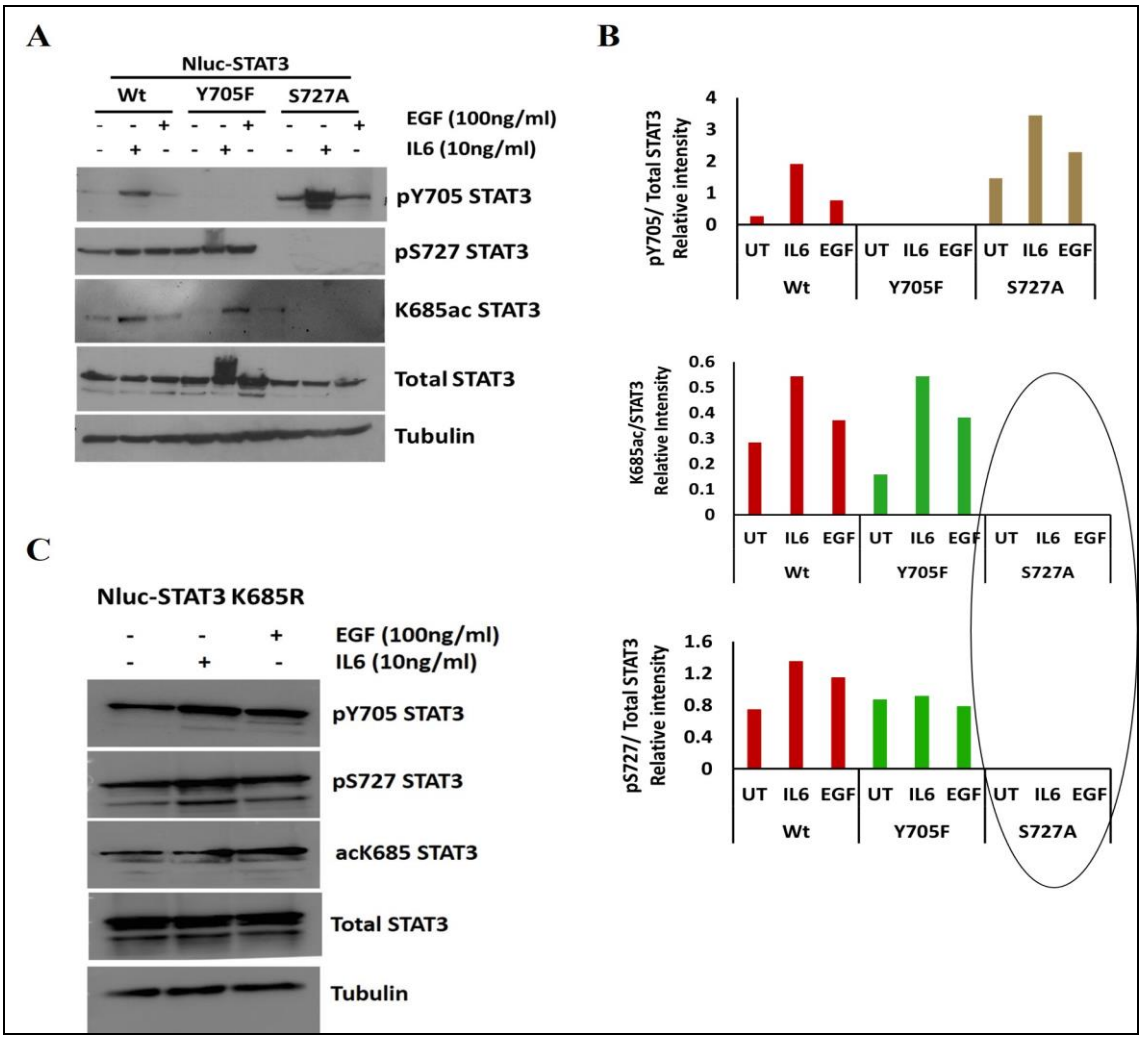

Figure 3.3. Canonical (pY705) and noncanonical (pS727 & K685ac) STAT3 activation are independent of each other. *(A) Immunoblot of Nluc-STAT3 PTM mutants stably expressed in MCF 7 cells. Post 24hours of serum starvation, the cells were stimulated with either IL6(10ng/ml) or EGF (100ng/ml) for 2hours and one set of unstimulated cells were kept as control. Each clone was probed for total and activated (pY705, pS727 and K685ac) STAT3 levels. (B) Densitometric analysis for each*

blot in (A). Activated STAT3 (pY705, pS727 or K685ac) level was normalised with total STAT3 expression for individual sample. (C) Immunoblot of Nluc-STAT3 K685R clone with or without ligand stimulus (IL6 or EGF) and probed for total, pY705, pS727 and K685ac STAT3 expression.

3.3.3 Noncanonical STAT3 pathway (pS727 and K685ac) controls cell proliferation and survival functions in breast cancer cells

STAT3 signaling is known to play a key role in controlling cell growth and proliferation under both normal and oncogenic conditions. Hence, we further investigated the implications of individual PTM site loss on STAT3 molecule, upon its ability to influence the cell survival functions in MCF 7 cells. Results from EdU cell proliferation assay revealed that in comparison to Wt or canonical Y705F mutant, with the loss of noncanonical pS727 (S727A) and K685ac (K685R) PTM sites more than 2-fold reduction ($p<0.01$ and $p<0.05$ respectively) in cell proliferation ability was observed **(Figure 3.4A)**. The depletion in cell proliferation ability of the clones was also evident with the long-term cell survival assay. Both S727A and K685R clones formed significantly less ($p<0.001$) number of colonies as compared to wild type counterpart. Though with Y705F mutant also the number of colonies formed were significantly less ($p<0.01$), however the average number of colonies formed within the same time frame of the assay was much higher than the other two mutants (S727A or K685R) **(Figure 3.4B).** Collectively these observations clearly indicate that as compared to canonical arm (pY705), it is the noncanonical activation (pS727 and K685ac) pathway that majorly controls the STAT3 dependent cell survival and proliferation functions in breast cancer cells.

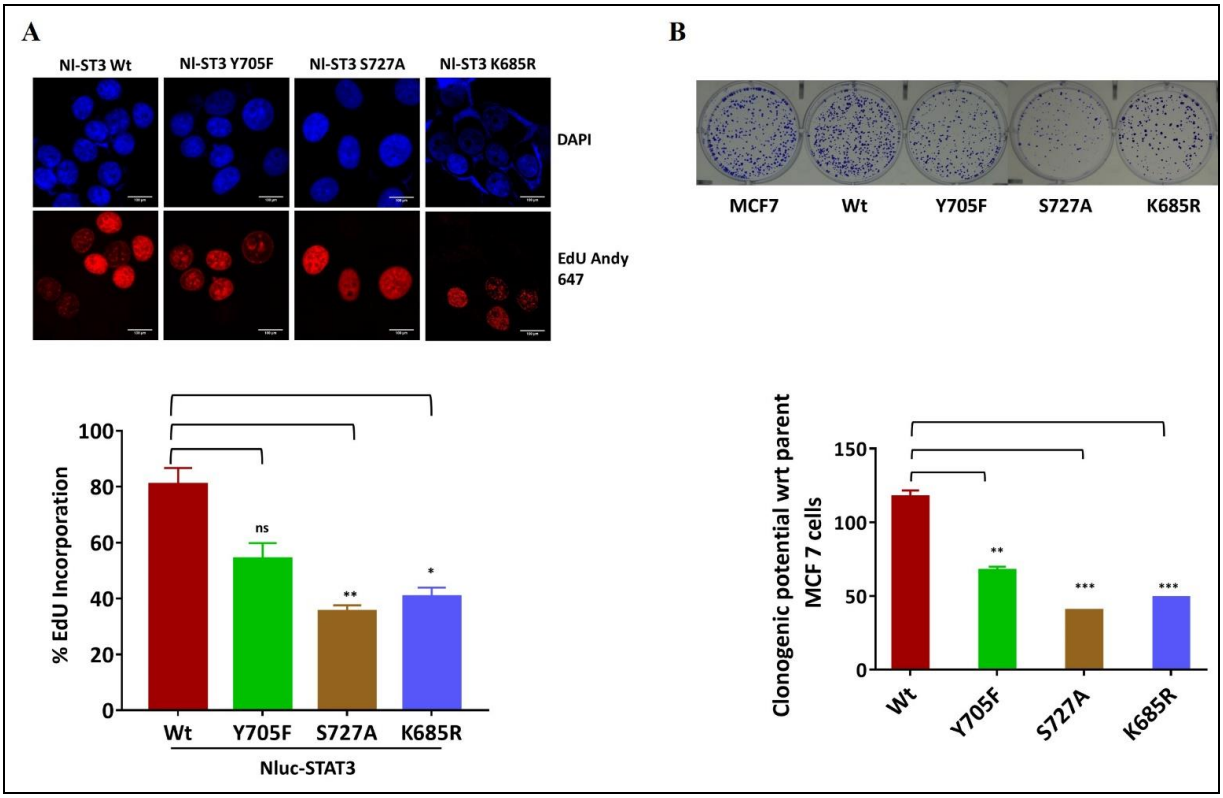

Figure 3.4. Effect of STAT3 PTM mutants on cell survival and proliferation. *(A) Microscopy images of EdU cell proliferation assay of MCF 7 cells (STAT3 KD) overexpressing STAT3 point mutants. Cells were stained with Anti-EdU-AndyFluor647antibody and DAPI was used to mark the nucleus. Bottom graph represents percentage of cells positive for EdU staining in each clone (n=300 cells per clone). (B) Representative image of colonies formed in clonogenic assay for individual STAT3 mutant stained with 0.5% crystal violet stain. Bottom graph represents the clonogenic potential of individual STAT3 PTM mutant clone w.r.t parental MCF 7 cells. Each graph represents mean value ± SEM. Significance levels are * $p<0.05$, ** $p<0.01$, and *** $p<0.001$ and ns as non-significant.*

3.3.4 Differential PTM marks alter STAT3 transcriptional regulation activity

To determine whether the differential PTM status of STAT3 molecule imparts any altered transcriptional activity or target preference, we monitored the expression levels of three well

known direct targets of STAT3 i.e. Cyclin D1, TWIST1 and SOCS3 using quantitative real time PCR. As a result of Wt STAT3 overexpression, transcript levels of both Twist1 and Socs3 was significantly enhanced ($p<0.01$). However, with all three mutants (Y705F, S727A and K685R) the mRNA expression of both the genes dropped down significantly ($p<0.05$). Specifically, for S727A mutant, the decrease in Twist1 transcript level was much more drastic ($p<0.001$) as compared to Y705F or K685R clones **(Figure 3.5A-B)**. For another target i.e. Cyclin D1, not much change was observed in mRNA transcript levels either with Wt or PTM mutant clones' expression **(Figure 3.5C)**. Similar observations were made even at Cyclin D1 protein levels using immunoblotting **(Figure 3.5D)**. These observations clearly indicate that both Twist1 and Socs3 expression requires presence of all the three (pY705, pS727 and K685ac) activation marks on STAT3 molecule while Cyclin D1 levels can be maintained even if one of the STAT3 activation site is intact.

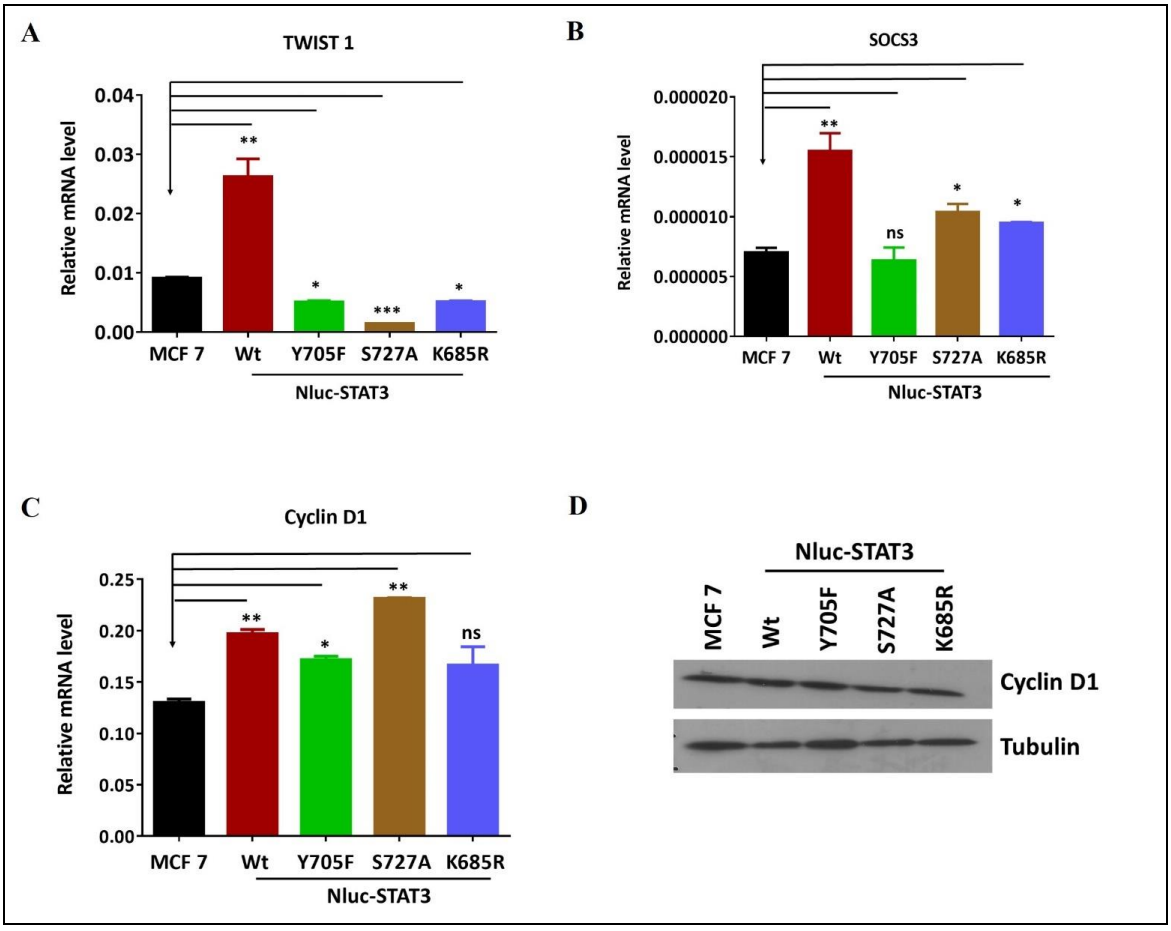

Figure 3.5. Effect of STAT3 PTM mutants on downstream transcriptional activity. *(A-C) Graphs representing relative mRNA levels of TWIST1, SOCS3 and CYCLIN D1, respectively, transcripts in different STAT3 PTM mutants. (D) Immunoblot of Cyclin D1 protein levels in respective MCF 7 STAT3 PTM line. Tubulin was used as loading control. Each graph represents mean value ± SEM. Significance levels are * p<0.05, ** p<0.01, and *** p<0.001 and ns as non-significant.*

Further as a novel target; Her2, E-Cadherin and ERα showed differential expression pattern in STAT3 mutant clones. As observed with immunofluorescence assay, the expression and membrane localization of Her2 protein was unaltered in either Wt or Y705F mutant while it increased significantly in S727A and K685R clones **(Figure 3.6A)**. This difference in Her2 expression pattern was also evident at the protein level across all the PTM mutant clones as determined using immunoblotting **(Figure 3.6B)**. Another molecule that showed altered expression was E-Cadherin. Similar to Her2 protein, E-Cadherin expression was unaffected in both Wt and Y705 overexpression clones, while it enhanced significantly in S727A and K685R mutants **(Figure 3.6C).** For ERα, the protein levels did not change much in Wt, Y705 and S727A clones while a significant downregulation was observed specifically in K685R mutant **(Figure 3.6D).** These results indicate that the noncanonical arm of STAT3 plays a key role in regulating expression of Her2, E-Cadherin and ERα either directly or indirectly while the expression of general STAT3 targets are equally maintained in breast cancer cells.

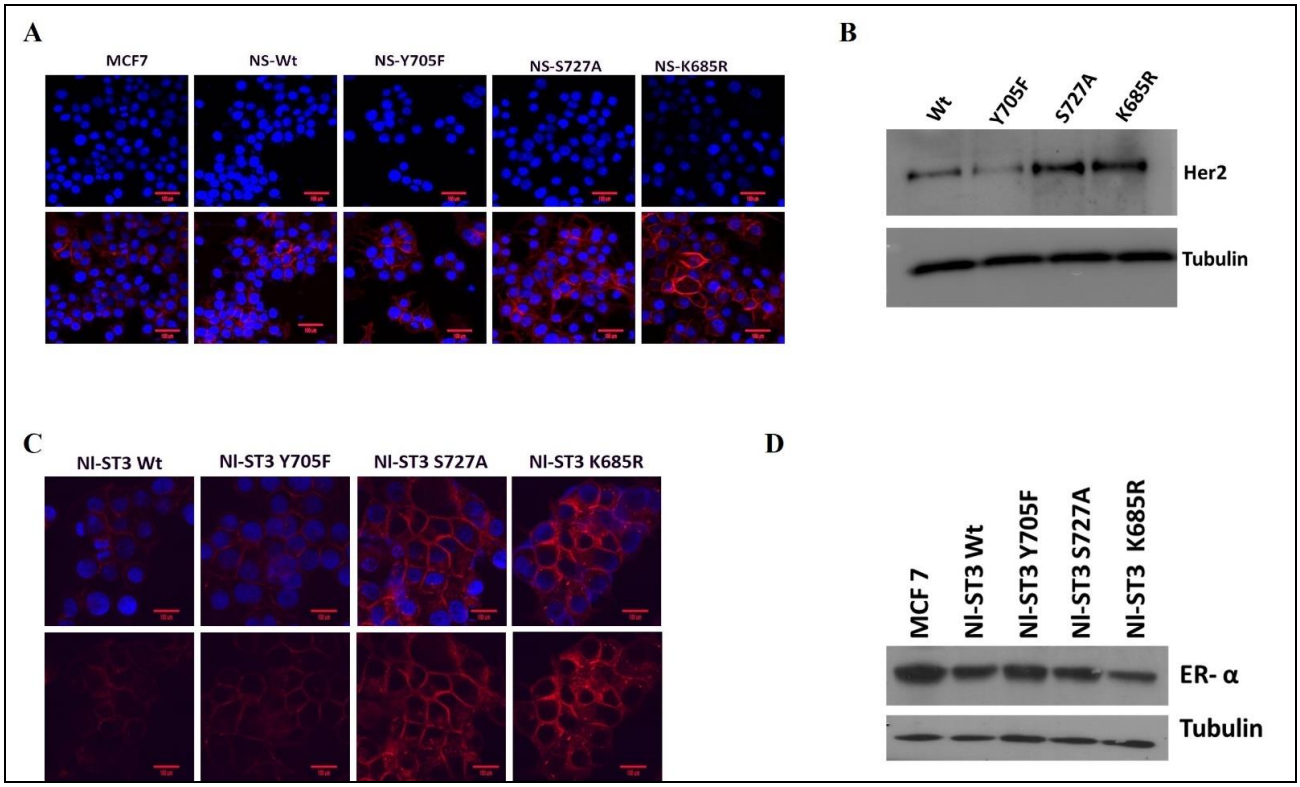

Figure 3.6. Effect of STAT3 PTM mutants on downstream transcriptional activity. *(A) Immunofluorescence microscopy images of Her2 protein expression in individual STAT3 PTM mutants. Her2 was stained with dylight633 and DAPI was used to stain the nucleus. (B) Immunoblot for expression level of Her2 protein in respective STAT3 PTM mutants. (C) Immunofluorescence microscopy images of E-Cadherin protein expression in individual STAT3 PTM mutants. E-Cadherin was stained with dylight633 and DAPI was used to stain the nucleus. (D) Expression level of ER alpha protein in different STAT3 PTM mutants as determined using immunoblotting. Tubulin is used as loading control.*

3.3.5 pS727 activation is essential for stable STAT3 homodimerization

Based on data from the literature, it is evident that homodimerization of STAT3 is a rate limiting step, that is essential for STAT3 pathway induction. Post activation the nuclear-cytoplasmic distribution of STAT3 homodimer changes as the activated from localizes more to the nucleus. Hence, we next raised the question that how different PTM sites on STAT3

influence its homodimerization ability and how dimer formation is affected when these specific sites are lost. To achieve this, we took advantage of the Phopsho-STAT3 BRET sensor developed in Chapter 2 **(Figure 3.7A)**. To thoroughly investigate the role of individual PTM sites in governing STAT3 homodimerization, we prepared a library of STAT3 Phospho BRET constructs (NLuc-STAT3 and Turbo-STAT3) carrying mutation in respective PTM site either alone or in combination (double or triple mutants) **(Figure 3.7B)**. We first determined the effect of single PTM site loss on STAT3 homodimerization and BRET signal. Upon expression of single point mutants BRET constructs in MCF 7 STAT3 knock down background cells, we computed the IL6 induced change in BRET ratio and compared that with the uninduced condition. Over here we observed that upon IL6 trigger a significant gain is evidently seen across all the mutants tested (Wt, Y705F, S727A and K685R). However, of all the mutants, Cl3 (S727A) had a dramatic decrease in the IL6 induced change in BRET signal (~3.5 fold) as compared to wild type Cl1 (Wt). While both Cl2 (Y705F) and Cl4 (K685R) achieved BRET signal equivalent to Cl1 upon IL6 trigger ($p<0.01$) **(Figure 3.7C)**. The observations made from live cell BRET assay was further validated by *in vitro* Co-IP experiment. Both Nluc-STAT3 and Turbo-STAT3 PTM mutant constructs were co-expressed in STAT3 knock down MCF 7 cells and cell lysate was prepared either in absence or presence of IL6 treatment (10ng/ml). As a measurement of homodimerization we pulled down the complex with anti- Turbo antibody and probed with anti-Nluc or anti-Turbo antibody for binding. Over here, in comparison to Wt, Y705F and K685R clones, S727A mutant showed significantly reduced band intensity (2.68-fold as compared to Wt) in the immunoblot of pull-down complex **(Figure 3.7D)** indicating formation of very fewer stable homodimers. Data from both live cell BRET assay and *in vitro* pull-down study strongly confirms the dominant role of pS727 and not pY705 or K685ac, as major PTM site influencing STAT3 homodimerization.

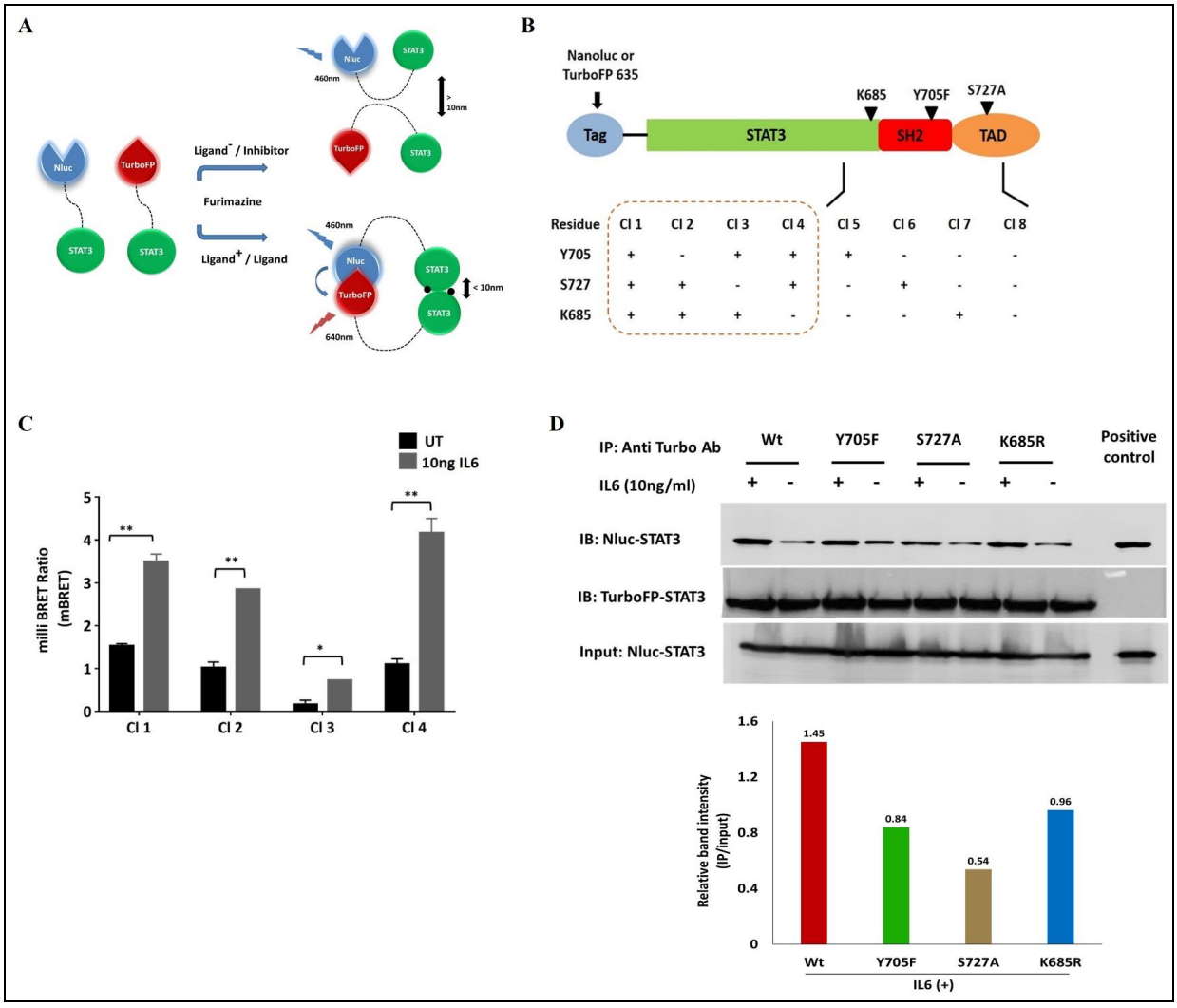

Figure 3.7. STAT3 phospho-BRET sensor to study STAT3 dimerization in live cell. *(A) Schematic representation for working model of Phospho STAT3 BRET sensor (explained in Chapter 2). (B) Clonal library of STAT3 BRET construct having respective PTM site mutated in Wt-STAT3 either alone or in combination. (C) Corrected BRET ratios for Nluc-STAT3 Cl1-4 in response to IL6 (10ng/ml) stimulation. Black bar represents unstimulated condition and bleed through signal was subtracted using Nluc-STAT3 Cl1-4 expressing controls. (D) Co-IP blot of respective STAT3 PTM mutants from (C) i.e. Cl1-4. Immunoprecipitation was done using anti-TurboFP antibody and immunoblotting was done using anti-Nluc or anti-TurboFP antibody. Positive control is lysate from MCF 7 cells expressing only Nluc-STAT3 wild type contract. Bottom graph represents densitometric analysis for band intensity in pull down complex normalised to input control. For all BRET studies, acquisition was done in 500nm-donor channel and 640nm-acceptor channel using IVIS*

*spectrum with integration time of 30sec/filter. Furimazine was used as luciferase substrate (1:1000 diluted). Each graph represents mean value ± SEM. Significance levels are * p<0.05, ** p<0.01, and *** p<0.001 and ns as non-significant.*

Based on these initial observations, we further screened the entire library of PTM mutants (Cl1-8) in STAT3 KD **(Figure 3.8A)** MCF 7 cells and stimulated with IL6 to determine the contribution of individual site in dimerization event. In Cl3 (S727A)- single site mutant and from Cl5-Cl7 -dual site mutant, a significant decrease in IL6 induced BRET signal was observed as compared to Cl1,2 and 4. Further, except for Cl5, both Cl6 and Cl7 majorly remained ineffective for the IL6 stimulation. For Cl7 ($Y705^-$/ $S727^-$) and Cl8 ($Y705^-$/ $S727^-$ /$K685^-$) a negative ratio in uninduced condition and a nonsignificant change with IL6 induction confirmed significant abrogation in STAT3 homodimerization event **(Figure 3.8B)**. Similar observation was made even in 3'UTR STAT3 KD MDA MB 231 cells having expression of BRET mutant library **(Figure 3.8C)**. These results clearly reveal the individual role of pY705, pS727 and K685ac PTMs in STAT3 dimerization and identifies pS727 PTM site as major contributor of activation mechanism, for driving STAT3 homodimerization and activation process.

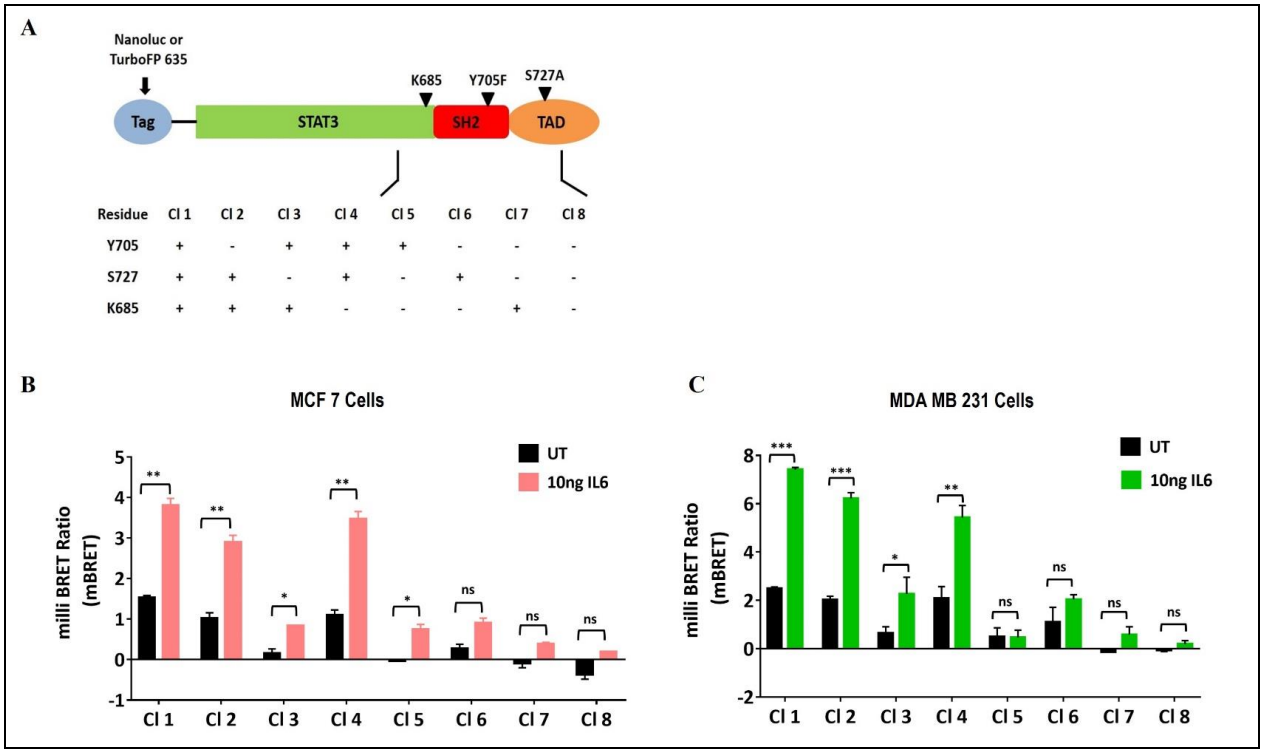

Figure 3.8. STAT3 phospho-BRET sensor to study STAT3 dimerization in live cell. (A) *Clonal library of STAT3 BRET construct having respective PTM site mutated in Wt-STAT3 either alone or in combination. (B-C) Corrected BRET ratios calculated for the entire STAT3 PTM mutant library (Cl1-Cl8) using IL6 as ligand (10ng/ml) in MCF 7 and MDA MB 231 cells, respectively. Black bar represents uninduced condition and pink or green depicts IL6 stimulated condition. For all BRET studies, acquisition was done in 500nm-donor channel and 640nm-acceptor channel using IVIS spectrum with integration time of 30sec/filter. Furimazine was used as luciferase substrate (1:1000 diluted). Each graph represents mean value ± SEM. Significance levels are * $p<0.05$, ** $p<0.01$, and *** $p<0.001$ and ns as non-significant.*

3.3.6 Niclosamide (NSA), the anti-helminthic drug can be repurposed as a target inhibitor blocking both the major STAT3 activation signals

Pertaining to at least the two different activation arms that can trigger STAT3 activation independently, it reveals the importance of targeting both the pathways to switch off STAT3

signaling completely. In this scenario, if one of the activation sites is blocked/mutated and cells are treated with inhibitor that inhibits the alternative arm too, a complete inhibition in STAT3 activity can thus be achieved **(Figure 3.9A)**. Therefore, in an attempt to achieve this, we selected two different STAT3 inhibitors; niclosamide that was previously known to block both pY705 and pS727 STAT3 activation and Stattic that is majorly a pY705 blocker **(Figure 3.9B also Chapter 2 Figure 2.10C)**, and tested for their specific effect against STAT3 pathway in various PTM mutants background. Long term cell survival assay revealed that both Wt and Y705F clones showed similar level of surviving fraction (~50% survival) post 5µM NSA or Stattic treatment ($p<0.01$). Though with NSA the percent survival in Y705F (33.23%, $p<0.01$) was significantly less than that of Stattic. In S727A mutant the percent surviving fraction obtained was 11.61% for NSA and 19.19% for Stattic ($p<0.001$) and in K685R, 18.22% for NSA and 38.59% for Stattic ($p<0.001$ and 0.01, respectively) **(Figure 3.9C)**. Overall, it showed that if canonical arm is blocked by site specific PTM mutation (Y705F), treating with drug inhibitor like NSA, that blocks pS727 noncanonical pathway, a synergetic effect is obtained. The same cannot be achieved upon treating with inhibitors like Stattic that is ineffective against pS727 PTM. On contrary, if pS727 site is already lost (S727A), treatment with either NSA or Stattic will be equally effective to block the STAT3 mediated cell survival signals. Hence, effective inhibition of STAT3 as achieved with NSA (pY705 and pS727 blocker) is a more promising approach to shut down the dual STAT3 pathway and downstream oncogenic functions.

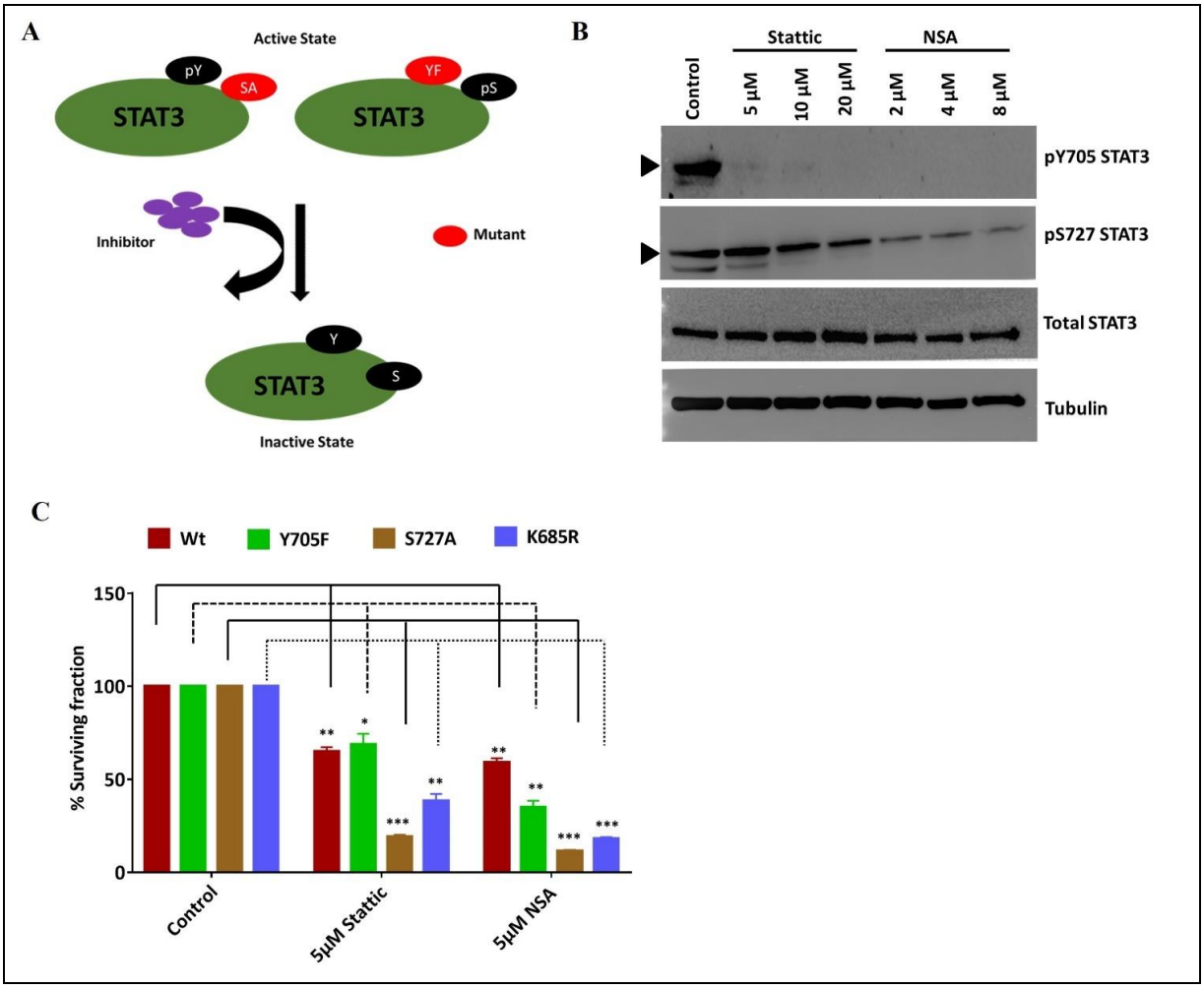

Figure 3.9. Effect of Niclosamide and Stattic treatment on STAT3 inhibition. *(A) Schematic representation for effective blocking STAT3 pathway. If one of the PTM site either pY705 or pS727 is already mutated or lost, then using inhibitor or drug molecule that blocks the intact PTM (either pY705 or pS727) site will result in complete inhibition of the STAT3 molecule. (B) Immunoblot of MCF 7 cells treated with differential concentration of Stattic or Niclosamide for 24hrs. Each blot was probed for total and activated (pY705 and pS727) STAT3 levels and tubulin was using as loading control. (C) Percent surviving fraction in respective STAT3 mutant cell line in response to Niclosamide and Stattic treatment. Colonies formed in the clonogenic assay were stained and counted on day 14th. Each graph represents mean value ± SEM. Significance levels are * $p<0.05$, ** $p<0.01$, and *** $p<0.001$ and ns as non-significant.*

3.4 Discussion

Based on limited knowledge available on alternate STAT3 activation mechanism. This study, taking example of breast cancer as model system, deciphers the essential role played by noncanonical STAT3 pathway over its canonical counterpart in controlling activation, dimerization, transcription activity and downstream biological functions of the STAT3 molecule.

In order to develop a clear understanding of independent or interdependent mode of operation for canonical and noncanonical STAT3 pathway, we engineered a 3'UTR STAT3 shRNA knock down MCF 7 cell line model stably expressing clonal library of Phospho STAT3 BRET constructs (Nluc-STAT3 and TurboFP-STAT3) carrying mutation either in single or multiple PTM sites. Using this model system, we determined that in response to IL6 or EGF stimulation, Y705F mutant can be induced for both pS727 and K685ac expression while in S727A clone though pY705 activation is intact, K685ac was completely blocked. These observations clearly indicate that phosphorylation event at Y705 and S727 site operates independently, while, K685ac was found to be dependent upon prior presence of pS727 activation mark. At functional and phenotypic level, we found that breast cancer cells devoid of S727 and K685 activation marks showed significantly lower proliferation rate and less percentage of surviving fraction as compared to wild type or Y705F clones. Additionally, with Y705F mutant not much difference in phenotypic aspects was seen. These observations clearly indicate that in case of breast cancer cells it is the noncanonical pathway (pS727 and K685ac) that primarily controls the cell survival and proliferation functions as compared to classical canonical (pY705) counterpart.

For STAT3 to localize to nucleus and work as an active transcription factor, homodimerization is very crucial. So far it was known that pY705 mediated STAT3

activation primarily controls STAT3 homodimerization and downstream biological functions (Berishaj *et al*, 2007). However, recently many literature suggests that pS727 or K685ac (O'Shea *et al*, 2005; Yuan *et al*, 2005) can independently activate STAT3 molecule even in absence of pY705 PTM (Hazan-Halevy *et al*, 2010). Therefore, taking advantage of the proximity dependent Phospho STAT3 BRET sensor developed in Chapter 2, we next determined the contribution of individual PTM site in regulating STAT3 dimerization event. For the first time in this study we report that in cells with pS727 activation site loss, the STAT3 homodimerization is significantly affected upon IL6 stimulation. Further when single site loss (Cl3- S727A) is accompanied by mutation at other PTM sites i.e. Cl5,7 and 8, a drastic drop in BRET homodimerization signal confirmed precise loss in proximity of the two STAT3 monomers. However, in Wt, Cl2 (Y705F) and Cl4 (K685R) mutants, under similar experimental conditions, a significant gain in BRET signal indicates sufficient STAT3 homodimerization. The observations from live cell BRET study was further validated using Co-IP assay where S727A mutant showed more than 2-fold reduction in dimer formation ability as compared to Wt.

Coming to the downstream function, STAT3 acts as a transcriptional regulator of downstream targets, where STAT3 dimer binds directly to many genes of oncogenic relevance (Carpenter & Lo, 2014). Therefore, to assess this potential, the transcriptional regulation ability of different STAT3 PTM mutants was verified for a few key genes of relevance in breast cancer like Cyclin D1, SOCS3 and TWIST 1(Carpenter & Lo, 2014). Not much change in the transcript levels of these known targets was observed in different PTM background indicating that all the mutants are transcriptionally active and both arms of STAT3 activation can control their expression equally. However, Her2, E-Cadherin and ERα showed altered expression w.r.t to different STAT3 PTM status. Her2 and E-Cadherin expression increased significantly in S727A and K685R mutants in comparison to Wt or

Y705F as observed with both immunoblotting and Immunofluorescence assay. While ERα levels dropped significantly in K685R mutant. With respect to Her2 being controlled by STAT3 there is only one report in which the authors found out that leptin mediated STAT3 activation increases Hsp90 expression that in turn stabilizes Her2 protein in breast cancer (Giordano *et al*, 2013). We assume that similar downstream effect would too have occurred in our models also, thereby enhancing Her2 expression in the cells. Whereas reduced level of ERα in K685R mutant indicates that acetylated STAT3 is required for maintaining its expression either directly or indirectly in breast cancer. All these observations point out critical role played by noncanonical pathway (pS727 and K685ac) in controlling STAT3 activation, homodimerization and downstream transcriptional functions.

Based on data gathered in this study, it is evident that in breast cancer cells, noncanonical pathway plays predominant role of controlling STAT3 mediated downstream biological functions. And to inactivate the STAT3 molecule blocking both pY705 and pS727 activation is important. However, in current scenario majority of the drug inhibitors available against STAT3 have been tested for their ability to block pY705 activation without much attention towards the pS727 inhibition (Chen *et al*, 2018). Therefore, in this study, we test verify two STAT3 inhibitors Niclosamide and Stattic **(discussed in chapter 2)** for their ability to target STAT3 activation in different PTM mutant background of STAT3 molecule. Our data revealed that as compared to Stattic, well known STAT3 inhibitor, Niclosamide is a more potent drug candidate. With ability of niclosamide to block both pY705 and pS727 activation simultaneously, the percent surviving faction was significantly reduced in all the mutant background (Y705F, S727A and K685R) as compared to Wt. While Stattic being only a pY705 blocker showed effective reduction in surviving faction majorly for S727A mutant. Hence for complete blocking of STAT3 pathway, identifying inhibitors like Niclosamide is a much more rational and strategic approach.

3.5 Significance of the Study

Pertaining to two different activation mechanisms -canonical and noncanonical pathway, that can trigger STAT3 activation, this chapter throws significant light on minute molecular details and bring strong evidences in favour of noncanonical pathway as an essential arm of STAT3 signaling operating in breast cancer cells.

Using an efficient engineered model system and combinatorial PTM mutant library we have identified independent occurrence of canonical and noncanonical STAT3 pathway activation, that was not known earlier. Further for the first time in this study, using live cell Phospho BRET sensor we have shown that pS727 residue plays a key role in regulating stable STAT3 homodimerization. While other PTM sites like pY705 or K685ac are less significant. This observation goes against the previous published report where K685 was identified as key player in STAT3 dimerization event (Yuan *et al*, 2005). However, the results from our study goes parallel with two recent published articles, where based on crystal structure of dimeric STAT3 and using a BiFC sensor in another study, no drastic difference in STAT3 dimerization was observed upon K685 site loss. (Belo *et al*, 2019).

The stable homodimers formed in response to pS727 activation than translocate to nucleus and control expression of genes involved in cell proliferation and survival of breast cancer cells. Hence for blocking STAT3 activity, the targeting approach is now required to be modulated and pS727 inhibition should be considered in parallel to pY705 blocking **(Figure 3.10)**. In these lines, we have identified repurposed anti-helminthic drug Niclosamide, which is a dual blocker of STAT3 molecule (pY705 and pS727), and have shown its anti-cancer activity against MCF 7 breast cancer cells. In future more such inhibitors should be identified to facilitate successful STAT3 targeting.

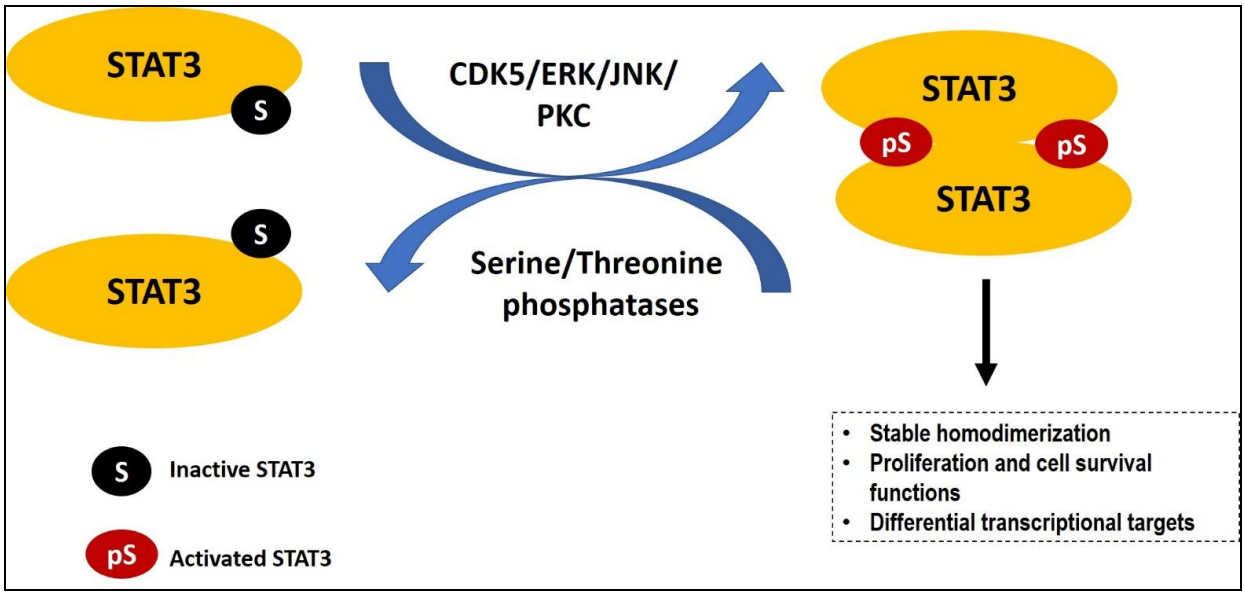

Figure 3.10. Noncanonical (pS727) pathway activation and function in breast cancer. *Schematic representation of how pS727 PTM mediated stable STAT3 homodimerization controls essential cell survival, proliferation and transcriptional functions for STAT3 molecule in breast cancer.*

Chapter 4

Role of STAT3 Signaling in Triple Negative Breast Cancer

Objective 3: To study the association of STAT3 PTMs (e.g. pY705, pS727 and K685ac) with respect to breast cancer outcome

4.1 Introduction

Breast cancer (BC) is highly heterogeneous disease with different histological type, molecular signatures, clinical outcome and response to therapeutic treatment. Based on gene expression profiling and IHC staining for ERα, progesterone and Her2 receptor, BC can be classified into 4 major subtypes- Luminal A, Luminal B, Her2 high and Triple negative breast cancer (TNBC). Of all the subtypes known, TNBCs, represents the most aggressive subtype with poor prognosis (Fragomeni *et al*, 2018) (He *et al*, 2019).

As the name suggest, triple negative breast cancer or TNBCs are characterised by absence of estrogen receptor, progesterone receptor or Her2 amplification (Yao *et al*, 2017). TNBCs are a heterogeneous group of tumours as identified both pathologically and clinically and comprises of overall 12-20% of breast cancer cases. Due to lack of targeted therapy, cytotoxic chemotherapy drugs and DNA damaging agents continues to be a mainstay approach for treatment in adjuvant, neoadjuvant or metastatic settings (Qin *et al*, 2019). Of all the TNBC patients that receive neoadjuvant chemotherapy, only 30% show pathologically complete response (pCR) with good survival. However, the remaining patients with leftover tumor cells in the breast or lymph nodes after pre-operative therapy, have high chances of relapse with metastasis and overall poor survival (Balko *et al*, 2014).Considering the highly heterogeneous nature of the disease, so far there are no targeted therapies available and there are very limited number of inhibitors that have shown some success in clinical trials. Targeted therapies using PARP inhibitors, anti-EGFR and immunotherapies though have given promising clinical results however further critical investigations is still required (Yao *et al*, 2017). Recently efforts have been shifted to identify targetable or overexpressed

molecules as an alternative treatment approach. Genomic profiling of TNBCs have identified many such aberrantly activated and overexpressed signaling molecules, of which, one of them is STAT3. Growing number of evidences strongly suggest that STAT3 could be a potential therapeutic candidate against TNBCs (Qin *et al*, 2019).

Signal transducer and activation of transcription 3 (STAT3), is known to be overexpressed in more than 60% of overall breast cancer cases (Alvarez *et al*, 2005; Walker *et al*, 2009). Once activated (pY705), STAT3 relays oncogenic signal from activated receptors on cell surface to nucleus, where it functions as a transcription factor to control expression of genes involved in growth and proliferation of cancer (Shalini Dimri, 2017).Though STAT3 is reported to be present in other BC subtypes, it is reported to be strongly associated with the triple negatives. In TNBCs, STAT3 is constitutively activated and it controls expression of target genes involved in initiation of tumor, progression, metastasis, immune evasion , imparting resistance to chemotherapy and overall poor survival (Qin *et al*, 2019). Apart from this, STAT3 is also reported to physiologically interact with other protein and transcription factors like TCPTP (Shields *et al*, 2013), GLI1 (Sirkisoon *et al*, 2018) and GRIM-19 (Zhou *et al*, 2013) that either indirectly or directly controls STAT3 pathway activation. Recently, new role of STAT3 has been identified in TNBCs where it localizes to mitochondria and interacts with electron transport chain, regulate calcium homeostasis and controls ROS generation (Wegrzyn *et al*, 2009). Activation of STAT3 and its downstream oncogenic functions driven by pY705 activation is well defined in breast cancer, however the alternate noncanonical STAT3 pathway (pS727) majorly remain unexplored. With respect to BC there are few reports that strongly suggest a strong association between noncanonical pS727 STAT3 activation and hormone negative BC type ; pS727 STAT3 is reported to have negative correlation with ER status of the BC tissue sample (Yeh *et al*, 2006), acetylated STAT3 at K685 residue interacts with DNMT1 and suppresses expression of ERα gene and pS727

mediated STAT3 activation is essential for interaction with CBP300/p300 for full transactivation of the molecule (Lee *et al*, 2012; Wang *et al*, 2005). Though reports are available even in case of melanoma (Sakaguchi *et al*, 2012), chronic lymphocytic leukaemia (Hazan-Halevy *et al*, 2010) lung adenocarcinoma as well as in glioblastoma (Ouedraogo *et al*, 2016) for independent occurrence of pS727 mediated STAT3 activation and functions, not much is known about its role and expression in context of TNBCs.

Despite extensive efforts, there is an unfulfilled need for therapeutic targeting and innovation of treatment for TNBCs. Recent data from both preclinical and clinical studies indicates critical role of STAT3 molecule in TNBCs (Qin *et al*, 2019) and thus a deeper understanding of the STAT3 pathway will strongly provide novel and alternative approaches for STAT3 mediated targeted therapy against this subtype of BC. Taking this idea in consideration, in the present study we have retrospectively investigated the role of less explored noncanonical (pS727) and well known canonical STAT3 pathway together in TNBC cohort. Further as therapeutic approach, we have shown how dual blocking of STAT3 (pY705 and pS727) as achieved with NSA both *in vitro* and *in vivo* is a better treatment approach for STAT3 positive TNBC tumours.

4.2 Materials and Methods

4.2.1 Materials

Stattic (#S7024) was purchased from Selleckchem, (USA) and Niclosamide (#N3510) from Sigma-Aldrich (USA). EGF (#AF-100-15) and IL6 (#200-06) were from Peprotech (USA). D-Luciferin Firefly, potassium salt (# L-8220) was bought from Biosynth (Switzerland). Mouse-anti-STAT3 (#9139), rabbit-anti-pY705 STAT3 (#9145) antibodies were purchased from Cell Signalling (USA) and rabbit-anti-pS727-STAT3 (#E121-31) was bought from Abcam. Anti-CD44 APC (#559942) was bought from BD biosciences and anti-CD24

(#MA1-10154) was purchased Invitrogen. Secondary antibodies like anti-mouse HRP (#ab6728), rabbit- HRP/DAB detection IHC kit (#ab80436) was from Abcam and anti-rabbit-HRP (#31460) was from Invitrogen. iClick EdU AndyFluor647 cell proliferation kit was bought from Genecopia (USA, #A006). IVIS Spectrum pre-clinical *in vivo* imaging system was from Perkin Elmer (USA). It is equipped with 20nm bandpass filters ranging from 500-850nm.

4.2.2 Clinical samples and Ethics statement

The protocol for IHC study of total, pY705 and pS727 STAT3 was reviewed and approved in the Institutional Ethical Committee III (IEC III) meeting. Waiver of consent from the patients was also approved for the protocol by the IEC committee. For a total of 76 TNBC cases, formalin fixed and paraffin embedded (FFPE) tumour tissue blocks were procured from the ACTREC biorepository. For each case core biopsy block from breast cancer excision and paired post NACT (neoadjuvant chemotherapy) specimen was taken. The study cohort majorly comprises of patients in the age group from 24-72 years recruited between 2012-2017. Clinical characteristics of the patients is given in **Table 4.1.** All the cases were grade III, infiltrating ductal carcinomas (IDCs) and TNBC subtype with median tumor size of 6.50cm. Neoadjuvant chemotherapy regime majorly comprises of docetaxel, paclitaxel, carboplatin given either alone or in combination for 4-5 cycles followed by surgery. We also procured tumor tissue blocks for melanoma (n=4), lung adenocarcinoma (n=4) and few other breast cancer subtypes cancer i.e. $Her2^{+}$ (n=5) and ER^{+}/PR^{+} (n=5).

Characteristics	N (Proportion)
Total cases	76
Age	Median=47 years (24-72 years)
Gender	Female
Tumor Size	6.50±2.40 cm (median)
Grade	III
Histologic Type	IDC
ER/PR/Her2 Status	TNBC
Menopausal Status	
Pre-Menopausal	46
Post Menopausal	28
Peri Menopausal	2
NACT Response	
Complete Response (CR)	18 (25.35%)
Incomplete or partial response	53 (74.64%)

Table 4.1. Demographic information of the patients involved in the study.

4.2.3 Immunohistochemistry (IHC)

Standard IHC protocol was followed as reported previously (Chatterjee *et al*, 2013). Briefly, 5 µm thick FFPE tissue section was taken on a glass slide and de-paraffinized by performing sequential xylene washes for three times/10mins each. Rehydration of the tissue was done by alcohol washes in gradient from 100% to 75%. Endogenous hydrogen peroxidase activity was blocked using 0.3% H_2O_2 solution. For antigen retrieval, Sodium citrate buffer pH 6.0 was used and samples were boiled in microwave. Following antigen retrieval protein blocking was done using IHC kit from Abcam ((#ab80436). Primary antibody incubation was given for overnight at 4ºC in humidified chamber (anti-STAT3 1:1000, anti-pY705 STAT3 1:500 and anti-pS727 STAT3 1:1000). Next day, samples were processed for HRP incubation and DAB staining as per the manufacturer's instructions.

4.2.4 IHC Scoring Methods

For pathologist-based scoring Allred method was employed. In Allred scoring method two parameters are considered ; proportion of cells stained (0- no stain,1- les are considered than 1%, 2- 1-10%,3-11-33%,4-35-66 % and 5- 67-100% cell stained) and intensity of the staining (0- negative, 1- weak,2- intermediate and 3- strong stain). Hence a total score is assigned out of 8 (Qureshi & Pervez, 2010).

For digital scoring of DAB stain IHC profiler plugin in the ImageJ software was used. Over here scoring is done as mentioned previously (Chatterjee *et al*, 2013)**.** The final score obtained is between 0-3 i.e. 0= negative, 1+ = weak positive, 2+ = positive and 3+ = strong positive. Depending upon localization of protein of interest cytoplasmic or nuclear mode of analysis can be selected (Varghese *et al*, 2014).

4.2.5 Recombinant DNA Plasmid reconstruction

For knockdown studies, shRNA oligos against 3'UTR region of STAT3 were annealed and cloned in pLL3.7-GFP vector under U6 promoter using HpaI and XhoI restriction sites as per the standard protocol (De *et al*, 2008).

Fwd 3'UTRshRNA STAT3 – 5'GCTACATACTCCTGGCATTGC3'

Rev 3'UTRshRNA STAT3 – 5'GCAATGCCAGGAGTATGTAGC 3'

4.2.6 Real Time PCR

Total RNA from the cells was extracted using RNA extraction minikit (QIAGEN). 2µg RNA was used for preparation of cDNA using SuperScript III (Invitrogen) kit as per the manufacturer's instructions. Real time PCR was done using Sybr green reagent and GAPDH was used as normalization control. Primer sequence for STAT3, OCT4 and SOX2 and GAPDH gene is as follows:

Fwd STAT3: 5' GGAGGAGTTGCAGCAAAAAG

Rev STAT3: 5’ TGTGTTTGTGCCCAGAATGT

Fwd GAPDH: 5' TGCACCACCAACTGCTTAGC

Rev GAPDH: 5'GGCATGGACTGTGGTCATGAG

Fwd OCT4: 5'GTGGAGAGCAACTCCGATG

Rev OCT4: 5'TGCAGAGCTTTGATGTCCTG

Fwd SOX2: 5'AACCCCAAGATGCACAACTC

Rev SOX2: 5'GCTTAGCCTCGTCGATGAAC

4.2.7 Cell culture

MDA MB231 cells were cultured in L-15 medium (Sigma, USA) without $NaHCO_3$ supplemented with 10% FBS (Gibco, USA) and 1% Pen-step (Invitrogen, USA) in a CO_2 free incubator at 37ºC. MDA MB 231-Luc D3H2LN cells were cultured in DMEM medium supplemented 10% FBS (Gibco, USA) and 1% Pen-step (Invitrogen, USA) and maintained in 5% CO_2 incubator at 37ºC.

For knocking down endogenous STAT3 expression in MDA MB 231 cells, we prepared lentiviral particles in HEK293FT cells by transfecting with pLL3.7-GFP lentiviral vector containing 3’UTR STAT3 shRNA cassette along with virus envelope plasmids. MDA MB 231 cells were stably transduced with the virus containing shRNA against STAT3 and high GFP assisted FACS sorting was performed to enrich knocked down clones with subsequent passages.

4.2.8 Immunoblotting

Cell were trypsinized, harvested and washed with by 1XPBS. Cell pellet was resuspended in 1X cell lysis buffer containing - 10 mM Tris-HCl (pH 7.5), 140 mM NaCl, 5 mM EDTA, 2mM EGTA, 100mM NaF,100mM Na_3VO_4 ,100mM PMSF and protease inhibitor cocktail. Lysis was performed by sonication method at 10% amplitude with 10sec on/off cycle. The sample was centrifuged at 14000rpm/30min/4ºC and supernatant was collected in separate tube. Protein estimation was done using Bradford reagent and approx. 50-60µg protein was loaded on 7.5% SDS-PAGE gel. Protein transfer was done in semidry Trans blot assembly at 15V for 1hr at room temperature. Blocking was performed in 5% non-fat dry milk for 1hr at room temperature followed by primary antibody incubation [STAT3 1:1000, pY705 STAT3 1:500, pS727 STAT3 1:1000, K685ac STAT3 1:500, α-Tubulin 1:1000] overnight/4ºC. Next day, secondary-HRP antibody treatment was given followed by developing the blot using ECL substrate in ChemiDoc system (Biorad, USA).

4.2.9 Flow cytometry

For CD24 and CD44 staining, $1X10^6$ were collected in a tube and washed with FACS buffer ((PBS, 5%FBS and 0.1% sodium azide) two times at 1000rpm/5min/4ºC. Final pellet was resuspended in 100µl FACS buffer containing 10µl anti-CD44-APC and 10µl anti-CD24-PE antibody. Samples were incubated in dark on ice for 1hr.Cells were washed twice with chilled FACS buffer at 1000rpm/5min/4ºC and final pellet was resuspended in 100µl FACS buffer. Acquisition was done in BD FACS Aria with respective filters for APC and PE emission.

4.2.10 Cell survival and proliferation assay

For EdU cell proliferation assay, EdU AndyFluor647 proliferation kit was used. Briefly, cells seeded at an appropriate density on a coverslip. Next day, EdU was added to each sample and

incubated for 24hrs.Processing of the coverslips was done as per the manufacturer's instructions. Images were acquired in LSM780 (Leica) microscope with 633nm filter for EdU and 460nm filter for DAPI.

For clonogenic assay, 1000 cells were counted and seeded in a 6-well plate in duplicates. Clones were allowed to form for 14days, after which the colonies were fixed with chilled methanol and stained with 0.5% crystal violet stain.

4.2.11 Live cell luciferase assay

For live cell luciferase assay, MDA MB 231-LucD3H2LN cells were seeded at the density of 5000 cells/well in duplicate. Next day niclosamide or Stattic treatment was given at variable concentration. After every 24hrs of the treatment, luminescence signal was acquired in IVIS spectrum using open filter settings upon addition of D-luciferin substrate (1:100 diluted).

4.2.12 Soft agar assay

For anchorage independent growth assay $1X10^3$ cells were seeded in triplicate in 6-well plate. The bottom layer was prepared with 1% low melting agarose density and top layer was 0.8% agarose in 2X medium with 5% FBS. On every 3^{rd} day 50µl 2x medium was added to each well. Colonies were allowed to form for 22 days.

4.2.13 Breast cancer xenograft model and *in vivo* anti-cancer study

All animal experiments were performed in compliance with the standard protocol laid down by Institutional animal ethics committee (IAEC) for handling and care of small animals for experimental purpose. For developing breast cancer tumour xenograft model, $5X10^6$ luciferase labelled MDA MB 231-LucD3H2LN were implanted orthotopically at the 5^{th} mammary fat pad of 6-8 weeks old female NOD/SCID mice in a maximum volume of 50µl. Once tumor are grown upto the size of $100mm^3$, mice were randomly segregated into two

groups; control group and treatment group. Niclosamide treatment (50mg/kg) was given consecutively for 21 days via intraperitoneal injection. Tumour growth was monitored by performing non-invasive bioluminescence imaging (BLI) on every 7^{th} day of the treatment by injecting 3mg D-luciferin (100µl in saline) via intraperitoneal route. Luminescence signal was acquired in IVIS spectrum with open filter settings. Post treatment termination, mice were sacrificed and organs were taken out for *ex-vivo* BLI imaging to monitor distant metastasis. Tumour volume was determined using digital Vernier Caliper on every 7^{th} day of the treatment using the following formula: [length (mm) x $(\text{breadth})^2$ $(\text{mm})^2$] / 2.

4.2.14 Statistical analysis

For all statistical analysis SPSS 10.00 software was used. For all *in vitro* and *in vivo* analysis student t-test was employed. p value < 0.05 was considered as statistically significant. For clinical data analysis Kruskal Wallis H test was used for non-normal distribution and one-way ANOVA was employed for normal distribution. For comparing variables within the group, Chi square test, student t-test, Mcnemar test and post hoc test was employed.

4.3 Results

4.3.1 pS727 STAT3 is predominately activated and shows positive association with the TNBC subtype

To determine which pathway governs STAT3 activation in TNBCs, we performed IHC analysis for total, pY705 and pS727 STAT3 markers in 76 core biopsy and paired post NACT specimens. The demographic information about the study cohort is given in **Table 4.1**. For quantitative assessment of DAB staining, we employed two different scoring approaches; pathologist based (Allred method) and digital scoring method (IHC profiler). IHC staining for

both total and pS727 STAT3 showed strong to moderate positive nuclear localization with weak to moderate cytoplasmic staining. While pY705 was majorly negative or low positive for both nuclear and cytoplasmic expression. As a positive control for staining intensity, oral cancer tissue samples were used for total and pY705 STAT3 while a previously identified TNBC tissue was used for batchwise intensity variation for pS727 expression **(Figure 4.1A)**. Quantitatively, of the 76-core biopsy and post NACT specimens analysed using Allred scoring method, 86.2% (66/76) were found to be positive for STAT3 expression with more than 92.1% of them constitutively phosphorylated at pS727 residue. In comparison, pY705 form was found to be present in only 15.8% of STAT3 positive cases ($p<0.001$) **(Figure 4.2A)**. The observations made using Allred scoring method was further cross-verified by using our IHC profiler digital scoring method. IHC profiler scoring also confirmed strong nuclear positivity for total STAT3 (2+ to 3+ score) is associated with abundant pS727 positivity (2+ to 3+ score) for majority of the cases (71/76). While pY705 expression was either negative or low positive (1+) in all the STAT3 positive cases **(Figure 4.2B)**.

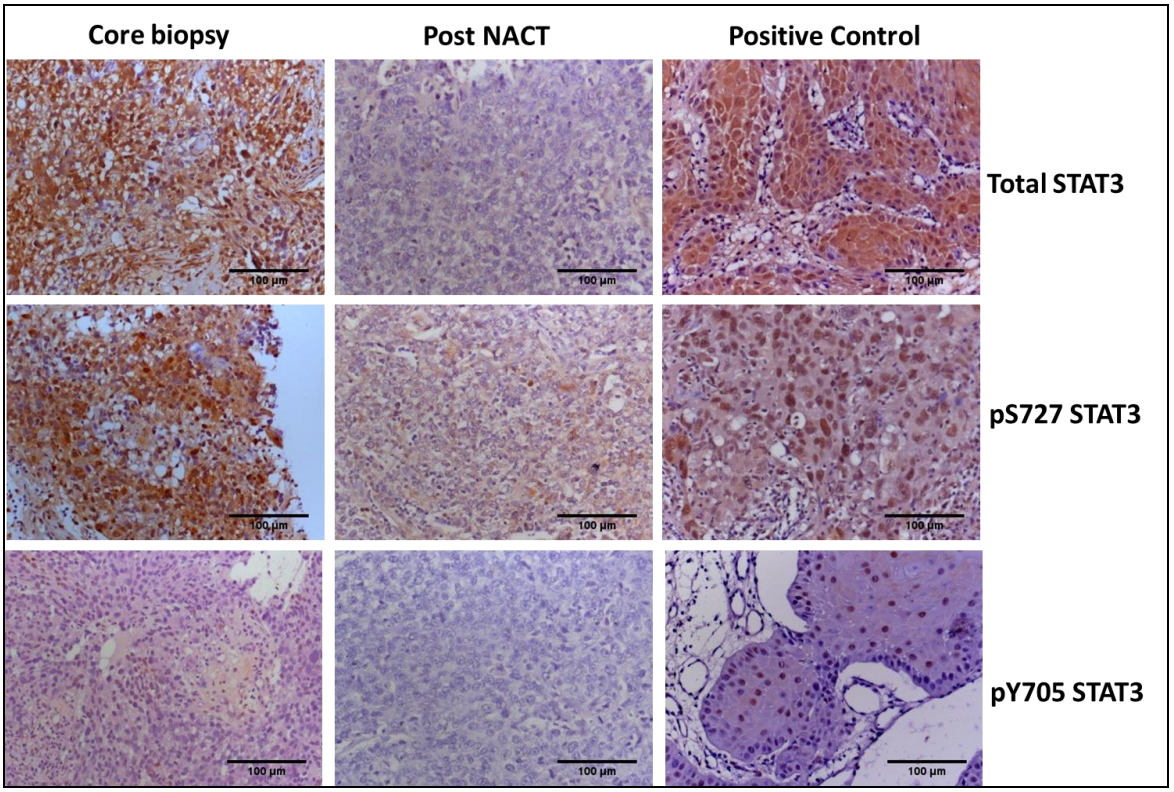

Figure 4.1. IHC DAB staining of total and PTM forms of STAT3 in TNBC tissue samples*. (A) Bright field IHC microscopy images of core biopsy and paired post NACT TNBC samples stained with DAB for total, pS727 and pY705 markers individually. Oral cancer tissue sample was used as positive control for total and pY705 STAT3, while a TNBC case was used for pS727 staining control. Scale bar represent 100µ.*

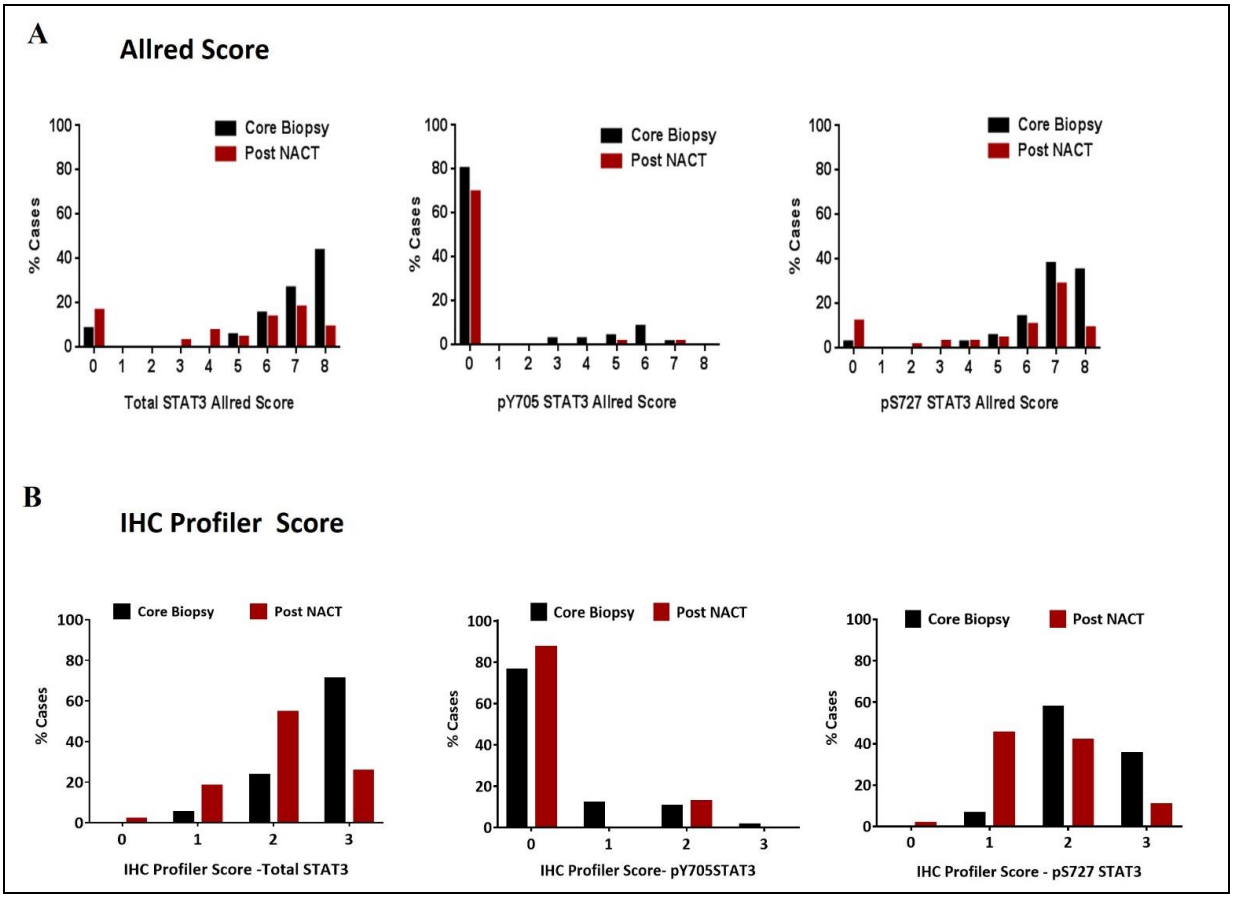

Figure 4.2. Quantitative IHC scoring for expression of total and phospho forms of STAT3 in TNBC tissue samples. *(A) Distribution of pathologist-based Allred scoring for total, pY705 and pS727 STAT3 expression in 76 core biopsy and paired post NACT specimens. A total score is assigned out of 8 (intensity of stain and percent positive cells). (B) Distribution of IHC profiler score (0-3+) for 76 core biopsy and paired post NACT specimens*

Furthermore, though the chemotherapy regime was not given with the perspective of targeting STAT3, however the number of positive cases for both total STAT3 and its PTM activated forms reduced significantly when compared between pre and post-chemotherapy samples. The frequency of percent positive cases dropped from 86.2% to 63.2% ($p<0.001$) for total STAT3, 92.1% to 64.4% ($p<0.001$) for pS727 and 15.8% to 3.4% ($p<0.01$) for pY705 respectively **(Figure 4.3A-C)** as observed with both the scoring methods**.**

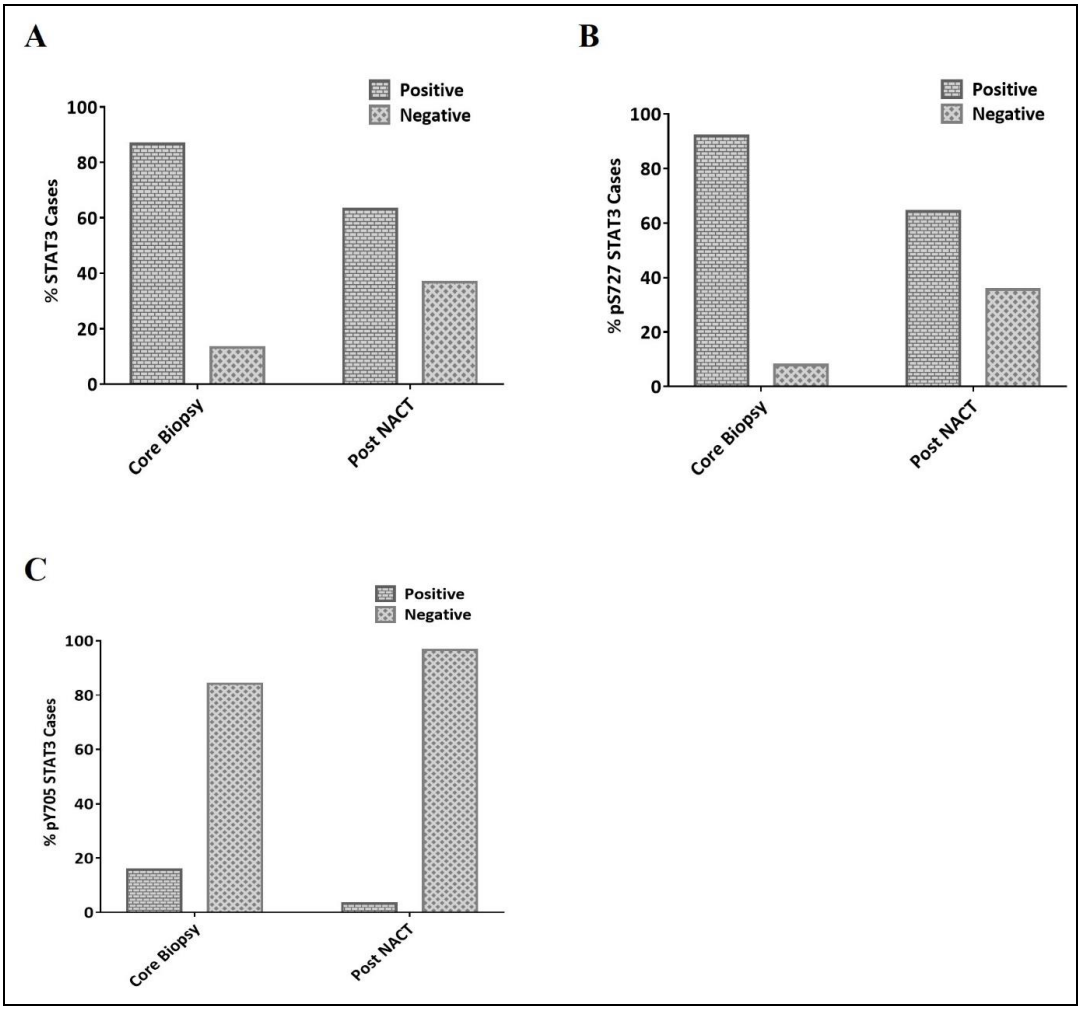

Figure 4.3. Effect of chemotherapy on expression of total and phospho forms of STAT3 in TNBC cases. *(A-C) Distribution of percent cases positive or negative for total, pS727 and pY705 STAT3 expression, respectively in 76 core biopsy and paired post NACT TNBC samples.*

Pertaining to similar expression pattern observed between total and pS727 STAT3 expression in tissue samples, we further performed independent correlation analysis to verify our observations. Person correlation value (**r**) of 0.49 ($p<0.0005$) showed significantly strong to moderate positive association between total and pS727 STAT3 expression in core biopsy specimens as analysed with two different scoring methods (Allred and IHC profiler scores). However, pY705 continued to show insignificantly low positive association ($r = 0.2086$, $p<0.$

0.0808) with total STAT3 expression **(Table 4.2)**. In post NACT specimens also similar pattern was obtained. Both total and pS727 STAT3 expression had Person correlation value (**r**) of 0.54 for Allred method and 0.47 for IHC profiler indicating moderate to strong positive association, while for pY705 and total STAT3, the Person correlation value (**r**) was 0.12 for Allred method and 0.23 for IHC profiler method, highlighting weak positive association. These observations clearly indicate that pS727 mediated non-canonical STAT3 signaling predominates over pY705 canonical arm in TNBC subtype of breast cancer.

	Core Biopsy samples			Post NACT Samples		
Samples	**N**	**Pearson Correlation Coefficient (r)**	**p Value**	**N**	**Pearson Correlation Coefficient (r)**	**p Value**
(IHC Profiler Method)						
Total STAT3 Vs. pS727	76	**0.4985**	0.0005	55	**0.5497**	0.0005
Total STAT3 Vs. pY705	76	0.187	0.09	55	0.129	0.054
(Allred Scoring Method)						
Total STAT3 Vs. pS727	76	**0.4987**	0.0005	55	**0.4776**	0.0006
Total STAT3 Vs. pY705	76	0.2086	0.0808	55	0.2342	0.1091

Table 4.2. Pearson's correlation analysis of total STAT3 expression with pY705 or pS727 expression in core biopsy and post NACT specimens using two different scoring methods. Pearson's correlation coefficient (r) = 0.1-0.3 small, 0.3-0.5= moderate, more than 0.5= strong positive association.

4.3.2 Correlation of Total STAT3 and its PTMs expression with different clinicopathological parameters

Clinical characteristics of the TNBC patients involved in the study are listed in **Table 4.1**. The median age of the patients was 47 years (range: 24-72 years) and the average tumour size was 6.50±2.40 cm in diameter. When the expression pattern of total STAT3, pS727, pY705 was correlated with different clinicopathological parameters, a positive association of pS727 STAT3 expression was observed with apoptosis ($p<0.001$) and necrosis ($p<0.017$) in core biopsy specimens. Both total STAT3 and pS727 also showed positive correlation with mitotic score in core biopsy ($p<0.001$) as well as in paired post-NACT samples ($p<0.017$, $p<0.008$). Lymphocytic infiltration was seen high in post NACT cases with high total STAT3, pS727 and pY705 expression ($p=0.010$, 0.004 and 0.044 respectively) **(Table 4.3)**. A chi-square test of independence was also performed to examine the relationship between STAT3, pS727 and pY705 expression score with response status after NACT. No significant difference in the expression pattern of total and phospho forms of STAT3 was observed with respect to the pathological response after neoadjuvant chemotherapy. However, based on medical case records, cases with high STAT3 score or positive cases (89.58%) tend to have an incomplete response when compared with STAT3 negative cases (61.11%) **(Figure 4.4A-C)**. No such observations of response status post NCAT was seen for pS727 and pY705 expression. Also, no significant difference in the expression of STAT3, pS727 and pY705 was observed with respect to age, menopausal status or stromal fibrosis in both before and after chemotherapy specimens.

			Core Biopsy				Post NACT		
		N	Negative	Positive	p- value	N	Negative	Positive	p- value
STAT3	Apoptosis	72	5	67	**0.051**	58	13	45	0.73
	Necrosis	71	41	30	0.678	59	39	20	0.768
	Mitosis	72	3	69	**0.001**	57	12	35	**0.017**
	Stromal Fibrosis	70	19	51	0.237	57	16	41	0.094
	Lymphocytic Infiltration	65	20	45	0.163	57	21	36	**0.01**
pY705 STAT3	Apoptosis	72	5	67	0.081	58	13	45	0.3
	Necrosis	71	41	30	0.716	59	39	20	0.551
	Mitosis	72	3	69	0.393	57	12	35	0.701
	Stromal Fibrosis	70	19	51	0.2	57	16	41	0.484
	Lymphocytic Infiltration	65	20	45	0.637	57	21	36	**0.044**
pS727 STAT3	Apoptosis	72	5	67	**0.001**	58	13	45	0.119
	Necrosis	71	41	30	**0.017**	59	39	20	0.301
	Mitosis	72	3	69	**0.001**	57	12	35	**0.008**
	Stromal Fibrosis	70	19	51	0.296	57	16	41	0.435
	Lymphocytic Infiltration	65	20	45	0.511	57	21	36	**0.004**

Table 4.3. Clinical correlation of different clinicopathological parameters with total and pY705 or pS727 STAT3 expression before and after neoadjuvant chemotherapy. Significance levels are *p < 0.05, **p < 0.01, and ***p < 0.001.

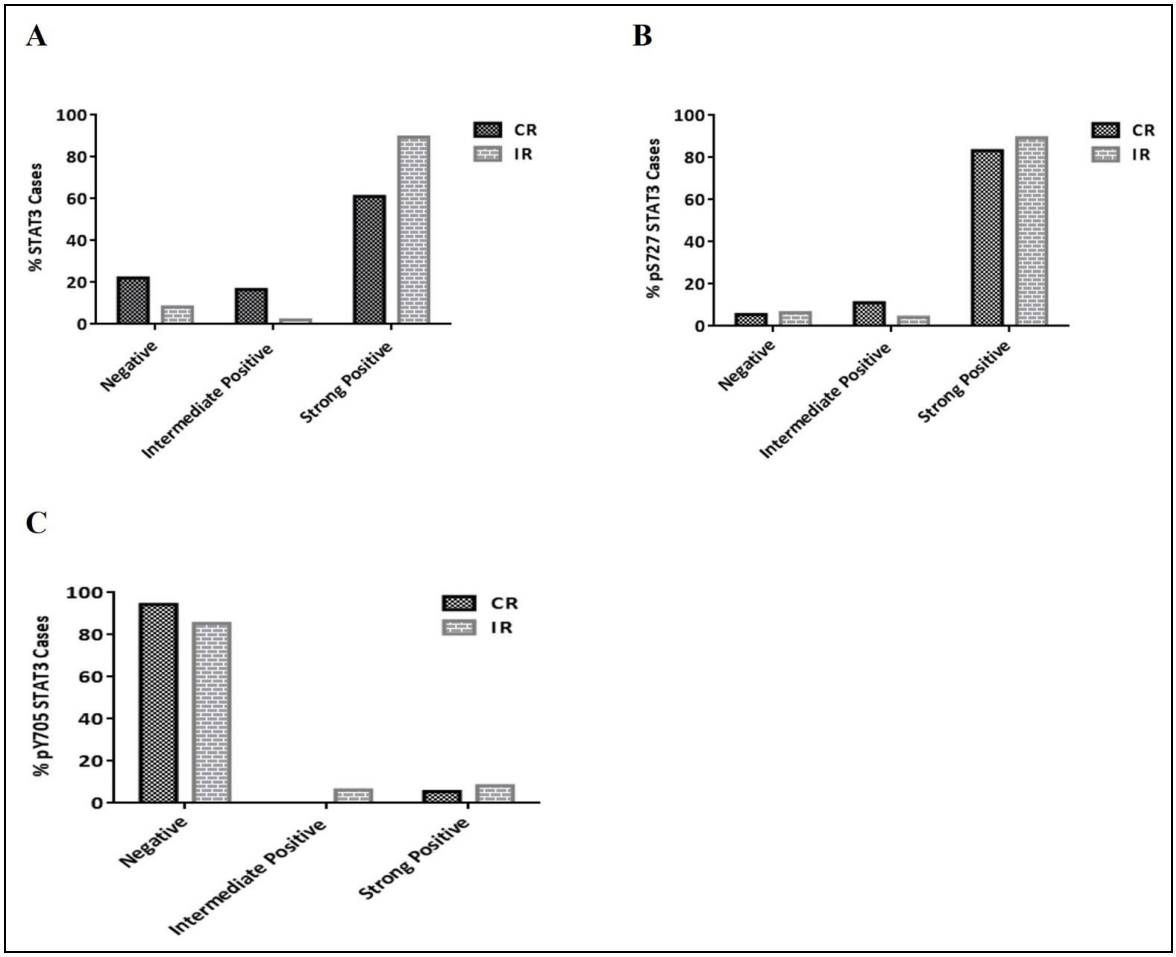

Figure 4.4. Correlation of total and phospho forms of STAT3 expression with response to neoadjuvant chemotherapy. *(A-C) Graphs representing percent cases with negative, intermediate or strong positive expression for total, pS727 and pY705 STAT3, respectively, with respect to response to chemotherapy i.e. CR= complete response and IR = incomplete response. Significance levels are *p < 0.05, **p < 0.01, and ***p < 0.001.*

4.3.3 Expression of total, pY705 and pS727 STAT3 in other cancers and breast cancer subtypes

The differential pattern of STAT3 activation as observed in the TNBC patient samples intrigued us to investigate whether this is specific to TNBCs or it is seen in other BC subtypes, as well as in different type of cancers. To address this, we procured formalin fixed

and paraffin embedded (FFPE) tumour tissue blocks for Melanoma (n=4), lung adenocarcinoma (n=4), Luminal A BC subtype (n=5) and $Her2^{+}$ (n=5) cases. IHC staining for total, pY705 and pS727 STAT3 was performed for individual cases and nuclear localization score was determined using digital scoring method. In both melanoma and lung adenocarcinoma samples total STAT3 expression was completely absent (Score=0), hence even pY705 and pS727 had IHC profiler score of 0 **(Figure 4.5A)**. In luminal A subtype, total STAT3 expression was either moderate or weak positive in cytoplasm with no nuclear localization as observed in 3 out of 5 cases, except for two cases where moderate nuclear intensity was seen. Eventually, pS727 expression was negative in all the respective cases, while pY705 was found weak positive only in one case. Her2 subtype majorly had weak nuclear or cytoplasmic stain for total STAT3 expression. pY705 expression was absent in all the cases while pS727 was positive (weak positive) only in one case **(Figure 4.5B-C)**. Overall, the distinct pS727 mediated STAT3 activation as observed in TNBCs was not seen in other BC subtype or the two different cancer types tested.

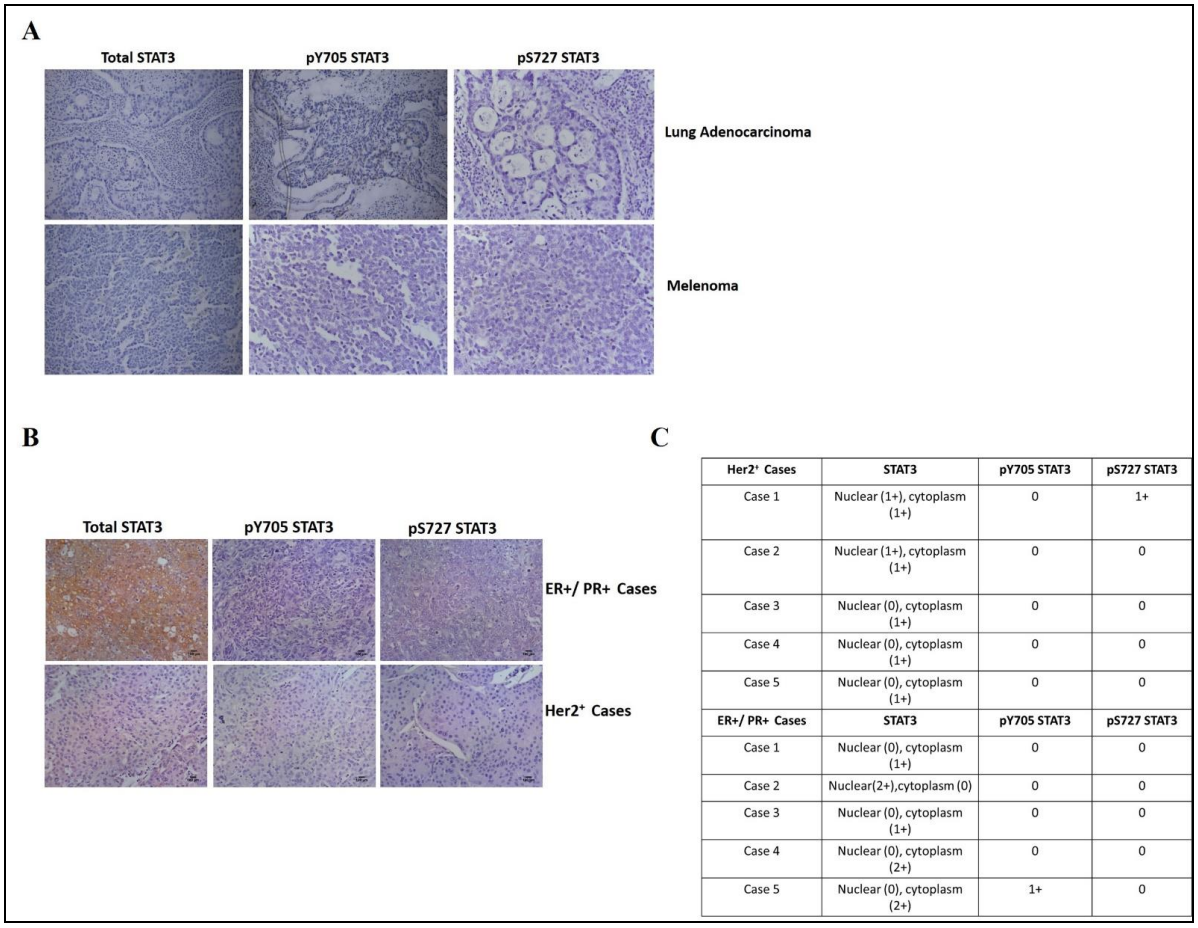

C

Her2+ Cases	STAT3	pY705 STAT3	pS727 STAT3
Case 1	Nuclear (1+), cytoplasm (1+)	0	1+
Case 2	Nuclear (1+), cytoplasm (1+)	0	0
Case 3	Nuclear (0), cytoplasm (1+)	0	0
Case 4	Nuclear (0), cytoplasm (1+)	0	0
Case 5	Nuclear (0), cytoplasm (1+)	0	0
ER+/ PR+ Cases	**STAT3**	**pY705 STAT3**	**pS727 STAT3**
Case 1	Nuclear (0), cytoplasm (1+)	0	0
Case 2	Nuclear(2+),cytoplasm (0)	0	0
Case 3	Nuclear (0), cytoplasm (1+)	0	0
Case 4	Nuclear (0), cytoplasm (2+)	0	0
Case 5	Nuclear (0), cytoplasm (2+)	1+	0

Figure 4.5. Expression of total and STAT3 PTM forms in other breast cancer subtypes as well as in other cancer type. *(A) Microscopy images of IHC DAB stain for total, pY705 and pS727 STAT3 expression in lung adenocarcinoma (n=4) and melanoma (n=4) tissue samples. (B) Microscopy images of IHC DAB stain for total, pY705 and pS727 STAT3 expression in Luminal (n=5) and Her2 high (n=5) tissue samples. (C) IHC profiler score for nuclear expression of total, pS727 and pY705 STAT3 expression in Her2 high and luminal subtype of breast cancer cases (0-3+).*

4.3.4 STAT3 signalling is essential for growth, proliferation and maintenance of $CD44^{high}/CD24^{low/-}$ stem cell pool in triple negative breast cancer cells

Compelling number of evidences point towards the role of STAT3 signalling in growth of ER negative tumours. Clinical data from our study also supports the upregulation of STAT3

pathway in TNBCs. Hence, to further investigate the role of STAT3 signaling in growth and survival of hormone negative breast cancer subtype, we engineered MDA MB 231 cell line with endogenous STAT3 expression knocked down using 3'UTR shRNA approach. GFP positive stable KD clone was enriched by performing high GFP assisted cell sorting consecutively for 3-rounds, to finally achieve a 97% pure knockdown population **(Figure 4.6A)**. The effect of shRNA mediated STAT3 knockdown was confirmed at both mRNA and protein level. Quantitative real time PCR analysis showed more than 3-fold reduction ($p<0.01$) in STAT3 mRNA transcript levels post knockdown **(Figure 4.6B).** While immunoblotting for total and different PTM forms of STAT3 showed very less or no protein expression from the knockdown cell lysates **(Figure 4.6C),** thus confirming effective suppression of STAT3 protein expression in engineered 3'UTR shRNA MDA MB 231 model.

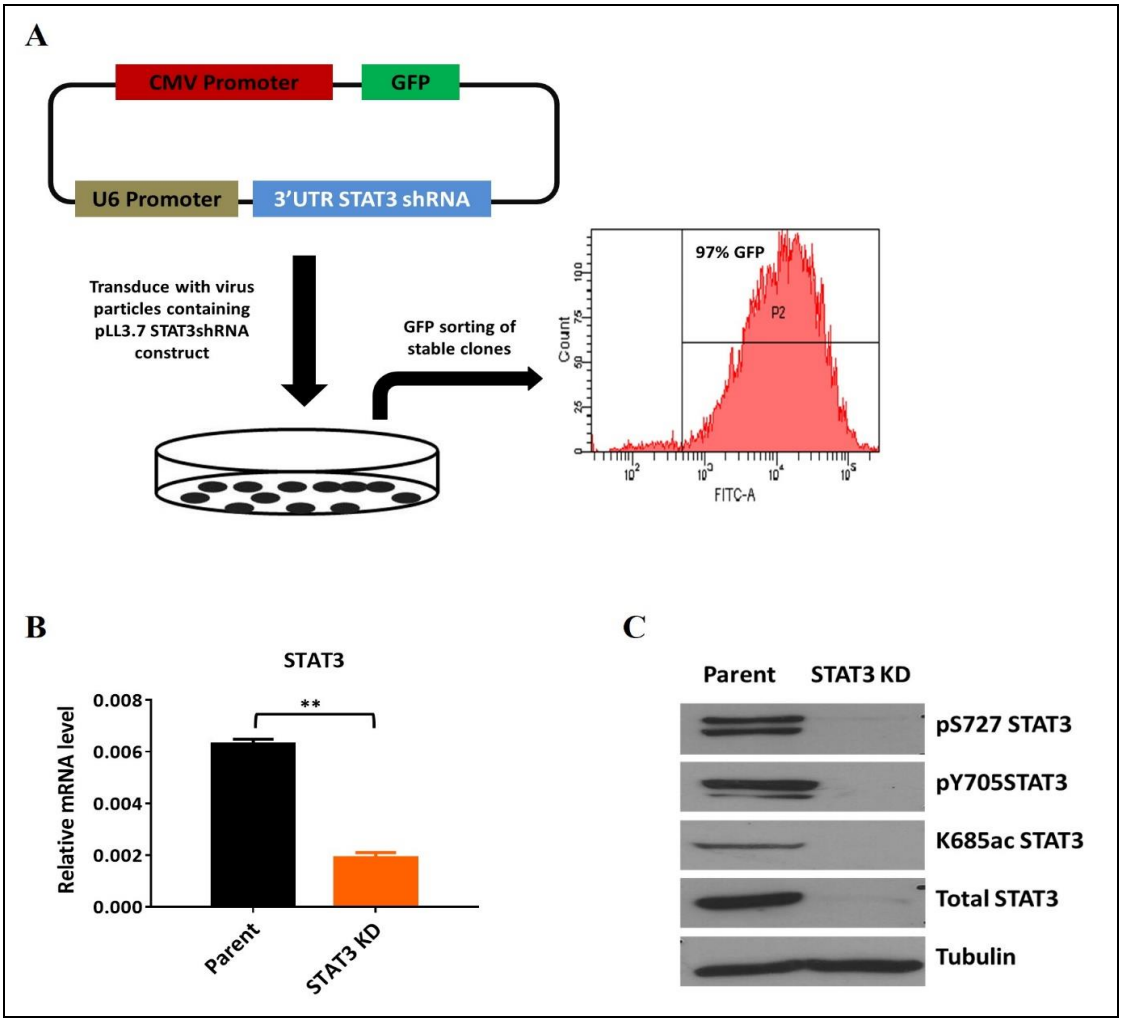

Figure 4.6. Engineering 3'UTR knockdown STAT3 MDA MB 231 cell line. *(A) Schematics for generation of MDA MB 231 cells having stable knock down of endogenous STAT3 expression using 3'UTR shRNA approach with lentivirus plasmid (pLL3.7). Positive clones were enriched with FACS sorting for GFP positive cells to obtain a final 97% pure knockdown population. (B) Relative mRNA transcript levels of STAT3 upon stable knockdown. GAPDH was used as normalization control. (C) Immunoblot of parent and STAT3 knockdown clones probed for expression of total and PTM activated forms (pY705, pS727 and K685ac) of STAT3. Tubulin is used as a loading control. Each bar represents mean value ± SEM. Significance levels are ns p> 0.05, *p< 0.05, **p< 0.01, and ***p< 0.001.*

Comparing the effect of STAT3 loss on functional and phenotypic aspects of TNBC cell line showed expected results. One of the important functions of STAT3 signaling is to control cell

proliferation. Hence when EdU incorporation assay was performed, parent MDA MB 231 cells showed 58% EdU incorporation while KD clones only had 25% cell labelled for EdU. A difference of more than 2.5-fold reduction ($p<0.01$) in cell proliferation ability was evident with the STAT3 loss **(Figure 4.7A**). The effect of STAT3 depletion was also seen with long term cell survival assay where with KD clones formed significantly smaller number of colonies ($p<0.01$) than parent counterparts. Also, the size of the colonies formed was appreciably small **(Figure 4.7B)**. Comparing the anchorage independent growth potential for the two population, with STAT3 loss MDA MB 231 cells lost the tumorigenic potential and a drop of more than 5-fold was observed in colony forming ability for the KD population on low adherent surface **(Figure 4.7C)**.

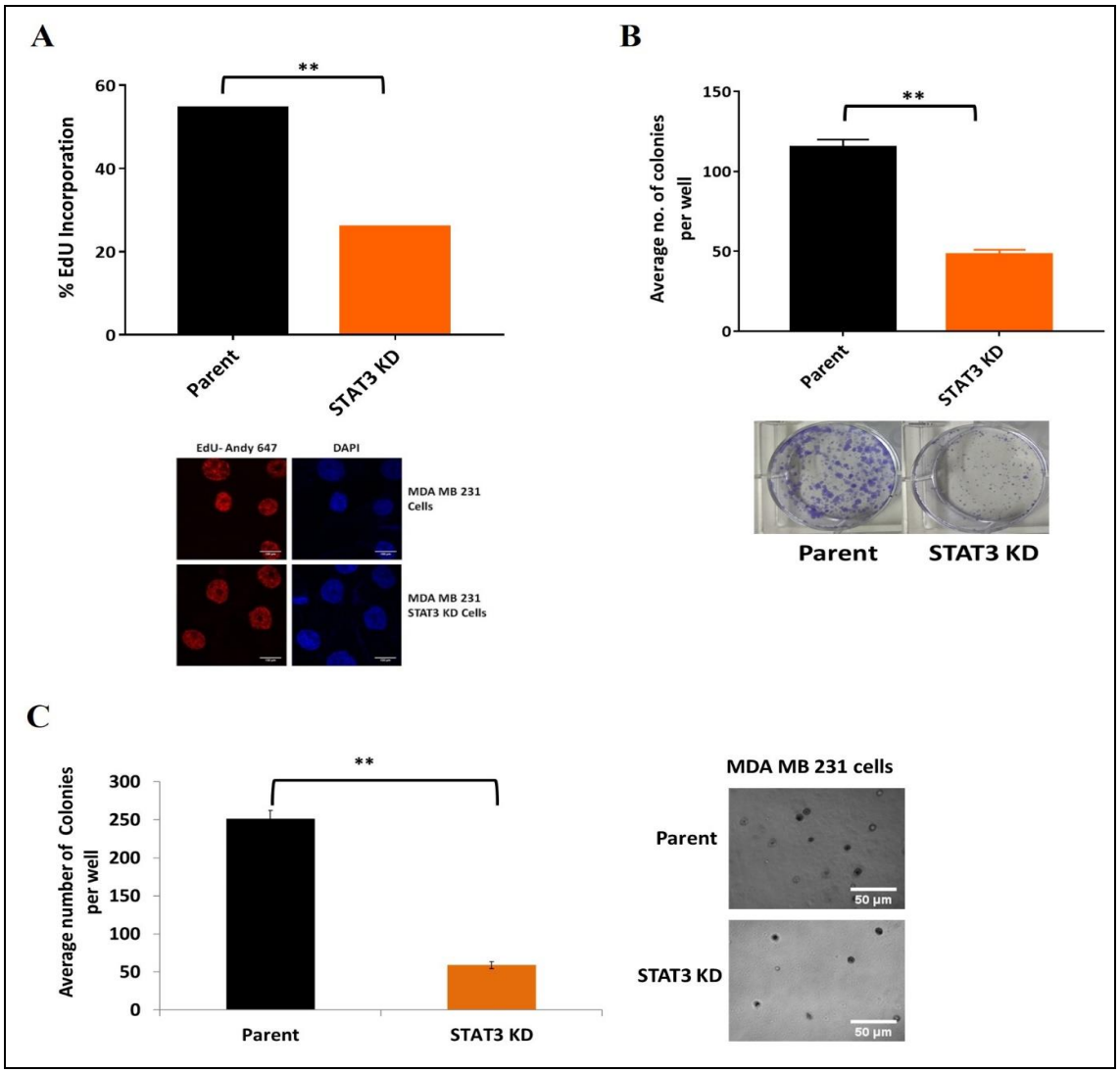

Figure 4.7. Effect of STAT3 knockdown on growth and proliferation of MDA MB 231 cells. *(A) Graph representing percent EdU positive cells in both parent and KD cells post 24hrs of EdU incubation (n=300 cells). Bottom image represents EdU positive cells stained with AndyFluor647 and nucleus with DAPI. (B) Average number of colonies formed post 14 days of seeding for clonogenic assay. Bottom image represents 6 well plate showing colonies stained using crystal violet stain. (C) Graph representing average number of colonies formed on low percentage agarose surface with parent and KD cells. Adjacent image represents colonies formed in the soft agar assay for individual population. Each bar represents mean value ± SEM. Significance levels are ns p> 0.05, *p< 0.05, **p< 0.01, and ***p< 0.001.*

Further, basal like breast cancer cells have stem cell population characterized by $CD44^{high/+}/CD24^{low/-}$ cell surface markers. Flow cytometry analysis for both CD44 and CD24 markers showed a drastic shift in the stem cell pool. From 82.2% in MDA MB 231 parent population, the $CD44^{high/+}/CD24^{low/-}$ stem cell pool dropped down to only 3.4% in knockdown population **(Figure 4.8A)**. To further affirm the effect of STAT3 loss on stem cell population of TNBC cells, quantitative real time PCR analysis for other stem cell markers like Oct-4 and Sox-2 was performed **(Figure 4.8B-C)**. As expected, in STAT3 KD clones the expression level of both the stem cell markers was significantly downregulated ($p<0.05$ and 0.01 respectively). Collectively, from above *in vitro* observations it is evident that STAT3 signaling not only controls growth and proliferation of TNBC cells, but is also essential for maintenance of stem cell pool for this subtype.

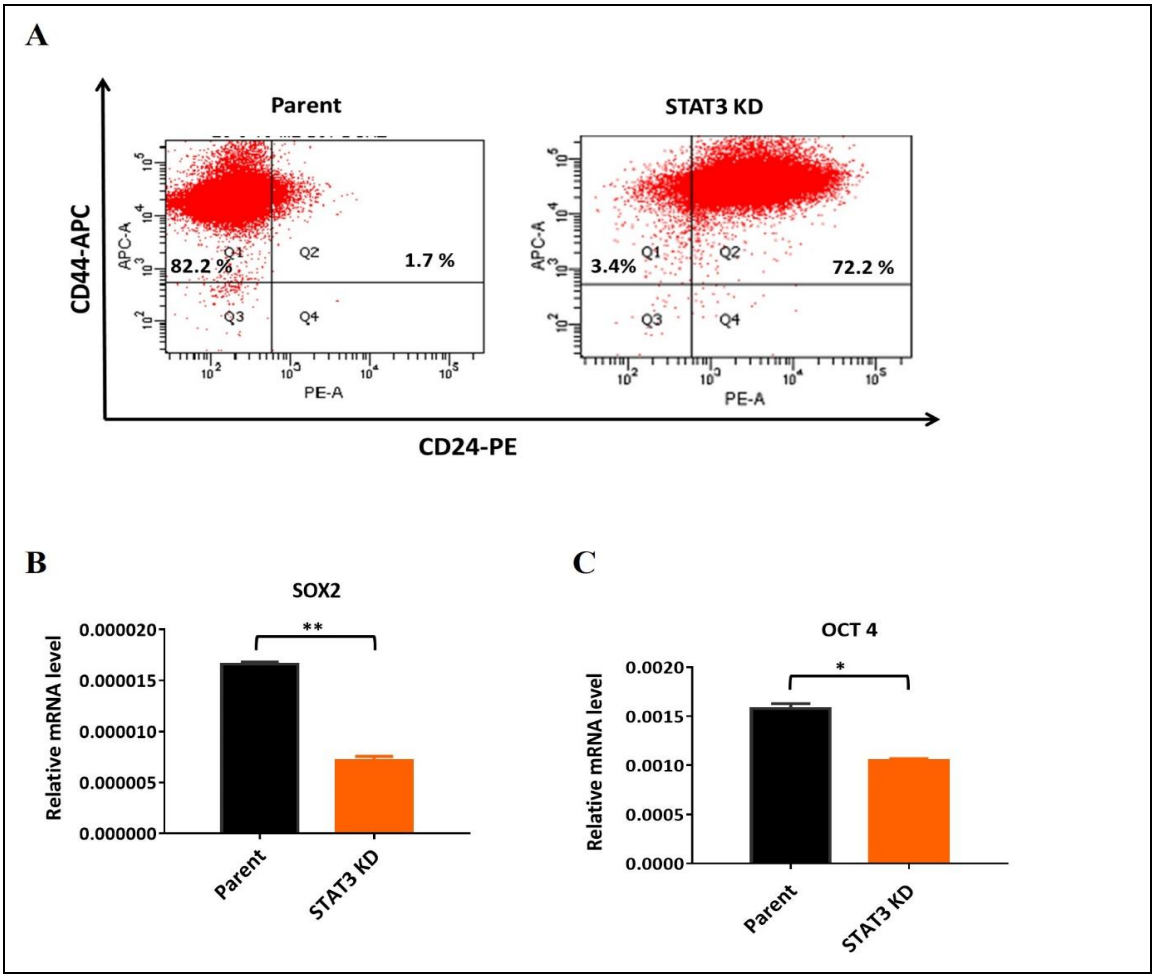

Figure 4.8. Effect of STAT3 knockdown on Stem cell population in MDA MB 231 cells. *(A) Flowcytometric distribution of stem cell population based on CD44 (anti-APC) and CD 24 (anti-PE) surface markers in parent and KD clones. (B-C) Relative mRNA transcript levels of stem cell markers Sox2 and Oct4 in parent and STAT3 KD population. GAPDH was used as normalization control. Each bar represents mean value ± SEM. Significance levels are ns p> 0.05, *p< 0.05, **p< 0.01, and ***p< 0.001.*

4.3.5 Niclosamide mediates its anti-tumour activity by targeting both arms of STAT3 signaling

As observed previously, Niclosamide by the virtue of being a dual blocker significantly attenuated STAT3 activation in MCF PTM mutant expressing cells. To further, affirm whether the similar inhibitory action of Niclosamide is even mediated in TNBC BC subtype, we treated parent MDA MB 231 cells with increasing dose of Niclosamide and determined site-specific inhibition of total and phospho-PTM sites on STAT3 molecule using immunoblotting. As expected, in MDA MB 231 cells also both Stattic and NSA significantly blocked STAT3 activation via inhibition of phosphoY705 residue in a dose specific manner, where NSA concentration (2µM) required was at least 5-fold lower than Stattic (10µM) **(Figure 4.9A-B)**. Additionally, as seen with MCF7 cells, in MDA MB 231 cells also NSA showed specific dose-dependent inhibition of pS727 (2-4µM) activation, for which Stattic was completely ineffective despite escalating the dose to a much higher concentration (upto 20µM). Taking advantage of the BRET sensor developed in Chapter 2, we further demonstrated that NSA dependent decrease in both pY705 and pS727 levels drastically depleted the homodimerization ability of the STAT3 molecule ($p<0.01$). The inhibitory effect achieved with NSA treatment could not be rescued despite triggering with even high dose of EGF ligand (100ng). While Stattic treatment also successfully blocked the STAT3 homodimerization event, however because of being only pY705 specific blocker, the effect was immediately lost as soon as EGF mediated induction was given **(Figure 4.9C-E)**. Hence NSA mediated perturbation of STAT3 signaling in TNBCs is more drastic and stronger in comparison to Stattic.

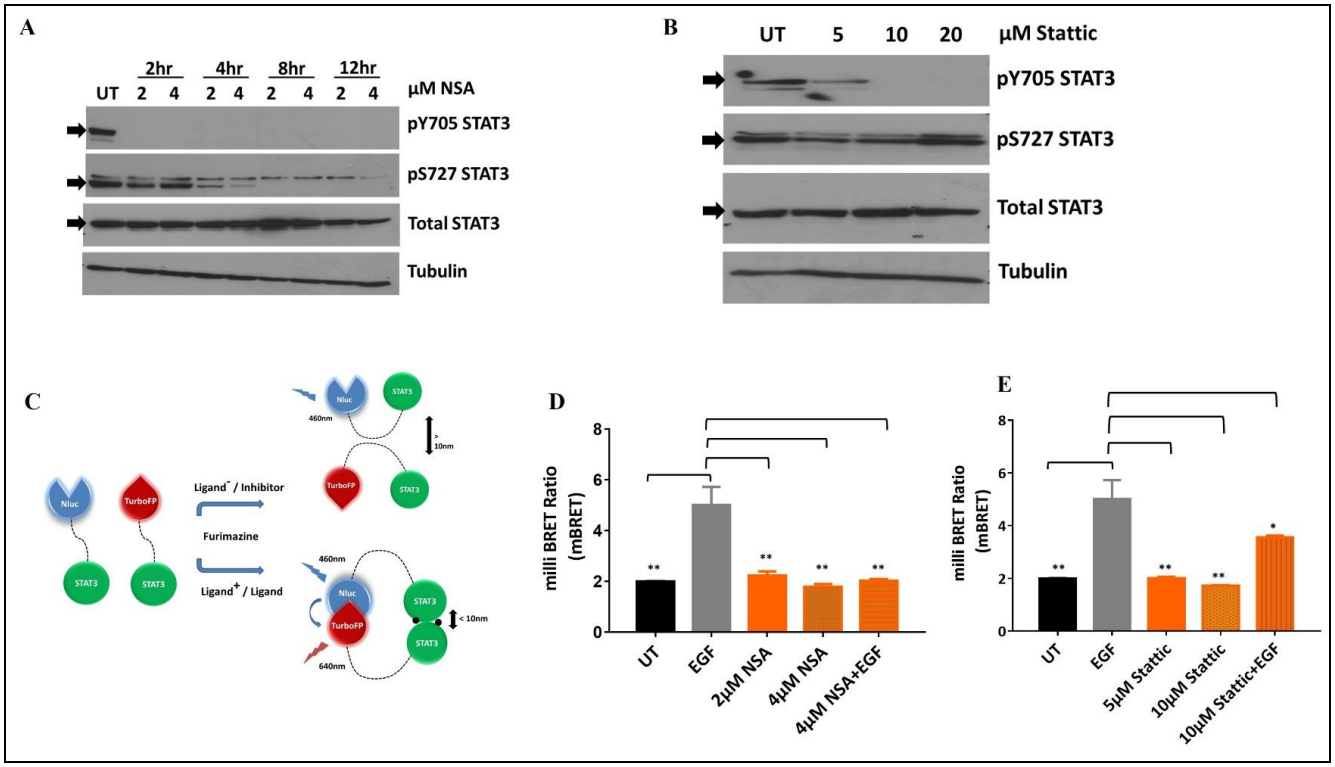

Figure 4.9. Effect of Niclosamide and Stattic on STAT3 activation in MDA MB 231 cells. *(A-B) Immunoblot of cell lysates from MDA MB 231 cells upon treatment with niclosamide (at different time points) and Stattic (24hrs), respectively, at variable concentration. Each blot was probed for total and PTM activated forms (pY705 and pS727) of STAT3 and tubulin was used as a loading control. (C) Schematics of working model for Phospho STAT3 BRET sensor. (D-E) Corrected BRET ratio graph for MDA MB 231 cells expressing phospho STAT3 BRET sensor upon treatment with niclosamide and Stattic either in presence or absence of EGF. Each bar represents mean value ± SEM. Significance levels are ns p> 0.05, *p< 0.05, **p< 0.01, and ***p< 0.001.*

Further, to test verify the importance of differential STAT3 inhibitory functions in TNBC cell proliferation ability, live cell luciferase assay with parental MDA MB 231 LucD3H2LN cells was performed **(Figure 4.10A)**. Over here NSA being dual blocking agent, successfully inhibited the growth of MDA MB 231 cells with even 5 times lower drug concentration than Stattic [2μM NSA ($p<0.01$) vs. 10μM Stattic ($p=ns$)] for a duration of upto 96hrs **(Figure**

4.10B-C). While, a further increase in the inhibitor concentrations led to significant cell death ($p<0.001$) with both the drugs. The potent effect of Niclosamide was even seen in long term cell survival assay where depleting endogenous STAT3 pool in MDA MB 231 cells significantly enhanced the sensitivity of the cells towards drug induced cell death **(Figure 4.10D-E)**. As compared to parent, in STAT3 KD condition, NSA dependent cell death was induced even with 1µM (30% surviving fraction, $p<0.01$) concentration that further increased when 2µM (10% surviving fraction, $p<0.001$) dose was used. While with Stattic, the effect was seen significantly only when high drug concentration was given (10µM, 10% surviving fraction, $p<0.001$). Therefore, unlike Stattic, NSA acts as a dual phospho-PTM blocker, resulting in significantly higher inhibition of STAT3 activation in TNBC cell line. Hence, based on the evidences gathered here and chapter 2, the new molecular basis of NSA drug function is revealed, which is important towards possible repurposing of NSA as an anti-cancer agent in activated STAT3 positive TNBCs cases.

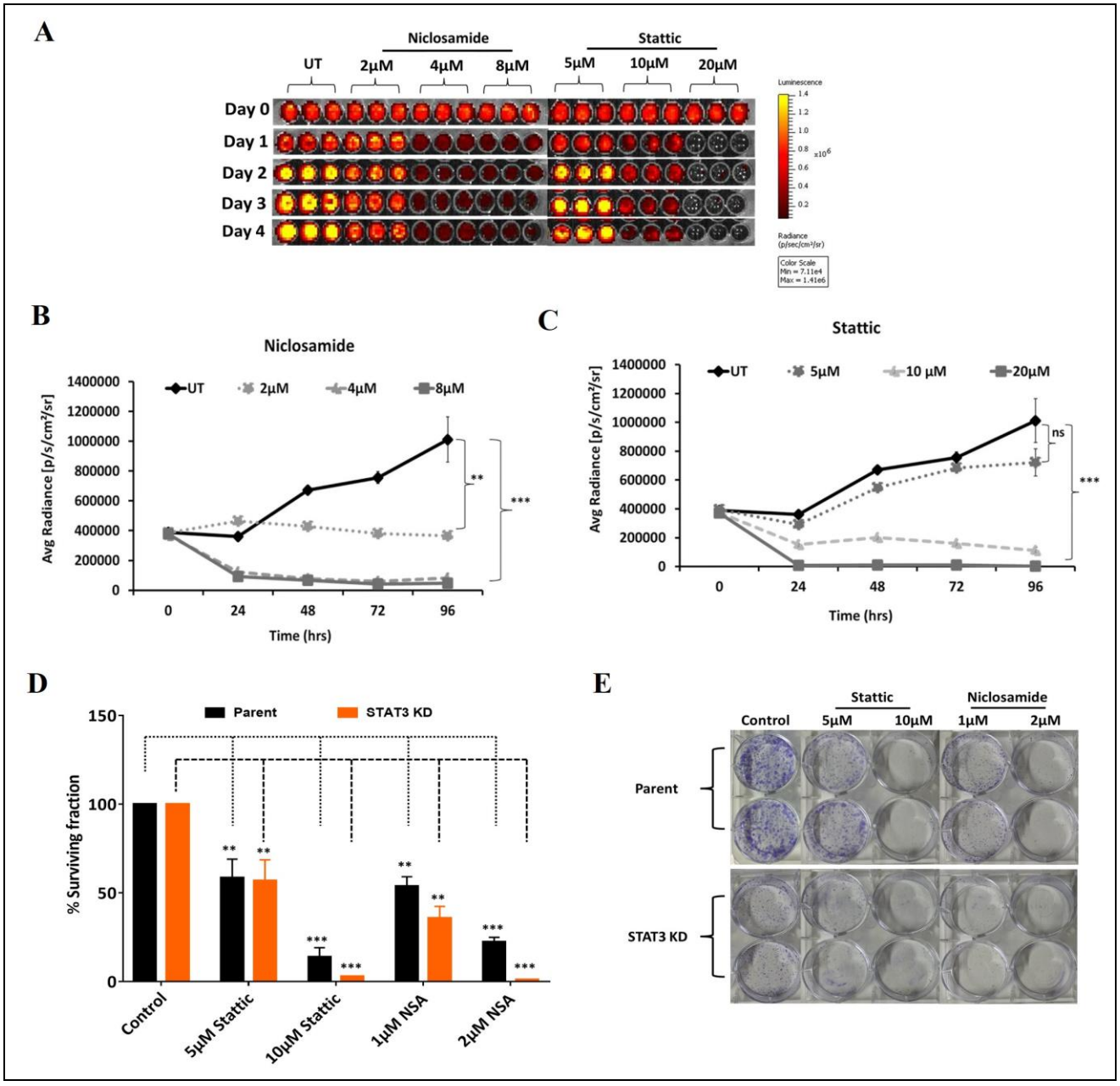

Figure 4.10. In vitro anti-cancer activity of niclosamide against TNBC cell line. *(A) Representative image of 96 well plate showing luciferase signal at different time points from MDA MB 231-LucD3H2LN cells treated with Stattic or niclosamide at different concentrations. (B-C) Representative graph of average radiance from cells in (A) upon treatment with niclosamide and Stattic, respectively, at different time points post treatment. (D) Percent surviving fractions in parent and STAT3 knockdown MDA MB 231 cells upon treatment with niclosamide or Stattic. (E) Representative clonogenic plate image of cells stained with 0.5% crystal violet stain to mark the*

*colonies. Each bar represents mean value ± SEM. Significance levels are ns p> 0.05, *p< 0.05, **p< 0.01, and ***p< 0.001.*

4.3.6 *In vivo* anti-tumour efficacy of Niclosamide against STAT3 in triple negative breast cancer tumour xenograft model

Based on observations made from clinical data it is evident that noncanonical pS727 STAT3 pathway predominates in TNBCs and oncogenic signaling from STAT3 molecule is essential for growth and survival of MDA MB 231 TNBC cell line. In this context, we have further shown that effective inhibition of STAT3 pathway as achieved with dual blocking effect (pY705 and pS727) of Niclosamide inhibitor is a preferred treatment approach. Hence to finally evaluate the anti-cancer effect of NSA *in vivo*, we developed orthotopic tumour xenograft model.

For *in vivo* efficacy study, 5X10^6 luciferase labelled MDA MB231-Luc (D3H2LN) cells were implanted orthotopically at the 5th mammary fat pad of female Balb/C NOD-SCID mice. Tumour growth was constantly monitored using serial non-invasive Bioluminescence imaging (BLI). When tumours attained approx. size of 2-3 mm (100mm^3), the mice were randomly segregated into two groups; control and treatment. Drug treated group received 50mg/kg body weight Niclosamide consecutively for 21 days via intraperitoneal injection, while control group was administered with vehicle (saline) solution **(Figure 4.11)**. On every 7th day of the treatment, tumour growth was monitored both by non-invasive BLI imaging as well as by digital recording of tumour volume **(Figure 4.12A)**. Over here, quantitative assessment of BLI signal from the two groups showed that, mice receiving NSA treatment for 21 days had a 3-fold reduction ($p<0.001$) in tumour BLI signal as compared to control growth **(Figure 4.12B)**. Tumour volume determined for the treatment group also followed the similar

trend, where a difference of more than 10-fold ($p<0.001$) was achieved upon NSA administration **(Figure 4.12C)**. MDA MB 231 cells are reported to be very aggressive with frequent tendency of *in vivo* metastasis. Hence, ex-vivo BLI imaging of lungs and bone was performed post termination of treatment schedule. In comparison to control group, mice with NSA treatment showed a smaller number of metastatic lung nodules **(Figure 4.12D)**. Further, bone metastasis was determined by removing femur bone from same side of the body as that of primary tumour growth. While control group had significant bone mets, no BLI signal for metastatic MDA MB 231 cells was seen in treated group **(Figure 4.12E)**, indicating that NSA treatment was able to successfully block bone metastasis in TNBCs. The body weight determined for both control and treatment group during the course of study showed no significant difference, further confirming that NSA administration as such has no adverse effect on the health of the mice **(Figure 4.12F)**. Taken, together these results strongly confirm the *in vivo* anti-cancer effect of NSA as an effective drug against TNBCs.

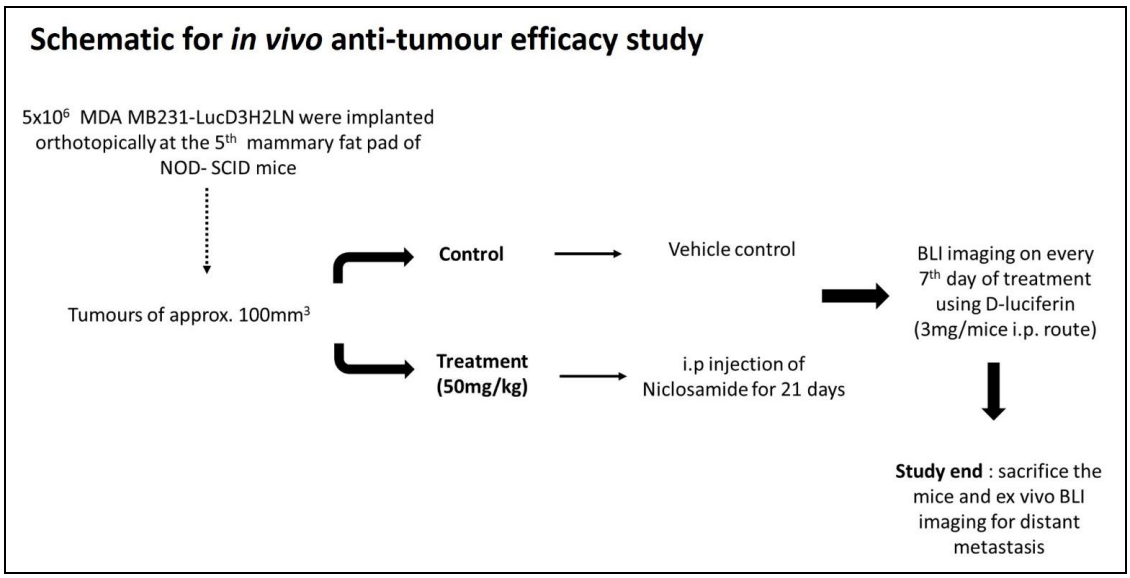

Figure 4.11. Schematics of the in vivo efficacy study for niclosamide using orthotopic tumor xenograft model from MDA MB 231 cells.

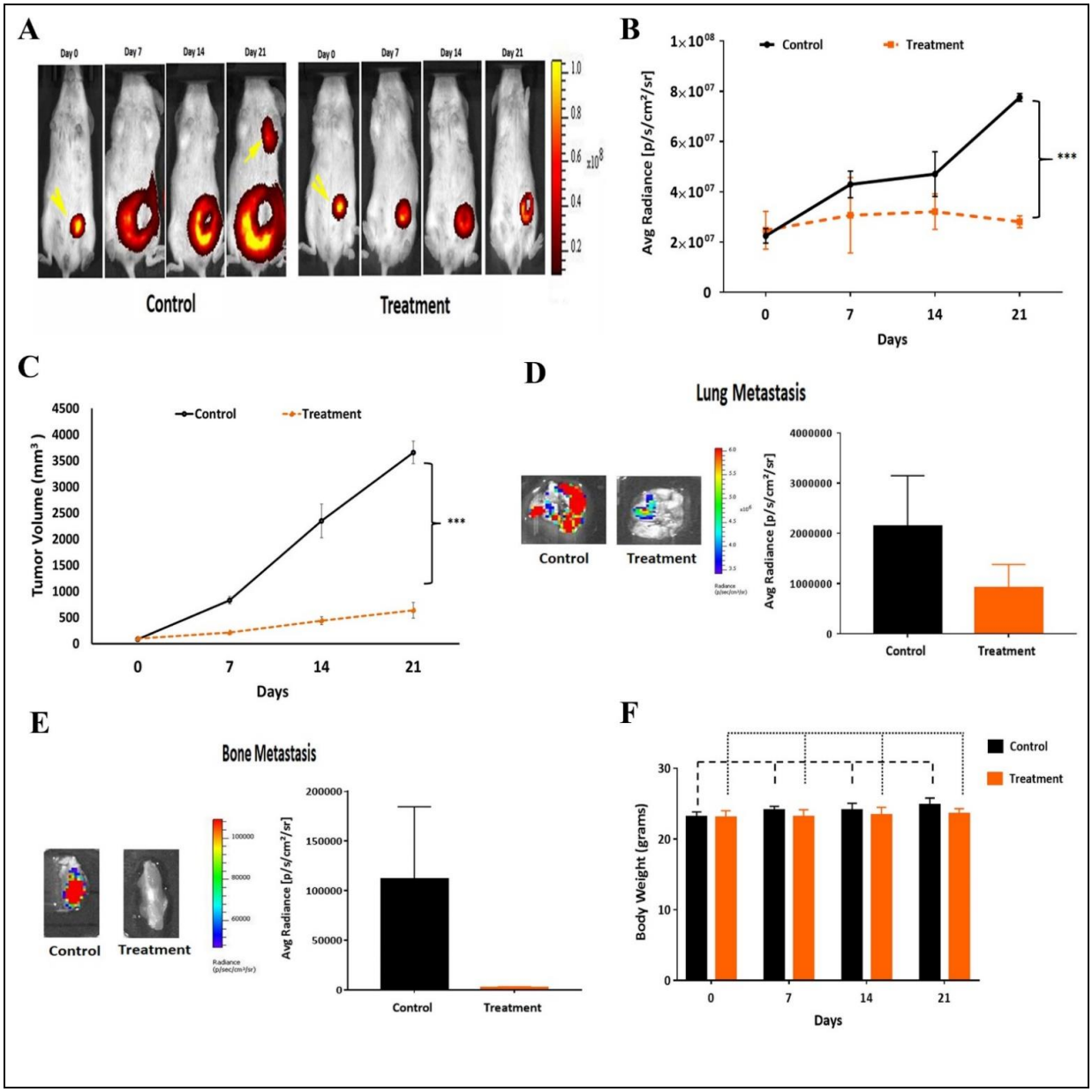

Figure 4.12. In vivo anti-tumour efficacy of niclosamide against TNBC tumor xenograft model. *(A) Representative images of mice from control and treatment group at different time points of the imaging. (B) Quantitative average bioluminescence imaging (BLI) signal from control and treatment group at every 7th day of the treatment for 21 days. (C) Tumour volume graph for the same cohort in (B) in mm$^{3.}$ (D) Representative ex vivo image of lungs showing BLI signal from control and treatment group. Adjacent graph represents quantitative average BLI signal from the lungs for two groups. (E) Representative ex vivo image of femur bone showing BLI signal from control and treatment group. Adjacent graph represents quantitative average BLI signal from the thigh bone for the two groups.*

*(F) Body weight of mice (in grams) from control and treatment group during the course of the study. Each bar represents mean value ± SEM. Significance levels are ns p> 0.05, *p< 0.05, **p< 0.01, and ***p< 0.001.*

4.4 Discussion:

STAT3 being a downstream molecule in activation hierarchy , lies at the converging point for many upstream oncogenic pathways such as PI3K/Akt (Alonzi *et al*, 2001), MAPK/ERK (Gough *et al*, 2013) and Notch (Kamakura *et al*, 2004) etc. Activation of STAT3 is primarily driven by classical canonical pY705 activation that controls its homodimerization, nuclear translocation and transcriptional activities. However, in the past many reports have emerged, that identifies new PTM sites (K685ac, pS727, K140me etc.) on STAT3 which can equally control its transcriptional and biological functions in different cancer types. Such reports has introduced a huge shift in clinical paradigm of STAT3 signaling and now pY705 is no more considered as a sole indictor for STAT3 pathway activation (Lee *et al*, 2012; Sellier *et al*, 2013; Yang *et al*, 2010; Yeh *et al*, 2006). Results from experimental, preclinical and patient related studies have identified noncanonical STAT3 pathway (pS727 and K685ac) as an alternative arm for STAT3 to mediate its immediate biological functions.

Increasing number of evidences strongly suggest key role of STAT3 signaling in growth of ER negative tumours. However, till date there is no clinical data available for STAT3 activation in receptor negative subtype of breast cancer (TNBC) cases. To delineate this further, we performed IHC analysis for both canonical and noncanonical STAT3 activation marks in triple negative breast cancer cases (TNBC). Quantitative scoring of DAB staining for total, pY705 and pS727 STAT3 levels in 76 paired core biopsy and post NACT samples showed more than 86% cases are positive for total STAT3 expression. Among all STAT3

positive cases 90% of them were high positive for pS727 expression while pY705 was evident in only 15% STAT3 positive cases. Considering high expression of pS727 STAT3, a strong to moderate positive Pearson's correlation was thus obtained between total and pS727 STAT3 score. For all quantitative analysis we always validated our observations with two scoring methods- Allred and IHC profiler that showed high concordance. To determine whether this differential STAT3 activation is specific to TNBCs, we extended our study to melanoma, lung adenocarcinoma and other subtypes of breast cancer cases. Surprisingly, since total STAT3 was either negative or low positive in most of these samples, pS727 or pY705 expression was naturally absent. Further, correlating expression of total and PTM forms of STAT3 with clinicopathological parameters, we found that total STAT3 and pS727 expression was high in core biopsy cases with high apoptotic, necrotic and mitotic score. While lymphocytic infiltration was seen more in cases with high STAT3, pS727 and pY705 expression in the post NACT specimens. These observations clearly indicate that pS727 mediated noncanonical STAT3 activation is the predominant mode for STAT3 to function in TNBC subtype of breast cancer.

Intrigued by the observations from clinical study, we further demonstrated the significance of STAT3 signaling for TNBCs *in vitro*. By engineering a 3'UTR STAT3 knockdown MDA MB 231 cell line model functional role STAT3 signaling is revealed. Loss of STAT3 expression in MDA MB 231 cell line not only affected the overall survival, proliferation and tumorigenic potential but it also led to a significant reduction in $CD44^{high}/CD24^{low}$ CSC pool by downregulating expression of some of the important stem cell markers like Oct4 and Sox2. Collectively, observations from *in vitro* experiments further highlight the dominant functional role of STAT3 signaling for TNBCs.

Considering the prevalence of two alternate arms (canonical pY705 and noncanonical pS727) that can activate STAT3 molecule in TNBCs, it is thus evident that to therapeutically target

STAT3 molecule, blocking both activation pathways is important. To achieve this, **as** discussed in Chapter 2 and 3, we have shown that Niclosamide is a potent inhibitor that can block STAT3 activation in MCF 7 cells. We thus explored the potential of this drug to work as an anti-cancer agent against TNBCs subtype of breast cancer. As expected, by the virtue of being dual blocker (pY705 and pS727) of STAT3 molecule, Niclosamide significantly reduced the cell survival functions in TNBCs in comparison to pY705 specific Stattic compound. To further validate the anti-cancer effect of niclosamide against TNBCs in preclinical settings, we developed a tumor xenograft model by implanting MDA MB 231-LucD3H2LN cells orthotopically at the mammary fat pad of NOD/SCID. Niclosamide treatment significantly retarded the primary tumor growth as compared to untreated controls. Further, frequency of distant metastasis and growth at secondary site such as lungs and bone were also affected, where a decrease of more than 50% in BLI signal was obtained.

In conclusion, the results here from both clinical and experimental set up provide convincing evidences for noncanonical pS727 PTM as dominant and independent mode for activation of STAT3 pathway in TNBCs. With the promising STAT3 inhibition dependent anti-cancer activity of niclosamide against TNBCs, in future it can be combined with existing chemotherapeutic drugs to increase treatment effect and achieve therapeutically complete response. Hence more efforts should now be employed in identifying inhibitors like niclosamide (dual STAT3 blocker) that can serve as a promising candidate for therapy less TNBC subtype.

4.5 Significance of the Study:

Paving way for the significance of alternate STAT3 activation arm, this chapter brings novel insights onto the role played by noncanonical pS727 STAT3 oncogenic pathway in TNBC subtype of breast cancer. Considering the prevalent expression of pS727 PTM form in TNBCs that essentially controls majority of the STAT3 dependent downstream biological functions like; cell proliferation, survival, tumorigenic potential as well as maintaining the constant stem cell pool, targeting STAT3 would be a rational therapeutic approach. With the two different signaling arms- canonical pY705 and noncanonical pS727 regulating STAT3 activation, it is thus evident that to target and inhibit STAT3 completely, it is extremely essential to remodify the drug development and targeting approach.

For tumours having classical canonical pY705 activation as predominant pathway driving STAT3 functions, treatment with inhibitors like Stattic is a more straightforward approach. Stattic is a well-known specific pY705 blocker that effectively target the STAT3 addicted cancer cells by suppressing pY705 activation and STAT3 homodimerization. As expected, with specific targeting of the cancer cells using drugs against the overexpressed target molecule, the therapy response is eventually enhanced. Using Stattic against pY705 positive tumours is thus, a more preferred clinical approach.

However, in case of tumours like, for e.g. TNBCs overexpressing the noncanonical pS727 STAT3 pathway, using inhibitors like Stattic will lead to incomplete inhibition of the STAT3 pathway. In this scenario, cancer cells expressing pY705 form of STAT3 will be targeted however the major population that is pS727 positive will be unaffected. This will not only lead to incomplete therapy response but will also produce cytotoxic effects upon dose escalation to achieve better treatment outcome. On contrary, using inhibitors like Niclosamide that are dual blockers of STAT3 pathway i.e. pY705 and pS727, will effectively

target both the populations of STAT3 despite its heterogenous expression in the tumor sample **(Figure 4.13)**. The treatment outcome obtained with this particular strategy will be more effective and less cytotoxic. Hence, strong efforts in the direction to find more such inhibitors like Niclosamide are extremely essential to target STAT3 oncogenic pathway.

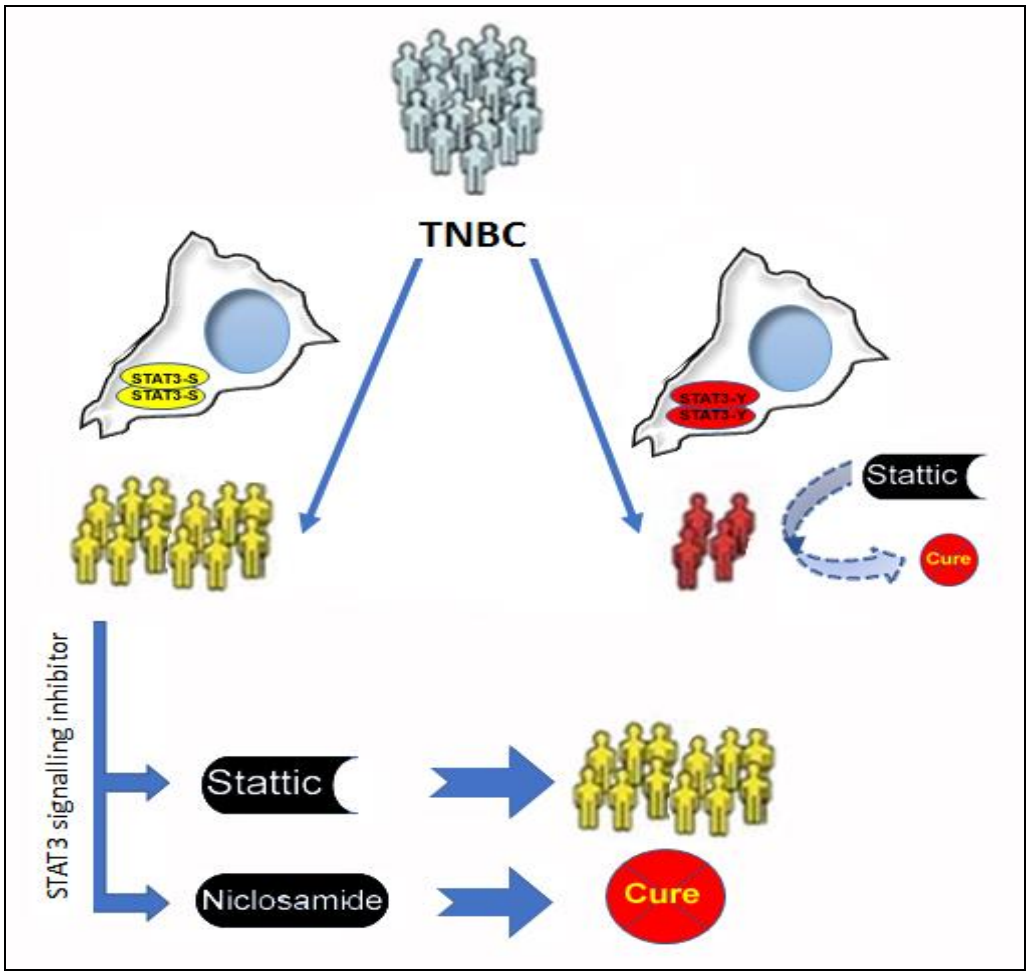

Figure 4.13. Targeting STAT3 signaling in TNBCs. *For a TNBC cohort overexpressing the canonical pY705 activation arm, targeting with Stattic (pY705 blocker) is an effective approach to achieve complete treatment response. However, for cases having predominant pS727 STAT3 positive population, use of STAT3 drug inhibitors like Stattic (only pY705 blocker) will lead to incomplete STAT3 inhibition and hence result in therapy failure. While using dual blockers like Niclosamide (pY705 and pS727) will effectively work on both pY705 and pS727 positive population to achieve complete STAT3 inhibition mediated treatment outcome.*

References

Abhijit De RA, Akshi Jasani (2014) Engineering Aspects of Bioluminescence Resonance Energy Transfer Systems. In *Engineering in Translational Medicine*, Cai W (ed), pp 257-300. London: Springer

Akira S (1999) Functional roles of STAT family proteins: lessons from knockout mice. *Stem cells* **17:** 138-146

Akira S, Nishio Y, Inoue M, Wang XJ, Wei S, Matsusaka T, Yoshida K, Sudo T, Naruto M, Kishimoto T (1994) Molecular cloning of APRF, a novel IFN-stimulated gene factor 3 p91-related transcription factor involved in the gp130-mediated signaling pathway. *Cell* **77:** 63-71

Alonzi T, Middleton G, Wyatt S, Buchman V, Betz UA, Muller W, Musiani P, Poli V, Davies AM (2001) Role of STAT3 and PI 3-kinase/Akt in mediating the survival actions of cytokines on sensory neurons. *Molecular and cellular neurosciences* **18:** 270-282

Alvarez JV, Febbo PG, Ramaswamy S, Loda M, Richardson A, Frank DA (2005) Identification of a genetic signature of activated signal transducer and activator of transcription 3 in human tumors. *Cancer research* **65:** 5054-5062

Angers S, Salahpour A, Joly E, Hilairet S, Chelsky D, Dennis M, Bouvier M (2000) Detection of beta 2-adrenergic receptor dimerization in living cells using bioluminescence resonance energy transfer (BRET). *Proceedings of the National Academy of Sciences of the United States of America* **97:** 3684-3689

Arai R, Nakagawa H, Kitayama A, Ueda H, Nagamune T (2002) Detection of protein-protein interaction by bioluminescence resonance energy transfer from firefly luciferase to red fluorescent protein. *Journal of bioscience and bioengineering* **94:** 362-364

Arora T, Liu B, He H, Kim J, Murphy TL, Murphy KM, Modlin RL, Shuai K (2003) PIASx is a transcriptional co-repressor of signal transducer and activator of transcription 4. *The Journal of biological chemistry* **278:** 21327-21330

Avalle L, Camporeale A, Morciano G, Caroccia N, Ghetti E, Orecchia V, Viavattene D, Giorgi C, Pinton P, Poli V (2019) STAT3 localizes to the ER, acting as a gatekeeper for ER-mitochondrion Ca(2+) fluxes and apoptotic responses. *Cell death and differentiation* **26:** 932-942

Avalle L, Poli V (2018) Nucleus, Mitochondrion, or Reticulum? STAT3 a La Carte. *International journal of molecular sciences* **19**

Baird GS, Zacharias DA, Tsien RY (2000) Biochemistry, mutagenesis, and oligomerization of DsRed, a red fluorescent protein from coral. *Proceedings of the National Academy of Sciences of the United States of America* **97:** 11984-11989

Balko JM, Giltnane JM, Wang K, Schwarz LJ, Young CD, Cook RS, Owens P, Sanders ME, Kuba MG, Sanchez V, Kurupi R, Moore PD, Pinto JA, Doimi FD, Gomez H, Horiuchi D, Goga A, Lehmann BD, Bauer JA, Pietenpol JA, Ross JS, Palmer GA, Yelensky R, Cronin M, Miller VA, Stephens PJ, Arteaga CL (2014) Molecular profiling of the residual disease of triple-negative breast cancers after neoadjuvant chemotherapy identifies actionable therapeutic targets. *Cancer discovery* **4:** 232-245

Banerjee K, Keasey MP, Razskazovskiy V, Visavadiya NP, Jia C, Hagg T (2017) Reduced FAK-STAT3 signaling contributes to ER stress-induced mitochondrial dysfunction and death in endothelial cells. *Cellular signalling* **36:** 154-162

Banerjee K, Resat H (2016) Constitutive activation of STAT3 in breast cancer cells: A review. *International journal of cancer* **138:** 2570-2578

Barre B, Vigneron A, Perkins N, Roninson IB, Gamelin E, Coqueret O (2007) The STAT3 oncogene as a predictive marker of drug resistance. *Trends in molecular medicine* **13:** 4-11

Becker S, Groner B, Muller CW (1998) Three-dimensional structure of the Stat3beta homodimer bound to DNA. *Nature* **394:** 145-151

Belo Y, Mielko Z, Nudelman H, Afek A, Ben-David O, Shahar A, Zarivach R, Gordan R, Arbely E (2019) Unexpected implications of STAT3 acetylation revealed by genetic encoding of acetyl-lysine. *Biochimica et biophysica acta General subjects* **1863:** 1343-1350

Berclaz G, Altermatt HJ, Rohrbach V, Siragusa A, Dreher E, Smith PD (2001) EGFR dependent expression of STAT3 (but not STAT1) in breast cancer. *International journal of oncology* **19:** 1155-1160

Berishaj M, Gao SP, Ahmed S, Leslie K, Al-Ahmadie H, Gerald WL, Bornmann W, Bromberg JF (2007) Stat3 is tyrosine-phosphorylated through the interleukin-6/glycoprotein 130/Janus kinase pathway in breast cancer. *Breast cancer research : BCR* **9:** R32

Bhuckory S, Kays JC, Dennis AM (2019) In Vivo Biosensing Using Resonance Energy Transfer. *Biosensors* **9**

Bito T, Sumita N, Ashida M, Budiyanto A, Ueda M, Ichihashi M, Tokura Y, Nishigori C (2011) Inhibition of Epidermal Growth Factor Receptor and PI3K/Akt Signaling Suppresses Cell Proliferation and Survival through Regulation of Stat3 Activation in Human Cutaneous Squamous Cell Carcinoma. *Journal of skin cancer* **2011:** 874571

Blaskovich MA, Sun J, Cantor A, Turkson J, Jove R, Sebti SM (2003) Discovery of JSI-124 (cucurbitacin I), a selective Janus kinase/signal transducer and activator of transcription 3 signaling pathway inhibitor with potent antitumor activity against human and murine cancer cells in mice. *Cancer research* **63:** 1270-1279

Boeuf H, Hauss C, Graeve FD, Baran N, Kedinger C (1997) Leukemia inhibitory factor-dependent transcriptional activation in embryonic stem cells. *The Journal of cell biology* **138:** 1207-1217

Bonni A, Sun Y, Nadal-Vicens M, Bhatt A, Frank DA, Rozovsky I, Stahl N, Yancopoulos GD, Greenberg ME (1997) Regulation of gliogenesis in the central nervous system by the JAK-STAT signaling pathway. *Science* **278:** 477-483

Boute N, Lowe P, Berger S, Malissard M, Robert A, Tesar M (2016) NanoLuc Luciferase - A Multifunctional Tool for High Throughput Antibody Screening. *Frontiers in pharmacology* **7:** 27

Bromberg JF, Horvath CM, Besser D, Lathem WW, Darnell JE, Jr. (1998) Stat3 activation is required for cellular transformation by v-src. *Molecular and cellular biology* **18:** 2553-2558

Bromberg JF, Wrzeszczynska MH, Devgan G, Zhao Y, Pestell RG, Albanese C, Darnell JE, Jr. (1999) Stat3 as an oncogene. *Cell* **98:** 295-303

Cao X, Tay A, Guy GR, Tan YH (1996) Activation and association of Stat3 with Src in v-Src-transformed cell lines. *Molecular and cellular biology* **16:** 1595-1603

Carpenter RL, Lo HW (2014) STAT3 Target Genes Relevant to Human Cancers. *Cancers* **6:** 897-925

Chang AY, Hsu E, Patel J, Li Y, Zhang M, Iguchi H, Rogoff HA (2019) Evaluation of Tumor Cell-Tumor Microenvironment Component Interactions as Potential Predictors of Patient Response to Napabucasin. *Molecular cancer research : MCR* **17:** 1429-1434

Chatterjee S, Malhotra R, Varghese F, Bukhari AB, Patil A, Budrukkar A, Parmar V, Gupta S, De A (2013) Quantitative immunohistochemical analysis reveals association between sodium iodide symporter and estrogen receptor expression in breast cancer. *PloS one* **8:** e54055

Chen Q, Lv J, Yang W, Xu B, Wang Z, Yu Z, Wu J, Yang Y, Han Y (2019) Targeted inhibition of STAT3 as a potential treatment strategy for atherosclerosis. *Theranostics* **9:** 6424-6442

Chen W, Daines MO, Khurana Hershey GK (2004) Turning off signal transducer and activator of transcription (STAT): the negative regulation of STAT signaling. *The Journal of allergy and clinical immunology* **114:** 476-489; quiz 490

Chen Y, Ji M, Zhang S, Xue N, Xu H, Lin S, Chen X (2018) Bt354 as a new STAT3 signaling pathway inhibitor against triple negative breast cancer. *Journal of drug targeting* **26:** 920-930

Chiu NH, Christopoulos TK (1999) Two-site expression immunoassay using a firefly luciferase-coding DNA label. *Clinical chemistry* **45:** 1954-1959

Choi JY, Li WL, Kouri RE, Yu J, Kao FT, Ruano G (1996) Assignment of the acute phase response factor (APRF) gene to 17q21 by microdissection clone sequencing and fluorescence in situ hybridization of a P1 clone. *Genomics* **37:** 264-265

Chung CD, Liao J, Liu B, Rao X, Jay P, Berta P, Shuai K (1997) Specific inhibition of Stat3 signal transduction by PIAS3. *Science* **278:** 1803-1805

Chung S.S. NG, Y. Wu, and J.V. Vadgama. (2014) STAT3 activation in HER2-overexpressing breast cancer promotes epithelial-mesenchymal transition and cancer stem cell traits. *International journal of oncology* **44:** 403-411

Ciruela F, Vilardaga JP, Fernandez-Duenas V (2010) Lighting up multiprotein complexes: lessons from GPCR oligomerization. *Trends in biotechnology* **28:** 407-415

Clevenger CV (2004) Roles and regulation of stat family transcription factors in human breast cancer. *The American journal of pathology* **165:** 1449-1460

Cocchiola R, Romaniello D, Grillo C, Altieri F, Liberti M, Magliocca FM, Chichiarelli S, Marrocco I, Borgoni G, Perugia G, Eufemi M (2017) Analysis of STAT3 post-translational modifications (PTMs) in human prostate cancer with different Gleason Score. *Oncotarget* **8:** 42560-42570

Copeland NG, Gilbert DJ, Schindler C, Zhong Z, Wen Z, Darnell JE, Jr., Mui AL, Miyajima A, Quelle FW, Ihle JN, et al. (1995) Distribution of the mammalian Stat gene family in mouse chromosomes. *Genomics* **29:** 225-228

Darnell JE, Jr. (1997) STATs and gene regulation. *Science* **277:** 1630-1635

Darnell JE, Jr., Kerr IM, Stark GR (1994) Jak-STAT pathways and transcriptional activation in response to IFNs and other extracellular signaling proteins. *Science* **264:** 1415-1421

Dasgupta M, Unal H, Willard B, Yang J, Karnik SS, Stark GR (2014) Critical role for lysine 685 in gene expression mediated by transcription factor unphosphorylated STAT3. *The Journal of biological chemistry* **289:** 30763-30771

De A (2011) The new era of bioluminescence resonance energy transfer technology. *Current pharmaceutical biotechnology* **12:** 558-568

De A, Jasani A, Arora R, Gambhir SS (2013) Evolution of BRET Biosensors from Live Cell to Tissue-Scale In vivo Imaging. *Frontiers in endocrinology* **4:** 131

De A, Yaghoubi SS, Gambhir SS (2008) Applications of lentiviral vectors in noninvasive molecular imaging. *Methods in molecular biology* **433:** 177-202

Decker T, Kovarik P (2000) Serine phosphorylation of STATs. *Oncogene* **19:** 2628-2637

Dimri S, Basu S, De A (2016) Use of BRET to Study Protein-Protein Interactions In Vitro and In Vivo. *Methods in molecular biology* **1443:** 57-78

Don-Doncow N, Marginean F, Coleman I, Nelson PS, Ehrnstrom R, Krzyzanowska A, Morrissey C, Hellsten R, Bjartell A (2017) Expression of STAT3 in Prostate Cancer Metastases. *European urology* **71:** 313-316

Dragulescu-Andrasi A, Chan CT, De A, Massoud TF, Gambhir SS (2011) Bioluminescence resonance energy transfer (BRET) imaging of protein-protein interactions within deep tissues of living subjects. *Proceedings of the National Academy of Sciences of the United States of America* **108:** 12060-12065

Drinovec L, Kubale V, Nohr Larsen J, Vrecl M (2012) Mathematical models for quantitative assessment of bioluminescence resonance energy transfer: application to seven transmembrane receptors oligomerization. *Frontiers in endocrinology* **3:** 104

Dunst S, Tomancak P (2019) Imaging Flies by Fluorescence Microscopy: Principles, Technologies, and Applications. *Genetics* **211:** 15-34

Durbin JE, Hackenmiller R, Simon MC, Levy DE (1996) Targeted disruption of the mouse Stat1 gene results in compromised innate immunity to viral disease. *Cell* **84:** 443-450

El Khamlichi C, Reverchon-Assadi F, Hervouet-Coste N, Blot L, Reiter E, Morisset-Lopez S (2019) Bioluminescence Resonance Energy Transfer as a Method to Study Protein-Protein Interactions: Application to G Protein Coupled Receptor Biology. *Molecules* **24**

England CG, Ehlerding EB, Cai W (2016) NanoLuc: A Small Luciferase Is Brightening Up the Field of Bioluminescence. *Bioconjugate chemistry* **27:** 1175-1187

Ferrajoli A, Faderl S, Van Q, Koch P, Harris D, Liu Z, Hazan-Halevy I, Wang Y, Kantarjian HM, Priebe W, Estrov Z (2007) WP1066 disrupts Janus kinase-2 and induces caspase-dependent apoptosis in acute myelogenous leukemia cells. *Cancer research* **67:** 11291-11299

Fonseca C, Voabil P, Carvalho AS, Matthiesen R (2013) Tools for protein posttranslational modifications analysis: FAK, a case study. *Methods in molecular biology* **1007:** 335-358

Fragomeni SM, Sciallis A, Jeruss JS (2018) Molecular Subtypes and Local-Regional Control of Breast Cancer. *Surgical oncology clinics of North America* **27:** 95-120

Giordano C, Vizza D, Panza S, Barone I, Bonofiglio D, Lanzino M, Sisci D, De Amicis F, Fuqua SA, Catalano S, Ando S (2013) Leptin increases HER2 protein levels through a STAT3-mediated up-regulation of Hsp90 in breast cancer cells. *Molecular oncology* **7:** 379-391

Gkouveris I, Nikitakis N, Avgoustidis D, Karanikou M, Rassidakis G, Sklavounou A (2017) ERK1/2, JNK and STAT3 activation and correlation with tumor differentiation in oral SCC. *Histology and histopathology* **32:** 1065-1076

Gough DJ, Koetz L, Levy DE (2013) The MEK-ERK pathway is necessary for serine phosphorylation of mitochondrial STAT3 and Ras-mediated transformation. *PloS one* **8:** e83395

Green AA, McElroy WD (1956) Crystalline firefly luciferase. *Biochimica et biophysica acta* **20:** 170-176

Gurskaya NG, Fradkov AF, Terskikh A, Matz MV, Labas YA, Martynov VI, Yanushevich YG, Lukyanov KA, Lukyanov SA (2001) GFP-like chromoproteins as a source of far-red fluorescent proteins. *FEBS letters* **507:** 16-20

Hahn YI, Kim SJ, Choi BY, Cho KC, Bandu R, Kim KP, Kim DH, Kim W, Park JS, Han BW, Lee J, Na HK, Cha YN, Surh YJ (2018) Curcumin interacts directly with the Cysteine 259 residue of STAT3 and induces apoptosis in H-Ras transformed human mammary epithelial cells. *Scientific reports* **8:** 6409

Han Y, Amin HM, Franko B, Frantz C, Shi X, Lai R (2006) Loss of SHP1 enhances JAK3/STAT3 signaling and decreases proteosome degradation of JAK3 and NPM-ALK in ALK+ anaplastic large-cell lymphoma. *Blood* **108:** 2796-2803

Hassan M, Klaunberg BA (2004) Biomedical applications of fluorescence imaging in vivo. *Comparative medicine* **54:** 635-644

Hazan-Halevy I, Harris D, Liu Z, Liu J, Li P, Chen X, Shanker S, Ferrajoli A, Keating MJ, Estrov Z (2010) STAT3 is constitutively phosphorylated on serine 727 residues, binds DNA, and activates transcription in CLL cells. *Blood* **115:** 2852-2863

He L, Lv Y, Song Y, Zhang B (2019) The prognosis comparison of different molecular subtypes of breast tumors after radiotherapy and the intrinsic reasons for their distinct radiosensitivity. *Cancer management and research* **11:** 5765-5775

He P, Li D, Zhang B (2014) Losartan attenuates renal interstitial fibrosis and tubular cell apoptosis in a rat model of obstructive nephropathy. *Molecular medicine reports* **10:** 638-644

Hemmann U, Gerhartz C, Heesel B, Sasse J, Kurapkat G, Grotzinger J, Wollmer A, Zhong Z, Darnell JE, Jr., Graeve L, Heinrich PC, Horn F (1996) Differential activation of acute phase response factor/Stat3 and Stat1 via the cytoplasmic domain of the interleukin 6 signal transducer gp130. II. Src homology SH2 domains define the specificity of stat factor activation. *The Journal of biological chemistry* **271:** 12999-13007

Ho HH, Ivashkiv LB (2006) Role of STAT3 in type I interferon responses. Negative regulation of STAT1-dependent inflammatory gene activation. *The Journal of biological chemistry* **281:** 14111-14118

Hoshino H (2009) Current advanced bioluminescence technology in drug discovery. *Expert opinion on drug discovery* **4:** 373-389

Huang G, Yan H, Ye S, Tong C, Ying QL (2014) STAT3 phosphorylation at tyrosine 705 and serine 727 differentially regulates mouse ESC fates. *Stem cells* **32:** 1149-1160

Huang S (2007) Regulation of metastases by signal transducer and activator of transcription 3 signaling pathway: clinical implications. *Clinical cancer research : an official journal of the American Association for Cancer Research* **13:** 1362-1366

Hughes K, Watson CJ (2018) The Multifaceted Role of STAT3 in Mammary Gland Involution and Breast Cancer. *International journal of molecular sciences* **19**

Imada K, Leonard WJ (2000) The Jak-STAT pathway. *Molecular immunology* **37:** 1-11

Irie-Sasaki J, Sasaki T, Matsumoto W, Opavsky A, Cheng M, Welstead G, Griffiths E, Krawczyk C, Richardson CD, Aitken K, Iscove N, Koretzky G, Johnson P, Liu P, Rothstein DM, Penninger JM (2001) CD45 is a JAK phosphatase and negatively regulates cytokine receptor signalling. *Nature* **409:** 349-354

Ji K, Zhang M, Chu Q, Gan Y, Ren H, Zhang L, Wang L, Li X, Wang W (2016) The Role of p-STAT3 as a Prognostic and Clinicopathological Marker in Colorectal Cancer: A Systematic Review and Meta-Analysis. *PloS one* **11:** e0160125

Jing N, Li Y, Xu X, Sha W, Li P, Feng L, Tweardy DJ (2003) Targeting Stat3 with G-quartet oligodeoxynucleotides in human cancer cells. *DNA and cell biology* **22:** 685-696

Johnston PA, Grandis JR (2011) STAT3 signaling: anticancer strategies and challenges. *Molecular interventions* **11:** 18-26

Kamakura S, Oishi K, Yoshimatsu T, Nakafuku M, Masuyama N, Gotoh Y (2004) Hes binding to STAT3 mediates crosstalk between Notch and JAK-STAT signalling. *Nature cell biology* **6:** 547-554

Kamran MZ, Patil P, Gude RP (2013) Role of STAT3 in cancer metastasis and translational advances. *BioMed research international* **2013:** 421821

Kaplan MH, Sun YL, Hoey T, Grusby MJ (1996) Impaired IL-12 responses and enhanced development of Th2 cells in Stat4-deficient mice. *Nature* **382:** 174-177

Kiu H, Nicholson SE (2012) Biology and significance of the JAK/STAT signalling pathways. *Growth factors* **30:** 88-106

Kotha A, Sekharam M, Cilenti L, Siddiquee K, Khaled A, Zervos AS, Carter B, Turkson J, Jove R (2006) Resveratrol inhibits Src and Stat3 signaling and induces the apoptosis of malignant cells containing activated Stat3 protein. *Molecular cancer therapeutics* **5:** 621-629

Kretzschmar AK, Dinger MC, Henze C, Brocke-Heidrich K, Horn F (2004) Analysis of Stat3 (signal transducer and activator of transcription 3) dimerization by fluorescence resonance energy transfer in living cells. *The Biochemical journal* **377:** 289-297

Krueger KE, Srivastava S (2006) Posttranslational protein modifications: current implications for cancer detection, prevention, and therapeutics. *Molecular & cellular proteomics : MCP* **5:** 1799-1810

Kulesza DW, Przanowski P, Kaminska B (2019) Knockdown of STAT3 targets a subpopulation of invasive melanoma stem-like cells. *Cell biology international* **43:** 613-622

Lacey VK, Parrish AR, Han S, Shen Z, Briggs SP, Ma Y, Wang L (2011) A fluorescent reporter of the phosphorylation status of the substrate protein STAT3. *Angewandte Chemie* **50:** 8692-8696

Lankadasari MB, Aparna JS, Mohammed S, James S, Aoki K, Binu VS, Nair S, Harikumar KB (2018) Targeting S1PR1/STAT3 loop abrogates desmoplasia and chemosensitizes pancreatic cancer to gemcitabine. *Theranostics* **8:** 3824-3840

Laudisi F, Cherubini F, Monteleone G, Stolfi C (2018) STAT3 Interactors as Potential Therapeutic Targets for Cancer Treatment. *International journal of molecular sciences* **19**

Lee H, Zhang P, Herrmann A, Yang C, Xin H, Wang Z, Hoon DS, Forman SJ, Jove R, Riggs AD, Yu H (2012) Acetylated STAT3 is crucial for methylation of tumor-suppressor gene promoters and inhibition by resveratrol results in demethylation. *Proceedings of the National Academy of Sciences of the United States of America* **109:** 7765-7769

Lee JL, Wang MJ, Chen JY (2009) Acetylation and activation of STAT3 mediated by nuclear translocation of CD44. *The Journal of cell biology* **185:** 949-957

Leonard WJ, O'Shea JJ (1998) Jaks and STATs: biological implications. *Annual review of immunology* **16:** 293-322

Levi J, De A, Cheng Z, Gambhir SS (2007) Bisdeoxycoelenterazine derivatives for improvement of bioluminescence resonance energy transfer assays. *Journal of the American Chemical Society* **129:** 11900-11901

Levitzki A (1992) Tyrphostins: tyrosine kinase blockers as novel antiproliferative agents and dissectors of signal transduction. *FASEB journal : official publication of the Federation of American Societies for Experimental Biology* **6:** 3275-3282

Li J, Cui G, Sun L, Wang SJ, Li YL, Meng YG, Guan Z, Fan WS, Li LA, Yang YZ, You YQ, Fu XY, Yan ZF, Huang K (2013) STAT3 acetylation-induced promoter methylation is associated with downregulation of the ARHI tumor-suppressor gene in ovarian cancer. *Oncology reports* **30:** 165-170

Lin GS, Chen YP, Lin ZX, Wang XF, Zheng ZQ, Chen L (2014) STAT3 serine 727 phosphorylation influences clinical outcome in glioblastoma. *International journal of clinical and experimental pathology* **7:** 3141-3149

Liu B, Gross M, ten Hoeve J, Shuai K (2001) A transcriptional corepressor of Stat1 with an essential LXXLL signature motif. *Proceedings of the National Academy of Sciences of the United States of America* **98:** 3203-3207

Liu LJ, Leung KH, Chan DS, Wang YT, Ma DL, Leung CH (2014) Identification of a natural product-like STAT3 dimerization inhibitor by structure-based virtual screening. *Cell death & disease* **5:** e1293

Liu X, Robinson GW, Wagner KU, Garrett L, Wynshaw-Boris A, Hennighausen L (1997) Stat5a is mandatory for adult mammary gland development and lactogenesis. *Genes & development* **11:** 179-186

Loening AM, Fenn TD, Wu AM, Gambhir SS (2006) Consensus guided mutagenesis of Renilla luciferase yields enhanced stability and light output. *Protein engineering, design & selection : PEDS* **19:** 391-400

Loening AM, Wu AM, Gambhir SS (2007) Red-shifted Renilla reniformis luciferase variants for imaging in living subjects. *Nature methods* **4:** 641-643

Luker GD, Luker KE (2008) Optical imaging: current applications and future directions. *Journal of nuclear medicine : official publication, Society of Nuclear Medicine* **49:** 1-4

Machleidt T, Woodroofe CC, Schwinn MK, Mendez J, Robers MB, Zimmerman K, Otto P, Daniels DL, Kirkland TA, Wood KV (2015) NanoBRET--A Novel BRET Platform for the Analysis of Protein-Protein Interactions. *ACS chemical biology* **10:** 1797-1804

Marampon F, Bossi G, Ciccarelli C, Di Rocco A, Sacchi A, Pestell RG, Zani BM (2009) MEK/ERK inhibitor U0126 affects in vitro and in vivo growth of embryonal rhabdomyosarcoma. *Molecular cancer therapeutics* **8:** 543-551

Maritano D, Sugrue ML, Tininini S, Dewilde S, Strobl B, Fu X, Murray-Tait V, Chiarle R, Poli V (2004) The STAT3 isoforms alpha and beta have unique and specific functions. *Nature immunology* **5:** 401-409

Migone TS, Lin JX, Cereseto A, Mulloy JC, O'Shea JJ, Franchini G, Leonard WJ (1995) Constitutively activated Jak-STAT pathway in T cells transformed with HTLV-I. *Science* **269:** 79-81

Mo XL, Fu H (2016) BRET: NanoLuc-Based Bioluminescence Resonance Energy Transfer Platform to Monitor Protein-Protein Interactions in Live Cells. *Methods in molecular biology* **1439:** 263-271

Muller-Taubenberger A, Anderson KI (2007) Recent advances using green and red fluorescent protein variants. *Applied microbiology and biotechnology* **77:** 1-12

Murray PJ (2007) The JAK-STAT signaling pathway: input and output integration. *Journal of immunology* **178:** 2623-2629

Nadiminty N, Lou W, Lee SO, Lin X, Trump DL, Gao AC (2006) Stat3 activation of NF-{kappa}B p100 processing involves CBP/p300-mediated acetylation. *Proceedings of the National Academy of Sciences of the United States of America* **103:** 7264-7269

Nair RR, Tolentino JH, Hazlehurst LA (2012) Role of STAT3 in Transformation and Drug Resistance in CML. *Frontiers in oncology* **2:** 30

Neel BG, Tonks NK (1997) Protein tyrosine phosphatases in signal transduction. *Current opinion in cell biology* **9:** 193-204

Nie Y, Erion DM, Yuan Z, Dietrich M, Shulman GI, Horvath TL, Gao Q (2009) STAT3 inhibition of gluconeogenesis is downregulated by SirT1. *Nature cell biology* **11:** 492-500

Nishihara R, Paulmurugan R, Nakajima T, Yamamoto E, Natarajan A, Afjei R, Hiruta Y, Iwasawa N, Nishiyama S, Citterio D, Sato M, Kim SB, Suzuki K (2019) Highly bright and stable NIR-BRET with blue-shifted coelenterazine derivatives for deep-tissue imaging of molecular events in vivo. *Theranostics* **9:** 2646-2661

O'Shea JJ, Gadina M, Schreiber RD (2002) Cytokine signaling in 2002: new surprises in the Jak/Stat pathway. *Cell* **109 Suppl:** S121-131

O'Shea JJ, Kanno Y, Chen X, Levy DE (2005) Cell signaling. Stat acetylation--a key facet of cytokine signaling? *Science* **307:** 217-218

Otto-Duessel M, Khankaldyyan V, Gonzalez-Gomez I, Jensen MC, Laug WE, Rosol M (2006) In vivo testing of Renilla luciferase substrate analogs in an orthotopic murine model of human glioblastoma. *Molecular imaging* **5:** 57-64

Ouedraogo ZG, Muller-Barthelemy M, Kemeny JL, Dedieu V, Biau J, Khalil T, Raoelfils LI, Granzotto A, Pereira B, Beaudoin C, Guissou IP, Berger M, Morel L, Chautard E, Verrelle P (2016) STAT3 Serine 727 Phosphorylation: A Relevant Target to Radiosensitize Human Glioblastoma. *Brain pathology* **26:** 18-30

Pardanani A, Hood J, Lasho T, Levine RL, Martin MB, Noronha G, Finke C, Mak CC, Mesa R, Zhu H, Soll R, Gilliland DG, Tefferi A (2007) TG101209, a small molecule JAK2-selective kinase inhibitor potently

inhibits myeloproliferative disorder-associated JAK2V617F and MPLW515L/K mutations. *Leukemia* **21:** 1658-1668

Pilati C, Amessou M, Bihl MP, Balabaud C, Nhieu JT, Paradis V, Nault JC, Izard T, Bioulac-Sage P, Couchy G, Poussin K, Zucman-Rossi J (2011) Somatic mutations activating STAT3 in human inflammatory hepatocellular adenomas. *The Journal of experimental medicine* **208:** 1359-1366

Prabakaran S, Lippens G, Steen H, Gunawardena J (2012) Post-translational modification: nature's escape from genetic imprisonment and the basis for dynamic information encoding. *Wiley interdisciplinary reviews Systems biology and medicine* **4:** 565-583

Qin HR, Kim HJ, Kim JY, Hurt EM, Klarmann GJ, Kawasaki BT, Duhagon Serrat MA, Farrar WL (2008) Activation of signal transducer and activator of transcription 3 through a phosphomimetic serine 727 promotes prostate tumorigenesis independent of tyrosine 705 phosphorylation. *Cancer research* **68:** 7736-7741

Qin JJ, Yan L, Zhang J, Zhang WD (2019) STAT3 as a potential therapeutic target in triple negative breast cancer: a systematic review. *Journal of experimental & clinical cancer research : CR* **38:** 195

Qureshi A, Pervez S (2010) Allred scoring for ER reporting and it's impact in clearly distinguishing ER negative from ER positive breast cancers. *JPMA The Journal of the Pakistan Medical Association* **60:** 350-353

Rebe C, Vegran F, Berger H, Ghiringhelli F (2013) STAT3 activation: A key factor in tumor immunoescape. *Jak-Stat* **2:** e23010

Regis G, Pensa S, Boselli D, Novelli F, Poli V (2008) Ups and downs: the STAT1:STAT3 seesaw of Interferon and gp130 receptor signalling. *Seminars in cell & developmental biology* **19:** 351-359

Ren Z, Cabell LA, Schaefer TS, McMurray JS (2003) Identification of a high-affinity phosphopeptide inhibitor of Stat3. *Bioorganic & medicinal chemistry letters* **13:** 633-636

Ren Z, Mao X, Mertens C, Krishnaraj R, Qin J, Mandal PK, Romanowski MJ, McMurray JS, Chen X (2008) Crystal structure of unphosphorylated STAT3 core fragment. *Biochemical and biophysical research communications* **374:** 1-5

Rumyantsev KA, Turoverov KK, Verkhusha VV (2016) Near-infrared bioluminescent proteins for two-color multimodal imaging. *Scientific reports* **6:** 36588

Sakaguchi M, Oka M, Iwasaki T, Fukami Y, Nishigori C (2012) Role and regulation of STAT3 phosphorylation at Ser727 in melanocytes and melanoma cells. *The Journal of investigative dermatology* **132:** 1877-1885

Schindler C, Levy DE, Decker T (2007) JAK-STAT signaling: from interferons to cytokines. *The Journal of biological chemistry* **282:** 20059-20063

Schroder M, Kroeger KM, Volk HD, Eidne KA, Grutz G (2004) Preassociation of nonactivated STAT3 molecules demonstrated in living cells using bioluminescence resonance energy transfer: a new model of STAT activation? *Journal of leukocyte biology* **75:** 792-797

Schust J, Sperl B, Hollis A, Mayer TU, Berg T (2006) Stattic: a small-molecule inhibitor of STAT3 activation and dimerization. *Chem Biol* **13:** 1235-1242

Segatto I, Baldassarre G, Belletti B (2018) STAT3 in Breast Cancer Onset and Progression: A Matter of Time and Context. *International journal of molecular sciences* **19**

Segovia-Mendoza M, Gonzalez-Gonzalez ME, Barrera D, Diaz L, Garcia-Becerra R (2015) Efficacy and mechanism of action of the tyrosine kinase inhibitors gefitinib, lapatinib and neratinib in the treatment of HER2-positive breast cancer: preclinical and clinical evidence. *American journal of cancer research* **5:** 2531-2561

Seliger HH, Mc EW (1960) Spectral emission and quantum yield of firefly bioluminescence. *Archives of biochemistry and biophysics* **88:** 136-141

Sellier H, Rebillard A, Guette C, Barre B, Coqueret O (2013) How should we define STAT3 as an oncogene and as a potential target for therapy? *Jak-Stat* **2:** e24716

Sethi G, Chatterjee S, Rajendran P, Li F, Shanmugam MK, Wong KF, Kumar AP, Senapati P, Behera AK, Hui KM, Basha J, Natesh N, Luk JM, Kundu TK (2014) Inhibition of STAT3 dimerization and acetylation by garcinol suppresses the growth of human hepatocellular carcinoma in vitro and in vivo. *Molecular cancer* **13:** 66

Shah K, Weissleder R (2005) Molecular optical imaging: applications leading to the development of present day therapeutics. *NeuroRx : the journal of the American Society for Experimental NeuroTherapeutics* **2:** 215-225

Shalini Dimri S, Abhijit De (2017) Approaching non-canonical STAT3 signaling to redefine cancer therapeutic strategy. *Integrative Molecular Medicine* **4:** 10

Shaner NC, Campbell RE, Steinbach PA, Giepmans BN, Palmer AE, Tsien RY (2004) Improved monomeric red, orange and yellow fluorescent proteins derived from Discosoma sp. red fluorescent protein. *Nature biotechnology* **22:** 1567-1572

Shcherbo D, Merzlyak EM, Chepurnykh TV, Fradkov AF, Ermakova GV, Solovieva EA, Lukyanov KA, Bogdanova EA, Zaraisky AG, Lukyanov S, Chudakov DM (2007) Bright far-red fluorescent protein for whole-body imaging. *Nature methods* **4:** 741-746

Shi L, Zheng H, Hu W, Zhou B, Dai X, Zhang Y, Liu Z, Wu X, Zhao C, Liang G (2017) Niclosamide inhibition of STAT3 synergizes with erlotinib in human colon cancer. *OncoTargets and therapy* **10:** 1767-1776

Shields BJ, Wiede F, Gurzov EN, Wee K, Hauser C, Zhu HJ, Molloy TJ, O'Toole SA, Daly RJ, Sutherland RL, Mitchell CA, McLean CA, Tiganis T (2013) TCPTP regulates SFK and STAT3 signaling and is lost in triple-negative breast cancers. *Molecular and cellular biology* **33:** 557-570

Shimoda K, van Deursen J, Sangster MY, Sarawar SR, Carson RT, Tripp RA, Chu C, Quelle FW, Nosaka T, Vignali DA, Doherty PC, Grosveld G, Paul WE, Ihle JN (1996) Lack of IL-4-induced Th2 response and IgE class switching in mice with disrupted Stat6 gene. *Nature* **380:** 630-633

Shuai K (2000) Modulation of STAT signaling by STAT-interacting proteins. *Oncogene* **19:** 2638-2644

Shuai K, Schindler C, Prezioso VR, Darnell JE, Jr. (1992) Activation of transcription by IFN-gamma: tyrosine phosphorylation of a 91-kD DNA binding protein. *Science* **258:** 1808-1812

Sirkisoon SR, Carpenter RL, Rimkus T, Anderson A, Harrison A, Lange AM, Jin G, Watabe K, Lo HW (2018) Interaction between STAT3 and GLI1/tGLI1 oncogenic transcription factors promotes the aggressiveness of triple-negative breast cancers and HER2-enriched breast cancer. *Oncogene* **37:** 2502-2514

Song H, Wang R, Wang S, Lin J (2005) A low-molecular-weight compound discovered through virtual database screening inhibits Stat3 function in breast cancer cells. *Proceedings of the National Academy of Sciences of the United States of America* **102:** 4700-4705

Srivastava J, DiGiovanni J (2016) Non-canonical Stat3 signaling in cancer. *Molecular carcinogenesis* **55:** 1889-1898

Stryer L, Haugland RP (1967) Energy transfer: a spectroscopic ruler. *Proceedings of the National Academy of Sciences of the United States of America* **58:** 719-726

Suraweera A, O'Byrne KJ, Richard DJ (2018) Combination Therapy With Histone Deacetylase Inhibitors (HDACi) for the Treatment of Cancer: Achieving the Full Therapeutic Potential of HDACi. *Frontiers in oncology* **8:** 92

Takeda K, Kaisho T, Yoshida N, Takeda J, Kishimoto T, Akira S (1998) Stat3 activation is responsible for IL-6-dependent T cell proliferation through preventing apoptosis: generation and characterization of T cell-specific Stat3-deficient mice. *Journal of immunology* **161:** 4652-4660

Takeda K, Noguchi K, Shi W, Tanaka T, Matsumoto M, Yoshida N, Kishimoto T, Akira S (1997) Targeted disruption of the mouse Stat3 gene leads to early embryonic lethality. *Proceedings of the National Academy of Sciences of the United States of America* **94:** 3801-3804

Takeda K, Tanaka T, Shi W, Matsumoto M, Minami M, Kashiwamura S, Nakanishi K, Yoshida N, Kishimoto T, Akira S (1996) Essential role of Stat6 in IL-4 signalling. *Nature* **380:** 627-630

Teglund S, McKay C, Schuetz E, van Deursen JM, Stravopodis D, Wang D, Brown M, Bodner S, Grosveld G, Ihle JN (1998) Stat5a and Stat5b proteins have essential and nonessential, or redundant, roles in cytokine responses. *Cell* **93:** 841-850

Tell RW, Horvath CM (2014) Bioinformatic analysis reveals a pattern of STAT3-associated gene expression specific to basal-like breast cancers in human tumors. *Proceedings of the National Academy of Sciences of the United States of America* **111:** 12787-12792

Thierfelder WE, van Deursen JM, Yamamoto K, Tripp RA, Sarawar SR, Carson RT, Sangster MY, Vignali DA, Doherty PC, Grosveld GC, Ihle JN (1996) Requirement for Stat4 in interleukin-12-mediated responses of natural killer and T cells. *Nature* **382:** 171-174

Timofeeva OA, Gaponenko V, Lockett SJ, Tarasov SG, Jiang S, Michejda CJ, Perantoni AO, Tarasova NI (2007) Rationally designed inhibitors identify STAT3 N-domain as a promising anticancer drug target. *ACS chemical biology* **2:** 799-809

Tkach M, Rosemblit C, Rivas MA, Proietti CJ, Diaz Flaque MC, Mercogliano MF, Beguelin W, Maronna E, Guzman P, Gercovich FG, Deza EG, Elizalde PV, Schillaci R (2013) p42/p44 MAPK-mediated Stat3Ser727 phosphorylation is required for progestin-induced full activation of Stat3 and breast cancer growth. *Endocrine-related cancer* **20:** 197-212

Tomita N, Ogihara T, Morishita R (2003) Transcription factors as molecular targets: molecular mechanisms of decoy ODN and their design. *Current drug targets* **4:** 603-608

Tsien RY (1998) The green fluorescent protein. *Annual review of biochemistry* **67:** 509-544

Turkson J, Bowman T, Adnane J, Zhang Y, Djeu JY, Sekharam M, Frank DA, Holzman LB, Wu J, Sebti S, Jove R (1999) Requirement for Ras/Rac1-mediated p38 and c-Jun N-terminal kinase signaling in Stat3 transcriptional activity induced by the Src oncoprotein. *Molecular and cellular biology* **19:** 7519-7528

Turkson J, Jove R (2000) STAT proteins: novel molecular targets for cancer drug discovery. *Oncogene* **19:** 6613-6626

Turkson J, Kim JS, Zhang S, Yuan J, Huang M, Glenn M, Haura E, Sebti S, Hamilton AD, Jove R (2004a) Novel peptidomimetic inhibitors of signal transducer and activator of transcription 3 dimerization and biological activity. *Molecular cancer therapeutics* **3:** 261-269

Turkson J, Zhang S, Mora LB, Burns A, Sebti S, Jove R (2005) A novel platinum compound inhibits constitutive Stat3 signaling and induces cell cycle arrest and apoptosis of malignant cells. *The Journal of biological chemistry* **280:** 32979-32988

Turkson J, Zhang S, Palmer J, Kay H, Stanko J, Mora LB, Sebti S, Yu H, Jove R (2004b) Inhibition of constitutive signal transducer and activator of transcription 3 activation by novel platinum complexes with potent antitumor activity. *Molecular cancer therapeutics* **3:** 1533-1542

Udy GB, Towers RP, Snell RG, Wilkins RJ, Park SH, Ram PA, Waxman DJ, Davey HW (1997) Requirement of STAT5b for sexual dimorphism of body growth rates and liver gene expression. *Proceedings of the National Academy of Sciences of the United States of America* **94:** 7239-7244

Varghese F, Bukhari AB, Malhotra R, De A (2014) IHC Profiler: an open source plugin for the quantitative evaluation and automated scoring of immunohistochemistry images of human tissue samples. *PloS one* **9:** e96801

Verma N, Keinan O, Selitrennik M, Karn T, Filipits M, Lev S (2015) PYK2 sustains endosomal-derived receptor signalling and enhances epithelial-to-mesenchymal transition. *Nature communications* **6:** 6064

Vigneron A, Gamelin E, Coqueret O (2008) The EGFR-STAT3 oncogenic pathway up-regulates the Eme1 endonuclease to reduce DNA damage after topoisomerase I inhibition. *Cancer research* **68:** 815-825

Vinkemeier U, Cohen SL, Moarefi I, Chait BT, Kuriyan J, Darnell JE, Jr. (1996) DNA binding of in vitro activated Stat1 alpha, Stat1 beta and truncated Stat1: interaction between NH2-terminal domains stabilizes binding of two dimers to tandem DNA sites. *The EMBO journal* **15:** 5616-5626

Wake MS, Watson CJ (2015) STAT3 the oncogene - still eluding therapy? *The FEBS journal* **282:** 2600-2611

Walker SR, Nelson EA, Zou L, Chaudhury M, Signoretti S, Richardson A, Frank DA (2009) Reciprocal effects of STAT5 and STAT3 in breast cancer. *Molecular cancer research : MCR* **7:** 966-976

Wang R, Cherukuri P, Luo J (2005) Activation of Stat3 sequence-specific DNA binding and transcription by p300/CREB-binding protein-mediated acetylation. *The Journal of biological chemistry* **280:** 11528-11534

Weber-Nordt RM, Egen C, Wehinger J, Ludwig W, Gouilleux-Gruart V, Mertelsmann R, Finke J (1996) Constitutive activation of STAT proteins in primary lymphoid and myeloid leukemia cells and in Epstein-Barr virus (EBV)-related lymphoma cell lines. *Blood* **88:** 809-816

Weber A, Hengge UR, Bardenheuer W, Tischoff I, Sommerer F, Markwarth A, Dietz A, Wittekind C, Tannapfel A (2005) SOCS-3 is frequently methylated in head and neck squamous cell carcinoma and its precursor lesions and causes growth inhibition. *Oncogene* **24:** 6699-6708

Wegenka UM, Buschmann J, Lutticken C, Heinrich PC, Horn F (1993) Acute-phase response factor, a nuclear factor binding to acute-phase response elements, is rapidly activated by interleukin-6 at the posttranslational level. *Molecular and cellular biology* **13:** 276-288

Wegrzyn J, Potla R, Chwae YJ, Sepuri NB, Zhang Q, Koeck T, Derecka M, Szczepanek K, Szelag M, Gornicka A, Moh A, Moghaddas S, Chen Q, Bobbili S, Cichy J, Dulak J, Baker DP, Wolfman A, Stuehr D, Hassan MO, Fu XY, Avadhani N, Drake JI, Fawcett P, Lesnefsky EJ, Larner AC (2009) Function of mitochondrial Stat3 in cellular respiration. *Science* **323:** 793-797

Wen Z, Darnell JE, Jr. (1997) Mapping of Stat3 serine phosphorylation to a single residue (727) and evidence that serine phosphorylation has no influence on DNA binding of Stat1 and Stat3. *Nucleic acids research* **25:** 2062-2067

Wen Z, Zhong Z, Darnell JE, Jr. (1995) Maximal activation of transcription by Stat1 and Stat3 requires both tyrosine and serine phosphorylation. *Cell* **82:** 241-250

Widder EA (2010) Bioluminescence in the ocean: origins of biological, chemical, and ecological diversity. *Science* **328:** 704-708

Wormald S, Hilton DJ (2004) Inhibitors of cytokine signal transduction. *The Journal of biological chemistry* **279:** 821-824

Wu M, Song D, Li H, Yang Y, Ma X, Deng S, Ren C, Shu X (2019) Negative regulators of STAT3 signaling pathway in cancers. *Cancer management and research* **11:** 4957-4969

Wu P, Brand L (1994) Resonance energy transfer: methods and applications. *Analytical biochemistry* **218:** 1-13

Wu P, Wu D, Zhao L, Huang L, Shen G, Huang J, Chai Y (2016) Prognostic role of STAT3 in solid tumors: a systematic review and meta-analysis. *Oncotarget* **7:** 19863-19883

Xu Q, Briggs J, Park S, Niu G, Kortylewski M, Zhang S, Gritsko T, Turkson J, Kay H, Semenza GL, Cheng JQ, Jove R, Yu H (2005) Targeting Stat3 blocks both HIF-1 and VEGF expression induced by multiple oncogenic growth signaling pathways. *Oncogene* **24:** 5552-5560

Xu X, Sun YL, Hoey T (1996) Cooperative DNA binding and sequence-selective recognition conferred by the STAT amino-terminal domain. *Science* **273:** 794-797

Xu Y, Piston DW, Johnson CH (1999) A bioluminescence resonance energy transfer (BRET) system: application to interacting circadian clock proteins. *Proceedings of the National Academy of Sciences of the United States of America* **96:** 151-156

Yang J, Huang J, Dasgupta M, Sears N, Miyagi M, Wang B, Chance MR, Chen X, Du Y, Wang Y, An L, Wang Q, Lu T, Zhang X, Wang Z, Stark GR (2010) Reversible methylation of promoter-bound STAT3 by histone-modifying enzymes. *Proceedings of the National Academy of Sciences of the United States of America* **107:** 21499-21504

Yao H, He G, Yan S, Chen C, Song L, Rosol TJ, Deng X (2017) Triple-negative breast cancer: is there a treatment on the horizon? *Oncotarget* **8:** 1913-1924

Yeh YT, Ou-Yang F, Chen IF, Yang SF, Wang YY, Chuang HY, Su JH, Hou MF, Yuan SS (2006) STAT3 ser727 phosphorylation and its association with negative estrogen receptor status in breast infiltrating ductal carcinoma. *International journal of cancer* **118:** 2943-2947

Yu CL, Meyer DJ, Campbell GS, Larner AC, Carter-Su C, Schwartz J, Jove R (1995) Enhanced DNA-binding activity of a Stat3-related protein in cells transformed by the Src oncoprotein. *Science* **269:** 81-83

Yuan ZL, Guan YJ, Chatterjee D, Chin YE (2005) Stat3 dimerization regulated by reversible acetylation of a single lysine residue. *Science* **307:** 269-273

Yue P, Turkson J (2009) Targeting STAT3 in cancer: how successful are we? *Expert opinion on investigational drugs* **18:** 45-56

Yuriev E (2014) Challenges and advances in structure-based virtual screening. *Future medicinal chemistry* **6:** 5-7

Zhang HF, Lai R (2014) STAT3 in Cancer-Friend or Foe? *Cancers* **6:** 1408-1440

Zhang J, Campbell RE, Ting AY, Tsien RY (2002) Creating new fluorescent probes for cell biology. *Nature reviews Molecular cell biology* **3:** 906-918

Zhang Q, Raje V, Yakovlev VA, Yacoub A, Szczepanek K, Meier J, Derecka M, Chen Q, Hu Y, Sisler J, Hamed H, Lesnefsky EJ, Valerie K, Dent P, Larner AC (2013) Mitochondrial localized Stat3 promotes breast cancer growth via phosphorylation of serine 727. *The Journal of biological chemistry* **288:** 31280-31288

Zhang X, Guo A, Yu J, Possemato A, Chen Y, Zheng W, Polakiewicz RD, Kinzler KW, Vogelstein B, Velculescu VE, Wang ZJ (2007) Identification of STAT3 as a substrate of receptor protein tyrosine phosphatase T. *Proceedings of the National Academy of Sciences of the United States of America* **104:** 4060-4064

Zhong Z, Wen Z, Darnell JE, Jr. (1994) Stat3: a STAT family member activated by tyrosine phosphorylation in response to epidermal growth factor and interleukin-6. *Science* **264:** 95-98

Zhou T, Chao L, Rong G, Wang C, Ma R, Wang X (2013) Down-regulation of GRIM-19 is associated with STAT3 overexpression in breast carcinomas. *Human pathology* **44:** 1773-1779

Materials and Methods

1. Reagents

Inhibitors or Growth Factors

Neratinib (#S2150), Losartan (#S1359), Stattic (#S7024) and Fingolimod (#S5002) were purchased from **Selleckchem** (USA). CI-994(#1742), AR-42 (#2716), Chidamide (#2261) and MS-275 (#1590) were from Biovision (USA). Wortmanin (#W1628), Niclosamide (#N3510) and Curcumin (#08511) were from **Sigma** (USA). ERK inhibitor U0126 (#9903) was purchased from **Cell signaling** (USA).

Both EGF (#AF-100-15) and IL6 (#200-06) were procured from **Peprotech** (USA).

Commercially Available Kits Used in the Study

Expose Mouse and Rabbit Specific HRP/DAB Detection IHC Kit (ab80436) from Abcam, iClick EdU AndyFluor647 cell proliferation kit from Genecopia (USA, #A006), RNeasy Mini Kit (74106) for RNA extraction from Qiagen, PureLink Quick Plasmid Miniprep Kit (K210010) from Invitrogen, QIAquick PCR and Gel cleanup kit (28115) from Qiagen and SuerScript III First-strand synthesis system (18080051) from Invitrogen.

Cell Culture Materials

RPMI (31800-02), DMEM (12800-017), Heat inactivated FBS (10082-147), Antibiotic-Antimycotic (15240-062), 0.25% Trypsin-EDTA (25200-072), Lipofectamine 2000 transfection reagent and Zeocin (R25005) all were purchased from Invitrogen (USA). L-15 (Leibovitz) medium (L4386) was from Sigma (USA). Ultrapure water (Resistivity = 18 MΩ cm) obtained from MilliQ water plant (Millipore, Billerica,USA) was autoclaved and further utilised for preparing all solutions, reagents and cell culture medium. Disposable sterile plastic ware tissue culture grade was obtained from **Nunc**. Disposable plastic ware (certified DNase, RNase, and protease-free) was obtained from **Axygen**.

List of antibodies used in the study

Antibody Name	Catalogue Number	Company
Mouse-anti-Total STAT3	9139	Cell Signalling (USA)
Rabbit-anti-pY705 STAT3	9145	Cell Signalling (USA)
Rabbit-anti-pS727 STAT3	E121-31	Abcam (USA)
Rabbit-anti-K685ac STAT3	2523	Cell Signalling (USA)
Mouse-anti-α Tubulin	T9026	Sigma (USA)
Rabbit-anti-Cyclin D1	ab134175	Abcam (USA)
Mouse-anti-Her2	ab8054	Abcam (USA)
Goat-anti-Rabbit Dylight 633	35562	Thermo Fischer (USA)
Goat-anti-Mouse Dylight 633	35512	Thermo Fischer (USA)
Rabbit-anti-Nanoluciferase	Commercially not available (provided as a gift)	Promega (USA)
Mouse-anti-RFP	125244	Abcam (USA)
Mouse-anti human-CD44 APC	559942	BD Biosciences (USA)
Mouse-anti-CD24 (SN3) human-PE	MA1-10154	Invitrogen (USA)
Rabbit-anti-mouse IgG-HRP	ab6728	Abcam (USA)
Goat-anti-rabbit IgG-HRP	31460	Invitrogen (USA)

Chemical Reagents

Poly L-Lysine (P8920), TRIS (T1378), Tween-20 (P9416), BSA (A7030), DAPI (D8417), β -mercaptoethanol (M3148), PIPES (P2949), CaCl2 (C7902), MnCl2 (M8054), MgCl2 (M4880), NaCl (71736), Ampicillin salt (A9518), DEPC (D5758), DMSO (D8418), EDTA, Ethidium bromide (E8751), L-15 (L4386), Para

formaldehyde (P6148), Triton X-100 (T8787), HEPES (H4034), Ponceau stain (P7170), Bradford reagent (B6916), Formamide (F9037), DAB enhanced liquid substrate system (D3939), Sodium citrate (W302600) were from **Sigma.**

Methanol (Merck 106009), Glacial Acetic Acid (Merck 100063), Ethanol (SD fine chemical 58051), Boric acid (Merck 194810), Formaldehyde (CB4F640180), Protease inhibitor cocktail (Merck 535140) and Prism ultra-protein ladder (ab116028) was obtained from **Abcam.**

10X DNA loading dye (10816-015), agarose powder (15510-027, MicroAmp optical 384-well reaction plate with Barcode (4309849) and MicroAmp optical adhesive film kit (4313663) and MTT (M6494) reagent was from **Invitrogen (Applied biosystems).**

Xylene (32297) and Pfu Fusion polymerase (F-530S) and 10mM dNTPs (R0191) were from **Thermo Fischer**. D-luciferin (L8220) for *in vivo* imaging was obtained from **Biosynth International, Switzerland** and Furimazine (N1110) from **Promega corporation.** Vectashield (H1000) was obtained from **Vector laboratories** and both Luria broth and agar were obtained from **HiMedia** (M557 & M575). All restriction enzymes, T4 DNA ligase, Taq DNA polymerase (M0273L), molecular biology buffers and DNA gel ladder were obtained from **NEB**.

Equipment's

Agarose gel casting assembly, Protein gel casting assembly (well comb, thick and thin plates), SDS and agarose gel electrophoresis unit, semi dry trans blot assembly and power pack were purchased from **BioRad**. IVIS Spectrum pre-clinical *in vivo* imaging system and IVIS Lumina were from **Perkin Elmer**. Quant Studio 12K Flex RT PCR machine was from **Applied Biosystems**.

2. Bacterial culture work

For all bacterial culture work DH5α strain of *E. coli* was used and grown in Luria Bertani (LB) medium or agar plate with appropriate antibiotic section marker. LB medium was prepared by dissolving 20g of powdered Luria broth powder (Himedia) in 1000ml of autoclaved double distilled water (ddH_2O) and sterilised by autoclaving. For LB agar

plates, 35g Luria broth powder was dissolved in 1000ml ddH_2O and autoclaved for sterilization. After autoclaving, appropriate antibiotic marker was added to the LB agar broth (37ºC temperature) and poured onto 90mm sterile plastic bacterial plates (Tarsons).

2.1 Preparation of competent cells

Preparation of Super optimal broth (SOB): Super optimal broth consists of following two solutions that are mixed only upon prior to use.

Solution A: For 100ml SOB, 2% Bactotryptone, 0.5% Yeast extract, 10mM NaCl and 2.5mM KCl was dissolved in 100ml sterile autoclaved MilliQ. The SOB was then autoclaved and kept at room temperature for 24hrs for sterility check.

Solution B: For solution B, 10mM $MgCl_2$ and 10mM $MgSO_4$ were weighed and dissolved in autoclaved MilliQ. They were further sterilised by passing through 0.2µ syringe filter.

Just before use solution B was added to solution A.

Transformation Buffer: 10mM PIPES sodium salt, 15mM calcium chloride ($CaCl_2$) and 250mM potassium dichloride (KCl_2) were weighed and dissolved in 50ml autoclaved MilliQ. pH of the solution was adjusted to 6.7 using 5N NaOH and then 55mM $MnCl_2$ was added. The final volume was made upto 100ml and the solution was sterilized by passing through 0.2µ syringe filter. The buffer was stored at -20ºC till further use.

Procedure:

1. Glycerol stock of DH5α *E. coli* strain was streaked onto sterile LB agar plate without antibiotics selection and kept overnight at 37ºC incubator for growth.
2. Next day, single colony from overnight grown DH5α *E. coli* plate was inoculated in 100ml SOB buffer and kept at 18ºC/ 150rpm for 2-3 days till optical density (O.D) reaches to about 0.6.
3. Once the O.D reaches 0.6, the flask with bacterial growth was kept on ice for 20mins. Cells were harvested by centrifugation at 4000rpm/4ºC for 10mins.
4. The pellet was resuspended in 20ml ice cold transformation buffer and incubated in ice for 10mins followed by centrifugation at 4000rpm/4ºC for 10mins. (This step was repeated twice for better efficiency competent cells)

5. The final pellet was resuspended in 1.860ml of transformation buffer and 140µl DMSO (7%) was added to it.
6. Aliquots of 100µl competent cells were made in sterile 1.5ml microfuge tubes and snap frozen using liquid nitrogen (N_2). The cells were stored in -80ºC for further use.

2.2 Bacterial Transformation

1. For transforming plasmid DNA, 100µl competent cells were thawed on ice and 1-4ng of uncut plasmid DNA / 10µl of ligation reaction mix / 10µl of DpnI digested site directed mutagenesis plasmid product was added to the cells.
2. The mixture of cells and plasmid was incubated in ice for 30mins with gentle tapping in between at every 10mins. After this the cells were given heat shock at 42ºC for 90sec and kept for cooling in ice for 5mins.
3. 900µl LB medium was added to the cells and kept for revival at 37ºC/180rpm for 60 mins.
4. The cells were then centrifuged at 2000rpm for 5mins at room temperature and 900µl supernatant was removed. The final pellet was resuspended in 100ul of left over supernatant and plated onto LB agar plate with required selection marker.
5. For growth of the colonies the plates were incubated at 37ºC for 16hours and sealed with parafilm before storing at 4ºC for 1 week.

3. Molecular cloning and Site directed mutagenesis

3.1 Polymerase chain reaction (PCR)

For PCR amplification of STAT3, TurboFP and Nanoluciferase gene following reaction set was used:

Components	**Volume (µl)**
Autoclaved MilliQ	15.5
10X High fidelity buffer (Thermo Fischer)	5
Template DNA (20ng/µl)	1
Forward Primer (100pmol/µl)	1
Reverse Primer (100pmol/µl)	1
dNTP mix ((10mM, Thermo Fischer)	1
Phusion Enzyme	0.5
Total Volume	**25ul**

PCR reaction conditions were as follows:

PCR Steps	Temperature and Time		
	STAT3	**TurboFP635**	**Nanoluc**
Initial denaturation	95ºC – 3min	95ºC – 3min	95ºC – 3min
Denaturation	95ºC – 30sec	95ºC – 30sec	95ºC – 30sec
Primer annealing	54ºC – 25sec	52ºC – 25sec	52ºC – 25sec
Primer extension	72ºC – 2min	72ºC – 1min	72ºC – 1min
Final extension	72ºC – 15min	72ºC – 10min	72ºC – 10min
Hold	4ºC- ∞	4ºC- ∞	4ºC- ∞

3.2 Agarose gel electrophoresis

Procedure

1. Depending upon size of DNA to be resolved, agarose gel (0.6-2%) was prepared by dissolving required amount of agarose powder (Himedia) in 1X TBE buffer (Tris Borate-EDTA buffer) by boiling in microwave. For visualization of DNA 0.5 µg/ml of EtBr dye (10mg/ml Stock) was added to the solubilised agarose.
2. Agarose solution was poured onto the plate, assembled in the agarose gel casting assembly and allowed to solidify.
3. Once the gel is solidified, it was transferred onto DNA agarose gel electrophoresis tank filled with 1XTBE buffer.
4. Samples were prepared in 10X DNA loading dye (Thermo Fischer, USA) that contains glycerol for viscosity and bromophenol blue for tracking DNA movement in the gel.
5. Samples were run along with reference DNA ladder (NEB) at required voltage and time and visualised using UV Gel dock system.

3.3 DNA Gel Extraction

PCR amplified products or restriction enzyme digested DNA ran on agarose gel were excised and purified using QIAquick Gel Extraction Kit (Qiagen). The protocol is as follows:

1. DNA fragment of interest was excised from the agarose gel under UV light using a sterile and clean scalpel.
2. The gel was weighed and 3 volumes of QG buffer was added to one volume of gel (i.e. 100mg gel = 100µl gel volume so 300 µl QG buffer should be added).
3. Reaction was incubated at 50ºC for 10mins or till the gel is completely dissolved. The tube was gently vortexed after every 2-3mins of incubation.
4. Add one volume of isopropanol to the sample and mix by vortexing.
5. Transfer entire solution to QIAquick spin column provided with 2ml collection tube. Incubate the reaction for 5mins at room temperature for binding of DNA to column.
6. Centrifuge the tubes at 13000rpm/1min/RT and discard the flow through.
7. Add 750µl Buffer PE to the column and incubate for 2mins. Centrifuge the tubes at 13000rpm/1min/RT. (Repeat this step 2 times if required to improve the 260/230 ratio)
8. Dry spin the column by centrifugation at 13000rpm/1min/RT.
9. Transfer the column to 1.5ml sterile microfuge tube and add 30-50µl warm autoclaved milliQ. Incubate the column with milliQ for 5-10mins at RT.
10. Centrifuge the sample at 13000rpm/2min/RT. Discard the column and preserve the eluted DNA product at -20ºC

3.4 Restriction Digestion

Restriction enzymes (RE) used are; NheI, SalI, SacI, XhoI, BamHI, EcoRI and BglII (from NEB). Compatible buffers: 1.1, 2.1, 3.1 and cut smart buffer (NEB) were selected based on RE pair.

For digesting the PCR purified product or parent vector for insertion, the restriction enzyme reaction was set up as per requirement. Depending upon single or double digestion the reaction volume can be adjusted and the compatible buffer with maximum activity for the enzyme is always selected. Basic RE digestion reaction is given below. The digestion reaction mix is incubated at 37ºC for overnight.

Components	Volume (µl)
Nuclease free water	32
10X Buffer*	5
DNA (1µg)	1
Enzyme 1	1
Enzyme 2	1
Total Volume	**50**

*Depending upon compatibility of the two enzymes, the buffer is selected

3.5 DNA Ligation

For ligating digested DNA and insert, ligation reaction was set depending upon the concentration of the insert. For all ligation reaction in the study a ratio of 1:3 was followed i.e. one part of DNA and 3 parts of insert in molar quantity. The amount of insert to be taken was calculated from NEB ligation calculator (http://nebiocalculator.neb.com/#!/ligation).

1. Ligation reaction was set up as given in below table. T4DNA ligase buffer was thawed at room temperature and vortexed till all precipitates are dissolved.

Components	Volume (µl)
Nuclease free water	APR
10X T4 DNA ligase buffer	2
Digested vector (ng)	30-50ng
Insert DNA (ng)	As per molar ratio
T4 DNA Ligase	1
Total Volume	**20**

2. Reaction mixture was prepared and mixed by pipetting up and down multiple times or vortex gently. (As a control, in parallel another ligation reaction without insert was also kept)
3. The reaction was incubated at 22ºC for 5hrs (STAT3 insertion) or 16ºC for overnight (TurboFP or Nluc cloning). To stop the reaction, the enzyme was heat inactivated at 65ºC for 5mins. The reaction can be stored at -20ºC or proceed for transformation.

4. For transformation, 10µl ligation mix was added to 100µl thawed competent cells (transformation efficiency 10^7 – 10^8) and transformation was performed as per the protocol mentioned previously.
5. Transformed *E. coli* cells were plated onto LB agar plate with required selection marker and incubated overnight at 37ºC for a maximum of 16hrs.
6. Next day, colonies were inoculated in LB medium and plasmid was extracted using QIAprep Spin Miniprep Kit.
7. Colonies were screened either by PCR or restriction enzyme digestion. Final positive clones were further confirmed by sequencing using automated DNA sequencer (Applied Biosystems- ABI) installed in genomics facility, ACTREC.

3.6 Plasmid DNA extraction

Plasmid DNA was extracted using QIAprep Spin Miniprep Kit (#27106) and steps were followed as per the manufacturer's instructions.

1. 5ml of overnight grown bacterial culture was centrifuges at 3000rpm/5min at room temperature.
2. Bacterial pellet was resuspended in 250µl Buffer P1 and transferred to 1.5ml microcentrifuge tube.
3. Buffer P2 was added to the lysate and it was mixed thoroughly by inverting the tubes 10times. The tubes were incubated in buffer P2 for 5mins at RT.
4. 350µl Buffer P3 was added to lysate and tubes were inverted 5-6times to thoroughly mix the sample. Above mixture was then centrifuged at 14000rpm for 10mins at RT. Supernatant was transferred to QIAprep 2.0 Spin columns and incubated for 5mins at RT.
5. The column was centrifuges at 14000rpm for 1min. Flow through was discarded and 750µl buffer PE was added to the column.
6. The tubes were centrifuged at 14000rpm for 1min. Flow through was discarded and tubes were given a dry spin for additional 1min.
7. The columns were transferred to 1.5ml sterile microfuge tubes and 30µl warm autoclaved milliQ was added.
8. The tubes were incubated for 5mins at RT and centrifuged at 14000rpm for 2min.
9. Eluted DNA was stored at -20ºC till further use.

3.7 Site Directed Mutagenesis

Site directed mutagenesis (SDM) is a classical *in vitro* approach of introducing mutation at a specific site in known DNA sequence. Apart from introducing mutation other DNA alterations like insertion, deletion or substitution can also be performed. SDM is a versatile technique that modifies gene sequence and can be used to study structural and functional property of a protein, interaction of transcription factors to specific promoter sequence or promoter activity.

Primer designing rules:

1. Both the primer pair should contain the desired mutation and should bind to the same DNA sequence on opposite strands.
2. Primers should be approximately 25-30bp in length, with desired nucleotide of change exactly in the middle flanked by equal number of nucleotides from both the sides.
3. Primer should be free of palindromic and repetitive DNA sequences.
4. Forward and reverse primers designed should be complementary to each other.
5. GC content of the primers should be approx. 40% and it should terminate with one or more C or G nucleotides.
6. The Tm of the primers should be equal to or greater than 78ºC and it is calculated by the following formula:

   T m = 81.5 + 0.41(%GC) - 675 / N - % mismatch (where N is the primer length in base pairs)
7. Primer concentration in the PCR reaction should be in excess.

SDM can be done for any double stranded DNA by using the following steps:

DNA template preparation: The plasmid of interest was transformed in *E. coli* bacteria and using plasmid miniprep extraction kit, DNA was isolated from parental *E. coli* cells. The plasmid from *E. coli* cells contain methylated DNA which is sensitive to DpnI enzyme digestion.

PCR amplification:

Temperature cycling in PCR for SDM contains three important steps:

a) **Denaturation:** In this step, the template double stranded DNA is denatured to allow primer bonding

b) **Annealing**: In this step the mutagenic complementary primer pair binds to same DNA sequence on opposite stands

c) **Extension**: pfu turbo DNA polymerase does not displace the newly synthesised daughter DNA strand and stops the extension once parent DNA is copied, is used for extending the SDM primers. As a result, nicked double stranded DNA is formed in each cycle of amplification.

Components	Volume (µl)
Nuclease free water	34.5
5x high fidelity buffer	10
Forward Primer (150ng/µl)	1
Reverse Primer (150ng/µl)	1
dNTPs (10mM)	2
Template DNA (150ng/µl)	1
Pfu Turbo enzyme	0.5
Total Volume	**50**

DpnI digestion

DpnI endonuclease is a highly specific nuclease for methylated and hemi-methylated DNA stands (target sequence- 5'-Gm6ATC-3'). Hence upon treatment of mutagenic PCR product with DpnI enzyme, the parental methylated DNA will be degraded by the DpnI enzyme, leaving the daughter DNA strand with specific mutation intact. Reaction set up for DpnI digestion is as follows:

Components	Volume (µl)
Nuclease free water	2
10X Cut smart buffer (NEB)	2
SDM PCR Product	15
DpnI enzyme	1
Total Volume	**20**

DpnI digestion is performed overnight at 37ºC.

Transformation

After DpnI digestion, the nicked double stranded DNA is transformed in DH5α *E. coli* cells where the nicked DNA is repaired by the bacterial DNA ligase. The colonies obtained after transformation were grown in LB medium and plasmid DNA was extracted. Mutation at desired site was confirmed by sequencing.

4. Mammalian Cell Culture

Cell line maintenance and Sub culturing

Standard aseptic practice was followed for performing cell culture. All the adherent cell lines were maintained and sub-cultured in their respective media supplemented with 10% FBS, 100U/ml penicillin and 10µg/ml streptomycin solutions.

Sub culturing of Cells

1. Old medium was aspirated out of the culture plate using sterile glass pipette.
2. The cells were given two gentle washes with 1XPBS buffer.
3. 1ml trypsin-EDTA solution was added to the plate drop by drop from the top to cover the entire surface and the plates were kept in 37ºC incubator for 1-2mins.
4. Activity of trypsin was neutralized by adding 2ml complete medium (1 part of trypsin: 2 parts of medium).
5. Cells were collected by flushing the medium throughout the surface of the plate and transferred to 15ml tube followed by centrifugation at 1000rpm for 5mins at 4ºC.
6. Supernatant was discarded and pellet was resuspended in 1ml 1XPBS buffer and again centrifuged at 1000rpm for 5mins at 4ºC.
7. Final cell pellet was resuspended in 1ml complete medium. A portion of cell suspension was reseeded in new culture plate with fresh complete medium and the rest was discarded.

Cryopreservation

1. Adherent cells were trypsinized and collected in 15ml tube.
2. Cells were washed twice, once with complete medium and once with 1XPBS by centrifugation at 1000rpm for 5mins at 4ºC.
3. Final pellet containing 1-2X10^6 cells was resuspended well in 1ml freezing medium (950µl FBS and 50µl DMSO).
4. Vials were kept in freezing container filled with isopropanol and transferred to -80ºC.

5. The vials were transferred to liq N_2 next day for long term storage of the cells.

Revival of Cryopreserved vials

1. Vial removed from liquid N_2 was immediately transferred to water bath set at 37ºC.
2. Thawed cells were resuspended in 1ml complete medium and centrifuged at 1000rpm/5mins at 4ºC.
3. Supernatant was removed and cell were again resuspended in 1XPBS and centrifuged at 1000rpm/5mins at 4ºC.
4. Final pellet was resuspended in suitable culture medium and plated in 35 or 60mm dish containing complete medium with FBS and pen strep.
5. Cells were allowed to recover and revive at 37ºC incubator with 5% CO_2 supply for overnight.
6. Next day, Cell revival was confirmed by visualizing under the light microscope.

5. Transfection of mammalian cell lines

Transfection

All mammalian cell transfections performed in the study were done using Lipofectamine 2000 transfection reagent (Invitrogen). For transfection following steps were followed:

1. One day before transfection, cells were counted and seeded at an appropriate density as recommended by the manufacturer for respective plate format.
2. On day of transfection, the cells should be around 70% confluent for good efficiency.
3. In one tube lipofectamine was added to serum negative medium and in another tube DNA and serum negative medium mixture was prepared. Both the samples were incubated for 5mins at RT. [volume of medium, amount of DNA and volume of lipofectamine reagent was chosen based on manufacturer's instructions and plate format]
4. After 5mins, lipofectamine mix was added to DNA samples. The tubes were vortexed and incubated for another 20mins at RT.
5. In the meanwhile, the cells were washed with 1XPBS and supplemented with fresh complete medium.
6. After 20mins incubation is over, the transfection mix was added to respective plates form the top and the plates were gently stirred to allow mixing.
7. Cells were incubated with the transfection cocktail for 6hrs at 37ºC and 5% CO_2.

8. After 6hrs, the medium was replaced and cells were kept at 37ºC and 5% CO_2 till further use.

6. Cell survival assay

Clonogenic Assay

1. After treating the cells with either Stattic or Niclosamide, the cells were trypsinized and collected in 1.5ml sterile microcentrifuge tube.
2. Cells were washed with 1XPBS and counted in haemocytometer.
3. 1000 cells per well in 6-well plate were seeded for both treatment and control set in duplicates.
4. Cells were kept in incubator at 37ºC with 5% CO_2 for next 14days to allow colony formation from single cells
5. After every two or three days the old medium was replenished with fresh medium.
6. On 14^{th} day post seeding, the medium was removed and cells were washed twice with 1XPBS.
7. Colonies were fixed with chilled methanol for 10mins at 4ºC without agitation.
8. Methanol was removed and 0.5% crystal violet dye prepared in 25% methanol was added to the cells. The incubation was done for 5mins at room temperature.
9. After 5mins, crystal violet dye was removed and excess stain was removed by washing thoroughly with tap water.
10. Plates were allowed to air dry overnight at room temperature.
11. Next day number of colonies from each well (a bunch of atleast 50cells was counted as a single colony) was counted using high magnification lenses and percent surviving fraction was determined with respect to untreated controls.

7. Real Time PCR of quantitative gene expression

RNA Extraction

For extracting RNA from cells RNeasy mini kit (Qiagen) was used. The protocol is as follows:

1. 70-80% confluent monolayer cells were trypsinized and collected in 1.5ml sterile microcentrifuge tubes.
2. Cells were given two washed with 1XPBS at 1000rpm for 5mins at 4ºC.
3. Cell pellet was dissolved in 350µl RLT buffer by pipetting up and down.

4. Using hand homogenizer, the cells were homogenised continuously for 30sec.
5. 350µl, 70% alcohol prepared in DEPEC water was added to homogenised cells and mixed well.
6. Entire solution was loaded onto RNeasy spin column mounted over 2ml collection tube and allowed to bind for 5mins.
7. The column was centrifuged at 13000rpm for 30secs at RT and flow through was discarded.
8. 700µl RW1 buffer was added to the spin column and centrifuged at 13000rpm for 30secs at RT. Flow through was discarded.
9. 500µl RPE buffer was added to the columns and centrifuged at 13000rpm for 30secs at RT. Flow through was again discarded. This step was repeated twice.
10. The column was given a dry spin for 2mins at 13000rpm.
11. The column was placed on fresh 1.5ml sterile microcentrifuge tubes and 30µl RNAse free water added to the column. It was incubated for 10mins at RT.
12. Final elution was done by centrifugation at 13000rpm for 1min. RNA collected was immediately transferred to ice bucket.
13. RNA yield was determined using nanodrop quantification.

RNA quality check

Before cDNA preparation, the quality of RNA isolated was determined by running in denaturing agarose gel.

1% denaturing agarose gel: 0.6g agarose was weighed and dissolved in 42.5ml DEPEC water by boiling in microwave oven. The solution was allowed to cool down and 5ml of 10X MOPS buffer, 2.5ml of HCHO and 2.5µl EtBr was added to it. The solution was mixed well and poured in gel casting tray followed by insertion of comb. The gel was allowed to solidify for some time.

RNA electrophoresis

1. 1% denaturing agarose gel was placed in gel tank and the tank was filled with RNA tank buffer (10X MOPS 30ml, HCHO – 30ml and DEPEC water upto 300ml).
2. Sample preparation: 2µg RNA was loaded in each well. The sample was prepared as given in below table.

Components	Volume (µl)
10X MOPS	2
Formamide	3
HCHO	1
10X gel loading dye	1
RNA	2µg
RNAse free water	APR (total volume =10µl)

3. RNA sample were heated at 65ºC for 10mins and loaded onto 1% denaturing agarose gel. The gel was run at 80V for 45mins.
4. RNA bands were visualised in UV light using UV-gel doc system.

cDNA Synthesis

For cDNA synthesis, superscript III first strand synthesis system (Invitrogen) was used. The protocol is as follows:

1. The components of the kit were thawed in ice.
2. For cDNA synthesis two reaction tubes were prepared separately; A and B.
3. For tube A preparation following components were mixed in 0.6ml microcentrifuge tube:

Components	Volume (µl)
RNA (2µg)	APR
Oligo DT Primers	1
Random Hexamers	0.5
dNTPs (10mM)	1
DEPEC Water	APR
Total Volume	**10**

4. After mixing the components in tube A, it was heated in heat block at 65ºC for 5mins followed by incubation in ice.
5. For preparation of tube B, following components were mixed together in PCR tube:

Components	Volume (µl)
10X RT Buffer	2
25mM $MgCl_2$	4
DTT	2
RNAse Out	1
Super Script III enzyme	1
Total Volume	**10**

6. Solution from tube A (10µl) was added to solution in Tube B (10µl) and mixed well.
7. For cDNA synthesis, the tubes were place in PCR machine and following protocol was run.

Temperature (ºC)	Time (mins)
25	10
50	50
85	5

8. Once the cDNA synthesis cycle is complete, 1µl RNAse H was added to 20µl reaction and the tubes were incubated at 37ºC for 20mins.
9. The cDNA prepared was kept in ice.

Real Time PCR

1. For real time PCR, primer stock of 5pmol/µl was prepared for both forward and reverse primers.
2. Working solution of 20ng/µl cDNA was prepared from the main stock.
3. For Sybr green based real time PCR, following reaction mixture was prepared:

Component	Volume (µl)
SYBR Green (2X)	15
cDNA (20ng/ µl)	3
Forward Primer (5pmol/µl)	1.5
Reverse Primer (5pmol/µl)	1.5
RNAse free Water	9

4. The tube was mixed well and centrifuged.
5. The reaction was divided into three replicates and the plate was sealed. To avoid any air bubble the plate was tapped from the bottom and centrifuged.
6. PCR reaction was run in ABI Prism 7500 Quantstudio 12.0 software with following conditions:

PCR Step	Temperature (ºC)	Time
Initial denaturation	95	10mins
Denaturation	95	15sec
Primer annealing	60	30sec
Primer extension	72	30sec
Final extension	72	5min
Hold	72	5min

7. After the run is complete the reaction is analysed and Ct values are obtained.
8. Relative expression is derived by comparing the Ct values normalised with GAPDH expression as control for the same sample.

8. Immunoblotting

Preparation of cell lysate

1. Cells were harvested from 6-well plate by trypsinization and collected in a 1.5ml microcentrifuge tube. (For all the subsequent steps, samples were always kept in ice)
2. Cells were washed twice with 1XPBS.
3. The final pellet of the cells was resuspended in 50-60µl lysis buffer [10mM Tris-Cl pH 7.4, 0.27M Sucrose,1mM EDTA,1mM EGTA,1%TritonX100,1mM PMSF,100mM Sodium fluoride, 100mM Sodium orthovanadate and 10ul protease inhibitor cocktail (for 1ml lysis buffer)]
4. Cells were disrupted by sonication at 10% amplitude with 10sec On/Off cycle for three times.
5. Cell lysate was centrifuges at 14000rpm for 30mins at 4ºC.
6. Supernatant was transferred to fresh tube and protein estimation was done.

Protein Estimation

Protein estimation was done using Bradford's reagent (Sigma, USA).

Standard curve for BSA

For standard curve of BSA 1mg/ml working stock solution of BSA was prepared in autoclaved MilliQ and kept on ice. In 1.5ml sterile microcentrifuge tubes first MilliQ was added followed by addition of required amount of BSA. In the end, to all the tubes Bradford dye was added. Following concentrations were taken for standard curve:

BSA Amount (µg/µl)	Autoclaved MilliQ (µl)	BSA Volume (µl)	Bradford Dye (ml)
0	100	0	1
5	95	95	1
10	90	10	1
15	85	15	1
20	80	20	1
Unknown	98	2	1

The samples were incubated in dark for 5mins. The absorbance was taken at 595nm wavelength after blank subtraction. Based on absorbance value, linear regression graph was plotted to determine the equation of the line. From the equation of the line for standard curve, concentration of unknown sample was determined.

Sample preparation

1. For STAT3 and its PTM forms, generally 60-70µg protein was loaded.
2. Based on concentration, required protein amount was taken in 0.6ml microcentrifuge tube and 5X protein loading dye (containing 50% glycerol, 0.02% βME, 10% SDS, 250mM Tris-HCl and 0.5% bromophenol blue dye) was added. The final volume was adjusted for each sample using autoclaved MilliQ. However, the loading volume was never exceeded beyond 25µl, to avoid overflowing of the sample to next well.
3. The samples were boiled at 95ºC for 5mins and centrifuged at 2000rpm for 2mins at RT.

SDS-PAGE Gel electrophoresis

Depending upon the molecular weight of the target protein, the percentage of SDS-PAGE gel was selected. For STAT3 protein 7.5% SDS-PAGE gel always used.

1. The glass plates were washed and wiped with 70% alcohol before setting up in the gel casting assembly.

2. Resolving gel solution for 7.5% density was prepared and poured into the glass plates in casting assembly upto the required length. The top of the resolving gel was covered with layer of water to prevent drying of the gel during polymerization.
3. Once resolving layer is polymerised, 4% stacking gel solution was added on top and 10-well set comb was inserted.

Recipe for 7.5% Resolving Gel

Reagent	Volume
Autoclaved MilliQ	3.662ml
30% Acrylamide	1.9ml
1.5M Tris pH8.8	1.9ml
10% SDS	75µl
10% APS	100µl
TEMED	10 µl

Recipe for 4% Stacking Gel

Reagent	Volume
Autoclaved MilliQ	1.82ml
30% Acrylamide	0.4ml
1.5M Tris pH6.8	0.75ml
10% SDS	30µl
10% APS	15µl
TEMED	2µl

4. Once stacking gel is ready, the glass plates were replaced in the electrode clamp and set inside the SDS- PAGE gel running tank filled with 1X SDS running buffer.
5. Samples were loaded in respective wells along with a pre-stained protein ladder for determination of molecular size.
6. Gel electrophoresis was performed at 80V for 45mins. Once the samples entered the resolving gel, the voltage was increased upto 100V and the run was allowed to proceed till dye front is removed.

Semidry Protein Transfer

1. 1X transfer buffer containing methanol was prepared at kept at 0ºC for cooling.

2. Once electrophoresis is over, gel, fibre pads and nitrocellulose membrane were soaked in chilled transfer buffer for 5mins (for regeneration of the membrane).
3. In the semidry trans blot, on the base of the assembly, first one fibre pad was placed followed by nitrocellulose membrane. On top of the nitrocellulose membrane gel was laid and covered with another layer of fibre pad. The air bubbles were removed by uniformly pressing the sandwich of blot and membrane.
4. For semidry transfer, the run was performed at 15V for 1hr at room temperature.

Immunodetection

1. Once the semidry transfer is over, the blot was incubated with ponceau stain to determine the protein transfer.
2. The blot was washed thrice with 1XTBST for 5mins each till all the ponceau stain is removed.
3. Blocking was done using 5% milk in 1XTBST for 1hr at room temperature under constant agitation (100rpm)
4. After blocking, blots were incubated with primary antibody at 4ºC for overnight with constant agitation. [Ms-anti-STAT3 1:1000 (5% milk in 1XTBST), Rb-anti-pY705 STAT3 1:500, Rb-anti-pS727 STAT3 1:500 and Rb-anti-K685ac 1:500 prepared 5%BSA in 1XTBST]
5. Next day, the blots were washed trice with 1XTBST for 10mins each with vigorous shaking.
6. Secondary antibody incubation was given for 1hr at room temperature with constant agitation. [anti-Ms HRP in 5% milk and anti-Rb-HRP in 5% BSA prepared in 1XTBST]
7. Blots were again washed trice with 1XTBST for 10mins each with vigorous shaking.
8. Blots were developed in Biorad Chemidoc system using ECL substarte.

Stripping and Re-probing of Blot

1. For reprobing, the bots were washed trice with 1XTBST for 5mins each.
2. Blots were incubated in stripping buffer [3.125ml of Tris pH6.8, 10ml of 10% SDS, 50µl βME and volume made upto 25ml] at 55ºC for 30mins with slow stirring.
3. Following incubation, blots were again washed thrice with 1XTBST for 10mins each or till the βME smell is gone (whichever is earlier).

4. Blocking was done again either with 5% BSA or milk depending upon the protein of interest, for 1hr at room temperature.
5. Blots were reincubated with primary antibody of interest for overnight at 4ºC.
6. Re probing was done as mentioned above.

9. Co-Immunoprecipitation

Sample preparation

1. Cells expressing the Nluc-STAT3 and TuboFP-STAT3 constructs were harvested (from 60mm dish0 and collected in 1.5ml microcentrifuge tube.
2. Cells were washed once with 1XPBS at 1000rpm for 5mins at 4ºC.
3. Cell pellet was resuspended in 250µl ECS lysis buffer [50mM Tris-Cl pH 8.0, 125mM NaCl, 0.5% NP40, 5mM EDTA, 2mM EGTA, 100mM NaF, 100mM Na_3VO_4, 10µl/ml protease inhibitor and 2□l/ 1ml PMSF] and sheared using 26G syringe needle till the sample is clear.
4. Cell lysate was then centrifuging at 14000rpm for 30mins at 4ºC and supernatant was collected in another 1.5ml sterile microcentrifuge tube. The sample was kept in ice.
5. Protein estimation for all the samples were done using Bradford reagent as mentioned previously.

Preparation of Beads

1. Protein G-Sepharose beads were equilibrated by washing with NETN buffer [20mM Tris-Cl pH 8.0, 100mM NaCl, 0.1% NP40 and 1mM EDTA] thrice at 500rpm for 5mins /4ºC.
2. For blocking, the beads were resuspended in 1ml 5% BSA prepared in NETN buffer and kept on rotor at 13rpm for 3-4hrs at 4ºC.
3. Following blocking, the beads were washed thrice with NETN buffer at 500rpm for 5mins/4ºC.
4. Final beads slurry was resuspended in 1:1ratio with NETN buffer.

Binding and Immunoblotting

1. For binding 1µg protein cell lysate was taken in 1.5ml microcentrifuge tube and 1 µg anti-RFP antibody was added. 20µl bead was taken from 1:1 diluted slurry and volume of the reaction was made upto 1ml with NETN buffer.
2. Binding was performed overnight at 13rpm and 4ºC.

3. Next day, the sample was centrifuged at 1000rpm for 5mins at 4ºC and supernatant was collected (unbound fraction).
4. The beads were washed twice with NETN buffer for 5mins at 4ºC. Supernatant collected in each wash and stored.
5. Final beads were resuspended in 5X protein loading dye and boiled at 95ºC for 5mins. 10% input for each set was also prepared in parallel using 5X protein loading dye.
6. The samples were loaded onto 7.5% SDS PAGE gel. For loading the tip of the microtip was cut using scissor to allow aspiration of beads by the pipette.
7. SDS PAGE electrophoresis and immunodetection was performed as mentioned above.

10. Immunofluorescence

Cells were seeded on a coverslip at an appropriate density of 60-70% confluency and kept overnight at 37ºC with 5% CO_2. For immunofluorescence of STAT3 and its PTM forms following protocol was followed;

1. Medium from the cells were removed and cells were washed with 1X PBS three times for 5mins each.
2. Cells were fixed with 4% PFA for 20mins at 37ºC. [2g Paraformaldehyde powder was weighed and added in 50ml 1XPBS. For solubilization PFA solution was kept on magnetic heat block with constant stirring On. Once the solution becomes clear, heating was switched off and solution was allowed to cool till it reaches 37ºC]
3. PFA was removed and cells were permeabilised with 0.2% tritonX100 in 4% PFA for 10mins at RT.
4. Cells were washed thrice with 1XPBS for 5mins each at RT.
5. Blocking was done with 5% BSA in 1XPBS for 1hr at RT.
6. Cells were incubated with primary antibody [Total STAT, pS727 STAT3-1:100 and pY705 STAT3, K685ac STAT3 1:50 in 1XPBS] overnight at 4ºC in a humidified chamber.
7. Next day, cells were washed thrice with 1XPBS for 5mins each at RT.
8. Secondary antibody [goat anti-mouse dylight 633 and goat anti-rabbit dylight 633; 1:100 in 1XPBS] incubation was given for 1hr at room temperature in dark.
9. Cells were washed thrice with 1XPBS for 10mins each at RT.
10. Nucleus of the cells was stained with DAPI [1:200 dilution of 1mg/ml stock] and cells were washed thrice with 1XPBS for 5mins each at RT.

11. Coverslips were mounted on glass slides using Vecta Shield solution and corner of the coverslips were sealed with transparent nail paint.
12. Acquisition was done in LSM870 confocal microscope with 460nm filter for DAPI and 633nm filter for Dylight 633.

11. Immunohistochemistry

For immunohistochemistry of STAT3 protein in TNBC patient tissue samples following steps were followed:

1. 5µm thin tissue section was excised from FFPE (formalin fixed and paraffin embedded) tumour tissue blocks and taken on a poly-lysine coated glass slide.
2. Slides containing the tumor tissue section was kept overnight at 60ºC.
3. Next day, tumor tissue sections were deparaffinised by three sequential washes in xylene for 10mins each at room temperature.
4. Sections were then air dried to evaporate the xylene. The sections were then rehydrated by gradient washes in alcohol – 100%, 90% and 75% for 10mins each.
5. Slides were washed under running tap water for 15mins.
6. Sections were dipped in 1XTBS buffer for 10mins.
7. Endogenous peroxidase activity was blocked by incubating the sections with H_2O_2 solution provided with the IHC kit (#ab80436 Mouse and Rabbit specific HRP/DAB detection kit) for 10min at RT in dark.
8. The sections were washed twice in 1X TBST buffer for 5mins each.
9. **Antigen retrieval**: for retrieving the masked antigen, slides were dipped in 10mM Sodium citrate buffer and heated in microwave with following voltage; 800mW (mega Watts), 640mW and 480mW for 2mins each. Slides were allowed to cool till the room temperature.
10. The sections were washed thrice in 1X TBST buffer for 5mins each.
11. Add protein block to the section and incubate for 10mins at RT.
12. Remove protein block by tapping the slides and add primary antibody [Total STAT3, pS727 STAT3 1:100 and pY075, K685ac STAT3 1:50] in 1XTBS to the tissue sections. Incubate overnight at 4ºC in humidified chamber.
13. Next day, the sections were washed thrice in 1X TBST buffer for 5mins each.
14. If primary antibody used was anti-mouse, then mouse compliment was added to these sections and incubated for 10mins at RT. [since secondary antibody is only anti-rabbit

HRP, addition of compliment is important for mouse antibodies, else secondary antibody will not bind to these sections]

15. The sections were washed twice in 1X TBST buffer for 5mins each.
16. Goat-anti-rabbit HRP secondary antibody was applied to all the samples and incubated for 15mins at RT.
17. The sections were washed thrice in 1X TBST buffer for 5mins each.
18. DAB stain was prepared by mixing 20µl DAB chromogen with 980µl DAB diluent and mixed well. DAB stain was added to each section and incubated till brown stain appears.
19. The sections were washed thrice in 1X TBST buffer for 5mins each and kept in distilled water.
20. The sections were again dehydrated with gradient of alcohol and xylene.
21. Sections were counterstained for haematoxylin stain and mounted with DPX solution.
22. The sections were visualised and images were acquired in upright microscope (Carl Zeiss).

12.Live cell luciferase assay

a) For live cell luciferase assay, luciferase labelled cells either nanoluc or Fluc2, were counted and seeded in 96 black well plate with clear bottom in two different cell numbers.
b) Next day, 50µl luciferase substrate [1:1000 furimazine or 1:100 D-luciferin] was added to respective well.
c) Acquisition was done in IVIS spectrum, using open filter settings to collect the total light output. With subject height was 0.50cm and FOV as C, signal was acquired after every one min to capture the peak activity of respective luciferase enzyme.
d) For analysis, image with peak luciferase signal was taken. ROI was drawn on individual well and signal in terms of average radiance was determined.

13.Bioluminescence Resonance Energy Transfer Assay (BRET)

Bioluminescence resonance energy transfer (BRET) is a versatile approach of detecting protein-protein interactions directly from live cells. Following steps were followed for performing BRET assay with Phospho STAT3 BRET sensor:

1. **Preparation of BRET constructs**: gene of interest i.e. STAT3 was fused to either donor-Nanoluciferase or acceptor-TurboFP keeping a spatial separation of 12 a.a. and cloned in two separate vectors driven by CMV promoter. (Fusion can be generated in different orientations to select the best dipole alignment confirmation)
2. **Transfection and Treatment**
   a) For transfection cells were seeded at an appropriate density to achieve 70-80% confluency on day of transfection.
   b) Nluc-STAT3 and TurboFP-STAT3 plasmids were transfected in 1:1 ratio in one well (donor + acceptor) and in another well only Nluc-STAT3 was transfected (donor alone) using lipofectamine transfection reagent.
   c) 30hrs post transfection, cells were counted and reseeded in 96-black well plate (in triplicates) in serum negative medium and kept in 37ºC incubator with 5%CO_2.
   d) **Treatment:** 24hrs post serum starvation, cells were treated with either STAT3 inhibitors at different concentration or with receptor blocking antibody for required amount of time. The treatment is given in both donors alone and donor + acceptor transfected cells for all the concentrations and one set was left as untreated control.
   e) After treatment is over, cells were stimulated either with or without ligand (EGF or IL 10-100ng/ml prepared in serum negative medium) followed by addition of 50µl furimazine substrate (1:1000 diluted in serum negative medium).

3. **Acquisition**

   Acquisition was performed in IVIS spectrum pre-clinical *in vivo* imaging system. For donor signal 500nm filter and for acceptor 640nm filter sets were used with integration time of 30sec per filter. Subject height was set as 0.50cm (standard for plate imaging) and FOV (field of view) used was C, to capture the entire plate image. Binning was set as medium for all acquisition. Immediately after ligand and substrate addition, acquisition was performed for 60mins at an interval of every 5mins.

4. **Analysis**

   All imaging analysis were done on IVIS living imaging software 4.5. For calculating BRET ratio following steps were followed;

   a) Acquisition file was opened in IVIS software and scan for individual time point was loaded in the software.

b) For any particular time-point, an ROI of same size was drawn on all the wells in donor channel and then copied and pasted for the same sample in acceptor channel.
c) Signal in terms of average radiance is selected and the file is copied in MS excel.
d) Background correction is performed by subtracting signal from wells with untransfected cells.
e) BRET ratio is determined by dividing avg. radiance value for any sample in 640nm filter, by reading of the same sample in 500nm filter set (A640nm/D500nm). In this way A/D ratio was determined for both donor alone and donor + acceptor cells.
f) For corrected ratio determination or bleed through subtraction, A/D ratio of donor alone cells was subtracted from A/D ratio of donor + acceptor cells.

14. *In vivo* bioluminescence imaging

Preparation of cells

Luciferase expressing cells were grown and maintained in sterile culture conditions. The cells were amplified in T75 sterile culture flask at required number depending upon the no. of animals to be implanted. Prior to implanting, the luciferase activity of the cells was confirmed by live cell luciferase assay in 96 black well plate. For implanting in animal, the cells were grown at a confluency not exceeding 70-80% to ensure that maximum cell population is in log phase.

Impanation of cells

1. 70-80% confluent culture flasks were trypsinized and cells were harvested.
2. Cells were washed with 1XPBS to remove any traces of medium or trypsin.
3. Cells were counted using trypan blue dye to determine live cell count.
4. For breast cancer orthotopic tumor xenograft model, $5X10^6$ were required to be implanted at the mammary fat pad. Hence the final cell pellet was resuspended in 1XPBS buffer such that each 50µl volume corresponds to a total of $5X10^6$ cell.
5. For breast tumour xenograft development, 6-8 weeks old immunocompromised female NOD/SCID mice were taken. All animal experiments were done as per the standard guidelines for small animal handling and care, outlined by the Institutional

Animal Ethics Committee (IAEC). For all animal study protocols, approval was obtained from the IAEC committee.

Preparation of D-luciferin injection

1. 30mg D-luciferin was weighed and dissolved in 1ml sterile 1XPBS. D-luciferin solution is always freshly prepared.
2. 100µl D-luciferin from 30mg/ml stock (3mg/mice) was injected per mice via intraperitoneal route.
3. The substrate was allowed to distribute throughout the body of the mice for 5-10mins.

Animal anaesthesia

1. Mice were placed inside clear plexiglass anaesthesia chamber and monitored continuously during isoflurane release in the cabinet.
2. 2-3% gaseous isoflurane mixed with 5% O_2 was slowly released into the chamber to anaesthetised the mice.
3. The tube that supplies isoflurane is divided in two parts; one opens at the glass cabinet kept outside and the other end supplies isoflurane inside the IVIS imaging system.
4. After the mice were anaesthetised, they were transferred to the imaging chamber with their snout placed inside the nose cone that continuously supplies isoflurane during the acquisition.

Image Acquisition and Analysis

1. All in vivo imaging acquisition was performed in IVIS spectrum preclinical *in vivo* imaging system. The machine was calibrated and initialised as per the standard manufacturer's instructions.

2. The animal placed inside the imaging chamber is positioned such that the site from where signal is to be detected is facing towards the detector. This significantly minimises the path length for luminescent signal to travel through different organs before it reaches the detector and improves the signal strength.

3. In the software, for animal imaging following parameters are set; subject height= 1.5cm, FOV (field of view) = C (might vary depending upon the number of animals

and location of the signal), binning= medium (could be adjusted to increase sensitivity) and integration time = 5-10sec or auto if not known.

4. Image was acquired by pressing the "acquire image" button in the software. During acquisition, the machine switches off the light in the chamber to take luminescence signal image, after that the light is switched On and the photographic image of the mice is acquired. The final output file is a merged image of luminescence signal on mouse photographic image. The luminescence signal is represented in pseudo colour with scale bar indicating the minimum and maximum signal intensity.
5. For luminescence signal, sequential acquisition is performed with a delay time of 1min as long as the luminescent signal is increasing to capture the peak activity of the luciferase enzyme.
6. For data analysis, ROI was drawn on the site of luminescence signal and average radiance value was determined. For background correction, average radiance signal was taken from other site of the mice body without luminescence signal by copying the same ROI. Background value can be subtracted from the luminescent signal to give true signal strength.

List of Primers used in the study

Primer Name	Primer Sequence
SDM Primers	
Fwd STAT3 K685R mutant	5' GCATTCGGAAGGTATTGTCGGCCA
Rev STAT3 K685R mutant	5'TGGCCGACAATACCTTCCGAATGC
Fwd STAT3 S727A mutant	5’ ACCTGCCGATGGCCCCCCGCA
Rev STAT3 S727A mutant	5’TGCGGGGGGcCATCGGCAGGT
Fwd STAT3 Y705F mutant	5’AGCGCTGCCCCATTCCTGAAGACC
Rev Stat3 Y705F mutant	5’GGTCTTCAGGAATGGGGCAGCGCT
Fwd STAT3 K679R mutant	5’ CTGACATTCCCAGGGAGGAGGCATT
Rev STAT3 K679R mutant	5’ AATGCCTCCTCCCTGGGAATGTCAG
Fwd STAT3 K707R+K709R mutant	5’CATACCTGAgGACCAgGTTTATCTG
Rev STAT3 K707R+K709R mutant	5’CAGATA AACCTGGTCCTCAGGTATG
Real Time PCR Primers	
Fwd STAT3	5' GGAGGAGTTGCAGCAAAAAG
Rev STAT3	5’ TGTGTTTGTGCCCAGAATGT
Fwd SOCS3	5'ACCCTCCGCGCTCAGCCTTT
Rev SOCS3	5'AGCGGAGCAGGGAGTCCAAGT
Fwd TWIST1	5' GGCCGGAGACCTAGATG
Rev TWIST1	5' ACGGGCCTGTCTCGCTTTCT
Fwd Cyclin D1	5'TATTGCGCTGCTACCGTTGA
Rev Cyclin D1	5'CCAATAGCAGCAAACAATGTGAAA
Fwd Oct4	5'GTGGAGAGCAACTCCGATG
Rev Oct4	5'TGCAGAGCTTTGATGTCCTG
Fwd Sox2	5'AACCCCAAGATGCACAACTC
Rev Sox2	5'GCTTAGCCTCGTCGATGAAC
Fwd GAPDH	5' TGCACCACCAACTGCTTAGC
Rev GAPDH	5'GGCATGGACTGTGGTCATGAG

Buffers Recipe

10X Phosphate Buffered Saline (PBS) (pH 7.4)

80g NaCl,
2g KCl,
14.4g Na2HPO4,
2.4g KH2PO4
Dissolve in 800ml autoclaved MilliQ. Adjust pH to 7.4. Make volume upto 1000ml and autoclave. Store at 4ºC

10 X SDS Running buffer pH 8.3

Tris base 15.15 g,
Glycine 72 g,
SDS 5 g,
Dissolve the components and make volume upto 500 ml. Store at 4ºC

10X Transfer buffer

Tris base 36.3 g
Glycine 144 g
SDS 3.7 g
Dissolve the components and make final volume upto 1000 ml. Store at 4ºC. For freshly prepared 1X transfer buffer add 20% methanol before use.

1.5M Tris-Cl pH8.8

90.75g Tris base
8ml conc. HCl
300ml MilliQ
Adjust pH to 8.8 with conc. HCl and make final volume upto 500ml with double distilled water. Store at 4ºC.

1.0M Tris-Cl pH 6.8

60.54g Tris base
36ml conc. HCl
300ml MilliQ
Adjust pH to 6.8 with conc. HCl and make final volume upto 500ml with double distilled water. Store at 4ºC.

50X TBE: For Agarose gel electrophoresis.

108g Tris base
55g Boric acid
Dissolve in 900ml double distilled water. Add 9.3g Na2EDTA and allow to dissolve. Make final volume upto 1000ml and store at RT.

Am J Nucl Med Mol Imaging 2019;9(6):321-334
www.ajnmmi.us /ISSN:2160-8407/ajnmmi0104822

Original Article

Dynamic monitoring of STAT3 activation in live cells using a novel STAT3 Phospho-BRET sensor

Shalini Dimri[1,2], Rohit Arora[1], Akshi Jasani[1], Abhijit De[1,2]

[1]*Molecular Functional Imaging Lab, Advanced Centre for Treatment, Research and Education in Cancer, Tata Memorial Centre, Navi Mumbai, India;* [2]*Department of Life Sciences, Homi Bhabha National Institute, Mumbai, India*

Received November 12, 2019; Accepted December 11, 2019; Epub December 15, 2019; Published December 30, 2019

Abstract: Phosphorylation (pY705) mediated homodimerization is a rate-limiting step controlling STAT3 key oncogenic functions making it an attractive target for drug discovery. Hence, this study reports development of a sensitive and versatile STAT3 Phospho-BRET biosensor platform technology to monitor activation dynamics of STAT3 signalling directly from live cells. Categorically, we first demonstrate that NanoLuc donor and TurboFP635 acceptor serves as an excellent BRET system over other tested fluorophores like mOrange and TagRFP, both for live cells as well as *in vivo* optical imaging of protein-protein interactions. Based on initial multi-parametric optimizations, our Phospho-BRET sensor developed by fusing STAT3 with NanoLuc and TurboFP at the C-terminus, successfully captured the activation kinetics of STAT3 in response to different ligands (e.g. IL6 & EGF) and across multiple cancer cell types either with or without the endogenous STAT3 pool. Perturbation in EGF-mediated STAT3 BRET activation signal upon blocking with EGFR neutralizing antibody further confirms the specificity of the sensor to judge ligand-receptor pathway dependent STAT3 activation. Finally, we determine the high-throughput compatibility of the developed biosensor by testing a few known/unknown STAT3 inhibitors in a 96- and 384-well plate format. The results from this screen revealed that drug molecules such as curcumin and niclosamide are more efficient inhibitors over known molecule like Stattic. Thus, the STAT3 Phospho-BRET sensor is a first of its kind live cell platform technology developed for its use to study STAT3 pathway dynamics and screen potential drug molecules *in vivo*.

Keywords: Bioluminescence resonance energy transfer (BRET), nanoluciferase, TurboFP635, phosphorylation, STAT3, cancer, high-throughput screening, protein-protein interactions, niclosamide, Stattic

Introduction

Complex cellular behaviour in response to a wide variety of external stimuli is a highly regulated and controlled process driven by multiple protein-protein interactions (PPIs) [1]. Although numerous assays are available for detecting PPIs, capturing these interactions in a cellular context is still a challenging task [2]. Bioluminescence resonance energy transfer (BRET) is an attractive assay primarily used for monitoring PPIs and/or temporal conformational changes in natural cellular environment. It is a proximity dependent assay, where non-radiative energy from donor luciferase-substrate reaction is transferred to excite the acceptor-fluorophore typically located within 0-10 nm of physiological distance. Due to the enzymatic nature of the donor molecule, no external illumination is required, and thus this assay offers high signal to background ratio with excellent sensitivity [3]. Recently, several high quantum efficient luciferase or luciferase variants were reported [4]. One such key luciferase molecule is NanoLuc (Nluc), which is the smallest known (19 KDa), ATP-independent luciferase producing highest photon flux known so far [5]. Because of its high quantum efficiency, NanoLuc-based system has been utilized for several potential applications, including monitoring protein stability [6], protein-protein interactions (GPCRs, NanoBRET) [7, 8], protein-ligand interactions (Epo-Epo receptor, INSL3-RXFP2) [9, 10] as well as gene regulation and cell signalling [11, 12].

STAT3 is a key oncogenic signalling molecule primarily activated by pY705 phosphorylation

leading to its homodimerization and nuclear translocation, where it acts as a potent transcription factor for its target genes [13]. Pertaining to its essential role as an oncogenic player, identifying drugs through virtual screening of inhibitor library is a mainstay approach [14]. Subsequently, efforts have been made in the past to develop study methodology for detecting STAT3 activation in live cells [15]. There are reports on a synthetic optical reporter for Y705 residue (Trp564 mutated to 7-hydroxycoumarin-4-yl) [16]. A FRET-based sensor has also been used to study localization dynamics of STAT3 in live cells using CFP and YFP as partners [17]. However, pertaining to low sensitivity and lack of unified assay system for *in vitro* and *in vivo* validation, none of the methods developed so far, have shown potential to study perturbations in STAT3 signalling dynamics or screen potential inhibitors in a high-throughput format from living system.

Hence, the present study is an effort to develop a highly sensitive protein phosphorylation biosensor using BRET platform technology for deciphering live cell STAT3 dimerization kinetics as an oncogenic candidate. Further, we have also attempted to demonstrate high-throughput screening (HTS) compatibility of this sensor for judging inhibitory action of drugs against STAT3 pathway.

Materials and methods

Materials

EGF (#AF-100-15) and IL6 (#200-06) were bought from Peprotech (USA). NanoLuc plasmid and anti-Nluc antibody were provided as a generous gift from Promega. Anti–total STAT3 (#9139), anti-pY705 STAT3 (#D3A7), anti-EGFR blocking antibody (#54359) were from Cell signalling (USA). Anti-RFP antibody [RF5R] (ab12-5244), anti-mouse-HRP (#ab6728) from Abcam and anti-rabbit-HRP (#31460) from Invitrogen. Furimazine (#N1110) was from Promega and Lipofectamine 2000 (#11668019) reagent was from Thermo Fischer. Coelenterazine (native, #C-7001) was purchased from Biosynth International (Switzerland). Stattic (#S7024) was purchased from Selleckchem (USA). CI-994 (#1742), AR-42 (#2716), Chidamide (#2261) and MS-275 (#1590) were from Biovision (USA). Niclosamide (#N3510) and Curcumin (#08511) were from Sigma (USA). BRET measurements were done using IVIS Spectrum In Vivo Imaging System from Perkin Elmer (USA) equipped with filters ranging from 500-850 nm with 20 nm bandwidth and Cytation Imaging reader from Biotek (USA) with filter range from 400-680 nm and band pass of 20 nm.

Plasmid preparation

Fusion constructs of full length nanoluciferase (Nluc) with different fluorophores were prepared in a pCMV empty vector containing suitable flexible GGSGGS repeat linker. The Nluc gene was inserted at the C-terminus by cloning a PCR amplified (516 base pairs) full length sequence using XhoI and BamHI restriction sites while PCR amplified fluorophores (TurboFP, TagRFP and mOrange) were inserted at N-terminus without stop codon using EcoRI and BglII restriction sites. A linker length of 12 amino acids was maintained between the fusion gene sequences. For dipole orientation related studies, PCR amplified fragment of XhoI-mOrange-BamHI was cloned at the C-terminus of pCMV-GGS vector while Nluc was inserted at the N-terminus using EcoRI and BglII restriction sites separated by a linker of 12 amino acids. mOrange-Nluc (12 a.a.) fusion construct was prepared as above. Optimization of linker length was achieved by ligating EcoRI-mOrange-BglII at the N-terminus and XhoI-Nluc-BamHI at the C-terminus in pCMV vector containing GGS linker of length varying from 12 a.a., 18 a.a. to 24 a.a. For achieving a separation of 9 a.a. linker length, mOrange was inserted using NheI and HindIII restriction sites while Nluc containing stop codon was amplified and ligated with AgeI and BamHI sites.

Expression vectors pSTAT3-Nluc and pSTAT3-TurboFP were prepared by amplifying full length STAT3 sequence from STAT3 (Y705F)-TAL-Luc plasmid (gift from Afshin Dowlati, Addgene plasmid # 46933) [18] flanked by NheI and SalI restriction sites and inserting into pCMV-GGS-Nluc and pCMV-GGS-TurboFP vectors (10 a.a. linker separation) at the N-terminus. pNluc-STAT3 and pTurbo-STAT3 expression vectors were prepared by inserting PCR amplified XhoI-STAT3 (Y705F)-BamHI sequence with stop codon into the C-terminus of pNluc-GGS and pTurboFP-GGS vector with linker separation of 12 a.a. Mutant STAT3 (Y705F) was converted to wild type sequence by site-directed muta-

genesis (Forward primer: 5' AGCGCTGCCCCATACCTGAAGACC 3', reverse primer: 5' GGTCTTCAGGTATGGGGCAGCGCT 3') in all relevant constructs.

Cell culture and transfection

HT1080 and PC3 cells were cultured in DMEM medium (Gibco, USA) supplemented with 10% fetal bovine serum (Gibco, USA) and 1% penicillin/streptomycin (Invitrogen, USA). A549 and MCF7 cells were maintained in RPMI1640 (Gibco, USA) supplemented with 10% fetal bovine serum (Gibco, USA) and 1% penicillin/streptomycin (Invitrogen, USA). All cells were maintained at 37°C in a 5% CO_2 humidified atmosphere. One day prior to transfection 1×10^5 cells were seeded in a 12 well-flat bottom plate. Transfection was carried out at an optimal confluency of 80% using Lipofectamine 2000 transfection reagent as per manufacturer's instructions. For BRET studies expression vectors coding for donor and acceptor plasmid were transfected in 1:1 ratio. Post-transfection medium was replaced and cells were maintained in normal culture condition until used.

Acceptor stable cells were developed by transfecting TurboFP-STAT3 or STAT3-TurboFP plasmids in HT1080 cells followed by antibiotic selection of stable clones using Zeocin (Invitrogen) (500 µg/ml).

Immunoblotting

Briefly cells were suspended in lysis buffer containing 10 mM Tris-HCl (pH 7.5), 140 mM NaCl, 5 mM EDTA, 2 mM EGTA, 100 mM NaF, 100 mM Na_3VO_4, 100 mM PMSF and protease inhibitor cocktail. The mixture was lysed using sonicator and centrifuged at 14000 rpm for 30 min at 4°C. Supernatant was collected and protein estimation was done using Bradford reagent (Sigma, USA). Samples were prepared in 1× Laemmli buffer and boiled at 95°C for 3 mins. Protein samples (50-60 µg) were separated in 10% SDS-PAGE gel and transferred onto nitrocellulose membrane using semi-dry transfer assembly (15 V for 1 hr), followed by incubation with blocking buffer (5% non-fat dry milk in 1XTBS and 0.1% Tween 20) for 1 hr. The blots were incubated with primary antibody at a relevant dilution (anti-STAT3 1:1000, anti-pY705 STAT3 1:500, anti-NanoLuc 1:1000 and anti-RFP 1:1000) overnight at 4°C. Next day, blots were processed for incubation with HRP conjugated-secondary antibody (1:10,000 dilution) for 1 hr. Chemiluminescence signal was captured using ECL substrate in ChemiDoc system (Biorad, USA).

Quantitative real time PCR

Total RNA was extracted using RNA extraction minikit (QIAGEN) followed by cDNA preparation from 2 µg RNA using SuperScript III (Invitrogen) kit. Normalization was performed using GAPDH as internal control. Primer sequence for EGFR and GAPDH is as follows: EGFR Fwd: 5' AGGCACAAGTAACAGGCTCAC; EGFR Rev: 5' AAGGTCGTAATTCCTTTGCAC; GAPDH Fwd: 5' TGCACCACCAACTGCTTAGC; GAPDH Rev: 5' GGCATGGACTGTGGTCATGAG.

Fluorescence microscopy

HT1080 cells stably expressing the pCMV-STAT3-TurboFP and pCMV-TurboFP-STAT3 constructs were seeded on cover slips and fixed with 4% paraformaldehyde for 10 min at 37°C. DAPI was used for nuclear staining and images were acquired using Zeiss LSM 780 Confocal Microscope (Germany) with 633 nm filter for TurboFP635 and 460 nm for DAPI.

BRET imaging and analysis

24 hrs post transfection, cells expressing donor alone and donor-acceptor fusion constructs were trypsinized and seeded in a 96 black well plate with clear bottom. Cells were allowed to adhere overnight at 37°C with 5% CO_2. For BRET studies, 50 ul furimazine (1:1000 diluted in DMEM from main stock) was added to each well and acquisition was performed in IVIS spectrum. Emission spectra were captured from 500-680 nm with an integration time of 1 s/filter and 20 nm step increments.

For monitoring functionality of the STAT3 phosphorylation sensor, 24 hrs post transfection, donor alone and donor-acceptor co-transfected cells (20,000 cells/well in 96 and 5000 cells/well for 384 well format) were distributed in black well plates in serum-negative medium. After 24 hrs of serum starvation, cells were triggered with STAT3 pathway ligands (IL6 or EGF) in varying concentrations (5 ng-10 ng IL6, 10-100 ng EGF) reconstituted in serum-negative medium followed by addition of 50 ul

furimazine/well (1:1000 diluted). To study the effect of inhibitors on STAT3 activation, cells were first incubated with varying concentrations of different inhibitors for 24 hrs followed by EGF (100 ng) and substrate addition. For Ab blocking study, cells were preincubated with EGFR blocking antibody for 4 hrs (1:100 dilution) and then EGF (100 ng) along with luciferase substrate was added. One set was left untreated as control group. For all BRET analyses, ROIs were drawn on each well and Average Radiance was calculated in both donor channel (500 nm) and acceptor channel (580 nm-mOrange, 600 nm-TagRFP and 640 nm-TurboFP), for donor alone and donor-acceptor samples. Analysis was done in Living image software version 4.5 for IVIS spectrum.

For acquisition done on Cytation 5 Imaging reader, followed by substrate addition, spectral scan was performed from 400 nm to 680 nm keeping 20 nm band pass filter with an integration time of 1 sec/filter for all the samples. The output for each well was measured in Relative light units (RLU) that was further used for calculating BRET ratios.

In order to calculate BRET ratio, following equations were used [4, 19]:

$$\text{BRET Ratio} = \frac{BL_{emission}\ (\text{Acceptor } \lambda)}{BL_{emission}\ (\text{Donor } \lambda)} - \frac{C_f \times BL_{emission}\ (\text{Donor } \lambda)}{BL_{emission}\ (\text{Donor } \lambda)}$$

$$\text{Where, } C_f = \left(\frac{BL_{emission}\ (\text{Acceptor } \lambda)}{BL_{emission}\ (\text{Donor } \lambda)}\right)_{\text{Donor only}}$$

In vivo bioluminescence imaging

All *in vivo* experiments were performed in compliance with the standard protocol of the institutional animal ethics committee (IAEC), ACTREC. For performing *in vivo* BRET, equal number of HT1080 (3×10^6) cells stably expressing either Nluc alone (above) or TurboFP-Nluc fusion protein (bottom) were implanted subcutaneously on to the dorsal right flank of 6-8 weeks old nude mice (N=3). 30 mins post implantation, 100 µl furimazine (1:20 diluted in 1XPBS) was injected via intraperitoneal route and mice were anesthetised using 2.5% (vol/vol) gaseous isoflurane in oxygen. Acquisition was performed in IVIS spectrum equipped with CCD camera at 500 nm for donor channel and 640 nm for acceptor channel with integration time of 60 sec/filter. For calculating double ratio (DR), the following equation was used [20, 21]:

$$DR = \frac{\left(\frac{BL_{acceptor\ channel} \times \mu_t\ (\text{acceptor channel})}{BL_{donor\ channel} \times \mu_t\ (\text{donor channel})}\right)_{(\text{Donor + Acceptor})}}{\left(\frac{BL_{acceptor\ channel} \times \mu_t\ (\text{acceptor channel})}{BL_{donor\ channel} \times \mu_t\ (\text{donor channel})}\right)_{(\text{Donor alone})}}$$

Where, μ_t is total attenuation coefficient. Here, DR is independent of μ_t.

Statistical analysis

For all data analysis student *t*-test (paired and two-sided) was employed. *p*-value<0.05 was considered statistically significant.

Results and discussion

NanoLuc is an efficient donor for BRET partnering with multiple red fluorescent proteins

For successful developing of a BRET based STAT3 Phosphorylation sensor, careful selection of an appropriate acceptor pair with the NanoLuc (Nluc)-donor is essential. Hence, three red fluorescent proteins, i.e. mOrange (Ex_{Max} 548 nm/Em_{Max} 562 nm), TagRFP (Ex_{Max} 555 nm/Em_{Max} 584 nm) or TurboFP (Ex_{Max} 588 nm/Em_{Max} 635 nm) were selected and individually fused to Nluc with a separation of 12 a.a. flexible GGS linker (**Figure 1A**). The integrity of fusion and expression of the above-mentioned BRET pairs was confirmed by immunoblotting and probing with anti-RFP antibody (**Figure 1B**). Transient overexpression of the three BRET pairs in HT1080 cells show that due to its high quantum output, Nluc is able to transfer sufficient energy to excite all the three fluorescence proteins used here, resulting in their characteristic emission maxima detected using appropriate acceptor filters (mOrange-560 nm, TagRFP-580 nm and TurboFP-640 nm) (**Figure 1C**). Further, with decreasing spectral overlap with Nluc emission, TurboFP (322.57 mBU [mBU is milli BRET unit]) and TagRFP (277.79 mBU) always exhibit BRET ratios less than mOrange (460.72 mBU, P<0.001). However, the BRET ratio obtained with Furimazine as substrate for Nluc were always higher in comparison to when only coelenterazine was used [for e.g. mOr-

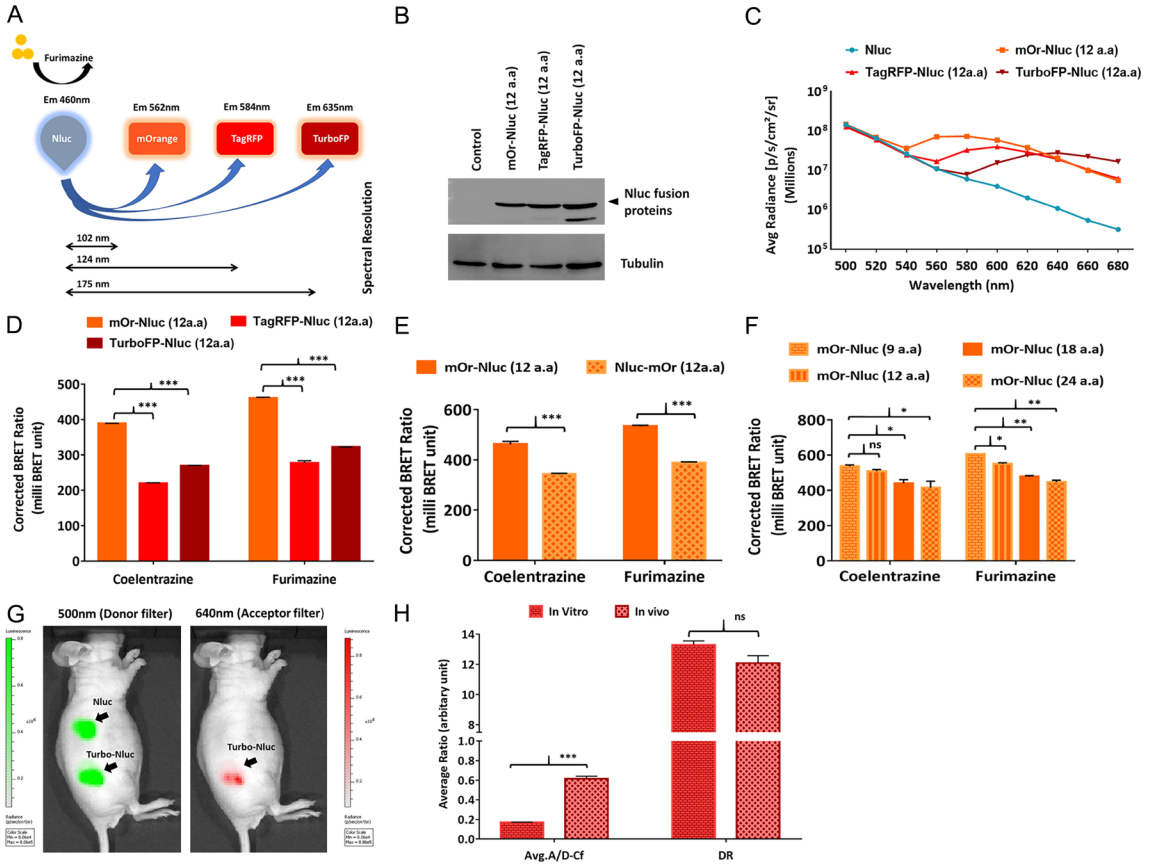

Figure 1. Development of Nanoluc based BRET system: A. Diagrammatic representation of spectral separation between Nluc (NanoLuc) emission and excitation maximum of different fluorophores in presence of furimazine substrate. B. Immunoblot of lysates from HT1080 cells expressing Nluc-fluorophores fusion proteins, probed with anti-RFP antibody. Upper band is the fusion protein in each case. Parental HT1080 cells were used as control. C. Spectral scan for Nluc fused with different fluorophores showing acceptor peak at respective filters (mOrange-560 nm, TagRFP-580 nm and TurboFP-640 nm) with Furimazine as substrate. D. Corrected BRET ratios (in milli BRET unit, mBU) for each of the Nluc-fluorophore fusion proteins in presence of two different substrates for Nluc (furimazine and coelenterazine). Spatial separation of 12 a.a. is kept constant between donor and acceptor in all fusion constructs. E. Graph representing the corrected BRET ratios for differentially oriented mOr-Nluc BRET pair. F. Effect of variable linker length from 9 a.a. to 24 a.a. on BRET ratio of mOr-Nluc (mBU) BRET pair. G. Representative image of nude mice implanted with HT1080 cells (3×10^6) stably expressing Nluc alone (top) and TurboFP-Nluc fusion protein (bottom) for *in vivo* BRET. Donor emission was collected at 500 nm filter and acceptor at 640 nm with 60 sec integration time per filter using furimazine as substrate. H. Graph representing comparison of corrected ratio (Avg.A/D-Cf) and double ratio calculated for both *in vitro* and *in vivo* BRET with Nluc and TurboFP BRET pair. All the above studies were done in HT1080 cells. Each graph represents mean ± SEM value, error bars represent SEM. Significance levels are *P<0.05, **P<0.01, and ***P<0.001 and ns for non-significant.

ange-Nluc; 460.72 mBU (furimazine) vs. 388.81 mBU (coelenterazine)] (**Figure 1D**). Overall, Nluc paired with mOrange showed the highest BRET efficiency using furimazine as a substrate when compared to other fluorophore acceptors.

Because energy transfer efficiency significantly relies on the geometric orientation of donor-acceptor moieties, fusion constructs of mOrange with Nluc were developed in different dipole orientations and transfected in HT1080 cells. Over here, Nluc oriented at the C-terminus (533 mBu) by the virtue of closest proximity shows significantly higher efficiency (P<0.001) of non-radiative energy transfer to mOrange as compared to the N-terminal orientation (388 mBu±0.0347), even with two different substrates (**Figure 1E**). Another important parameter that impacts BRET efficiency is the linker length between the donor and acceptor molecule. To verify this, constructs of Nluc separat-

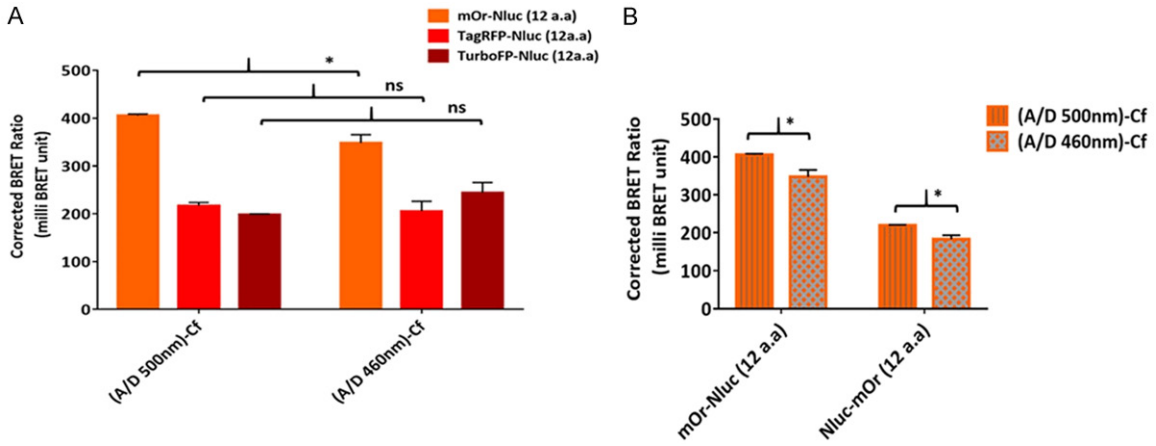

Figure 2. Comparison of BRET ratios using different donor channels for NanoLuc. A. Comparison of corrected BRET ratios obtained for mOrange-Nluc, TagRFP-Nluc or TurboFP-Nluc BRET pairs using different donor filters, 460 nm and 500 nm, in Cytation5 luminescence microplate reader. For all studies furimazine substrate was used. B. BRET ratio comparison done for N- or C-terminally tagged Nluc and mOrange BRET pairs using 500 nm or 460 nm donor filter. Each graph represents mean ± SEM value, error bars represent SEM. Significance levels are *P<0.05, ns indicates non-significant.

ed from mOrange with a variable GGS linker repeat sequence (9 a.a. to 24 a.a.) were expressed in HT1080 cells. With the difference in linker length from 9 a.a. to 12 a.a. (606.27 mBu and 550 mBu respectively) the RET efficiency of Nluc for mOrange majorly remains unaffected, however with further increment of linker length from 18 a.a. to 24 a.a. the corrected BRET ratios (478 mBu and 447 mBu respectively) drop significantly (P<0.01) (**Figure 1F**). Hence, C-terminal orientation of donor and N-terminal orientation of acceptor with an optimal linker length of 9-12 amino acids were considered, which also creates sufficient distance for protein folding in 3D conformation state for all control BRET pairs.

After obtaining a valid BRET pair using Nluc and TurboFP (emission maxima beyond 600 nm) combination *in vitro*, next we explore the potential of this pair to detect PPIs in deep tissues by performing *in vivo* BRET. HT1080 cells stably expressing either Nluc alone or TurboFP-Nluc fusion protein were injected subcutaneously onto the dorsal right flank of nude mice and imaged at respective donor (500 nm)-acceptor (640 nm) filter pairs (**Figure 1G**) Due to drastic difference in attenuation of signal for short wavelength emission, the bleed through subtracted corrected ratios (Avg. A/D-Cf) obtained for *in vivo* BRET (0.614 mBU) were 3-fold higher as compared to *in vitro* BRET (0.169 mBU, P<0.001). Hence double ratios were calculated (DR) that considerably minimized the effect of tissue attenuation on BRET measurements [20], as the latter is independent of total attenuation coefficient (**Figure 1H**). Similar DRs obtained both in case of mice (13.30 mBU) and cell culture BRET (12.07 mBU, P<0.05) confirms the ability of Nluc-TurboFP pair for sensitive detection of protein interactions even with deep tissue imaging in living subjects. Point to be noted here is that BRET ratios calculated using two different donor channels available on plate reader (i.e. 460±20 nm vs. 500±20 nm) show no significant difference in the BRET measurement efficiency (**Figure 2A**, **2B**). Therefore, even though Nluc-furimazine emission peak is at 460 nm, for BRET measurements done using IVIS spectrum, the 500 nm donor channel was used.

NanoLuc-TurboFP635 STAT3 BRET biosensor is a definite model for capturing STAT3 phosphorylation kinetics from live cells

Because of bright and stable luminescence from Nluc and high spectral resolution along with feasibility to be adopted for *in vivo* imaging with TurboFP made them an obvious choice for development of STAT3 phosphorylation driven homodimerization sensor (**Figure 3A**). Hence, fusion constructs of STAT3 either with Nluc donor or TurboFP acceptor were established in both the orientations (N- and C-terminus) with a

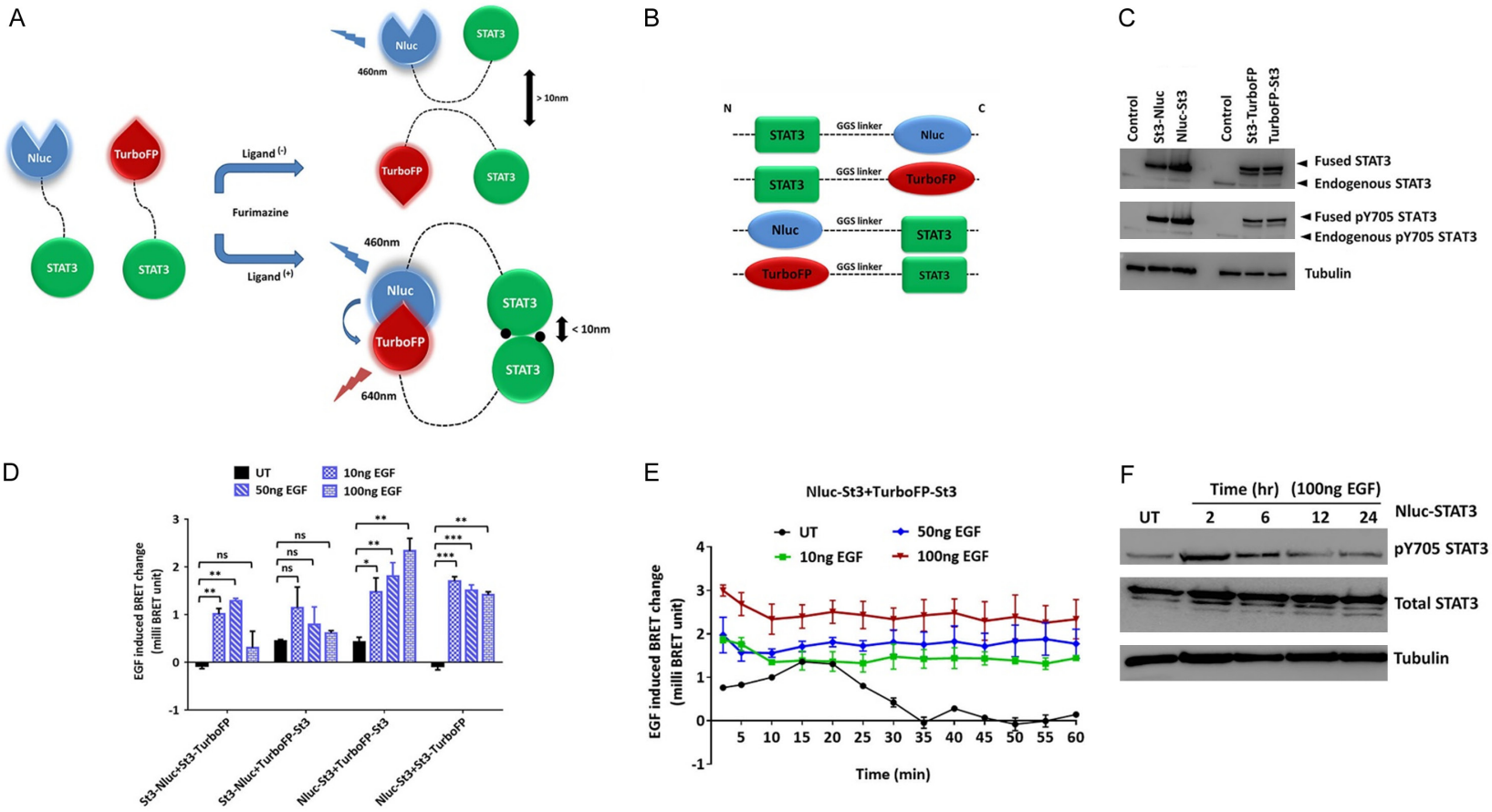

Figure 3. Development of STAT3 phosphorylation biosensor using Nluc and TurboFP BRET pair: A. Working model of STAT3 BRET sensor; STAT3 fused to either donor (Nluc) or acceptor (TurboFP) in the presence of substrate and ligand (that triggers activation and PTM of STAT3) undergoes dimerization and achieve a molecular distance less than 10 nm that allows energy from excited donor to be transferred to acceptor molecule. While in the absence of ligand or presence of inhibitor the two STAT3 molecules are far apart from each other allowing only donor signal to be detected without any energy transfer to the acceptor molecule. B. Schematic representation of all the four STAT3 BRET fusion constructs in different orientations. C. STAT3 BRET constructs transiently transfected in HT1080 cells shows expression of total STAT3 and activated from pY705-STAT3 along with the endogenous STAT3 pool. Upper band in each blot is the band of interest. D. Graph representing corrected BRET ratios (mBU) calculated for differentially oriented STAT3 BRET constructs transiently expressed in HT1080 cells at 30 mins post EGF treatment. E. Time kinetics graph (mBU) of BRET ratios for Nluc-St3+TurboFP-St3 BRET constructs transfected in HT1080 cells and stimulated with varying EGF concentration (0-100 ng). F. Immunoblot for time dependent phosphorylation and activation status of Nluc-St3 BRET fusion protein in response to EGF treatment (100 ng/ml). Phosphorylation is detected by probing for pY705 STAT3 and total STAT3 is determined by probing with anti-Nluc antibody in HT1080 cells. For all BRET studies Nanoluc activity was measured at 500 nm and for TurboFP at 640 nm in IVIS spectrum using furimazine as substrate. Each graph represents mean ± SEM value, error bars represent SEM. Significance levels are *P<0.05, **P<0.01, ***P<0.001 and ns as non-significant.

10 a.a. GGS linker separation and subjected to primary functional validation for proper protein formation (**Figure 3B**). Overexpression of these constructs in HT1080 cells and immunoblotting for total and pY705 STAT3 level confirms fusion protein translation and the ability to undergo spontaneous phosphorylation with endogenous cellular machinery (**Figure 3C**). In order to select an appropriate dipole orientation of STAT3 (ST3) BRET constructs where dimerization-driven BRET signal gain is maximum, a total of four probable combinations i.e. Nluc-ST3+TurboFP-ST3, Nluc-ST3+ST3-TurboFP, ST3-Nluc+ST3-TurboFP and ST3-Nluc+TurboFP-ST3 were established. Activation levels in each set were assayed by treatment with varying EGF concentrations (10-100 ng/ml) in comparison to serum-starved untreated cells and BRET ratios were calculated as described in Materials and Method section. Upon expression of these fusion constructs in HT1080 cells, treatment with the EGF ligand triggers an immediate response with a rapid increase in BRET signal within 5 min. A stable BRET signal is observed for upto 1 hour, for all the fusion combinations. However, of all the orientations tested, C-terminally oriented STAT3 BRET constructs (Nluc-ST3+TurboFP-ST3; 2.33 mBu, $P<0.01$ for 100 ng EGF) clearly stands out exhibiting a dose-dependent (10-100 ng EGF) significant gain in STAT3 activation and a subsequent increase in BRET signal (**Figure 3D**, **3E**). Additionally, to ensure that the gain in Phospho-BRET signal upon EFG treatment is a result of preceding phosphorylation event, Nluc-ST3 fusion expressing HT1080 cells were treated with EGF for different time points and pY705 activation levels were determined. As expected, EGF stimulation initiates Nluc-ST3 pY705 phosphorylation that drops down to basal level after 24 hrs (**Figure 3F**). This indicates that the fusion STAT3 is able sense the ligand trigger from cellular environment and can initiate the STAT3 signalling independently.

Further, in an attempt to achieve higher BRET signal, stable HT1080 cell line overexpressing acceptor-STAT3 fusion was established (**Figure 4A**). With constitutive expression of this fusion partner enhanced the BRET efficiency further. The result indicates that a BRET ratio of 1.57 mBU ($P<0.05$) obtained when acceptor stable cell population is transiently co-expressed for the donor-STAT3 combinations and incubated with only 10 ng EGF ligand. Point that also to be noted here is the Nluc-ST3 and Turbo-ST3 combination shows the highest BRET efficiency (1.61 mBu, $P<0.05$) when incubated with 100 ng EGF ligand (**Figure 4B**, **4C**). Hence, based on the above observations, donor/acceptor constructs with C-terminally orientated STAT3 were selected as final pair for further experiments.

STAT3 Phospho-BRET biosensor can detect STAT3 activation and dimerization in different cancer cell lines and with multiple ligands

Following the identification of Nluc/Turbo-STAT3 as optimal dipole orientation, we next sought to verify the applicability of developed BRET sensor as a working model to judge STAT3 activation across different cancer cell types and against variable pathway ligands. To achieve this, we transiently overexpressed the STAT3 Phospho-BRET sensor in a panel of multiple cancer cell lines including; MCF7 (breast cancer), HT1080 (Fibrosarcoma), PC3 (Prostate cancer), A549 (Adenocarcinomic human alveolar basal epithelial cells) cells and challenged with IL6 at variable concentration, another potential ligand of STAT3 pathway. Despite having a differential biological milieu, the STAT3 Phospho-BRET sensor sensitively captures the activation phenomenon, upon ligand stimulation across all the model cancer cell lines tested (HT1080 [2.14 mBU, $P<0.01$], PC3 [2.3 mBU, $P<0.05$], MCF7 [1.57 mBU, $P<0.05$] and A549 [4.43 mBU, $P<0.01$] for 10 ng IL6) (**Figure 5A-E**). PC3 being a STAT3 null (**Figure 5D**) and HT1080/A549/MCF7 being STAT3 positive, the compounding effect of variable endogenous STAT3 pool, also did not affect the strength of BRET signal achieved. Further, as expected the increment in BRET signal observed shows linear dependency upon ligand (IL6) concentration, except in case of MCF 7 cells. Surprisingly, pertaining to its potency, IL6 turned out to be a better ligand as it could achieve BRET ratio equivalent to EGF treatment (100 ng) with even 10-fold lower ligand concentration [for e.g. HT1080-10 ng IL6 (2.14 mBU) and 100 ng EGF (2.20 mBU)] (**Figure 5A**). These results clearly highlight the inherent strength of the STAT3 Phospho-BRET sensor to work as a sensing model irrespective of the genetic background of model cell line or stimulating ligand.

The differential BRET ratios achieved with the same EGF concentration (100 ng) across a panel of cancer cell lines, intrigued us to look for EGFR expression level. Over here, quantita-

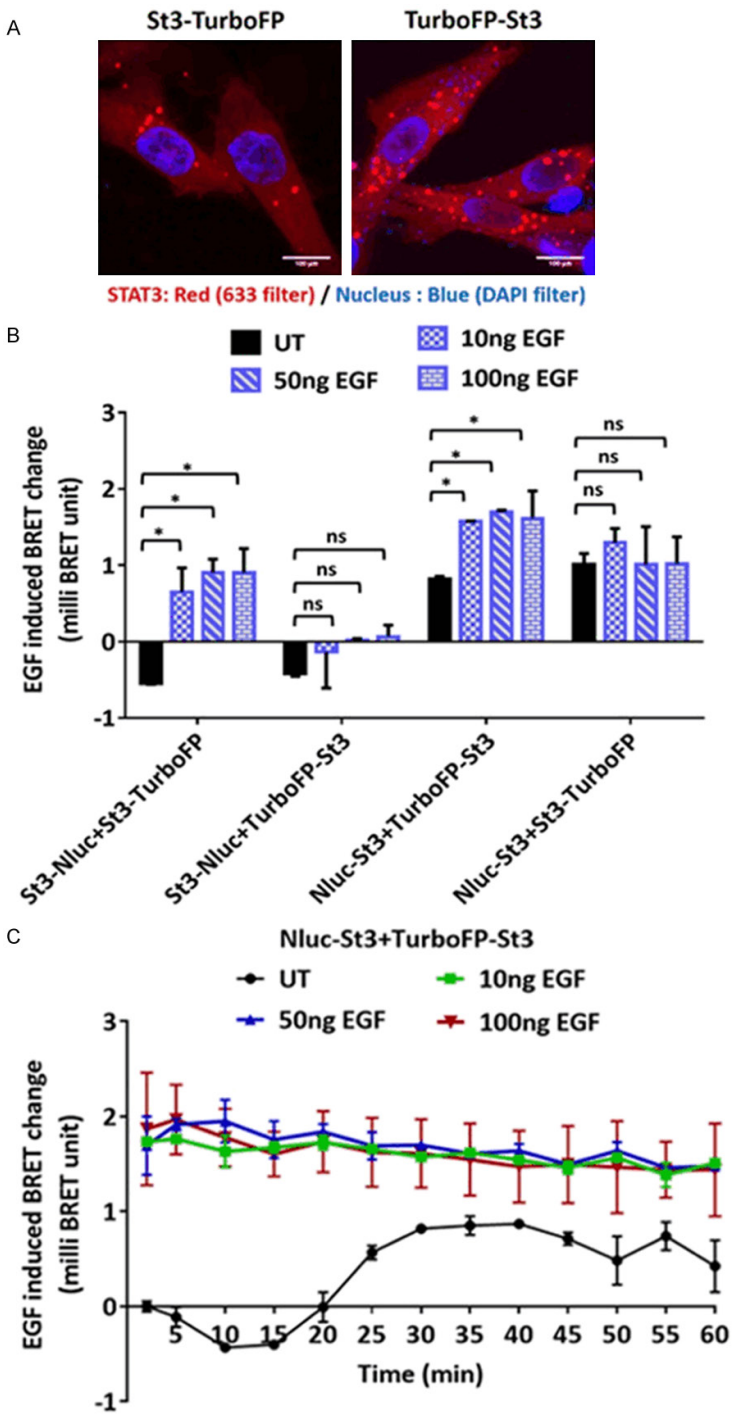

Figure 4. Activation kinetics of phospho-STAT3 BRET constructs in HT1080 acceptor stable cells in response to variable amount of EGF ligand. A. Fluorescence microscopy images of HT1080 cells stably expressing either the TurboFP-St3 or St3-TurboFP acceptor plasmids (uninduced). Nucleus is stained with DAPI and STAT3 signal was acquired at 633 nm filter for TurboFP. B. BRET ratios measured for differentially oriented donor-STAT3 constructs transiently expressed in acceptor-STAT3 stable background, post 30 min of EGF trigger. C. Dynamics of BRET ratios measured for Nluc-St3+TurboFP-St3 BRET construct for 60 min, post EGF induction at variable concentration (10 ng-100 ng) using furimazine as substrate. Nanoluc activity was measured at 500 nm and TurboFP at 640 nm filter at every 5 min for 1 hour. Y-axis represent corrected BRET ratio in milli BRET units (mBU) and X-axis represent time in minutes. Each graph represents mean ± SEM value, error bars represent SEM. Significance levels are *P<0.05, **P<0.01, ***P<0.001 and ns as non-significant.

tive assessment of EGFR transcript level with the BRET ratio gained in the respective cell line points towards the role of receptor density on cell surface as key factor influencing BRET signal (**Figure 5F**). Cells having high EGFR expression [e.g. A549, 4.17 mBU] respond more strongly to the same EGF concentration as compared to the low EGFR-expressing cell line [MCF7 (1.48 mBU) and HT1080 (2.20 mBU); 100 ng, P<0.05 and 0.01 respectively] (**Figure 5G**). Finally, to confirm the specificity of the sensor, prior blocking of EGF receptor with an EGFR neutralizing antibody in MCF7 cells successfully abrogates EGF-mediated STAT3 activation (1.15 mBU with EGF and 0.92 mBU with EGF+EGFR Ab, P<0.05) and a parallel attenuation in BRET signal gain (**Figure 5H**, **5I**). These data indicate that the activation response obtained with the STAT3 BRET sensor upon EGF treatment is a true event of EGF-EGFR mediated STAT3 phosphorylation and homodimerization. Collectively these observations clearly demonstrate the specificity and versatile nature of the developed STAT3 Phospho-BRET sensor as true representation of STAT3 activation events from live cell.

STAT3 Phospho-BRET biosensor is compatible for high-throughput screening of different STAT3 inhibitors

The need to find promising STAT3 inhibitors that can clear the

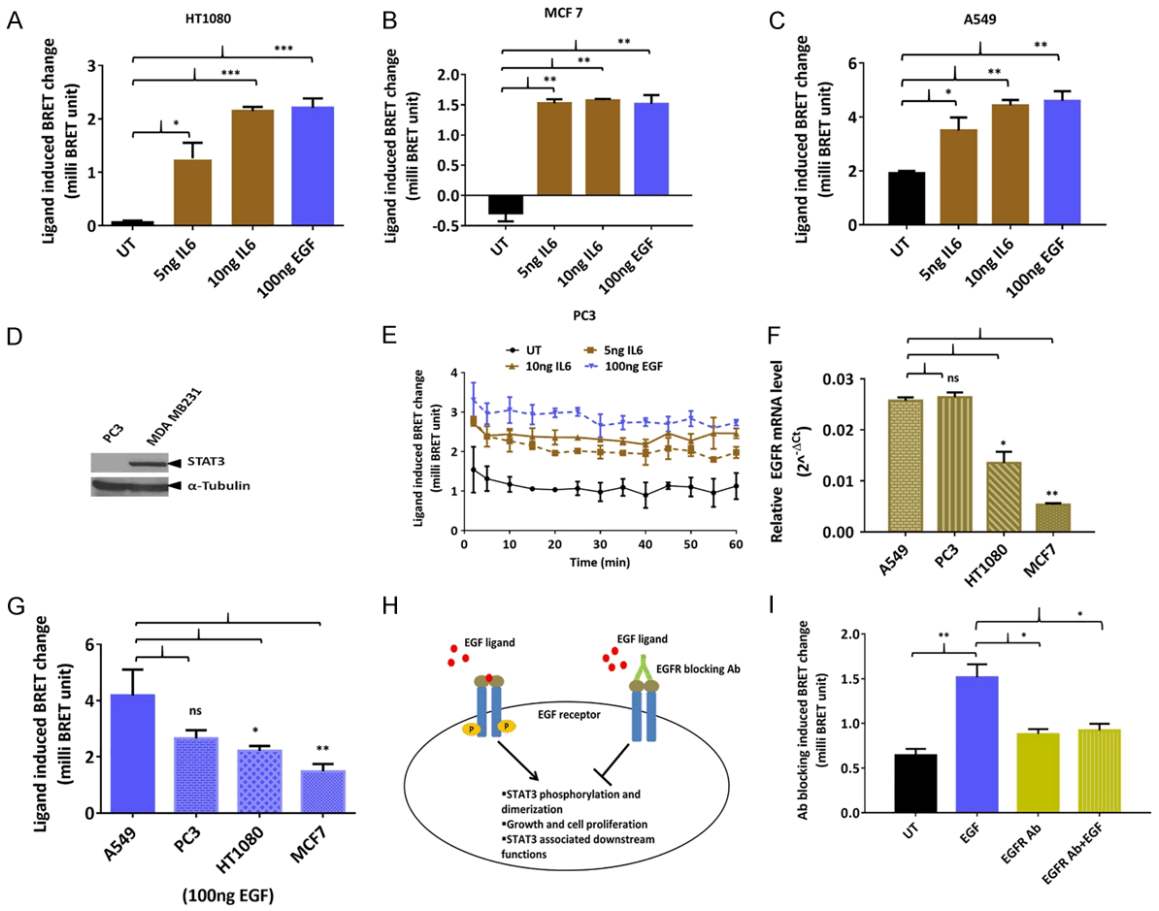

Figure 5. Specificity and sensitivity of phospho-STAT3 BRET biosensor: A. HT1080 cells transfected with Nluc-St3 and TurboFP-St3 wildtype BRET plasmids. Corrected BRET ratio graph (mBU) represent 30 min post ligand trigger condition with both IL6 and EGF as ligands. B, C. Representative graphs of corrected ratios (mBU) for MCF7 and A549 cells respectively showing activation of phospho-STAT3 BRET sensor 30 min post ligand trigger. D. Immunoblot of PC3 cells probed for endogenous STAT3 expression. MDA MB 231 cells were used as positive control. E. Kinetics of change in BRET ratio (mBU) in PC3 cells for STAT3 BRET sensor at varying ligand concentration. F. Relative EGFR mRNA level in different cancer cell lines tested. Normalization was done using GAPDH. G. Corrected BRET ratio values (mBU) for respective cancer cell lines expressing STAT3 BRET construct at 30 min post 100 ng EGF treatment. H. Schematic representation on mode of action of EGFR blocking antibody on STAT3 signaling. I. Representative graphs show corrected BRET ratios (mBU) for MCF7 cells expressing STAT3 BRET constructs either treated with or without EGFR blocking antibody in presence and absence of EGF (mean ± SEM, error bars represent SEM). Significance levels are *P<0.05, **P<0.01, ***P<0.001 and ns as non-significant.

clinical trials demands for a very robust and much more strategic approach in screening STAT3 inhibitors [22]. With the advantages shown by the developed STAT3 Phospho-BRET biosensor to precisely read modulations in the STAT3 pathway, we next sought to adapt it in HTS platform as a drug screening tool. For this, we performed BRET assays in MCF7 cells expressing genetically encoded STAT3 phospho-BRET sensor with relatively six-fold less adherent cell number in a 384-well plate and compared its sensitivity with a conventional 96 well plate format. A random screen of seven different compounds (either known or unknown STAT3 modulators) with differential concentrations either in absence or presence of EGF yield significant results. Out of the 7, four compounds [MS-275 (-0.157 mBU), Niclosamide (-0.287 mBU), Stattic (0.325 mBU) and Curcumin (-0.367 mBU) against EGF^+ (1.4 mBU)] shows significant attenuation in STAT3 activity despite giving EGF stimulation. While remaining three drugs [AR-42 (1.05 mBU), Chidamide (1.00 mBU) and CI994 (0. strategic 603 mBU) against EGF^+ (1.4 mBU)] though activated STAT3 but failed to achieve signal strength as equivalent

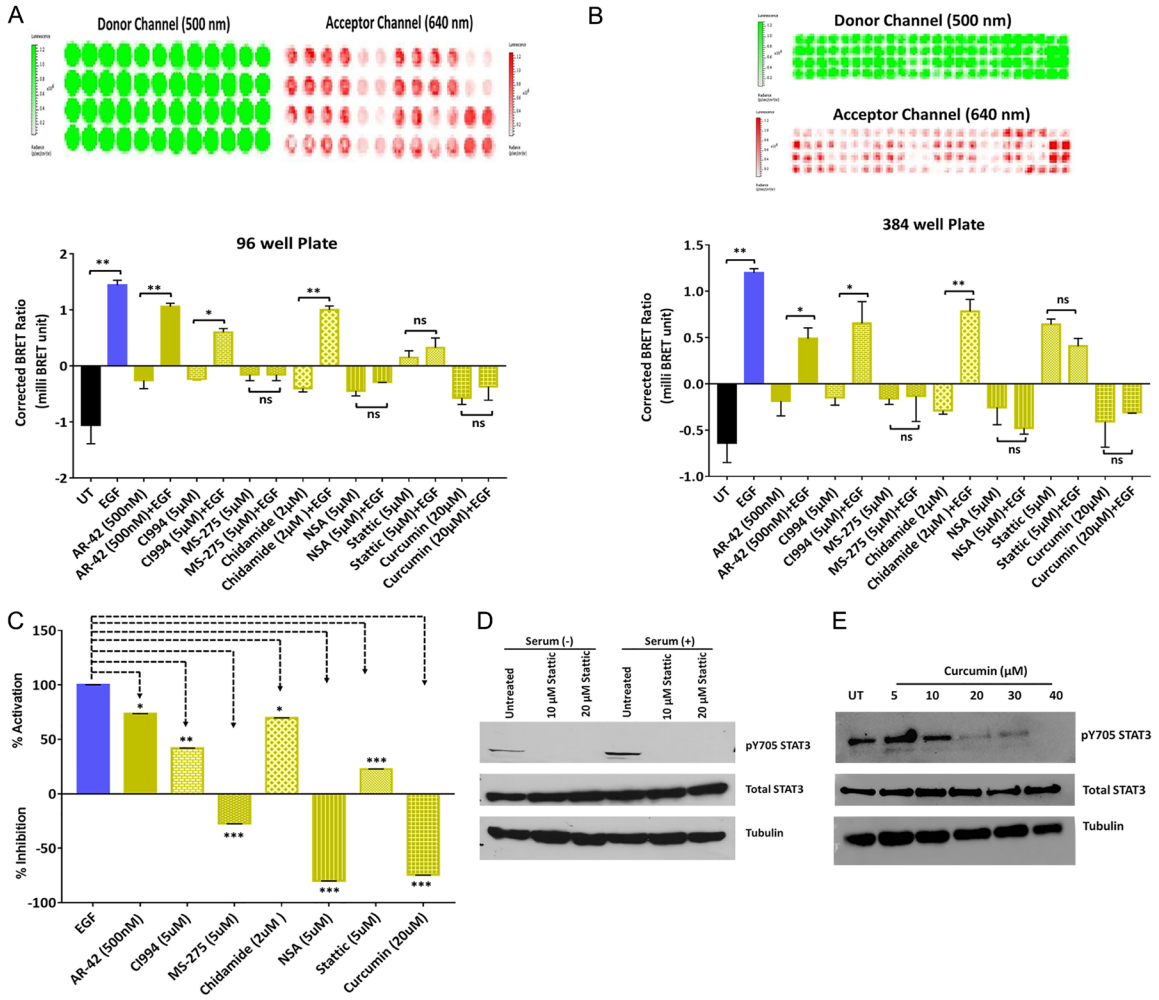

Figure 6. STAT3 Phospho-BRET biosensor is HTS compatible for STAT3 pathway inhibitor screen: A, B. Representative plate images of compound library screen using Phospho STAT3 BRET sensor in 96 and 384 black well plate, respectively, at specific donor and acceptor channels. Bottom graph in each case represents corrected ratios calculated for each drug concentration with or without EGF (100 ng). C. Percent inhibition or activation of BRET signal achieved with respect to EGF treated sample as control (100%). Percent activation is calculated by dividing corrected ratio of drug treated sample with EGF treated control *100. For percent inhibition the above calculated value is subtracted from 100. D, E. Immunoblot of MCF 7 cells treated with different concentrations of Stattic (either in serum positive or serum negative condition) and Curcumin, respectively. Each blot is probed for total and pY705 STAT3, with tubulin as loading control. Each bar represent mean ± SEM, error bars represent SEM. Significance levels are *P<0.05, **P<0.01, ***P<0.001 and ns as non-significant.

to EGF treated control (**Figure 6A**, **6B**). Surprisingly, of the inhibitory compounds identified, Curcumin (74% inhibition) [23] and niclosamide (80% inhibition) [24] were more potent than the previously well-known STAT3 inhibitor, Stattic (22% activation) [25], (**Figure 6C**). The reason for higher potency of both niclosamide and curcumin could be attributed to their ability to inhibit STAT3 activation by abrogating multiple other pathways that either directly or indirectly activate the STAT3 molecule [26, 27], while Stattic is more specifically a SH2 domain binder [25]. The remaining three compounds (i.e. Chidamide, CI-994 and AR-42), that show high BRET signal upon EGF trigger in the HTS screen were majorly HDAC inhibitors, that probably activated STAT3 by increasing overall acetylation of the genome with concomitant increase in inducers of STAT3 pathway [28].

While a majority of HTS assays rely on 96 well plate format, here we have shown that STAT3 phospho BRET sensor works even in 384 well

format while using the same imaging equipment for photonic quantification. A comparable bleed through subtracted BRET signal from two different plate formats (96 vs. 384) clearly shows uncompromised and sensitive signal detection ability of STAT3 phospho-BRET sensor despite adapting to the miniature platform. Finally, to confirm the STAT3 inhibitory mode of action for these drugs, Curcumin and Stattic were randomly selected as drug candidates from the BRET screen for *in vitro* validation. Here, treating MCF7 cells with differential doses of both Curcumin and Stattic (either in serum-positive or serum-starved conditions) respectively, shows a significant drop in activated pY705 STAT3 levels (**Figure 6D**, **6E**), thereby confirming loss of phosphorylation mediated drop in homodimerization signal as mechanistic basis for STAT3 Phospho-BRET sensor. Collectively, these results clearly demonstrate the ability of STAT3 Phospho-BRET sensor as a promising high-throughput, specific and multidrug screening tool against the oncogenic STAT3 pathway.

Conclusion

Pertaining to the excellent quantum efficiency, NanoLuc has form an efficient BRET donor for fluorophores such as mOrange, TagRFP and TurboFP with 100 nm or more spectral resolution and thus provide opportunity to work with BRET systems with minimal bleed through signal at donor and acceptor channel. For the TurboFP-Nluc pair, the furimazine substrate yields a reasonably higher BRET ratio (351.5 mBU) than a value when coelenterazine substrate is used (296.6 mBU). Considering the reasonable dynamic range obtained from TurboFP-Nluc BRET pair, alongside of its suitability for non-invasive molecular imaging, we have utilized this new BRET combination for developing a BRET biosensor that provides the monitoring ability of dynamic STAT3 phosphorylation directly from live cells in culture. STAT3, being an important oncogenic signalling pathway, it is a prime target for therapeutic intervention [29]. However, one of the major challenges is the lack of an appropriate assay system to help screen the inhibitors for their specific action against STAT3 signalling in the live cell environment. Though virtual screening and structure-based drug designing approaches strongly pave the path for identifying novel compounds, final validation both *in vitro* and *in vivo* is mandatory [30]. The STAT3 Phospho-BRET biosensor system is developed to bridge this technological gap, where as a measure of an immediate effect of protein phosphorylation, STAT3 forms homodimer, resulting in increased BRET ratio. After careful optimization of the dipole angular orientation, STAT3 placed at the C-terminus end of both the donor and the acceptor moiety is found to be the best orientation. Alongside of a thorough validation of this biosensor, we have further tested it for revealing the capacity to report real-time phosphorylation events occurring *in situ* using EGF and IL6 ligands in different types of cancer cells.

Pertaining to its ability to give a true read out of the STAT3 activation event, irrespective of either the genetic background of the cell model or differential ligand modulators (e.g. IL6 and EGF), this assay system holds true potentials of deciphering STAT3 biology. The biosensor is also expected to provide novel and specific measures of a range of compounds with inhibitory action on STAT3 signalling directly from live cells. Here, as a token measure of the HTS compatibility of the biosensor, we have shown that signal strength is equally sensitive in 96 well plate with 20 K cells vs. 384 well plate with only 5 K cells. Thus, in future this technology can be used for studying role of key post translational modifications in changing the dimerization status of STAT3 and screening potential inhibitors against this very important transcriptional regulatory protein involved in various oncogenic pathways.

Acknowledgements

The authors acknowledge funding support from Department of Biotechnology (DBT)-Bioengineering project [REF NO. BT/PR3651/MED/32/210/2011], Govt. of India, New Delhi and ACTREC for facilities. We acknowledge Promega for generously providing us with the NanoLuc plasmid and antibody.

Disclosure of conflict of interest

None.

Address correspondence to: Dr. Abhijit De, Molecular Functional Imaging Lab, Advanced Centre for Treatment, Research and Education in Cancer (ACTREC), Tata Memorial Centre, Sector 22, Kharghar,

Navi Mumbai 410210, India. Tel: +91-22-2740 5038; Fax: +91-22-2740 5085; E-mail: ade@actrec.gov.in

References

[1] Paulmurugan R and Gambhir SS. Novel fusion protein approach for efficient high-throughput screening of small molecule-mediating protein-protein interactions in cells and living animals. Cancer Res 2005; 65: 7413-7420.

[2] Berggård T, Linse S and James P. Methods for the detection and analysis of protein-protein interactions. Proteomics 2007; 7: 2833-2842.

[3] De A. The new era of bioluminescence resonance energy transfer technology. Curr Pharm Biotechnol 2011; 12: 558-568.

[4] De A, Rohit A and Jasani A. Engineering aspects of bioluminescence resonance energy transfer systems. in: Cai W, editor. Engineering in Translational Medicine. London: Springer; 2014. pp. 257-300.

[5] England CG, Ehlerding EB and Cai W. NanoLuc: a small luciferase is brightening up the field of bioluminescence. Bioconjug Chem 2016; 27: 1175-1187.

[6] Zhao J, Nelson TJ, Vu Q, Truong T and Stains CI. Self-assembling NanoLuc luciferase fragments as probes for protein aggregation in living cells. ACS Chem Biol 2016; 11: 132-138.

[7] Machleidt T, Woodroofe CC, Schwinn MK, Mendez J, Robers MB, Zimmerman K, Otto P, Daniels DL, Kirkland TA and Wood KV. NanoBRET--a novel BRET platform for the analysis of protein-protein interactions. ACS Chem Biol 2015; 10: 1797-1804.

[8] Salahpour A, Espinoza S, Masri B, Lam V, Barak LS and Gainetdinov RR. BRET biosensors to study GPCR biology, pharmacology, and signal transduction. Front Endocrinol (Lausanne) 2012; 3: 105.

[9] Song G, Wu QP, Xu T, Liu YL, Xu ZG, Zhang SF and Guo ZY. Quick preparation of nanoluciferase-based tracers for novel bioluminescent receptor-binding assays of protein hormones: using erythropoietin as a model. J Photochem Photobiol B 2015; 153: 311-316.

[10] Zhang L, Song G, Xu T, Wu QP, Shao XX, Liu YL, Xu ZG and Guo ZY. A novel ultrasensitive bioluminescent receptor-binding assay of INSL3 through chemical conjugation with nanoluciferase. Biochimie 2013; 95: 2454-2459.

[11] Lackner DH, Carré A, Guzzardo PM, Banning C, Mangena R, Henley T, Oberndorfer S, Gapp BV, Nijman SMB, Brummelkamp TR and Bürckstümmer T. A generic strategy for CRISPR-Cas9-mediated gene tagging. Nat Commun 2015; 6: 10237.

[12] Yasuzaki Y, Yamada Y, Ishikawa T and Harashima H. Validation of mitochondrial gene delivery in liver and skeletal muscle via hydrodynamic injection using an artificial mitochondrial reporter DNA vector. Mol Pharm 2015; 12: 4311-4320.

[13] Shalini D and De A. Approaching non-canonical STAT3 signaling to redefine cancer therapeutic strategy. Integr Mol Med 2017; 4: 10.

[14] Matsuno K, Masuda Y, Uehara Y, Sato H, Muroya A, Takahashi O, Yokotagawa T, Furuya T, Okawara T, Otsuka M, Ogo N, Ashizawa T, Oshita C, Tai S, Ishii H, Akiyama Y and Asai A. Identification of a new series of STAT3 inhibitors by virtual screening. ACS Med Chem Lett 2010; 1: 371-375.

[15] Schroder M, Kroeger KM, Volk HD, Eidne KA and Grütz G. Preassociation of nonactivated STAT3 molecules demonstrated in living cells using bioluminescence resonance energy transfer: a new model of STAT activation? J Leukoc Biol 2004; 75: 792-797.

[16] Lacey VK, Parrish AR, Han S, Shen Z, Briggs SP, Ma Y and Wang L. A fluorescent reporter of the phosphorylation status of the substrate protein STAT3. Angew Chem Int Ed Engl 2011; 50: 8692-8696.

[17] Kretzschmar AK, Dinger MC, Henze C, Brocke-Heidrich K and Horn F. Analysis of Stat3 (signal transducer and activator of transcription 3) dimerization by fluorescence resonance energy transfer in living cells. Biochem J 2004; 377: 289-297.

[18] Dabir S, Kluge A and Dowlati A. The association and nuclear translocation of the PIAS3-STAT3 complex is ligand and time dependent. Mol Cancer Res 2009; 7: 1854-1860.

[19] Dimri S, Basu S and De A. Use of BRET to study protein-protein interactions in vitro and in vivo. Methods Mol Biol 2016; 1443: 57-78.

[20] Dragulescu-Andrasi A, Chan CT, De A, Massoud TF and Gambhir SS. Bioluminescence resonance energy transfer (BRET) imaging of protein-protein interactions within deep tissues of living subjects. Proc Natl Acad Sci U S A 2011; 108: 12060-12065.

[21] De A, Jasani A, Arora R and Gambhir SS. Evolution of BRET biosensors from live cell to tissue-scale in vivo imaging. Front Endocrinol (Lausanne) 2013; 4: 131.

[22] Wake MS and Watson CJ. STAT3 the oncogene-still eluding therapy? FEBS J 2015; 282: 2600-2611.

[23] Hahn YI, Kim SJ, Choi BY, Cho KC, Bandu R, Kim KP, Kim DH, Kim W, Park JS, Han BW, Lee J, Na HK, Cha YN and Surh YJ. Curcumin interacts directly with the Cysteine 259 residue of STAT3 and induces apoptosis in H-Ras transformed human mammary epithelial cells. Sci Rep 2018; 8: 6409.

[24] Shi L, Zheng H, Hu W, Zhou B, Dai X, Zhang Y, Liu Z, Wu X, Zhao C and Liang G. Niclosamide inhibition of STAT3 synergizes with erlotinib in human colon cancer. Onco Targets Ther 2017; 10: 1767-1776.
[25] Schust J, Sperl B, Hollis A, Mayer TU and Berg T. Stattic: a small-molecule inhibitor of STAT3 activation and dimerization. Chem Biol 2006; 13: 1235-1242.
[26] Tomeh MA, Hadianamrei R and Zhao X. A review of curcumin and its derivatives as anticancer agents. Int J Mol Sci 2019; 20.
[27] Li Y, Li PK, Roberts MJ, Arend RC, Samant RS and Buchsbaum DJ. Multi-targeted therapy of cancer by niclosamide: a new application for an old drug. Cancer Lett 2014; 349: 8-14.
[28] Eckschlager T, Plch J, Stiborova M and Hrabeta J. Histone deacetylase inhibitors as anticancer drugs. Int J Mol Sci 2017; 18.
[29] Sellier H, Rébillard A, Guette C, Barré B and Coqueret O. How should we define STAT3 as an oncogene and as a potential target for therapy? JAKSTAT 2013; 2: e24716.
[30] Yuriev E. Challenges and advances in structure-based virtual screening. Future Med Chem 2014; 6: 5-7.

टाटा स्मारक केंद्र
TATA MEMORIAL CENTRE
कैंसर उपचार, अनुसंधान एवं शिक्षा का प्रगत केंद्र
ADVANCED CENTRE FOR TREATMENT RESEARCH & EDUCATION IN CANCER
ACTREC
• CANCER RESEARCH INSTITUTE
• CLINICAL RESEARCH CENTRE

To,
Dean
Homi Bhabha National Institute,
B.A.R.C., Anushakti Nagar,
Mumbai – 400085

10.08.2020

Sub: Final Ph.D. Thesis submission to HBNI
Name: **Ms. Shalini Dimri**
Enrollment No. LIFE09201304001

Dear Sir,

Please find enclosed the following documents in support of **Ms. Shalini Dimri** for final submission of Ph.D. thesis.

- One hard copy of the thesis as per HBNI template & one-page abstract + list of publications arising from the thesis & and list of Conference/Symposium papers.
- Soft copy of the thesis **single file as well as chapter wise** in PDF format in a CD (2 CDs)*.
- Name in Hindi
- Integrity certificate
- Integrity Report
- Report duly signed by the Viva Voce committee
- Certificate (by the guide) of changes incorporated in final thesis as per the suggestions of examiners if any.
- Duly signed Assessment report by Guide of the student
- Duly signed report of Examiner: -1
  - **Prof. Ramasamy Paulmurugan**
  - Department of Radiology
  - Stanford University School of Medicine
  - California, USA
- Duly signed report of Examiner: -2
  - **Dr. Veena K. Parnaik**
  - Nuclear Organization and Lamin Biology
  - Centre for Cellular and Molecular Biology (CCMB)
  - Hyderabad
- Copy of email correspondence if thesis is reviewed by examiners other than 1 & 2-NA
- UGC 11 criteria checklist duly signed by Dean Academic.

With Best Regards,

S. Chiplunkar 10/08/2020

Prof. S.V. Chiplunkar,
Chairperson, Academic &
Training Programme, ACTREC

13/8/2020

Dr. S. D. Banavali,
Dean (Academics)
T.M.C.

PROF. S. D. BANAVALI, MD
DEAN (ACADEMICS)
TATA MEMORIAL CENTRE
MUMBAI – 400 012.

(Prof. Dr. S. V. Chiplunkar)
Chairperson, Academic &
ACTREC

खारघर, नवी मुंबई - ४१० २१० इंडिया
दूरभाष : ९१-२२-२७४०५००० / २७४१२८९१
फॅक्स : ९१-२२-२७४०५०८५

Kharghar,
Navi Mumbai - 410210, INDIA.
Phone : 91-22-27405000 / 27412891
Fax : 91-22-27405085
E-mail : mail@actrec.gov.in
Website : www.actrec.gov.in

टाटा स्मारक केंद्र
TATA MEMORIAL CENTRE
कैंसर उपचार, अनुसंधान एवं शिक्षा का प्रगत केंद्र
ADVANCED CENTRE FOR TREATMENT RESEARCH & EDUCATION IN CANCER
ACTREC
• CANCER RESEARCH INSTITUTE
• CLINICAL RESEARCH CENTRE

To,
Dean HBNI,
B.A.R.C., Anushakti Nagar,
Mumbai – 400085

Date: 10.08.2020

Sub: Certification for the Award of Ph.D. degree.

Dear Sir,

Ms. Shalini Dimri, (ACTREC, Enrollment No. LIFE09201304001; Year-2013) has been working under my guidance for HBNI Ph.D. program in Life Sciences. The topic of her thesis is **"Molecular Imaging of STAT3 Signaling *in vivo*"**. Please find attached copies of the thesis evaluation reports received from the two external referees of the thesis. Both the examiners have recommended award of the Ph.D. degree. As there were no suggestions for any change in the thesis examined, the final thesis retains the same presentation details. The final Ph.D. *viva voce* of **Ms. Shalini Dimri** was held on **10.08.2020** in presence of the Doctoral Committee members and External Examiner **Prof. Veena K. Parnaik, CCMB-Hyderabad**. The committee recommended the award of HBNI Ph.D. degree in Life Sciences to **Ms. Shalini Dimri.**
Recommendation of the viva voce committee with report of the final viva voce examination, thesis evaluation reports from the approved examiners, one hard copy and two soft copies (CDs) of the thesis and Abstract are included herewith for your kind perusal.

We request you to award HBNI Ph.D. degree in Life Sciences to **Ms. Shalini Dimri.**

10.08.2020

Dr. Abhijit De
(Guide & Convener)

15/08/2020

Dr. S.V. Chiplunkar
(Chairperson, Doctoral Committee)

Forwarded Through:

15/08/2020

Prof. S.V. Chiplunkar,
Chairperson, Academic &
Training Programme, ACTREC

13/8/2020

Dr. S. D. Banavali,
Dean (Academics)
T.M.C.

PROF. S. D. BANAVALI, MD
DEAN (ACADEMICS)
TATA MEMORIAL CENTRE
MUMBAI – 400 012.

(Prof. Dr. S. V. Chiplunkar)
Chairperson, Academic &
Training Programme , ACTREC

Cc: Prof. S. V. Chiplunkar – **Convener, Board of studies in** Life Sciences, HBNI
Email : schiplunkar@actrec.gov.in

खारघर, नवी मुंबई - ४१० २१० इंडिया
दूरभाष : ९१-२२-२७४०५००० / २७४१२८९१
फॅक्स : ९१-२२-२७४०५०८५

E-mail : mail@actrec.gov.in
Website : www@actrec.gov.in

Kharghar,
Navi Mumbai - 410210, INDIA.
Phone : 91-22-27405000 / 27412891
Fax : 91-22-27405085

Thesis Abstract

Name: Ms. Shalini Dimri

Enrollment Number: LIFE09201304001

Thesis Title: Molecular Imaging of STAT3 Signaling *In Vivo*

STAT3 signaling via classical canonical (pY705) pathway is well established, however the role of non-canonical (S727phosphorylation and K685acetylation) pathways, is still emerging. The present study thus focuses on unravelling the interplay between canonical and noncanonical pathway by which STAT3 mediates its oncogenic functions in breast cancer. To understand the functional importance of individual PTM sites in regulating STAT3 activation, dimerization and downstream biological functions, we developed a highly sensitive phospho STAT3 biosensor using BRET (Bioluminescence Resonance Energy Transfer) methodology. STAT3 fused with Nanoluciferase (donor) and TurboFP635 (acceptor) at the C-terminus successfully captured the dynamics of STAT3 activation and dimerization in live cells across multiple different cancer cell lines, and using two different activating ligands (IL6 and EGF). Moreover, we showed the high throughput compatibility (384 plate format) of the sensor by screening compound library and identified potential activators and inhibitors of STAT3 pathway. Thereafter, to understand how the two pathways cross talk or dialogue with each other, we engineered 3'UTR STAT3 knockdown cell model with stable overexpression of Nluc-STAT3 PTM point mutants i.e. Wt, Y705F, S727A and K685R. Using this elegant model system, we first showed that both pY705 and pS727 activation are independent of each other while K685ac proceeds only after pS727 PTM *in vitro*. Testing these mutants (either alone or in combination) on BRET platform we further demonstrated that pS727 plays a dominant and independent role in dictating STAT3 homodimerization over pY705 and K685ac. As a functional consequence S727A and K685R mutants exhibited drastic decrease in overall cell survival, proliferation and preferential transcriptional regulation for downstream targets. Extending our observation to clinical scenario, we further determined the role of noncanonical STAT3 pathway in breast cancer oncogenesis. By performing immunohistochemistry analysis of total, pY705 and pS727 expression in 76 paired core biopsy and post NACT TNBC specimens, we found more than 90% STAT3 positive cases expressing pS727 PTM, contrary to only 15% cases with pY705 positivity. Finally, we identified niclosamide as potent dual blocker of STAT3 pathway (pY705 and pS727) with excellent anti-cancer activity against pre-clinical TNBC tumor model. Altogether, this study reports novel role and functioning of noncanonical pS727 STAT3 pathway in breast cancer.

Shalini
10.08.2020

Ms. Shalini Dimri

10.08.2020

Dr. Abhijit De (Guide)

Forwarded through:

S.Chiplunkar
10/08/2020

Prof. S.V. Chiplunkar,
Chairperson, Academic &
Training Programme, ACTREC

(Prof. Dr. S. V. Chiplunkar)
Chairperson, Academic &
Training Programme , ACTREC

13/8/2020

Dr. S. D. Banavali,
Dean (Academics)
T.M.C.

PROF. S. D. BANAVALI, MD
DEAN (ACADEMICS)
TATA MEMORIAL CENTRE
MUMBAI - 400 012.

List of Publications arising from the thesis

Journals

1. **"**Dynamic monitoring of STAT3 activation in live cells using a novel STAT3 Phospho-BRET sensor." **Shalini Dimri**, Rohit Arora, Akshi Jasani and Abhijit De, American Journal of Nuclear Medicine and Molecular Imaging, 2019;9(6):321-334.

2. "Noncanonical pS727 post translational modification dictates major STAT3 activation and downstream functions in breast cancer." **Shalini Dimri**, Renu Malhotra, Tanuja Shet, Smruti Mokal, Sudeep Gupta and Abhijit De. [Manuscript under Revision- Experimental Cell Research]

Patents

Provisional Indian Patent application filed with BCIL: "A Method for Detection of Protein Activation Using Phospho-BRET Imaging Sensor and Methods Thereof" (Ref. # 201921010208; filed on March 15, 2019).

Book chapters and Review articles

1. **Shalini Dimri**, Soumya Basu and Abhijit De. Use of BRET to Study Protein–Protein Interactions *in vitro*. The nuclear receptor superfamily, edited by Iain J. McEwan. Methods in Molecular Biology, Springer, New York 2016; 1443:57-78. **[Book Chapter]**

2. **Shalini Dimri**, Sukanya and Abhijit De. Approaching non-canonical STAT3 signaling to redefine cancer therapeutic strategy. Integrative Molecular Medicine,2017 4(1): 1-10 **[Review Article]**

Conferences and workshops

1. Attended and actively participated in workshop on - "Basic Course in Flow Cytometry-II-Hands on workshop" organized by Mumbai immunology group at ACTREC, 10-11th July 2014.

2. "Monitoring Stat3 Dimerization Dynamics in Live Cells Using Novel BRET Platform." Shalini Dimri, Rohit Arora and Abhijit De. 39th All India cell biology conference

(AICBC)-cellular organization and dynamics held in Thiruvananthapuram, Kerala, 06-08th December 2015.

3. "Monitoring activation dynamics of STAT3 in Live Cells Using Novel BRET Platform". Shalini Dimri, Rohit Arora and Abhijit De. 11th National Research Scholars meet in Life Sciences held in ACTREC, Mumbai, 17-18th December 2015 and received **second best poster award**.

4. "A novel molecular imaging sensor to elucidate functional role of non-canonical STAT3 activation in breast cancer." Shalini Dimri, Rohit Arora and Abhijit De.75th TMC platinum jubilee "A Conference of New Ideas in Cancer: Challenging Dogmas" held in Mumbai, 26-28th February 2016.

5. "A novel molecular imaging sensor for monitoring *in vivo* STAT3 protein phosphorylation highlights important functional and biological role of non-canonical STAT3 PTMs." Shalini Dimri, Rohit Arora, Renu Malhotra, Tanuja Shet, Sudeep Gupta and Abhijit De. International Congress of Cell Biology- "The Dynamic Cell- From molecules and Networks to form and function" held at Hyderabad, 27-31st January,2018.

6. "Non-canonical S727 STAT3 PTM activation governs its dimerization and downstream function in triple negative breast cancer." Shalini Dimri, Rohit Arora, Renu Malhotra, Tanuja Shet, Sudeep Gupta and Abhijit De. 25th Biennial Congress of the European Association for Cancer Research (EACR25) held at Amsterdam, Netherlands, 30th June – 03rd July 2018.

7. "Phospho-STAT3 BRET sensor for assessment of live cell STAT3 dimerization highlights functional and biological significance of non-canonical STAT3 activation in breast cancer." Shalini Dimri, Rohit Arora, Renu Malhotra, Tanuja Shet, Sudeep Gupta and Abhijit De. Society of Biological Chemists (SBC) Annual Meeting 2018- Mumbai Chapter held at Mumbai, 13th October 2018.

8. "A novel 'Phospho-STAT3 BRET' molecular sensor reveals non-canonical activation of STAT3 signaling in breast cancer." Shalini Dimri, Rohit Arora, Renu Malhotra, Tanuja Shet, Sudeep Gupta and Abhijit De. 7th Annual MPAI (Molecular Pathology Association of India) Meeting held at Mumbai, 12-13th January 2019 and received **best oral presentation award**.

Conference Abstracts (Published)

1. A novel molecular imaging sensor to elucidate functional role of non-canonical STAT3 activation in breast cancer. **Shalini Dimri**, Rohit Arora and Abhijit De. European Journal of Cancer, 2016 (54).

2. Non-canonical S727 STAT3 PTM activation governs its dimerization and downstream function in triple negative breast cancer. **Shalini Dimri**, Rohit Arora, Renu Malhotra, Tanuja Shet, Sudeep Gupta and Abhijit De. ESMO Open 2018; **3:** doi: 10.1136/esmoopen-2018-EACR25.706

Other Publications

1. Nishant Kumar Jain*, **Shalini Dimri***, Rajendra Prasad, Gayathri Ravichandran, V.G.M. Naidu, Abhijit De and Rohit Srivastava. Characteristics of molecularly engineered anticancer drug conjugated organic nanomicelles for site-selective cancer cell rupture and growth inhibition of tumor spheroids. (Manuscript Under Review- ACS Applied Bio Materials)

   (*Both the authors have contributed equally to the work)

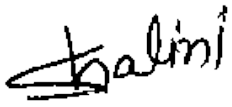

10.08.2020

Ms. Shalini Dimri

Homi Bhabha National Institute

Ph.D. Thesis Evaluation Report

1. **Name of the Constituent Institution: TMC- ACTREC**
2. **Name of the Student: Ms. Shalini Dimri**
3. **Enrolment No.: LIFE09201304001**
4. **Title of the Thesis:** Molecular Imaging of STAT3 Signaling in vivo.
5. **Name of the Board of Studies: Life Sciences**

Recommendations

Tick one of the following:

1. The thesis in its present form is commended for the award of the Ph.D. Degree. [X]
2. The thesis is commended for the award of the Ph.D. degree. However, my suggestions for improving the thesis may be considered at the time of the viva voce examination and if the viva voce board deems it appropriate, the same may be incorporated in the thesis based on the discussions during the viva voce examination. The revised thesis need not be sent to me. [ ]
3. The thesis should be revised as per the suggestions enclosed. I would like to see the revised thesis incorporating my suggestions before I give further recommendations. [ ]
4. The thesis is not acceptable for the award of the Ph.D. degree. [ ]

Date: 07-25-2020

(Signature):

RAMASAMY PAULMURUGAN, Ph.D.
Associate Professor
Molecular Imaging Program at Stanford (MIPS),
Canary Center for Cancer Early Detection
Department of Radiology
Stanford University School of Medicine
3155 Porter Drive, Room: 2236
Palo Alto, CA 94304
Phone: 650-725-6097, Fax: 650-721-6921
E-mail: paulmur8@stanford.edu

Please give your detailed report in the attached sheet. You may use additional sheets, if required.

Attached a separate document.

1. **Name of the Student: Shalini Dimri**
2. **Title of the Thesis: Molecular Imaging of STAT3 Signaling *In Vivo***
   ……..

DETAILED REPORT

Enclosed a separate document.

Name of Examiner:

(Signature):

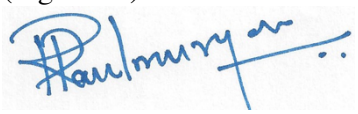

RAMASAMY
PAULMURUGAN, Ph.D.

STANFORD
UNIVERSITY
MEDICAL CENTER
Hospital & Clinics ▪ School of Medicine
Lucile Salter Packard Children's Hospital

DEPARTMENT OF RADIOLOGY

July 27, 2020

Sub: Evaluation report of the thesis entitled **"Molecular Imaging of STAT3 Signaling *In Vivo*"** by **Ms. Shalini Dimri** to **HOMI BHABHA NATIONAL INSTITUTE**, **TATA MEMORIAL CENTRE,** Mumbai, India, for the award of Doctor of Philosophy in Life Sciences.

General Report:

This study presents the research results of an important family of transcription factors called Signal Transducer and Activator of Transcription (STAT). STAT is a conserved family of transcription factors containing seven proteins that are involved in many regulatory pathways in cells at normal and in pathological conditions. STAT3 is an important member of this family that regulates oncogenic and cell survival signaling in cancer. Hence, STAT3 inhibitors are considered as highly recognized drug candidates for treating cellular diseases, including cancer. The posttranslational modifications (PTMs) of this protein at Y705, S727, and K685 play important roles in transcriptional regulation of this protein for its oncogenic signaling. This study developed BRET sensors to monitor the PTMs of this protein to delineate the interrelation between the modifications and the regulatory signaling. In addition, the study also provided insights on the use of this system in screening small molecules that can serve as drugs for treating diseases associated with STAT3 dysregulation. PTMs in STAT3, and activation of its downstream targets such as Cyclin D1, c-Myc, Socs3, etc., are important for its regulatory functions. In this study, by using BRET sensors, the candidate is trying to portray between the canonical pY705 PTM versus non-canonical pS727 and acK685 in STAT3 signaling. Specifically, this study evaluated this process in breast cancer in general, and TNBC in particular. STAT3 dimerization is important for its cytoplasmic trafficking for transcriptional activation. This study also addresses the importance of all three PTM's role in the dimerization of STAT3 protein in cells engineered to express different mutants. The candidate mainly focused on Nanoluc in combination with TurboRFP as donor and acceptor combination respectively, for developing the BRET sensors proposed in this study for STAT3 PTM evaluation. The work is planned very well and logically to STAT3 signalizing in cancer by developing BRET sensors in various combinations to identify optimal sensor for measuring STAT3 PTM with high signal to noise ratio, attempting to evaluate the identified sensor for its high throughput drug screening ability with the final application in studying STAT3 signaling in BC and TNBC.

Chapter 1: In this chapter, the candidate has given a brief introduction to support the importance of the study with an extensive review of the existing literature in BRET sensors, reporter gene imaging, breast cancer, and STAT3 signaling. The introduction and reviews were very detailed with logical justifications.

Chapter 2: In this chapter, the candidate explored different BRET sensor constructs to identify the correct orientation of Nanoluc and TurboRFP to present in STAT3 fusion protein for achieving

STAT3 PTM specific BRET signal with minimum background signal. The identified BRET sensor was evaluated in several cell lines with the treatment of ligand activators of STAT3 signaling. The results compared IL6 and EGF and found more activation by IL6. The other ligands such as Niclosomide and Stattic were also tested. After ligand evaluation, the cells stably expressing BRET sensor was applied in high throughput screening approach using a few bioactive compounds in different doses. The screening of 12 known bioactive drugs identified 3 strong new candidates such as Neratinib, MS-275, and ERK inhibitors as valuable drugs. These drugs were further utilized for anticancer therapeutic study in TNBC.

Chapter 3: In this chapter, the study evaluated the role of PTM dependent STAT3 signaling in breast cancer. The candidate first engineered 3'UTR STAT3 knockdown MCF7 cells with stable overexpression of individual STAT3 PTM mutants i.e. Wt, Y705F, S727A and K685R, fused to Nanoluc reporter gene for BRET imaging. Upon stable overexpression and treatment with IL6 or EGF as ligand, the results observed both pS727 and pY705 activation can take place independently while K685ac requires prior pS727 activation. Loss of noncanonical activation marks (S727A and K685R) results in losing cell proliferation in engineered MCF7 cells. TWIST1 and SOCS3 expression changed in Y727/K685 mutant. This in turn correlated with lower homodimer formation. Mutant BRET sensor with S727 activation (S727A) using IL6 and EGF showed variation and indicated this PTM's importance.

Chapter 4: In this chapter, the study evaluated STAT3 PTM (Y705 and S727) in clinical TNBC specimens. IHC analysis for total STAT3, pS727, and pY705 forms were performed in 76 TNBCs core biopsy and paired post NACT tumor tissues. The results showed strong correlation of STAT3 PTM with the disease. After establishing its clinical relation, the candidate generated MDA MB231 TNBC cells stably expressing shRNA targeting STAT3 by lentiviral transduction. The cells were evaluated for *in vitro* proliferation followed by *in vivo* anticancer study. Interestingly, STAT3 knock-down significantly altered cell proliferation while also altering stemness of TNBC cells by changing the expression profile of markers like CD44 and CD24. Knockdown of STAT3 in MDA MB 231 cells correlated with the depletion of CSC ($CD44^{+}/CD24^{-\text{or low}}$ with drop in Oct4 ($p<0.05$) and Sox2 ($p<0.01$) expression. *In vivo* therapeutic evaluation using Niclosamide showed a dual PTM blocking mediated antitumor effect against TNBC. Finally, the study tested pY705, pS727, and acK685 PTM in breast cancer outcome.

Organization of the thesis: The thesis is well organized starting with addressing reviewing up-to-date literature on STAT3 signaling and the reporter gene imaging, especially BRET sensors and its applications followed by the research results of this study.

Justification of publication: The candidate has published several manuscripts and presented data in different National and International conferences, which supports the value of the research project she studied.

Specific Comments (revisions required):

1. I found inappropriate use of words in several places. In addition, I found several spelling mistakes throughout the thesis. It is better to correct them in the copy that will be submitted to the library.
2. Some new BRET system using NIR wavelength in combination with the exploration of soret band of iRFP has been developed for improved imaging with long band pass filters. This system is not discussed in the thesis. If possible, add to the revised version of the copy submitted to the library (but not mandatory).
3. On page 59, the candidate mentioned a statement saying that there are no assay systems currently available for studying protein dimerization and post translational modification of proteins STAT3 biology, hence it forced the candidate to develop the current BRET system. It is not true. There are several systems available. Please rephrase this statement.
4. Figure 2.2: Results of TurboRFP signal measured *in vitro* and *in vivo* by using excitation filter followed by emission filter is missing. Similarly, Fig. 2.2C, the comparison is supposed to be BRET ratio of *in vitro* and *in vivo* conditions.
5. Reference citations within the chapter, it is important to italicize "*et al.,*" throughout the thesis.

Conclusion: In summary, it is a reasonably high impact thesis performed in a systematic and organized way with a very high level of technical skill to study an important oncogenic pathway in breast cancer, importantly in triple negative breast cancer which lacks targeted therapies and succumb many young women to the disease. Other than some of the minor issues in different chapters, it is a successful thesis studied with significant originality by applying a high level of technical skills. Hence, I consider this work as **highly commendable**. I am confident that the candidate acquired enough skills and potential to successfully pursue independent research and also possess knowledge to guide students at different levels.

Please feel free to contact me if any additional information is needed.

Sincerely,

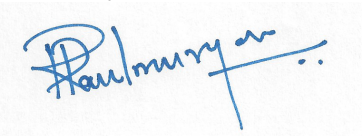

RAMASAMY PAULMURUGAN, Ph.D.
Associate Professor of Radiology
Molecular Imaging Program at Stanford (MIPS),
Canary Center for Cancer Early Detection
Department of Radiology
Stanford University School of Medicine
3155 Porter Drive, Room: 2236
Palo Alto, CA 94304
Phone: 650-725-6097, Fax: 650-721-6921
paulmur8@stanford.edu
https://med.stanford.edu/profiles/mips/ramasamy-paulmurugan
https://profiles.stanford.edu/ramasamy-paulmurugan

Homi Bhabha National Institute

Ph.D. Thesis Evaluation Report

1. **Name of the Constituent Institution: TMC- ACTREC**
2. **Name of the Student: Ms. Shalini Dimri**
3. **Enrolment No.: LIFE09201304001**
4. **Title of the Thesis:** Molecular Imaging of STAT3 Signaling in vivo.
5. **Name of the Board of Studies: Life Sciences**

Recommendations

Tick one of the following:

1. The thesis in its present form is commended for the award of the Ph.D. Degree. ☑

2. The thesis is commended for the award of the Ph.D. degree. However, my suggestions for improving the thesis may be considered at the time of the viva voce examination and if the viva voce board deems it appropriate, the same may be incorporated in the thesis based on the discussions during the viva voce examination. The revised thesis need not be sent to me. ☐

3. The thesis should be revised as per the suggestions enclosed. I would like to see the revised thesis incorporating my suggestions before I give further recommendations. ☐

4. The thesis is not acceptable for the award of the Ph.D. degree. ☐

Date: 5 June 2020

(Signature): V V Parnaik

Name of Examiner: Dr Veena K Parnaik
And affiliation: FNA
Former JC Bose Fellow
CCMB, Hyderabad

Please give your detailed report in the attached sheet. You may use additional sheets, if required.

1. **Name of the Student:** Ms. Shalini Dimri

2. **Title of the Thesis:** Molecular imaging of STAT3 signaling in vivo

DETAILED REPORT

In this thesis, the candidate Ms Shalini Dimri has described her studies on understanding the role of STAT3, a key transcription factor, with specific reference to cancer cells. This is an important area of work since changes in phosphorylation of STAT3 influence its activity in normal and cancer cells. The focus of the study is on comparing the roles of canonical and non-canonical phosphorylation pathways in mediating STAT3 activity, primarily using imaging techniques.

The candidate has written a detailed introduction to STATs in Ch.1. In Ch.2 the development of a novel and versatile imaging sensor for STAT3 phosphorylation dependent homo-dimerization is described. In Ch 3 evidence is presented for the importance of the non-canonical pathway of STAT3 modification in breast cancer cells. In Ch 4, experiments elucidating the importance of non-canonical STAT3 phosphorylation in TNBCs are described. The potential of STAT3 inhibitors for therapy using in vivo animals models of imaging is highlighted.

The presentation of the thesis, both written matter and images is excellent. The experiments have been carried out carefully with appropriate controls. The study highlights the skill and expertise of the candidate. The major part of the work has been published in good quality peer-reviewed journals.

I strongly recommend the thesis for award of the PhD degree.

Name of Examiner: Dr Veena K Parnaik

Signature and Date: V K Parnaik 5 June 2020

Homi Bhabha National Institute

Ph.D. Thesis Evaluation Report

1. **Name of the Constituent Institution:** TMC- ACTREC
2. **Name of the Student:** Ms. Shalini Dimri
3. **Enrolment No.:** LIFE09201304001
4. **Title of the Thesis:** "Molecular Imaging of STAT3 Signaling *in vivo*"
5. **Name of the Board of Studies:** Life Sciences

Recommendations

Tick one of the following:

1. The thesis in its present form is commended for the award of the Ph.D. Degree. [X]
2. The thesis is commended for the award of the Ph.D. degree. However, my suggestions for improving the thesis may be considered at the time of the viva voce examination and if the viva voce board deems it appropriate, the same may be incorporated in the thesis based on the discussions during the viva voce examination. The revised thesis need not be sent to me. [ ]
3. The thesis should be revised as per the suggestions enclosed. I would like to see the revised thesis incorporating my suggestions before I give further recommendations. [ ]
4. The thesis is not acceptable for the award of the Ph.D. degree. [ ]

Date: 08.08.2020

Dr. Abhijit De
Research Guide
Head, Molecular Functional Imaging Laboratory
PI and Scientific Officer "F"
ACTREC, Tata Memorial Centre

1. **Name of the Student:** Ms. Shalini Dimri
2. **Title of the Thesis:** Molecular Imaging of STAT3 Signaling *in vivo*

DETAILED REPORT

Breast cancer is a global disease with high incidence. There are many subtypes of breast cancer of which triple negative breast cancer (TNBC) is one aggressive type that shows high incidence of mortality due to cancer among woman. STAT3 is an important regulatory protein which when activated triggers higher expression of key gene sets (e.g. VEGF, Myc, Cyclin etc) required for growth and progression of cancer cells. Research literatures has majorly reported that STAT3 is activated at Y705 locus across multiple types of cancers. A key finding of this thesis work done by the candidate shows that STAT3 protein in TNBC cases is activated predominantly at a specific gene locus i.e. S727. In depth experimental analysis was done here which shows that phosphorylation at S727 is highly correlated with activated STAT3 protein present in TNBC cancer cells. Activated STAT3 then forms STAT3-STAT3 dimer, which is a significant step for cellular oncogenic activity. It is also shown here that activation via pS727 can cause phenotypic difference independent of canonical pY705 activation. Hence, this study evokes a new understanding of TNBC disease biology, where targeting pY705 alone will not therapeutically suffice inhibition of STAT3 signaling at least for TNBC. Towards this understanding three key technological solutions have been offered through this work– (i) develop a biophysical reporter assay system called phosphoBRET sensor; (ii) set out a live cell drug screen platform for screening of effective drug compounds against STAT3 activation and (iii) use of an anti-helminth medicine, Niclosamide is shown which can be repurposed as an anti-cancer drug by effectively inhibiting S727 and Y705 mediated STAT3 activation in TNBC tumor model.

This thesis work done is thorough and turned out to be sufficiently contributory and productive in terms of two first author research articles by the candidate in reputed international journals as well as a patent filed in India. I therefore wholeheartedly recommend the thesis for the degree award and also recommend for consideration for 'Best thesis category in life Science' by HBNI.

Signature with Date:

08-08-2020

Dr. Abhijit De
Research Guide
Head, Molecular Functional Imaging Laboratory
PI and Scientific Officer "F"
ACTREC, Tata Memorial Centre

Gmail **Shalini Dimri <yashree.dimri@gmail.com>**

Viva voce of Ms. Shalini Dimri

Academic Office <academic.office@actrec.gov.in> Tue, Aug 11, 2020 at 2:29 PM
To: Abhijit De <ade@actrec.gov.in>
Cc: Shalini Dimri <yashree.dimri@gmail.com>

Dear Sir,

For your reference please.

With Best Regards,

Mrs. Sharwari Joshi
Academic Office - HBNI
Advanced Centre for Treatment Research & Education in Cancer (ACTREC)
Tata Memorial Centre, Kharghar, Navi Mumbai – 410210, India
Phone: +91 -22 - 27405000 extn. 5557
Email: academic.office@actrec.gov.in
----- Forwarded by Academic Office/ACTREC on 11/08/2020 02:11 PM -----

From: "Veena K" <veenap@csirccmb.org>
To: "Academic Office" <academic.office@actrec.gov.in>
Date: 10/08/2020 04:44 PM
Subject: Re: Viva voce of Ms. Shalini Dimri

Dear Mrs Joshi,
As a member of the Viva Voce Committee, I certify that I have read the dissertation prepared by **Ms. Shalini Dimri** entitled "**Molecular Imaging of STAT3 Signaling *in vivo***" and recommend that it may be accepted as fulfilling the thesis requirement for the award of Degree of Doctor of Philosophy. I have also attended the Viva Voce presentation by Ms Shalini Dimri and certify that the presentation was excellent and she answered all the questions put to her. I recommend that she may be awarded the PhD degree.
I have attached the signed form.
Best wishes,
Veena K Parnaik

On Mon, Aug 10, 2020 at 12:11 PM Academic Office <academic.office@actrec.gov.in> wrote:

Dear Prof. Parnaik,

I am attaching the document for your signature. Requesting you to please sign the document and forward it to Academic office at above mail id after viva voce and give your recommendation by mail also.

With Best Regards,

Mrs. Sharwari Joshi
Academic Office - HBNI
Advanced Centre for Treatment Research & Education in Cancer (ACTREC)
Tata Memorial Centre, Kharghar, Navi Mumbai – 410210, India
Phone: +91 -22 - 27405000 extn. 5557
Email: academic.office@actrec.gov.in
----- Forwarded by Academic Office/ACTREC on 10/08/2020 12:05 PM -----

From: Academic Office/ACTREC
To: "Veena K" <veenap@csirccmb.org>

Gmail **Shalini Dimri <yashree.dimri@gmail.com>**

Viva voce of Ms. Shalini Dimri

Academic Office <academic.office@actrec.gov.in> Fri, Aug 14, 2020 at 4:21 PM
To: Shalini Dimri <yashree.dimri@gmail.com>

With Best Regards,

Mrs. Sharwari Joshi
Academic Office - HBNI
Advanced Centre for Treatment Research & Education in Cancer (ACTREC)
Tata Memorial Centre, Kharghar, Navi Mumbai – 410210, India
Phone: +91 -22 - 27405000 extn. 5557
Email: academic.office@actrec.gov.in
----- Forwarded by Academic Office/ACTREC on 14/08/2020 04:17 PM -----

From: "shubhada chiplunkar" <shubhachiplunkar@gmail.com>
To: "Academic Office" <academic.office@actrec.gov.in>
Date: 13/08/2020 09:03 PM
Subject: Re: Viva voce of Ms. Shalini Dimri

I attended the PhD viva voce examination of Ms Shalini Dimri through video conferencing on 10th August 2020 at 3pm.
As Chairperson of the DC Committee I attended the viva along with other DC members and External Examiner Dr Veena K Parnaik,
Senior Scientist & JC Bose Fellow.Ms Dimri presented her thesis work on "Molecular Imaging of STAT3 signaling *in vivo* ".
She made an excellent presentation of the thesis work and also defended the thesis well.
She answered both the Reviewers questions satisfactorily and also answered questions raised by the audience.
Based on the performance of the candidate , I strongly recommend award of PhD Life Science degree to Ms Dimri by HBNI.

S. Chiplunkar

Prof Dr. S.V. Chiplunkar
FORMER DIRECTOR
ACTREC, Tata Memorial Centre
Kharghar, Navi Mumbai 410210
PRESIDENT Immuno-Oncology Society of India (IOSI)
PRESIDENT Mumbai Immunology Group (MIG)
Education Committee Member of
International Union of Immunological Societies (IUIS)
[Quoted text hidden]

Gmail **Shalini Dimri <yashree.dimri@gmail.com>**

Viva voce of Ms. Shalini Dimri

Academic Office <academic.office@actrec.gov.in> Fri, Aug 14, 2020 at 4:23 PM
To: Shalini Dimri <yashree.dimri@gmail.com>

With Best Regards,

Mrs. Sharwari Joshi
Academic Office - HBNI
Advanced Centre for Treatment Research & Education in Cancer (ACTREC)
Tata Memorial Centre, Kharghar, Navi Mumbai – 410210, India
Phone: +91 -22 - 27405000 extn. 5557
Email: academic.office@actrec.gov.in
----- Forwarded by Academic Office/ACTREC on 14/08/2020 04:19 PM -----

From: Abhijit De/ACTREC
To: Academic Office/ACTREC@ACTREC
Cc: S V Chiplunkar/ACTREC@ACTREC, Sanjay Gupta/ACTREC@ACTREC, "shubhada chiplunkar" <shubhachiplunkar@gmail.com>, Sudeep Gupta/ACTREC@ACTREC, Venkatraman Prasanna/ACTREC@ACTREC
Date: 13/08/2020 11:44 AM
Subject: Re: Viva voce of Ms. Shalini Dimri

Dear Sharwari
The viva voce exam for Ms. Shalini Dimri was held in the CRI Auditorium on August 10, 2020 between 3-4:30 PM. There were over 40 people (DC members, other faculties and past and present students of ACTREC) attended either physically or online via skype link provided. The candidate made a very impressive presentation and answered all the queries. External examiner, Dr. Veena Parnaik highly appreciated the work done and recommended for the Doctoral degree award to the candidate.

All doctoral committee members are copied in my response here.
Thanks
Abhijit

Dr. Abhijit De
Principal Investigator and Scientific Officer 'F'
Head, Molecular Functional Imaging Laboratory

In Charge, Molecular Imaging Core Facility
ACTREC, Tata Memorial Centre
Sector 22, Kharghar
Navi Mumbai - 410210, INDIA
+91-22-27405038 (O)
SKYPE ID - abhijit.de09
https://actrec.gov.in/dr-abhijit-de

From: Academic Office/ACTREC
To: Sudeep Gupta/ACTREC@ACTREC, S V Chiplunkar/ACTREC@ACTREC, Venkatraman Prasanna/ACTREC@ACTREC, Sanjay Gupta/ACTREC@ACTREC
Cc: "shubhada chiplunkar" <shubhachiplunkar@gmail.com>, Abhijit De/ACTREC@ACTREC
[Quoted text hidden]

Gmail **Shalini Dimri <yashree.dimri@gmail.com>**

Viva voce of Ms. Shalini Dimri

Academic Office <academic.office@actrec.gov.in> Fri, Aug 14, 2020 at 4:03 PM
To: Abhijit De <ade@actrec.gov.in>
Cc: Shalini Dimri <yashree.dimri@gmail.com>

Dear Sir,

For your reference please.

With Best Regards,

Mrs. Sharwari Joshi
Academic Office - HBNI
Advanced Centre for Treatment Research & Education in Cancer (ACTREC)
Tata Memorial Centre, Kharghar, Navi Mumbai – 410210, India
Phone: +91 -22 - 27405000 extn. 5557
Email: academic.office@actrec.gov.in
----- Forwarded by Academic Office/ACTREC on 14/08/2020 03:59 PM -----

From: Venkatraman Prasanna/ACTREC
To: Academic Office/ACTREC@ACTREC
Cc: Abhijit De/ACTREC@ACTREC, S V Chiplunkar/ACTREC@ACTREC, Sanjay Gupta/ACTREC@ACTREC, "shubhada chiplunkar" <shubhachiplunkar@gmail.com>, Sudeep Gupta/ACTREC@ACTREC
Date: 14/08/2020 03:59 PM
Subject: Re: Viva voce of Ms. Shalini Dimri

I congratulate Shalini Dimri for a great presentation and defending her thesis very well
She graduates now to Dr Shalini Dimri
regards
prasanna

From: Academic Office/ACTREC
To: Sudeep Gupta/ACTREC@ACTREC, S V Chiplunkar/ACTREC@ACTREC, Venkatraman Prasanna/ACTREC@ACTREC, Sanjay Gupta/ACTREC@ACTREC
Cc: "shubhada chiplunkar" <shubhachiplunkar@gmail.com>, Abhijit De/ACTREC@ACTREC
Date: 10-08-2020 17:07
Subject: Viva voce of Ms. Shalini Dimri

10th August, 2020
Dear Sir/Madam,

Thank you for attending viva voce of Ms. Shalini Dimri today.

You are requested to give your viva recommendations by mail.

Thanking you,

Sincerely,

Mrs. Sharwari A. Joshi
Academic Office - HBNI
Advanced Centre for Treatment Research & Education in Cancer (ACTREC)
Tata Memorial Centre,

Gmail **Shalini Dimri <yashree.dimri@gmail.com>**

Viva voce of Ms. Shalini Dimri

Academic Office <academic.office@actrec.gov.in> Fri, Aug 14, 2020 at 4:37 PM
To: Abhijit De <ade@actrec.gov.in>
Cc: Shalini Dimri <yashree.dimri@gmail.com>

Dear Sir,

For your reference please.

With Best Regards,

Mrs. Sharwari Joshi
Academic Office - HBNI
Advanced Centre for Treatment Research & Education in Cancer (ACTREC)
Tata Memorial Centre, Kharghar, Navi Mumbai – 410210, India
Phone: +91 -22 - 27405000 extn. 5557
Email: academic.office@actrec.gov.in
----- Forwarded by Academic Office/ACTREC on 14/08/2020 04:32 PM -----

From: Sanjay Gupta/ACTREC
To: Academic Office/ACTREC@ACTREC
Date: 14/08/2020 04:35 PM
Subject: Re: Viva voce of Ms. Shalini Dimri

Congratulations to Shalini on gaining her Ph.D and now Dr. Shalini Dimri. She made excellent presentation and defended her thesis.

Dr. Sanjay Gupta, Ph.D.
PI & Scientific Officer 'G'
KS#352, CRI-ACTREC, TMC, Navi Mumbai
+91 (22) 27405086; 8652098209
Sent from HCL Verses

Academic Office --- Viva voce of Ms. Shalini Dimri ---
From: "Academic Office" <academic.office@actrec.gov.in>
To: "Sanjay Gupta" <sgupta@actrec.gov.in>
Date: Fri, 14 Aug 2020 16:06
Subject: Viva voce of Ms. Shalini Dimri

Gentle Reminder!!!

Dear Sir,

Thank you for attending viva voce of Ms. Shalini Dimri today.

You are requested to give your viva recommendations by mail.

Thanking you,

Sincerely,

With Best Regards,

Gmail **Shalini Dimri <yashree.dimri@gmail.com>**

Viva voce of Ms. Shalini Dimri

Academic Office <academic.office@actrec.gov.in> Tue, Aug 11, 2020 at 2:28 PM
To: Abhijit De <ade@actrec.gov.in>
Cc: Shalini Dimri <yashree.dimri@gmail.com>

Dear Sir,

For your reference please.

With Best Regards,

Mrs. Sharwari Joshi
Academic Office - HBNI
Advanced Centre for Treatment Research & Education in Cancer (ACTREC)
Tata Memorial Centre, Kharghar, Navi Mumbai – 410210, India
Phone: +91 -22 - 27405000 extn. 5557
Email: academic.office@actrec.gov.in
----- Forwarded by Academic Office/ACTREC on 11/08/2020 02:07 PM -----

From: Sudeep Gupta/ACTREC
To: Academic Office/ACTREC@ACTREC
Date: 11/08/2020 01:31 PM
Subject: Re: Viva voce of Ms. Shalini Dimri
Sent by: Director ACTREC

Approved and accepted.

Dr Sudeep Gupta

****

Dr. Sudeep Gupta, M.D., D.M.
Director ACTREC
Room 309/310, 3rd Floor, Paymaster Shodhika,
ACTREC (Advanced Centre for Treatment, Research and Education in Cancer)
Navi Mumbai - 410210, Maharashtra, India
Tel: +91-22-27405035 /37, +91-22-27405059, +91-22-30435059
Fax: +91-22-27405080
Email: sudeep.gupta@actrec.gov.in & sudeepgupta04@yahoo.com
Skype: sudeep.gupta07
Personal Secretary:
Tel: +91-22-27405035 /37 & +91-22-30435035 /37
Mob (only during working hours): +91-9869451641
E-mail: director@actrec.gov.in

Professor of Medical Oncology,
Past Convener, Gynecologic & Breast Oncology Working Groups,
Room No. 1109, 11th Floor, Homi Bhabha Block,
Tata Memorial Centre/Hospital & Homi Bhabha National Institute
Parel, Mumbai-400012, India
Tel (Off): +91 22 24177201
Fax (Off): +91 22 24177201

General Secretary,
Women's Cancer Initiative - Tata Memorial Hospital

Homi Bhabha National Institute

Recommendations of the Viva Voce Committee

As members of the Viva Voce Committee, we certify that we have read the dissertation prepared by **Ms. Shalini Dimri** entitled "**Molecular Imaging of STAT3 Signaling *in vivo***" and recommend that it may be accepted as fulfilling the thesis requirement for the award of Degree of Doctor of Philosophy.

S. Chiplunkar 10.08.2020

Chairperson – Dr. S.V Chiplunkar Date:

Abhijit De 10-08-2020

Guide – Dr. Abhijit De Date:

10 August 2020

External Examiner – Dr. Veena K. Parnaik Date:

Prasanna 10/8/2020.

Member – Dr. Prasanna Venkataraman Date:

Sanjay 10.08.2020

Member -Dr. Sanjay Gupta Date:

10/8/2020

Invitee- Dr. Sudeep Gupta Date

Final approval and acceptance of this thesis is contingent upon the candidate's submission of the final copies of the thesis to HBNI.

I hereby certify that I have read this thesis prepared under my direction and recommend that it may be accepted as fulfilling the thesis requirement.

Abhijit De 10-08-2020

Date: 10.08.2020
Place: Navi Mumbai

Dr. Abhijit De
Guide

Homi Bhabha National Institute

Report of Ph.D. Viva-Voce

Board of Studies in Life Sciences

A. General Details:

1. **Name of the Constituent Institution:** Tata Memorial Centre- ACTREC

2. **Name of the Student:** Ms. Shalini Dimri

3. **Enrolment Number:** LIFE09201304001

4. **Date of Enrolment in HBNI:** 01.09.2013

5. **Date of Submission of Thesis:** 02.03.2020

6. **Title of the Thesis:** Molecular Imaging of STAT3 Signaling *in vivo*

7. **Number of Doctoral Committee Meetings held with respective dates:**

Review Period	Date	Review Period	Date
1.Aug 2013-Aug 2014	20.10.2014	2.Aug 2014-Aug 2015	20.08.2015
3.Aug 2015-Aug 2016	17.11.2016	4.Aug 2016-Aug 2017	30.11.2017
5.Aug 2017-Aug 2019	11.06.2019	6. NA	

8. **Name and Affiliation of the Thesis Examiner 1:** Dr. Ramasamy Paulmurugan, Associate Professor of Radiology, Molecular Imaging Program at Stanford, Department of Radiology, Stanford University School of Medicine, California - USA

   Recommendations of the Examiner 2 (Thesis Evaluation) (i) accepted

9. **Name and Affiliation of the Thesis Examiner 2:** Dr. Veena K. Parnaik, Senior Scientist, JC Bose Fellow, Centre for Cellular and Molecular Biology (CCMB), Hyderabad

   Recommendations of the Examiner 2 (Thesis Evaluation) (i) accepted

B. Record of the Viva-Voce Examination

1. **Date of Viva Voce Examination:** 10.08.2020

2. **Name and affiliation of External Examiner**: Dr. Veena K. Parnaik, Senior Scientist, JC Bose Fellow, Centre for Cellular and Molecular Biology (CCMB), Hyderabad

3. **Whether there were other experts / faculty/students present? Please enclose a soft copy of attendance sheet indicating participation in person/over video as per proforma given below at (5)**

4. **Recommendations for the award of the Ph.D. degree: Recommended**
   (If Recommended, give summary of main findings and overall quality of thesis)

Chapter 1: Candidate provides background information on all aspects of the research work and raise key questions by laying out rationales.
Chapter 2: Covers research results obtained on objective 1, which essentially frames the core technical foundation of the total work. Candidate has secured her qualifying publication from this chapter and she is also a co-inventor in the Indian patent applied based on this work.

Chapter 3: Candidate evaluated the role of PTM dependent STAT3 signaling in breast cancer. Through meticulously designed experiments conducted in this chapter, the candidate has convincingly proved the hypothesis that in TNBC cases Non-canonical STAT3 PTM drives oncogenic potential and this operates independent of canonical activation.
Chapter 4: Candidate evaluated clinical aspects using patient sample to judge the practical link of the study in clinical condition of breast cancer. Work in this chapter has also contributed to find a solution through preclinical evaluation of a repurposed drug that can effectively prevent STAT3 activation both via canonical and non-canonical axis. Combining the major work done in chapter 3 and 4, she has communicated another high impact research article (which is under review currently).

Therefore, the thesis work done by Shalini Dimri is a very thorough piece of work, well designed and practical goal oriented. Candidate has secured multiple publications in reputed international and peer-reviewed journals. Her work contribution recognized as a co-inventor of an Indian patent filed from ACTREC is a unique example from ACTREC, amply suggests the credentials. Therefore, this PhD thesis work may be considered for best thesis award category in Life Science this year and candidate be awarded the PhD degree.

5. Attendance at Viva Voce (Doctoral Committee, External Examiner, others):

Sr No	Composition	Name	Attended in person or through video; if in person, signature
1.	**Chairperson**	Dr. Shubhada V. Chiplunkar	Skype Video
2.	**Convener** (Guide)	Dr. Abhijit De	10-08-2020
3.	**External Examiner**	Dr. Veena K. Parnaik	Skype Video
4.	**Member**	Dr. Prasanna Venkataraman	10/08/2020
5.	**Member**	Dr. Sanjay Gupta	Skype Video
6	**Invitee**	Dr. Sudeep Gupta	Not available
Others: Separate list attached			

10-08-2020

(Convener, Viva Voce Board)

Participants present in the auditorium		
S. No.	**Name**	**Designation**
1	Dr. Abhijit De	Principal Investigator
2	Dr. Pritha Ray	Principal Investigator
3	Dr. Prasanna Venkatraman	Principal Investigator
4	Dr. Manoj B. Mahimkar	Principal Investigator
5	Dr. Sorab Dalal	Principal Investigator
6	Dr. Rohan Khadilkar	Principal Investigator
7	Ms. Mansi Joshi	Student
8	Ms. Chetna Patnaik	Student
9	Mr. Sumit Kumar Mishra	Student
10	Mr. Arijit Mal	Student
11	Ms. Maitreyi Rathod	Student
12	Ms. Snehal Valvi	Student
13	Mrs. Renu Malhotra	Student
14	Mr. Aniket Bishnu	Student
15	Mr. Praveen Marathe	Student
16	Mr. Muddassir Ali Rashid	Student
17	Ms. Tarang Gaur	Student
18	Mr. Shubham Deshmukh	Student
19	Ms. Neha	Student
20	Mr. Abhilah	Student
21	Ms. Rucha Kulkarni	Student
22	Mr. Girish	Student
23	Ms. Nazia Chaudhary	Student
24	Ms. Aasna Parui	Student
25	Mr. Aakash	Student
26	Ms. Raikamal Paul	Student
27	Mr. Ajit Dhadve	Student
28	Mr. Saim Wasimulla	Student
29	Mr. Raghav Reddy Sunkara	Student
30	Ms. Sonam	Student
31	Mr. Joel Christie	Student
32	Ms. Deepkshikha Dutta	Student
Participants attended Viva Voce via Skype video call		
1	Mr. Ajay Wagh	Student
2	Mr. Amir Bukhari	Student
3	Ms. Anjali Singh	Student
4	Ms. Debashmita Sarkar	Student
5	Ms. Jyothi Nair	Student

6	Dr. Kakoli Bose	Principal Investigator
7	Ms. Mahalakshmi Ram	Student
8	Ms. Megha Mehrotra	Student
9	Ms. Mythreyi Narasimhan	Student
10	Dr. Nandini Verma	Principal Investigator
11	Mr. Pranay Dey	Student
12	Mr. Pratham Phadte	Student
13	Ms. Rajashree Kadam	Student
14	Mr. Rohan Chaubal	Student
15	Mr. Rohit Gaikwad	Student
16	Dr. Sanjay Gupta	Principal Investigator
17	Dr. Shubhada V. Chiplunkar	Principal Investigator
18	Dr. Ujjwala Warawdekar	Principal Investigator
19	Dr. Veena K Parnaik	External Examiner
20	Mr. Abhiram Natu	Student
21	Mr. Raghupathi Kummari	Student
22	Ms. Shalini Dimri	Student
23	ACTREC 02	Student
24	Dr. Abhijit De	Principal Investigator

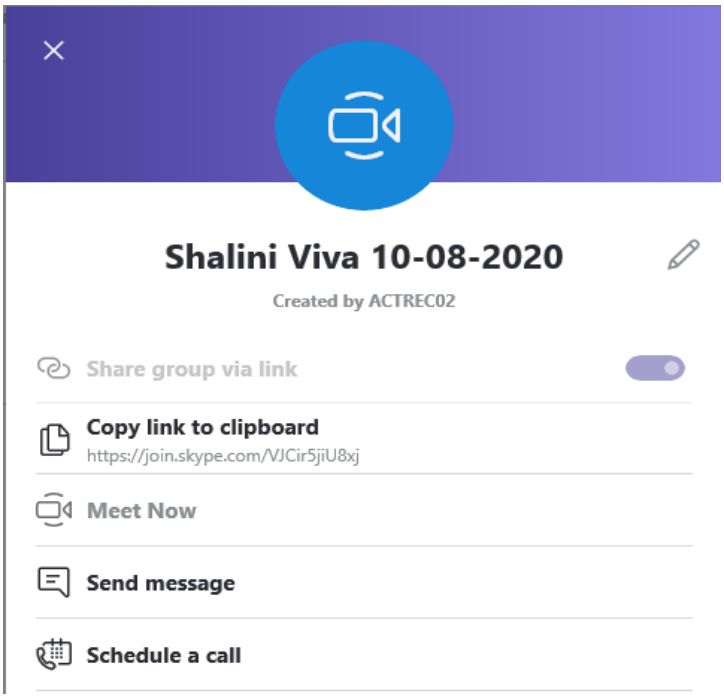

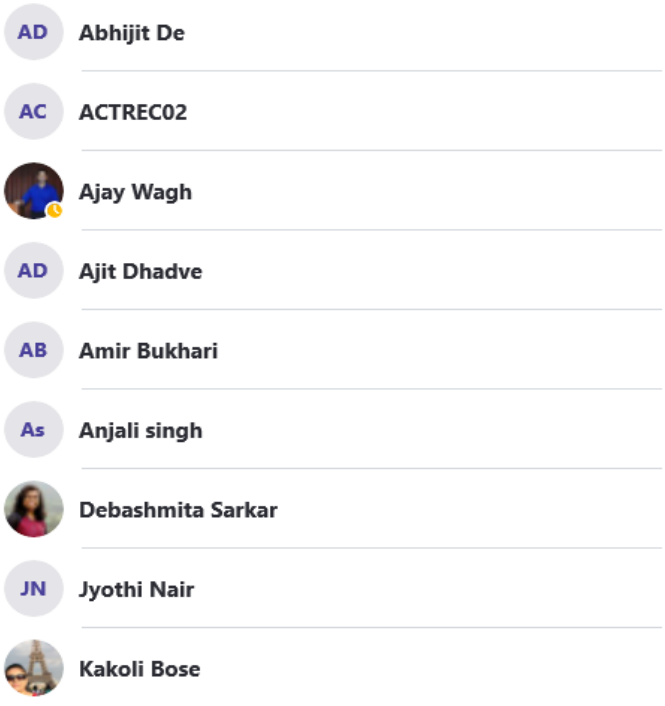

mr mahalakshmi ram

 mansi joshi

 Megha Mehrotra

 Nandini Verma

PD Pranay Dey

 Pratham Phadte

 Rajashree Kadam

RC Rohan Chaubal

RC Rohan Chaubal

RG Rohit Gawand

SG Sanjay Gupta

SC Shubhada Chiplunkar

UW Ujjwala Warawdekar

VP Veena Parnaik

 Shalini Dimri

GROUP GALLERY

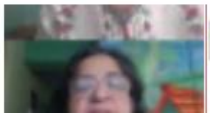

Molecular Imaging of STAT3 Signaling *In Vivo*

By

SHALINI DIMRI

[LIFE09201304001]

TATA MEMORIAL CENTRE

MUMBAI

A thesis submitted to the Board of Studies in Life Sciences

In partial fulfilment of requirements for the Degree of

DOCTOR OF PHILOSOPHY

of

HOMI BHABHA NATIONAL INSTITUTE

March, 2020

TABLE OF CONTENTS

DECLARATION

I, hereby declare that the investigation presented in the thesis has been carried out by me. The work is original and has not been submitted earlier as a whole or in part for a degree / diploma at this or any other Institution / University.

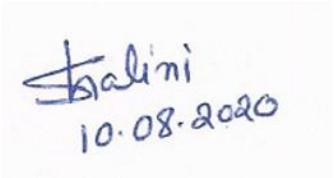

Ms. Shalini Dimri

DECLARATION

I, hereby declare that the investigation presented in the thesis has been carried out under my supervision. The work is original and has not been submitted earlier as a whole or in part for a degree / diploma at this or any other Institution / University.

Dr. Abhijit De

(Guide)

Alumni Form

(To be submitted by the student at the time of issue of PDC)

Name of Student: Ms. Shalini Dimri

Enrolment Number: LIFE09201304001

Date of enrolment: 01.09.2013

Academic Program and Discipline: HBNI, Life Sciences

Name of CI/OCC: TMC-ACTREC

Date of submission of thesis: 02.03.2020

Title of thesis: Molecular Imaging of STAT3 Signaling *in vivo*

Contact details for future correspondence: Mr. Rohit Dimri

Postal Address: C/O Rohit Dimri, RZ 532 First Floor, Gali No. 2, Kailash Puri, Palam, New Delhi 110045

Email address: yashree.dimri@gmail.com

Telephone number:

Landline: NA

Mobile: 09757012258, 09711004754

Employed / pursuing higher studies (give details): Applying for Post-Doctoral Programme

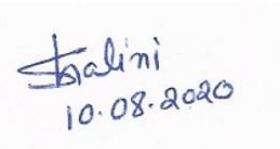

(Signature)

HOMI BHABHA NATIONAL INSTITUTE

Regd. Office : Training School Complex, Anushaktinagar, Mumbai 400 094.

Bank Transaction details for Fee Payment

1	Payment ID	**LIFE09201304001-130120122844**
2	Discipline	Life Sciences
3	CI Name	TMC Mumbai
4	Year of Enrollment	2013
5	Programme Name	Ph.D
6	Enrollment No.	LIFE09201304001
7	Student Name	Ms Ms Shalini Dimri
8	Gender :	Female
9	Date of Birth (DD/MM/YYYY) :	03/03/1989
10	Mobile No./Contact No. :	9757012258
11	Email ID (in block letters) :	yashree.dimri@gmail.com
12	Type of Fee :	Evaluation Fee
13	Amount of Fee :	Rs.10000
14	Bank Transaction ID	DUC5745149
15	Bank Transaction Date	13/01/2020

Date : Signature of the Candidate

To. : Dean, HBNI

Note : Kindly submit printout of the Above Page to HBNI Office for further processing

Note : If Bank Transaction ID / Transaction Date wrongly updated; Contact HBNI Office for Correction

Print

Student feedback Form

Sr. No.	Parameters	Student Feedback				
		Strongly Agree	Moderately Agree	Agree	Moderately Disagree	Strongly Disagree
1.	The courses offered are stimulating & broadening and help in improving overall domain knowledge		X			
2	There are adequate options for electives covering wide spectrum of subjects	X				
3.	The curriculum can be recommended to continue without change (if you recommend any change(s) please give details through mail to Dean, HBNI)			X		
4.	The curriculum provides necessary foundation and skill base for future career	X				
5	Associated projects and tutorials are useful		X			
6.	The examination system of the course does not put in any undue stress		X			
7	I have come across any instance of ragging in my campus					X
8.	All necessary ICT resources (eg. Computer, Internet, projector.) are available in classroom	X				
9.	State-of-the-art facilities are available to carry out research		X			
10.	Faculty have up-to-date knowledge of the courses		X			
11.	Faculty have Very Good teaching capability		X			
12.	Faculty encourage questions to be raised in the class.	X				
13.	Non-teaching staff are helpful and cooperative		X			
14	Hostel rooms are good, clean and have good facilities			X		
15.	Mess serves good and hygienic food			X		
16.	Recreation and common room facilities are adequate				X	
17.	Will recommend others to enrol for academic programs in HBNI	X				

छात्र का नाम: सुश्री शालिनी डिमरी

शोध का शीर्षक: विवो में STAT3 सिग्नलिंग की आणविक इमेजिंग

नामांकन संख्या: लाईफ09201304001

हस्ताक्षर: Shalini 10.08.2020

छात्र: सुश्री शालिनी डिमरी

हस्ताक्षर: 10.08.2020.

गाइड: डॉ. अभिजीत डे

Thesis Keyword

Name: Ms. Shalini Dimri

Enrolment No.: LIFE09201304001

Thesis Title: Molecular Imaging of STAT3 Signaling *in vivo*

Subject: Cancer biology

Sub-Category: Post Translational Modification and Signaling

Breast Cancer

Triple Negative Breast Cancer (TNBC)

Signal Transducer and Activator of Transcription 3 (STAT3)

Post translational modifications (PTMs)

Bioluminescence Resonance Energy Transfer (BRET)

Non-invasive Bioluminescence Imaging

Canonical pathway

Noncanonical pathway

High throughput Screening

Nanoluciferase

TurboFP635

Niclosamide

Stattic

Shalini
10.08.2020

Ms. Shalini Dimri

10.08.2020

Dr. Abhijit De

(Guide)

Thesis Highlight

Name of the Student: Ms. Shalini Dimri

Name of the CI/OCC: TMC-ACTREC **Enrolment No.:** LIFE09201304001

Thesis Title: "Molecular Imaging of STAT3 Signaling *in vivo*"

Discipline: Life Sciences **Sub-Area of Discipline:** Breast Cancer biology

Date of viva voce: 10.08.2020

STAT3 pathway is known to be primarily driven by classical canonical pY705 activation. In recent years, an alternate mechanism of STAT3 activation termed as noncanonical pathway is identified. Here, apart from pY705 other post translational modifications (PTMs) like Serine727-phosphorylation (pS727) and lysineK685-acetylation (K685ac) can equally activate the STAT3 signaling. However, the critical role of noncanonical STAT3 pathway in controlling STAT3 dimerization, functional and transcriptional activity in breast cancer still remains elusive.

Here by developing a novel BRET (Bioluminescence Resonance Energy Transfer) based STAT3 phosphorylation sensor, that can detect dynamic STAT3 dimerization in live cells, we have identified that pS727 noncanonical activation predominantly controls STAT3 homodimerization process (rate limiting step) in breast cancer cells. Further, stable homodimers of STAT3 formed under the influence of pS727 activation are majorly involved in controlling cell survival, proliferation and transcriptional functions of STAT3 in MCF 7 cells as compared to canonical pY705 PTM.

Extending our *in vitro* observations to clinical scenario, in TNBC patient samples, a strong nuclear pS727 expression was evidently seen in more than 90% total STAT3 positive cases while pY705 was found in only 15% cases. From therapy perspective, for pY705 STAT3 positive tumours Stattic (pY705 blocker) is a promising candidate. However, in case of TNBC, treatment with Stattic would result in therapy failure as it is ineffective against pS727 pathway (predominant mechanism). Over here dual blockers like Niclosamide (pY705 and pS727) would be a more appropriate choice as it can cause complete STAT3 pathway inactivation, resulting in treatment success. Considering prevalent role of noncanonical STAT3 pathway in TNBCs, in future more inhibitors like niclosamide should be identified.

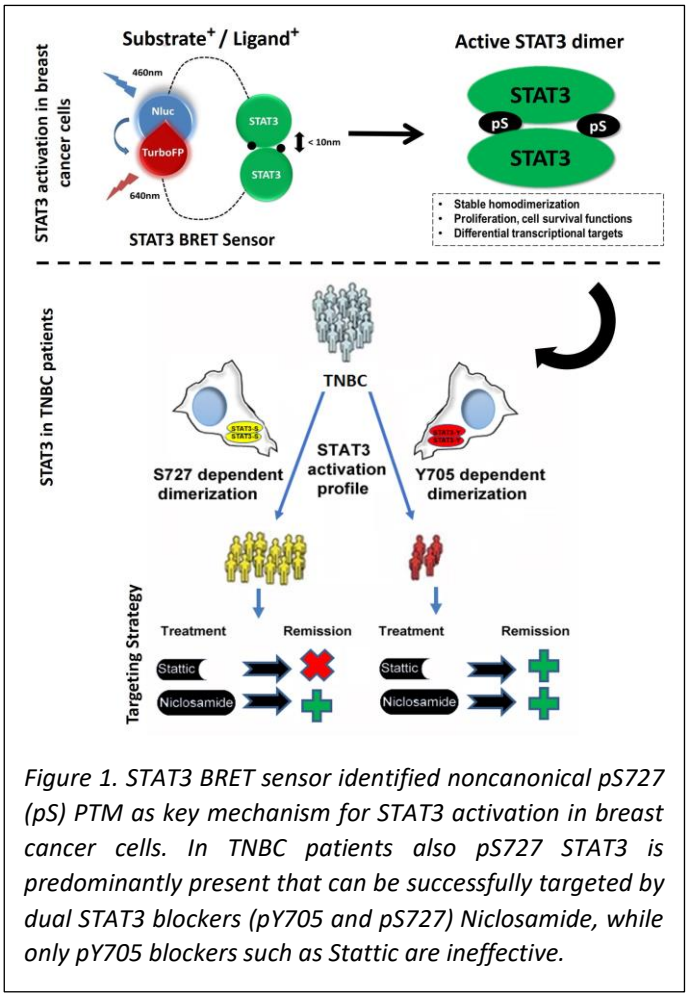

Figure 1. STAT3 BRET sensor identified noncanonical pS727 (pS) PTM as key mechanism for STAT3 activation in breast cancer cells. In TNBC patients also pS727 STAT3 is predominantly present that can be successfully targeted by dual STAT3 blockers (pY705 and pS727) Niclosamide, while only pY705 blockers such as Stattic are ineffective.

HOMI BHABHA NATIONAL INSTITUTE
CHECK LIST FOR 11 CRITERIA AS PER UGC (MINIMUM STANDARD AND PROCEDURE FOR AWARD OF PH.D. DEGREE) REGULATION 2009[1]

1. **NAME OF THE STUDENT:** Ms. Shalini Dimri
2. **NAME OF THE CONSTITUENT INSTITUTION:** Tata Memorial Centre, ACTREC
3. **ENROLMENT NO.:** LIFE09201304001
4. **BOARD OF STUDIES:** Life Sciences

SR. NO.	PARTICULAR	**Remark** (Tick the appropriate one)
1.	Mode of selection for Ph.D. Programme	~~Written Test~~ / ~~Interview~~ / **Both***
2.	Number of Ph.D. students under the guide ≤ 8 during the period	Yes / ~~No~~
3.	Reservation Policy applied for selection	~~Yes~~ / No
4.	Course work prescribed as per guidelines done	Yes / ~~No~~
5.	Annual Progress Reviews held	Yes / ~~No~~
6.	Test on Research Methodology was a part of the course work	Yes / ~~No~~
7.	Pre-synopsis presentation held	Yes / ~~No~~
8.	At least 1 journal paper published	Yes / ~~No~~
9.	At least of 2 papers in conference / seminar presented	Yes / ~~No~~
10.	Evaluation reports of Ph.D. Thesis from guide and two experts (one expert is out of state) received	Yes / ~~No~~
11.	Soft copy of Thesis submitted to HBNI	Yes / ~~No~~

***Cleared ACTREC Test**

S. Chiplunkar 10/08/2020

Dr. S.V. Chiplunkar
Chairperson, Academic
& Training Programme, ACTREC

13/8/2020

Dr. S. D. Banavali
Dean-ACADEMIC,
TMC

PROF. S. D. BANAVALI, MD
DEAN (ACADEMICS)
TATA MEMORIAL CENTRE
MUMBAI – 400 012.

TO
DEAN, HBNI

(Prof. Dr. S. V. Chiplunkar)
Chairperson, Academic &
Training Programme , ACTREC

Annexure I

CERTIFICATION ON ACADEMIC INTEGRITY

1. I, **Ms. Shalini Dimri** HBNI Enrolment No. LIFE09201304001 hereby undertake that, the Thesis titled ***"Molecular Imaging of STAT3 Signaling in vivo"*** is prepared by me and is the original work undertaken by me and free of any plagiarism. That the document has been duly checked through a plagiarism detection tool and the document is plagiarism free.

2. I am aware and undertake that if plagiarism is detected in my thesis at any stage in future, suitable penalty will be imposed as per the applicable guidelines of the Institute / UGC.

Shalini
10.08.2020

Ms. Shalini Dimri

Endowed by the Thesis Supervisor:
(I certify that the work done by the Researcher is plagiarism free)

Abhijit De. 10.08.2020.

Name: Dr. Abhijit De
Designation: PI and SO "F"
Department: Molecular Functional Imaging Laboratory
Centre: ACTREC- Tata Memorial Centre
Name of the CI/OCC: ACTREC-TMC

The Report is Generated by DrillBit Plagiarism Detection Software

Title: Thesis

Author Name:Shalini

Document : Shalini Thesis_DB (18189 KB)
Submission Id : 200217121302
Submitted Date : 17-Feb-2020 12:19:32 (IST)

DrillBit Similarity Report

6	51	A
SIMILARITY %	MATCHED FILES	GRADE

A-Satisfactory (0-10%)
B-Upgrade (11-40%)
C-Poor (41-60%)
D-Unacceptable (61-100%)

Sl.No	LOCATION	MATCHED SOURCES	%
1	3	esmoopen.bmj.com Internet Data	2
2	21	STAT3 knockdown by siRNA induces apoptosis in human cutaneous T-cell , by Navin K. Verma Ant- 2010 Publication	<1
3	28	microRNAs as potential regulators of myeloid-derived suppressor cell , by El-Gazzar, M.- 2014 Publication	<1
4	30	Sema4D expression and secretion are increased by HIF-1 and inhibit o, by Chen, Wu-gui Sun, - 2019 Publication	<1
5	35	www.doaj.org Publication	<1

Conclusion and Significance

Conclusion

STAT3 signaling is reported to be upregulated in majority of primary tumours and cancer cell lines. Since pY705 STAT3 is predominantly expressed in most tumours it is unanimously considered as an indicator of STAT3 pathway and is used as biomarker for drug development and therapeutic screening of potential STAT3 inhibitors. Classical approach for presence or absence of canonical pY705 activation mark is still used as stratification criteria for STAT3 based therapeutic approaches at both preclinical and clinical settings. However, with the identification of an alternate noncanonical (pS727 and K685ac) activation mechanism, the clinical paradigm of terming pY705 as sole activation mark for STAT3 pathway is changing. The present study here carefully demonstrates the role and functions of the two STAT3 activation arms and how they can be targeted effectively in a subset of breast cancer.

To better inhibit the STAT3 pathway, it is important to decipher the biology of STAT3 activation from natural cellular environment. However, so far there are no sensor-based approaches available that can determine the STAT3 pathway modulation in real time manner from live cells or living system. Hence taking advantage of the highly sensitive BRET based protein interaction methodology, this study for the first-time reports' development of a phosphorylation driven STAT3 homodimerization BRET sensor. With carful optimization we first established Nanoluc as a compatible donor for TurboFP red-sifted fluorophore as an acceptor pair. BRET sensor established by fusing STAT3 with Nluc or TurboFP at an optimized C-terminus orientation very precisely captured the STAT3 activation kinetics upon EGF stimulation in a time dependent manner. The biosensor developed also demonstrated equal sensitivity of monitoring STAT3 pathway perturbation even in cancer cell types of different origin (HT1080, PC3, A549, MCF7) expressing differential level of endogenous STAT3 as well as with variable pathway ligands (IL6 and EGF). With the obvious

advantages shown, the Phospho-BRET sensor was further adapted to high throughput screening platform, where it clearly identified the potential activators (AR42, CI-994 and Chidamide) and inhibitors (Curcumin, Niclosamide, ERK inhibitor, Neratinib and MS-275) of the STAT3 pathway. Of which, Niclosamide being dual blocker (pY705 and pS727) was found to be more potent STAT3 inhibitor than previously known Stattic compound, which can only block pY705 phospho- activation mark. Interestingly from the high throughput screen other novel inhibitors of STAT3 pathway such as neratinib (Her family blocker), ERK inhibitor and MS-275 (HDACi) with BRET inhibitory signal comparable to niclosamide and curcumin (known STAT3 inhibitors) were identified. Most importantly, in the parameter of the sensitivity the biosensor showed reproducible results with uncompromised sensitivity in comparison to conventional 96-well plate format, despite using minimal number of cells and substrate utility.

In order to determine how the two signaling arms (canonical and noncanonical) govern STAT3 activation and molecular functions in breast cancer cells, we engineered a 3'UTR STAT3 knocked down MCF7 cells, in which stable over expression of either wild type or point mutants of STAT3 PTMs (Y705F, S727A and K685R) were introduced. Over here we found that both canonical (pY705) and noncanonical (pS727 and K685R) activations can operate independently while pS727 PTM mark necessarily cooperate with K685ac. With differential downstream transcriptional execution, both pS727 and K685ac were identified to play a dominant and essential role in controlling proliferation and cell survival functions in BC cells over canonical pY705 PTM. Further taking advantage of the Phospho BRET sensor developed, we constructed a library of STAT3 clones harbouring mutation in individual PTM residue either alone or in combinations and subjected them to BRET platform in presence or absence of ligands (IL6 and EGF). Collective observation form all the mutants screened, identified pS727 and not Y705, as key residue required for stable STAT3 homodimer

formation in breast cancer cells. The critical observations made from our study here strongly contradict the existing literature where K685ac was termed as sole executor of STAT3 dimerization and biological functions. However surprisingly, recent reports from two independent groups parallel our observations. Based on molecular observation of STAT3 dimer at atomic level using X-ray crystallography approach and by utilizing BiFC (Bimolecular fluorescence complementation assay) sensor, these two studies independently identified that STAT3 dimerization event is independent of K685ac PTM, and that K685 gain or loss had minimal effect on the STAT3 dimeric complex.

Intrigued by the dominant role played by noncanonical pS727 activation in governing STAT3 homodimerization and downstream biological functions *in vitro* in breast cancer cells, we next decided to explore whether the same situation prevails even in clinical scenario. With convincing number of studies pointing towards STAT3 as key signaling pathway for triple negative breast cancers, we decided to perform retrospective analysis for pY705, pS727 and total STAT3 expression in 76 core biopsy and paired post NACT TNBC cases. Quantitative assessment of the IHC DAB staining with two different scoring methods identified pS727 (more than 90% positive cases) as predominant STAT3 PTM form present over pY705 (less than 15% positive cases). Also, the cases positive for total STAT3 showed moderate to strong positive Pearson correlation value with pS727 PTM mark while it was low positive for pY705 STAT3. This distinct preference of STAT3 pathway for pS727PTM was seen exclusively in TNBCs and not in other breast cancer subtypes (luminal and Her2 high) or other cancer tissue samples (melanoma and lung adenocarcinoma). However, a more conclusive observations can be made once the same analysis is performed with good sample size. The observations made from patient samples were in accordance with the above *in vitro* data and identified noncanonical pS727 pathway as key mode of operation for STAT3 functions in TNBCs. With the aberrant activation of STAT3 signaling seen in TNBCs, as

expected, knocking down its expression in MDA MB 231 cells (TNBC cell line) led to a significant decrease in cell proliferation, survival, and tumorigenic potential along with depletion in $CD44^{high}/CD24^{low}$ like stem cell pool. Based on clinical and *in vitro* data it is evident that STAT3 pathway is essential for survival of TNBCs. Hence to therapeutically target TNBC, we developed *in vivo* tumour xenograft model using reporter labelled MDA MB 231cells and treated the mice with, dual STAT3 blocker Niclosamide (as identified from the BRET inhibitor screen) inhibitor. With potent STAT3 inhibitory functions Niclosamide treatment not only retarded the primary tumour growth but it significantly reduced the metastasis to distant organs like lungs and bones.

In summary, based on experimental and clinical data gathered during the study, here for the first time we report that noncanonical pS727, but not the canonical pY705, is the key PTM driving major STAT3 activation and functions in TNBC subtype of breast cancer. We have further demonstrated that pS727 STAT3 PTM operates independently and is crucial requirement for STAT3 homodimerization, activation and downstream oncogenic functions in breast cancer cells. As a therapeutic target, Niclosamide, a repurposed anti-helminthic drug, is demonstrated as dual blocker of phospho-STAT3 (pY705 and pS727) and thus act with enhanced anti-cancer activity than Stattic (which specifically block pY705 only) both *in vitro* and *in vivo* condition. Finally, with the robust drug screening platform developed using Phospho-STAT3 BRET sensor, the way for comprehensive analysis of STAT3 signaling is paved and in future it is expected to provide with an opportunity to screen large combinatorial anti-STAT3 drug libraries using live cell across multiple cancer types.

Significance of the Study

The work done in the present study provides convincing evidences in favour of noncanonical pathway as key moderator of STAT3 dependent biological functions (dimerization, transcriptional and survival) in triple negative breast cancer and how a treatment approach against STAT3 should be redesigned and pursued for duel blocking of both canonical and noncanonical routes in tumours addicted to the STAT3 oncogene.

As implicated from results obtained, at least for TNBC cases, where canonical pY705 STAT3 is mostly inactive, use of some of the major inhibitors blocking only Y705 PTM may results in ineffective or partial inhibition of the STAT3 pathway and thus may result in incomplete treatment response. However, a thorough detection of other PTM activation marks in addition to the pY705 mark in the cancer tissue samples can rationally stratify the patients for specific PTM inhibitory approach and thus help in achieving the complete blockade of the STAT3 oncogenic molecule. As evidently seen, how Niclosamide treatment effectively blocks both canonical and noncanonical oncogenic STAT3 functions in breast cancer, identifying more such inhibitors blocking both pY705 and pS727 activation marks might offer a promising and a more potent therapeutic strategy. Over here, taking the advantage of the STAT3 Phospho-BRET biosensor approach, setting out a live cell, high throughput screening of inhibitor drug molecule might help in future. Since, based on literature evidences, noncanonical activation of STAT3 is reported in multiple other cancer types, a pan-cancer screening effort might also be helpful. Additionally, based on high throughput compatibility of the sensor, several other existing chemotherapeutic agents or FDA approved drugs can be repurposed for their use as anti-cancer agents either alone or in combination against the STAT3 molecule.

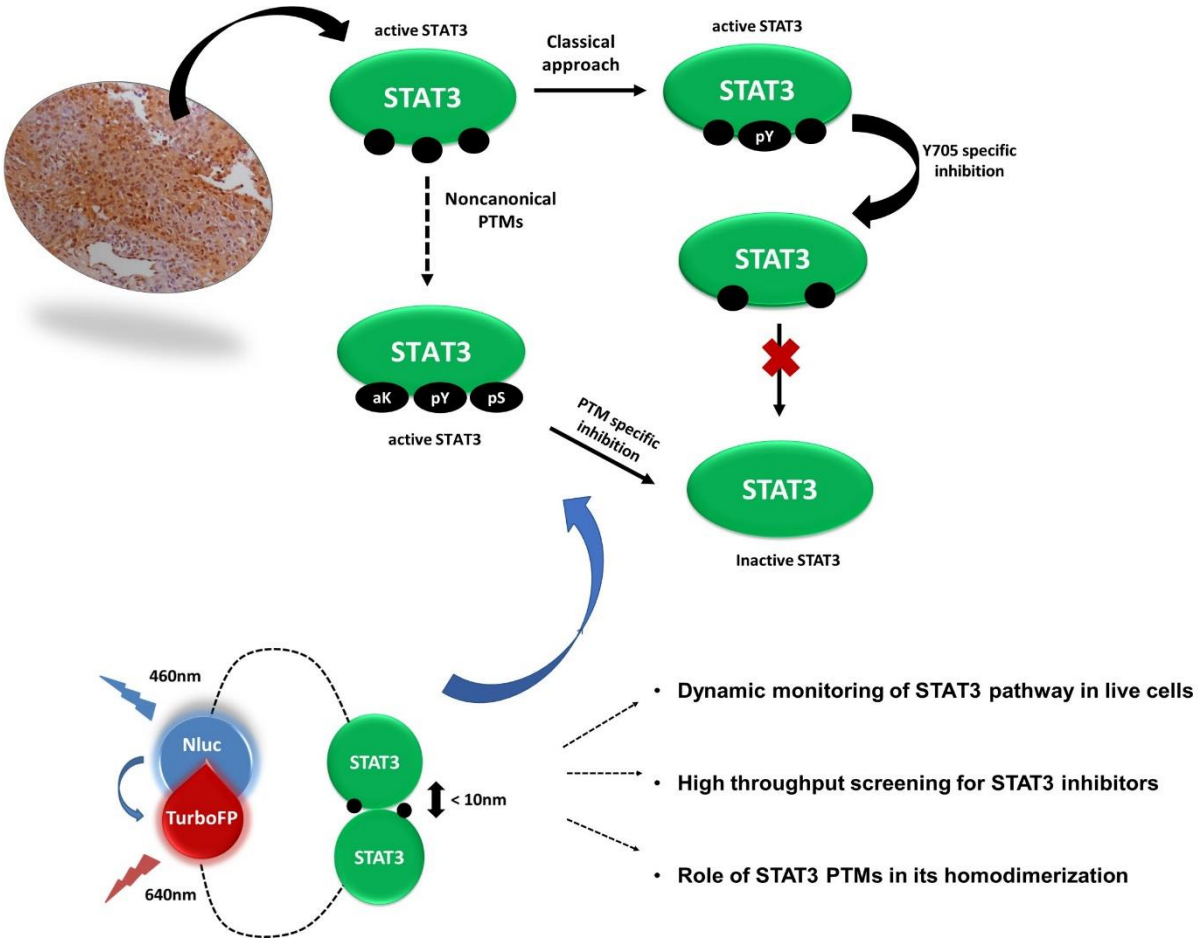

Modifying STAT3 targeting approach. *Following the classical method of pY705 detection in cancer tissue sample and inhibitors targeting it will result in partially blocked STAT3 molecule as the other sites will remain active in such treatment scenario. However, screening for other PTM marks in parallel will help in rectifying the treatment approach to be more global and thus help in achieving complete STAT3 inhibition. Taking advantage of high throughput screening tool like Phospho-STAT3 BRET sensor will significantly aid in understanding the biology of individual PTM site and identifying inhibitors for STAT3 with multitargeting approach.*

List of Figures

List of Tables

List of Abbreviations

3, 3’-diaminobenzidine tetra hydrochloride (DAB)
4, 6’-diamidino-2-phenylindole (DAPI)
Bioluminescence imaging (BLI)
Bioluminescence Resonance Energy Transfer (BRET)
Bovine serum albumin (BSA)
Breast cancer (BC)
Charge-coupled device (CCD)
Epidermal growth factor (EGF)
Epidermal growth factor receptor (EGFR)
Estrogen receptor alpha (ERα)
Food and Drug Administration (FDA)
Fetal bovine serum (FBS)
Formalin fixed paraffin embedded (FFPE)
Glyceraldehyde- 3-phosphate dehydrogenase (GAPDH)
Green fluorescent protein (GFP)
Histone deacetylase inhibitors (HDACi)
Horse radish peroxidase (HRP)
Human epidermal growth factor receptor (HER2)
Immunohistochemistry (IHC)
Infiltrating ductal carcinoma (IDC)
Interlukin-6 (IL6)
Mean fluorescence intensity (MFI)
Milli BRET Unit (mBU)
Molecular imaging (MI)
Nanoluciferase (NLuc)
Near-infrared (NIR)
Niclosamide (NSA)
Optical imaging (OI)
Real time polymerase chain reaction (RT-PCR)
Region of interest (ROI)
Signal Transducer and Activator of Transcription 3 (STAT3)
Site directed mutagenesis (SDM)
Triple Negative Breast Cancer (TNBC)
Post Translational Modifications (PTMs)